IMMUNO-ONCOLOGY OF GYNECOLOGICAL MALIGNANCIES

FROM BENCH TO BEDSIDE

Fenne L. Komdeur

COLOFON

Layout and cover design:	Design Your Thesis, www.designyourthesis.com
Printing:	Ridderprint B.V., www.ridderprint.nl
ISBN:	978-94-034-1114-9
ISBN (Ebook)	978-94-034-1113-2

Printing of this thesis was financially supported by the University of Groningen, University Medical Center Groningen, Graduate School of Medical Sciences and Vicinivax BV.

rijksuniversiteit
groningen

IMMUNO-ONCOLOGY OF GYNECOLOGICAL MALIGNANCIES

FROM BENCH TO BEDSIDE

Proefschrift

ter verkrijging van de graad van doctor aan de
Rijksuniversiteit Groningen
op gezag van de
rector magnificus prof. dr. E. Sterken
en volgens besluit van het College voor Promoties.

De openbare verdediging zal plaatsvinden op

woensdag 21 november 2018 om 16.15 uur

door

Fenne Lara Komdeur
geboren op 19 november 1988
te Nijmegen

Promotores
Prof. dr. H.W. Nijman
Prof. dr. C.A.H.H. Daemen

Copromotor
Dr. M. de Bruyn

Beoordelingscommissie
Prof. dr. J.P. Medema
Prof. dr. R.K. Weersma
Prof. dr. S.A. Scherjon

Paranimfen
Dr. F.A. Eggink
Dr. I.S. Bakker

TABLE OF CONTENTS

General introduction

GENERAL INTRODUCTION

The immune system plays a crucial role in recognition and elimination of (pre)malignant cells. Immune T cells in particular are highly skilled at surveying the body and identifying (pre) malignant cells to be eliminated. When T cells infiltrate the tumor micro-environment they are referred to as tumor-infiltrating lymphocytes (TIL). TIL have a pronounced effect on the survival of patients across malignancies. Moreover, it has also become abundantly clear that TIL can be targeted by cancer immunotherapy to induce lasting clinical benefit. In this thesis, we explored several aspects of TIL biology, including localization and differentiation, with the ultimate aim of developing novel therapeutic interventions.

TUMOR-IMMUNOLOGY

The identification of (pre)malignant cells by T cells is based on the recognition of so-called antigens. These antigens are either 'self' or 'non-self' proteins. Bacterial and viral pathogens are prototypical examples of non-self and are therefore easily recognized as foreign by the T cell. Nevertheless, as discussed in more detail below, tumor antigens can also be recognized by the T cell as non-self. Such tumor antigens are therefore prime targets for the immune system and can serve as a locus of immune activation against (pre)malignant cells.

This immune activation against the tumor starts with capture of tumor antigens by antigen presenting cells (APCs). After uptake of antigens, APCs migrate to draining lymph nodes and process antigens for presentation. Antigens are then presented in the form of small peptides in the context of major histocompatibility complex (MHC) molecules to T cells. When T cells encounter such a MHC-peptide complex, T cells recognize this complex via the T cell receptor. Upon specific recognition via the T cell receptor T cells become activated and undergo proliferation. The antigen-experienced, activated T cells can now exit the lymph node, enter the circulation and migrate towards the tumor bed. The T cell receptor on these T cells subsequently recognizes the specific MHC-peptide complex on tumor cells. After recognition, the T cell secretes perforins and granzymes to form pores in the membrane of the tumor cell and triggers lysis and/or apoptosis.[1]

The interaction between the immune system and (pre)malignant cells, also referred to as cancer immunoediting, is a dynamic process which can be divided in three phases.[2] The first phase, also called the elimination phase, involves the immune system recognizing and successfully eradicating (pre)malignant cells. This recognition and eradication of (pre)malignant cells by the immune system is also called immune surveillance. If eradication of the cancer is incomplete, an equilibrium phase -the second phase- is established. Herein, the immune system is only able

to exert limited control over malignant cells in which cancer cell growth is restricted by the immune cells, but the cancer is not eliminated. The final 'escape' phase involves tumor cells completely evading the immune system allowing unrestricted growth and metastasis.[3,4] At clinical presentation most cancers have already reached this point.[5] Nevertheless, as discussed in this thesis, therapeutic intervention by immunotherapy or even standard treatment can reverse this cancer-induced immune suppression and result in remarkable clinical benefit.

IMMUNOTHERAPY

Immunotherapy aims to eradicate cancer by inducing or augmenting anti-tumor immunity. To date, several immunotherapeutic modalities have been approved by the Food and Drug Administration (FDA) and many more are under clinical investigation (>1400 ongoing clinical trials). For the purpose of brevity, the immunotherapeutic modalities that will be discussed within this thesis are immune checkpoint blockade, therapeutic vaccination, and adoptive cellular transfer.

Immune checkpoint blockade (ICB) targets molecules involved in the activation/inhibition pathways of T cells (e.g. cytotoxic T-lymphocyte–associated antigen 4 [CTLA-4] and programmed cell death-1 [PD-1]). ICB leads to durable clinical responses, but only in a fraction of patients. There are ongoing studies to identify predictive biomarkers for the selection of patients for ICB treatment.[6] Major predictive markers for response to ICB include high levels of infiltrating T cells, high neo-antigenic load, high tumor mutational load (e.g. microsatellite instability), and PD-L1 expression.[7–10] On the contrary, failure to respond to ICB is thought to result from insufficient spontaneous tumor-specific T cell responses. A logical combination approach is therefore to increase the amount of tumor-specific T cells within the tumor. This can be achieved in multiple ways; actively by therapeutic vaccination or passively by adoptive cellular transfer.

Therapeutic vaccination aims to stimulate the immune system against tumor peptides. The main advantage of active therapeutic vaccination is the potential to initiate durable effects by the induction of immunological memory. Adoptive cellular transfer consists of the transfusion of *ex-vivo* stimulated or generated T cells, directed against a specific antigen. Initially, adoptive cellular transfer led to transient increases in tumor-specific T cells, for which multiple infusions were needed to initiate a long-lasting response. Currently, new T cell engineering techniques (e.g. second and third generation chimeric antigen receptor T cells [CAR T cells]) for adoptive cellular transfer are being developed and under clinical investigation and are also able to induce long-lasting immune responses.[11,12]

Most of these modalities have proven effective across cancer types, with mainly differences in the type of antigen targeted for effective therapy. Although many of the lessons learned from the studies described in this thesis can also be applied in a pan-cancer manner, the focus will remain on immunity in gynecological malignancies, and the possibilities for immunotherapy in these diseases.

IMMUNITY IN GYNECOLOGICAL MALIGNANCIES

Gynecological malignancies account for approximately 16% of the cancer cases among women worldwide (GLOBOCAN 2012) and include ovarian, uterine, cervical, vaginal, and vulvar cancers.[13] Although the initial primary treatment for most gynecological malignancies is effective, cancer recurrences frequently occur, and are often therapy resistant. As gynecological cancer burden and mortality remain high, new therapeutic strategies urgently need to be explored. In this thesis, we focus on the 3 most prevalent gynecological malignancies; cervical, endometrial and ovarian cancer.

Cervical cancer

Of all gynecological malignancies, cervical cancer is the most prevalent, and the fourth most common cancer among women, with an estimated 528,000 new cases worldwide. Further, approximately 266,000 women die from cervical cancer each year, accounting for 7.5% of all female cancer deaths. A large majority of the global cervical cancer burden occurs in the less developed regions, where it accounts for almost 12% of all female cancers. In addition, almost 9/10 cervical cancer deaths occur in the less developed regions. This large geographic variation in cervical cancer rates reflects differences in the availability of screening, and human papillomavirus (HPV) infection prevalence. Screening in particular allows for effective treatment by early detection and removal of precancerous lesions. Indeed, in countries where screening programs have been established, cervical cancer rates have decreased by as much as 65% over the past 40 years.[14–17] In addition, prognosis for patients treated in an early stage of this disease is good.

Persistent infection with HPV has been established as the causative agent for cervical cancer. Upon infection, HPV integrates into the genome of the host cells. This integration leads to the production and overexpression of the early viral proteins E6 and E7. The viral proteins E6 and E7 block the function of important tumor suppressor pathways, Rb and P53 respectively, leading to malignant transformation of the host cells. Persistent expression of the viral proteins E6 and E7 is needed to maintain the transformed phenotype. Therefore, the viral proteins E6 and E7 represent ideal tumor-specific antigens for the immune system in HPV-associated cancer.[18–20]

Endometrial cancer

The second most common gynecological malignancy is endometrial cancer. Worldwide, endometrial cancer is the sixth most common cancer in women, with an estimated 320,000 new cases and 50,000 deaths. In contrast to cervical cancer, the majority of endometrial cancer cases occur in developed countries where it accounts for 6% of all cancers in women, whereas in developing countries, endometrial cancer accounts for only 2% of cancers in women. The increased incidence and prevalence of endometrial cancer in developed countries can be explained by the increase in life expectancy, increased obesity rates, and reproductive factors such as younger age at menarche and late age at menopause, null parity, age of the first child, and long-term use of unopposed estrogens for hormone replacement therapy.[21] As endometrial cancer often presents at an early stage of disease and with clear symptoms, prognosis is fairly good.

In endometrial cancer, 17% of endometrial tumors are microsatellite unstable (MSI), which is caused by defects in the DNA- mismatch repair (dMMR) mechanisms. MSI/dMMR-deficient tumors have a high mutational load leading to the formation of neo-antigens expressed by the tumor cells. Neo-antigens can be recognized by the immune system as non-self and form a locus of immune attraction against the cancer cells. Therefore, MSI/dMMR-deficient tumors are characterized by high levels of infiltrated immune cells (e.g. CD8-positive cytotoxic T lymphocytes). For these neo-antigen rich tumors, treatment with ICB has proven to be highly effective in initial trials.[22,23] As such, the FDA has approved ICB for the treatment of this subset of endometrial cancer patients.[24]

Ovarian cancer

The third most common gynecological cancer in woman is ovarian cancer. While not the most prevalent gynecological cancer, ovarian cancer is the most lethal gynecological malignancy. Indeed, ovarian cancer is only the seventh most common cancer among women worldwide, with an estimated 239,000 new cases, but results in 152,000 deaths annually. The poor prognosis of the disease is largely due to diagnosis at advanced stage and therapy-resistant disease relapses. In contrast to cervical and endometrial cancer, there are neither sufficient screening methods nor early symptoms of disease that could lead to early detection of ovarian cancer.[25–27] Ovarian cancer can be divided into different histological subtypes of which epithelial ovarian cancer is the most common subtype (95%). Epithelial ovarian cancers derive from malignant transformation of the epithelium of the ovarian or fallopian tube surface. The remaining ovarian cancers arise from other ovarian cell types such as germ cell tumors, sex cord stromal tumors and mixed cell types.[28] Serous ovarian cancer is the most common subtype of epithelial ovarian

cancers (75%), whereas mucinous, endometrioid, clear cell, transitional cell, and undifferentiated tumors are less common.[29] The studies described within this thesis mainly focus on high-grade serous ovarian cancer (HGSC), as this is the most common and aggressive subtype.

HGSCs are characterized by TP53 mutations (~95%) and chromosomal instability leading to frequent DNA losses or gains.[30] Despite this chromosomal instability, mutational load and neo-antigen load in HGSC are relatively low. With the exception of TP53 mutations, other somatic mutations in oncogenes are relatively uncommon with the exception of BRCA1 and BRCA2 mutations. Approximately 13% of HGSCs are attributable to germline mutations in BRCA1/2. Additionally, 50% of HGSCs are defective in the homologous recombination (HR) DNA repair pathway. These HR-defects arise mostly from somatic and epigenetic mutations in BRCA1/2, but also other genes in the BRCA pathway can be involved. Interestingly, patients with a germline BRCA1/2 mutation have an improved survival and these tumors have higher levels of infiltrating T cells.[30] Nevertheless, in clinical trials only a subset of HGSC patients (~10%) responded to ICB.[31] To improve the response rate of ovarian cancer patients to ICB, T cell infiltration likely needs to be increased, e.g. by therapeutic vaccination against tumor-associated antigens as reviewed by *Leffers et al*.[32] or by adoptive cellular transfer.

Taken together, although the above described malignancies are different in origin and interaction with the immune system, their immunity eventually depends on recognition of antigens and subsequent infiltration of tumor-reactive T cells (e.g, CD8-positive cytotoxic T lymphocytes).

OUTLINE OF THE THESIS

As CD8-positive TIL appear crucial across malignancies, we first defined the CD8-positive immune infiltrate and it's prognostic value in gynecological malignancies; in high-grade serous ovarian cancer in **chapter 2**; endometrial cancer in **chapter 3**; and cervical cancer in **chapter 4**. We observed a strong prognostic benefit for patients with TIL that localize within the epithelial cancer islets of gynecological tumors, but not from TIL localized within the connective tissue of tumor, the stroma. We identified a distinguishing cell surface marker, CD103, for these cancer cell-associated epithelial TIL that performed consistently across gynecological malignancies (**chapters 2, 3 and 4**). In addition, in **chapters 5 and 6** we identified that less differentiated "younger" TIL in the cancer cell epithelium were of greater prognostic benefit to patients than "older" more differentiated TIL, and could even compensate in part for incomplete surgical removal of the tumor in high-grade serous ovarian cancer. Interestingly, while we did not observe immune modulating effects of chemotherapy on the tumor microenvironment, in **chapter 7** we identified a pronounced depletion of circulating myeloid cells during treatment with carboplatin and paclitaxel in epithelial ovarian cancer patients. Finally, in **chapter 4** we demonstrate that, a Semliki forest virus-based vaccine (Vvax001) targeting the cervical cancer oncogenes E6 and E7 was highly effective at inducing the prognostically beneficial intraepithelial CD103-positive TIL in cervical cancer *in vivo* associated with significant tumor reduction. Currently, we are therefore evaluating Vvax001 in a first-in-human phase I clinical study, as described in **chapter 8**.

REFERENCES

1. Mellman I, Coukos G, Dranoff G. Cancer immunotherapy comes of age. Nature [Internet] 2011 [cited 2014 Jul 9]; 480:480–9.
2. BURNET M. Cancer; a biological approach. I. The processes of control. Br Med J [Internet] 1957 [cited 2017 Oct 25]; 1:779–86.
3. Mittal D, Gubin MM, Schreiber RD, Smyth MJ. New insights into cancer immunoediting and its three component phases--elimination, equilibrium and escape. Curr Opin Immunol [Internet] 2014 [cited 2017 Aug 8]; 27:16–25.
4. Schreiber RD, Old LJ, Smyth MJ. Cancer immunoediting: integrating immunity's roles in cancer suppression and promotion. Science [Internet] 2011 [cited 2017 Aug 8]; 331:1565–70.
5. Hanahan D, Weinberg RA. Hallmarks of cancer: The next generation. Cell2011; 144:646–74.
6. Sharma P, Allison JP. The future of immune checkpoint therapy. Science (80-) [Internet] 2015 [cited 2017 Aug 17]; 348. l
7. Rizvi NA, Hellmann MD, Snyder A, Kvistborg P, Makarov V, Havel JJ, Lee W, Yuan J, Wong P, Ho TS, et al. Cancer immunology. Mutational landscape determines sensitivity to PD-1 blockade in non-small cell lung cancer. Science [Internet] 2015 [cited 2017 Aug 23]; 348:124–8.
8. Chen P-L, Roh W, Reuben A, Cooper ZA, Spencer CN, Prieto PA, Miller JP, Bassett RL, Gopalakrishnan V, Wani K, et al. Analysis of Immune Signatures in Longitudinal Tumor Samples Yields Insight into Biomarkers of Response and Mechanisms of Resistance to Immune Checkpoint Blockade. Cancer Discov [Internet] 2016 [cited 2017 Aug 23]; 6:827–37.
9. Snyder A, Makarov V, Merghoub T, Yuan J, Zaretsky JM, Desrichard A, Walsh LA, Postow MA, Wong P, Ho TS, et al. Genetic basis for clinical response to CTLA-4 blockade in melanoma. N Engl J Med [Internet] 2014 [cited 2017 Aug 23]; 371:2189–99.
10. Khagi Y, Kurzrock R, Patel SP. Next generation predictive biomarkers for immune checkpoint inhibition. Cancer Metastasis Rev [Internet] 2017 [cited 2017 Aug 17]; 36:179–90.
11. Barrett DM, Singh N, Porter DL, Grupp SA, June CH. Chimeric Antigen Receptor Therapy for Cancer. Annu Rev Med [Internet] 2014 [cited 2017 Oct 18]; 65:333–47.
12. Maude SL, Frey N, Shaw PA, Aplenc R, Barrett DM, Bunin NJ, Chew A, Gonzalez VE, Zheng Z, Lacey SF, et al. Chimeric Antigen Receptor T Cells for Sustained Remissions in Leukemia. N Engl J Med [Internet] 2014 [cited 2017 Oct 18]; 371:1507–17.
13. Torre LA, Bray F, Siegel RL, Ferlay J, Lortet-Tieulent J, Jemal A. Global cancer statistics, 2012. CA Cancer J Clin [Internet] 2015 [cited 2017 Jul 28]; 65:87–108.
14. Bray F, Lortet-Tieulent J, Znaor A, Brotons M, Poljak M, Arbyn M. Patterns and Trends in Human Papillomavirus-Related Diseases in Central and Eastern Europe and Central Asia. Vaccine [Internet] 2013 [cited 2017 Aug 8]; 31:H32–45.
15. Bruni L, Diaz M, Castellsagué X, Ferrer E, Bosch FX, de Sanjosé S. Cervical Human Papillomavirus Prevalence in 5 Continents: Meta-Analysis of 1 Million Women with Normal Cytological Findings. J Infect Dis [Internet] 2010 [cited 2017 Aug 8]; 202:1789–99.
16. Vaccarella S, Lortet-Tieulent J, Plummer M, Franceschi S, Bray F. Worldwide trends in cervical cancer incidence: Impact of screening against changes in disease risk factors. Eur J Cancer [Internet] 2013 [cited 2017 Aug 8]; 49:3262–73.
17. Forman D, de Martel C, Lacey CJ, Soerjomataram I, Lortet-Tieulent J, Bruni L, Vignat J, Ferlay J, Bray F, Plummer M, et al. Global Burden of Human Papillomavirus and Related Diseases. Vaccine [Internet] 2012 [cited 2017 Aug 8]; 30:F12–23.
18. Howley PM. Role of the human papillomaviruses in human cancer. Cancer Res [Internet] 1991 [cited 2016 Jan 11]; 51:5019s–5022s.
19. Nasseri M, Gage JR, Lorincz A, Wettstein FO. Human papillomavirus type 16 immortalized cervical keratinocytes contain transcripts encoding E6, E7, and E2 initiated at the P97 promoter and express high levels of E7. Virology [Internet] 1991 [cited 2016 Jan 11]; 184:131–40.

20. zur Hausen H. Papillomaviruses and cancer: from basic studies to clinical application. Nat Rev Cancer [Internet] 2002 [cited 2014 Jul 17]; 2:342–50.

21. Ali AT. Reproductive Factors and the Risk of Endometrial Cancer. Int J Gynecol Cancer [Internet] 2014 [cited 2017 Aug 17]; 24:384–93.

22. Le DT, Durham JN, Smith KN, Wang H, Bartlett BR, Aulakh LK, Lu S, Kemberling H, Wilt C, Luber BS, et al. Mismatch repair deficiency predicts response of solid tumors to PD-1 blockade. Science [Internet] 2017 [cited 2017 Oct 23]; 357:409–13.

23. Ott PA, Bang Y-J, Berton-Rigaud D, Elez E, Pishvaian MJ, Rugo HS, Puzanov I, Mehnert JM, Aung KL, Lopez J, et al. Safety and Antitumor Activity of Pembrolizumab in Advanced Programmed Death Ligand 1-Positive Endometrial Cancer: Results From the KEYNOTE-028 Study. J Clin Oncol [Internet] 2017 [cited 2017 Oct 18]; 35:2535–41.

24. FDA. Approved Drugs - FDA grants accelerated approval to pembrolizumab for first tissue/site agnostic indication [Internet]. [cited 2017 Oct 18];

25. Coleman M, Forman D, Bryant H, Butler J, Rachet B, Maringe C, Nur U, Tracey E, Coory M, Hatcher J, et al. Cancer survival in Australia, Canada, Denmark, Norway, Sweden, and the UK, 1995–2007 (the International Cancer Benchmarking Partnership): an analysis of population-based cancer registry data. Lancet [Internet] 2011 [cited 2017 Aug 8]; 377:127–38.

26. Vaughan S, Coward JI, Bast RC, Berchuck A, Berek JS, Brenton JD, Coukos G, Crum CC, Drapkin R, Etemadmoghadam D, et al. Rethinking ovarian cancer: recommendations for improving outcomes. Nat Publ Gr [Internet] 2011 [cited 2017 Aug 8]; 11.

27. Allemani C, Weir HK, Carreira H, Harewood R, Spika D, Wang X-S, Bannon F, Ahn J V, Johnson CJ, Bonaventure A, et al. Global surveillance of cancer survival 1995–2009: analysis of individual data for 25 676 887 patients from 279 population-based registries in 67 countries (CONCORD-2). Lancet [Internet] 2015; 385:977–1010.

28. Cannistra SA. Cancer of the ovary. N Engl J Med [Internet] 2004 [cited 2016 Feb 24]; 351:2519–29.

29. Berek JS, Crum C, Friedlander M. Cancer of the ovary, fallopian tube, and peritoneum. Int J Gynecol Obstet [Internet] 2015 [cited 2017 Aug 17]; 131:S111–22.

30. Cancer Genome Atlas Research Network TCGAR. Integrated genomic analyses of ovarian carcinoma. Nature [Internet] 2011 [cited 2017 Oct 4]; 474:609–15.

31. Ventriglia J, Paciolla I, Pisano C, Cecere SC, Di Napoli M, Tambaro R, Califano D, Losito S, Scognamiglio G, Setola SV, et al. Immunotherapy in ovarian, endometrial and cervical cancer: State of the art and future perspectives. Cancer Treat Rev [Internet] 2017 [cited 2017 Aug 15]; 59:109–16.

32. Leffers N, Daemen T, Helfrich W, Boezen HM, Cohlen BJ, Melief CJM, Nijman HW. Antigen-specific active immunotherapy for ovarian cancer. Cochrane database Syst Rev [Internet] 2014 [cited 2015 Aug 3]; 9:CD007287.

CD103+ intraepithelial T cells in high-grade serous ovarian cancer are phenotypically diverse TCRαβ+ CD8αβ+ T cells that can be targeted for cancer immunotherapy

FL Komdeur*, MCA Wouters*, HH Workel, AM Tijans, ALJ Terwindt, KL Brunekreeft, A Plat, HG Klip, FA Eggink, N Leffers, W. Helfrich, D.F. Samplonius, E. Bremer, GBA Wisman, T Daemen, EW Duiker, H Hollema, HW Nijman, M de Bruyn

*Authors contributed equally

Oncotarget. 2016 Nov 15;7(46):75130-75144

ABSTRACT

CD103+ tumor-infiltrating lymphocytes (TIL) have been linked to specific epithelial infiltration and a prolonged survival in high-grade serous epithelial ovarian cancer (HGSC). However, whether these cells are induced as part of an ongoing anti-HGSC immune response or represent non-specifically expanded resident or mucosal lymphocytes remains largely unknown. In this study, we first confirmed that CD103+ TIL from HGSC were predominantly localized in the cancer epithelium and were strongly correlated with an improved prognosis. We further demonstrate that CD103+ TIL were almost exclusively CD3+ TCRαβ+ CD8αβ+ CD4- T cells, but heterogeneously expressed T cell memory and differentiation markers. Activation of peripheral T cells in the presence of HGSC was sufficient to trigger induction of CD103 in over 90% of all CD8+ cells in a T cell receptor (TCR)- and TGFβR1-dependent manner. Finally, CD103+ TIL isolated from primary HGSC showed signs of recent activation and dominantly co-expressed key immunotherapeutic targets PD-1 and CD27. Taken together, our data indicate CD103+ TIL in HGSC are formed as the result of an adaptive anti-tumor immune response that might be reactivated by (dual) checkpoint inhibition.

INTRODUCTION

High-grade serous epithelial ovarian cancer (HGSC) is the most common cause of death from gynecological malignancies and is the fifth leading cause of female cancer death worldwide.[1] Despite successful initial treatment, 5-year survival is only 35% as almost all patients with advanced disease relapse. This poor prognosis has not improved in four decades and novel therapies for HGSC are urgently needed.[2] Herein, therapeutic exploitation of the immune system may be of value.

The immune system plays an important role in the development and control of HGSC, and the presence of tumor-infiltrating lymphocytes (TIL) in HGSC is associated with prolonged survival.[3–5] Indeed, infiltration of T cells, and particularly CD8+ cytotoxic T cells (CTL) is associated with an improved prognosis for HGSC patients.[4–6] Reactivating CTL is therefore an active area of investigation for therapy of HGSC. One issue that needs to be considered herein is the distribution of the CTL within the tumor. Whereas CTL localized in the tumor epithelium are associated with prolonged survival in HGSC patients, stromal CTL are not.[6] Therefore, developing immunotherapeutic strategies tailored to the specific biology of prognostically favorable intraepithelial CTL, whilst not activating potentially inflammatory stromal immune cells appears warranted.

The epithelial and stromal CTL populations in HGSC can be delineated by expression of the α_E integrin subunit CD103. In line with this, the total number of CD103+ TIL (irrespective of localization) was shown to be associated with improved prognosis.[7] By contrast, the total number of CD8+ TIL did not associate with an improved prognosis.[7] CD103+ TIL therefore represent an interesting population for therapeutic targeting. However, there are several remaining questions regarding CD103+ TIL that need to be addressed before these cells can be considered as key players in natural HGSC-directed immunological reactions.

For instance, CD103 is the prototypical marker for intraepithelial lymphocytes (IEL) and tissue-resident memory T cells (T_{RM}), and has been linked to persistence of T cells involved in immune surveillance after pathogenic infection of (barrier) tissue. Indeed, CD103 was reported to be expressed on influenza-specific CD8+ T cells in the human lung, Epstein-Barr virus (EBV)-specific cells in human tonsil, and on vesicular stomatitis virus (VSV)-specific CD8+ T cells in a mouse model system of VSV infection of the brain.[8–10] Since ovarian/tubal tissue constitutes a de facto barrier, CD103+ T cells in HGSC might simply represent "native" (not tumor-specific) IEL or T_{RM} cells expanded due to the inflammatory reaction within the tumor. Such cells would have limited potential for therapeutic targeting in HGSC and would represent a poor biomarker for selection

of patients for immunotherapy. By contrast, if CD103+ TIL in HGSC represent adaptive immune cells that are formed as part of an ongoing specific anti-cancer response in HGSC, these cells could be harnessed for adoptive cell therapy or targeted by e.g. immune checkpoint inhibitors.

To address these questions, we determined the ontogeny of CD103+ TIL in HGSC and explored whether these cells represent a promising target population for HGSC immunotherapy.

RESULTS

CD103 identifies intraepithelial CD8+ TIL with prognostic benefit in HGSC

First, we confirmed the recent reports on the prognostic benefit of CD103+ TIL in HGSC[7,11] in an independent cohort of advanced-stage HGSC patients treated with either primary surgery and adjuvant chemotherapy (PS; n=84), or neo-adjuvant chemotherapy followed by interval surgery (NACT; n=102).[12] CD3+, CD8+ and CD103+ TIL were present in tumors from most patients and the distribution of CD3+ and CD8+ TIL in tumor epithelium and stroma was similar (Fig. 1A). By contrast, CD103+ TIL were mainly found in the tumor epithelium (Fig. 1A). Total CD103+ TIL numbers did not differ significantly between patients that received PS or NACT therapy (not shown), as reported previously for epithelial CD8+ TIL in this cohort.[12] In line with the observed epithelial distribution, total CD103+ TIL counts per mm^2 in these patients correlated strongly to intraepithelial CD3+ and CD8+ TIL ($r=0.86$; $p<0.0001$ and $r=0.87$; $p<0.0001$, respectively), but weaker to stromal CD3+ and CD8+ TIL ($r=0.14$; $p=0.0008$ and $r=0.59$; $p<0.0001$, respectively) (Fig. 1B and 1C). Moreover, the relative distribution of epithelial CD3+ or CD8+ and total CD103+ TIL counts were similar (Fig. 1D). High total numbers of CD103+, but not total CD8+ TIL, were associated with a longer disease-specific survival (DSS) in patients treated with PS ($p=0.012$ and $p<0.809$, respectively) (Fig. 1E and 1F). As previously reported for epithelial CD8+ TIL[12], total CD103+ TIL did not confer prognostic benefit in patients treated with NACT ($p=0.583$) (Fig. 1G and supplementary Fig. S1). Taken together, our data confirm the restricted distribution of CD103+ TIL in the HGSC epithelium and suggest a CD3+ CD8+ phenotype for these cells.

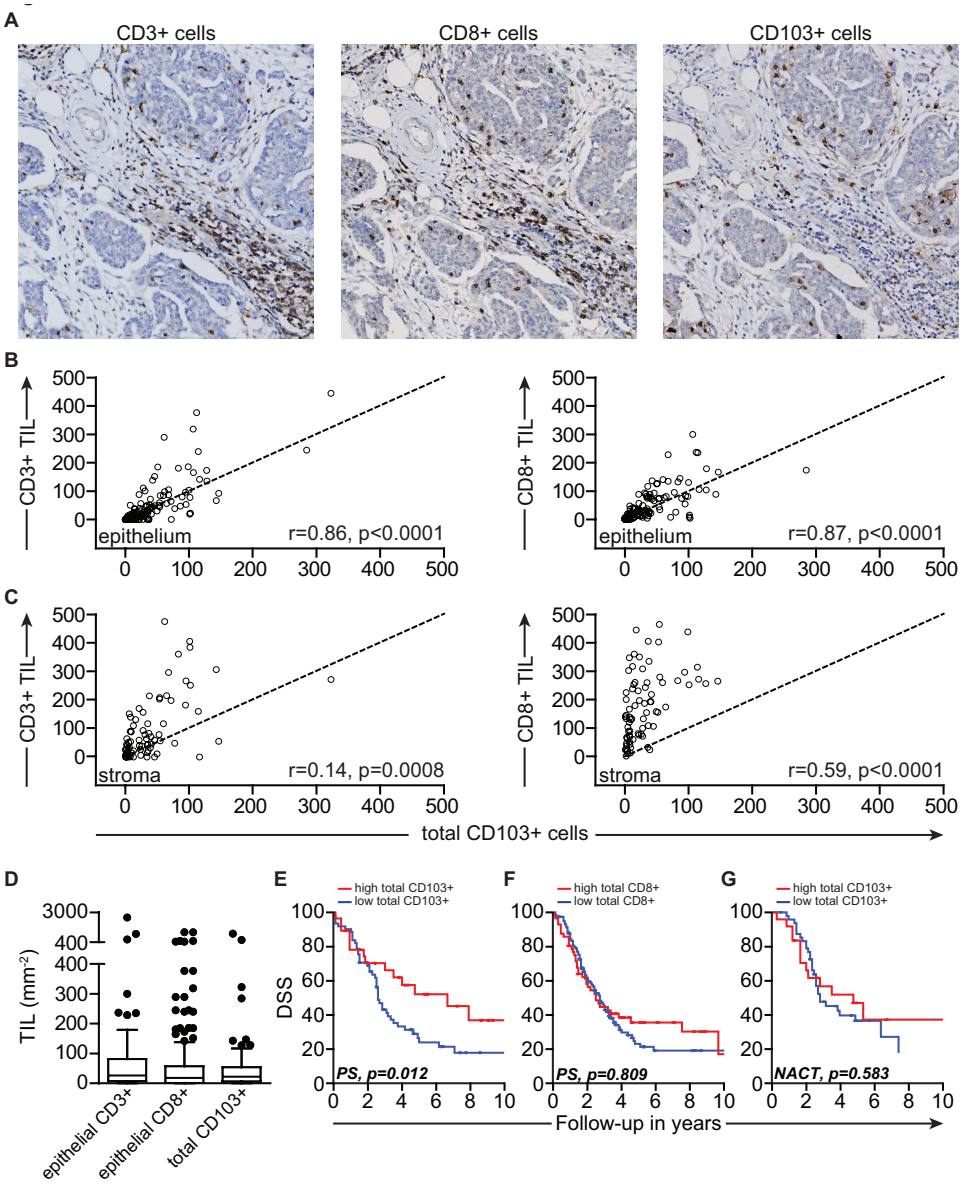

FIGURE 1. CD103 defines intraepithelial CD8+ TIL with prognostic benefit in HGSC patients. A) Representative images of HGSC tissue cores with infiltration of CD3+, CD8+ or CD103+ cells. **B)** Correlation of total CD103+ cells per tumor core versus epithelial CD3+ cells or epithelial CD8+ cells. Line insert represents a hypothetical perfect correlation on the x-and y-axis. **C)** Correlation of total CD103+ cells versus stromal CD3+ cells or stromal CD8+ cells. Line insert represents a hypothetical perfect correlation on the x-and y-axis. Spearman's rank correlation coefficient was used to determine correlation between epithelial and stromal CD3+ and CD8+ TIL and total CD103+ TIL. **D)** Box-plots of epithelial CD3+, epithelial CD8+ and total CD103+ cell counts per 1 mm² HGSC tissue. **E)** DSS (determined by Kaplan-Meier method with Log Rank test) of patients within the PS cohort according to infiltration of total CD103+ cells. **F)** DSS of patients within the PS cohort according to infiltration of total CD8+ cells. **G)** DSS of patients within the NACT cohort according to infiltration of total CD103+ cells.

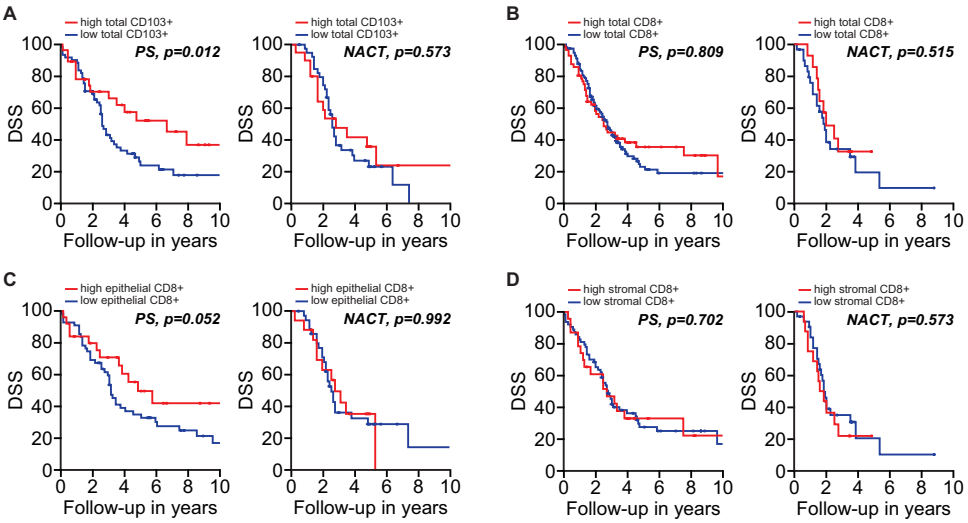

SUPPLEMENTARY FIGURE S1. CD103+ TIL are associated with improved prognosis in patients with high-grade serous epithelial ovarian cancer (HGSC). A) Disease-specific survival (DSS) (determined by Kaplan-Meier method with Log Rank test) of patients within the primary cytoreductive surgery (PS) and neo-adjuvant chemotherapy (NACT) cohort according to infiltration of total CD103+ cells. **B)** DSS of patients within the PS and NACT cohort according to infiltration of total CD8+ cells. **C)** DSS of patients within the PS and NACT cohort according to infiltration of epithelial CD8+ cells. **D)** DSS of patients within the PS and NACT cohort according to infiltration of stromal CD8+ cells.

CD103+ TIL in HGSC are almost exclusively classical CD3+ CD56- TCRαβ+ CD8αβ+ CD4- T cells with heterogeneous differentiation status

The marker CD103 has been shown to define IEL in mucosal tissues, T_{RM} cells in non-lymphoid tissues, T_{RM} cells in lung cancer tissue, but also characterizes T cell clones that have been in recent contact with cognate epithelial tumor cell lines.[13-19] Therefore, to address whether CD103+ TIL in HGSC represent expanded IEL, T_{RM}, or classical adaptive T cells that have migrated to HGSC tissue as a result of an ongoing immune response, we performed in-depth phenotyping on TIL isolated from primary HGSC tumors. As tissue dissociation and digestion may skew distribution of cell subsets and can even cause loss of cell surface antigens, we first studied CD103+ TIL infiltration in a side-by-side comparison of tissue and digests using 6 matched patient samples. Immunohistochemistry for detection of CD3, CD8 and CD103 was performed on full slides and complemented with flow cytometric analysis of the corresponding tumor digest. In all cases, CD103+ CD8+ cells were only observed in tumor digests when CD8+ and CD103+ cells could be detected in the tumor epithelium by immunohistochemistry (data not shown).

Marginal numbers of tumor-infiltrating NK-cells were observed by phenotyping the immune cell subpopulations in the tumor digests (n=10, Fig. 2A), a finding in line with our previous reports. Furthermore, NK-cells expressed CD103 in only 1/10 analyzed digests at percentages >1% (Fig.

2A). 10/10 patients had a detectable CD3+ CD103+ T cell infiltrate, although the majority of CD3+ TIL in the digests did not express CD103 (Fig. 2B) (distribution of subsets per patient in Supplementary Fig.2). Importantly, CD103+ and CD103- TIL predominantly expressed the αβ chains of the T cell receptor (TCR) in conjunction with CD3 (Fig. 2C). Moreover, no CD56 expression on these cells was detected (data not shown), excluding both γδ- and NKT cells as dominant CD103-expressing T cells in HGSC.

Within the total CD3+ TCRαβ+ T cell population, both CD8+ and CD4+ cells were detected at roughly a 1:1 ratio (Fig. 2D). By contrast, CD3+ TCRαβ+ CD103+ T cells were almost exclusively CD8+, with only marginal numbers of CD4+ cells detected (Fig. 2D, $p<0.0001$). Notably, all cells expressing the CD8α chain also expressed the CD8β chain, and no cells were found to co-express CD4. As IEL are characterized by co-expression of CD4 and CD8α (but not CD8β), this suggests that CD103+ T cells in HGSC are not of an IEL origin. Interestingly, a subset of ~20-30% of all CD3+ TCRαβ+ CD8αβ+ cells expressed both CD8α and β chains at a lower level of roughly 50% of the mean fluorescent intensity, irrespective of CD103 expression (Fig. 2E). The lower expression of CD8β has previously been reported in association with effector differentiation of T cells and suggests both CD103+ and CD103- T cells undergo similar differentiation in the HGSC microenvironment.

Finally, to address the resident memory status of the CD103+ TIL population, we analyzed expression of memory markers CD45RO, CCR7, CD27 and CD28 in conjunction with CD3, CD8 and CD103 expression in two additional HGSC digests (flow cytometric plots and gating strategy in Supplementary Fig. S3). In line with our recent report on the differential expression of CD27 and CCR7/CD45RO in HGSC, TIL in these HGSC digests could be readily typed to various populations such as central memory (T_{CM}), effector memory 1-4 ($T_{EM}1$-4) and terminally differentiated (T_{TD}) subtypes (Fig. 2F and 2G). Nevertheless, T_{CM}, T_{EM} and T_{TD} subtypes were observed in both CD103+ and CD103- CD8+ T cell populations and variation between CD103+ and CD103- cells was similar to variation between the two HGSC patient samples (Fig. 2F and 2G). These data support a heterogeneous differentiation status of CD103+ TIL, not directly in line with a T_{RM} phenotype.

Our data therefore suggest CD103+ TIL in HGSC represent T cells of a classical CD3+ CD56- TCRαβ+ CD8αβ+ CD4- phenotype of varying differentiation. This phenotype is consistent with cells that have infiltrated as a result of an adaptive immune response.

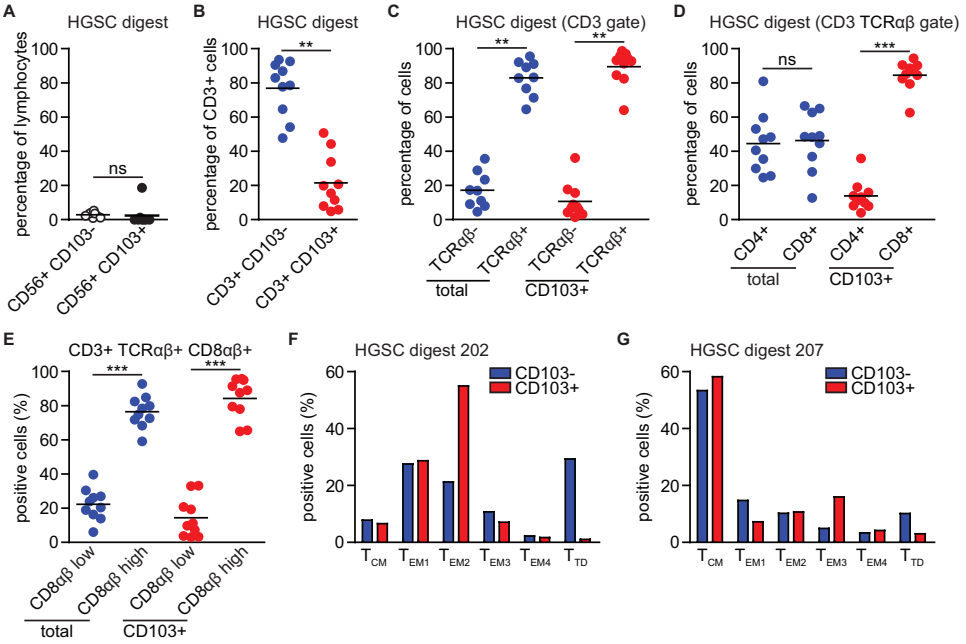

FIGURE 2. CD103+ TIL are almost exclusively classical CD3+ CD56- TCRαβ+ CD8αβ+ CD4- T cells with heterogeneous differentiation status. HGSC tumor tissue was subjected to enzymatic digestion and analyzed by flow cytometry. **A)** Dot plot representing the percentage of CD56+ CD103- cells and CD56+ CD103+ cells within the total lymphocyte population isolated from HGSC tumor digests (N=10). **B)** Percentage of CD103- cells and CD103+ cells within the CD3+ cell population. **C)** Percentage of TCRαβ- and TCRαβ+ cells within the total CD3+ population or within the CD3+ CD103+ subpopulation. **D)** Percentage of CD4+ and CD8+ cells within the total CD3+ TCRαβ+ population or within the CD3+ TCRαβ+ CD103+ subpopulation. **E)** Percentage of $CD8\alpha\beta_{low}$ and $CD8\alpha\beta_{high}$ cells within the total CD3+ TCRαβ+ CD8αβ+ population or within the CD3+ TCRαβ+ CD8αβ+ CD103+ subpopulation. **F)** Bar graph of phenotypical subtype for CD103+ cells and CD103- cells derived from HGSC tumor digest #202. **G)** Bar graph of phenotypical subtype for CD103+ cells and CD103- cells derived from HGSC tumor digest #207. T_{CM}: central memory T cell. T_{EM}: effector memory T cell. T_{TD}: terminally differentiated T cell. Differences were assessed by Mann-Whitney U or one-way ANOVA tests.

Activation in the presence of HGSC cells induces CD103 on peripheral blood CD8+ T cells through combined TCR- and TGFβR1-signaling

The non-IEL, non-T_{RM} phenotype of CD103+ TIL in HGSC prompted us to speculate that induction of CD103 occurs as a natural consequence of peripheral blood T cell activation after infiltrating the HGSC epithelium. To assess this, we co-cultured peripheral blood mononuclear cells (PBMC) with HGSC cell lines and determined expression of CD103 in the presence or absence of a CD3 agonistic antibody (n≥3 donors). As exemplified in Figure 3A, activation of T cells in the presence of HGSC cell line PEA-1 induced expression of CD103 on a subset of ~25% of PBMC. Similar percentages were observed in the presence of a panel of HGSC cell lines, but not when T cells were activated alone (Fig. 3A and 3B; n≥3 donors). In line with the *ex vivo* phenotyping data, co-culture of PBMC with OVCAR-3 cells predominantly induced CD103 on T cells of a CD8αβ+ phenotype, with much lower percentages observed in CD4+ cells (Fig. 3C and 3E). A small

subset of CD56- CD8- CD4- lymphocytes also upregulated CD103 in response to stimulation with anti-CD3 agonistic antibody in this setting (Fig. 3D and 3F), although the exact identity of these cells remains unclear. Of note, T cell proliferation did not correlate directly with the induction of CD103 on T cells (Compare Supplementary Fig. S4A with Fig. 3B), and both CD103+ and CD103- CD8+ cells underwent proliferation in co-culture with HGSC (exemplified for PEA-1 in Supplementary Fig. S4B).

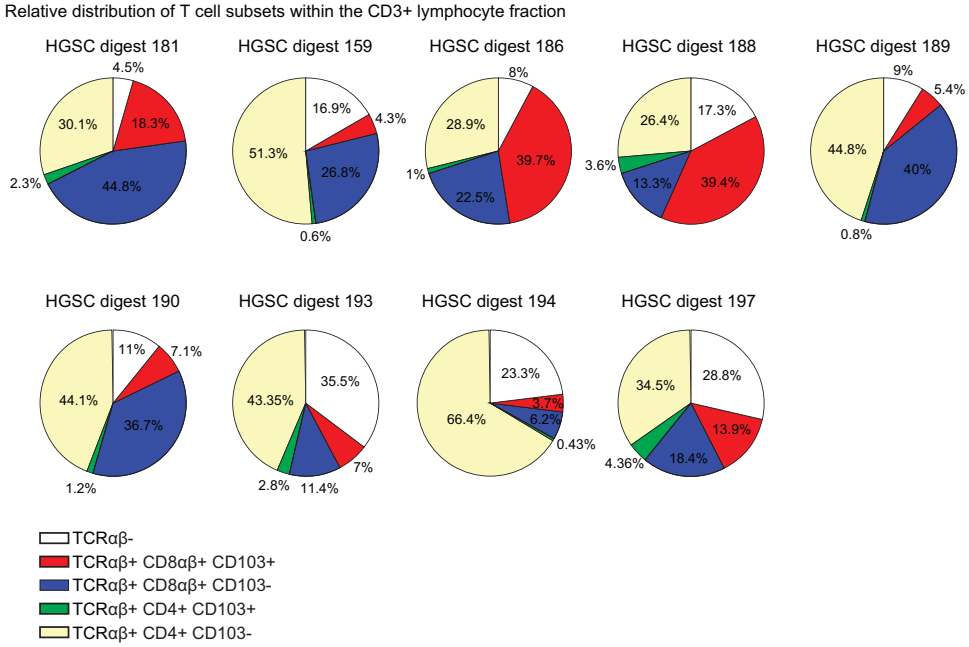

SUPPLEMENTARY FIGURE S2. Relative distribution of T cell subsets of each individual patient from Figure 2. HGSC tumor tissue was subjected to enzymatic digestion and analyzed by flow cytometry. Digests were stained using Zombie Aqua live/dead stain and antibodies against CD3, CD56, TCRαβ, CD8α, CD8β, CD4 and CD103. Distribution of T cell subsets within the CD3+ lymphocyte fraction was determined and plotted as a pie chart for each individual patient.

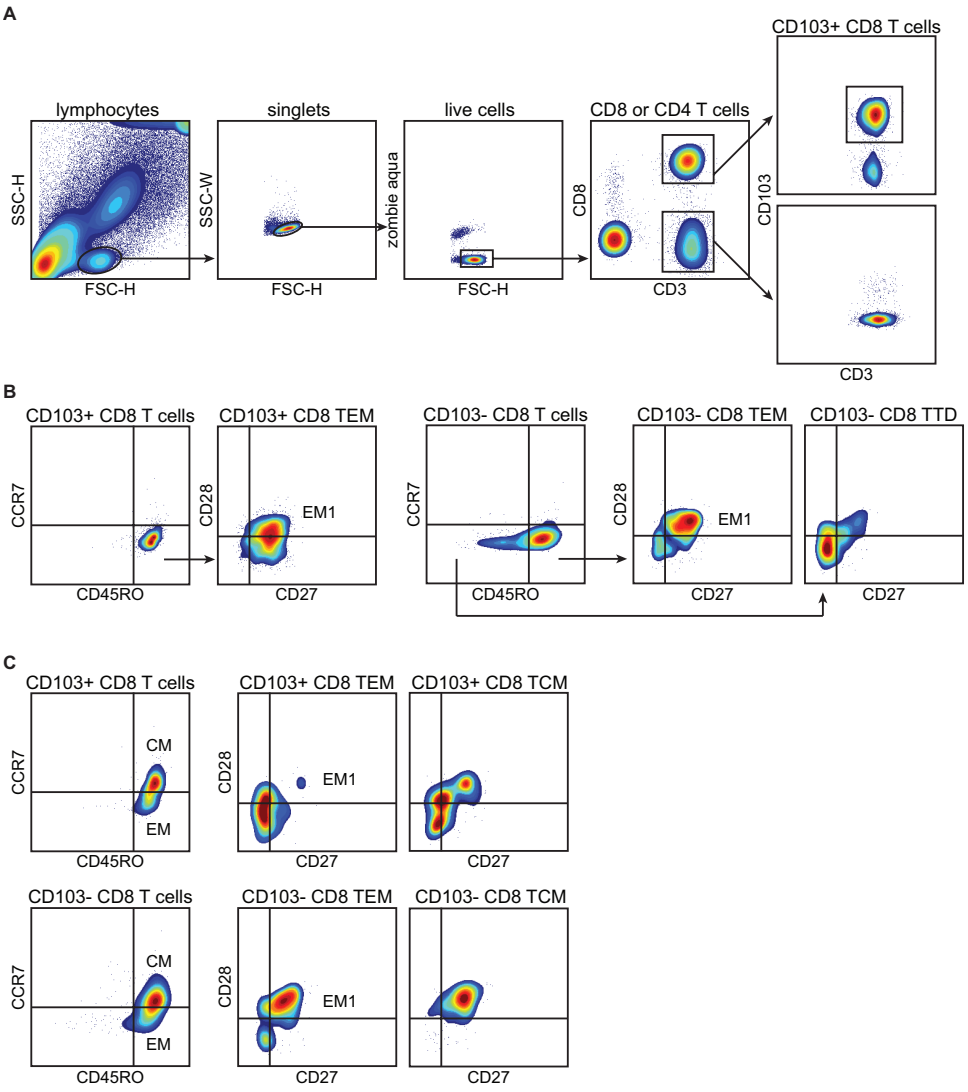

SUPPLEMENTARY FIGURE S3. Flow cytometric plots and gating strategy. HGSC tumor tissue was subjected to enzymatic digestion and analyzed by flow cytometry. **A)** Gating strategy for identifying live CD3+ CD8+ CD103+ and CD3+ CD8+ CD103- T cells. **B)** Flow cytometric plots for HGSC tumor digest #202 used in the quantification depicted in Figure 2G of the manuscript. **C)** Flow cytometric plots for HGSC tumor digest #207 used in the quantification depicted in Figure 2G of the manuscript. T_{CM}: central memory T cell. T_{EM}: effector memory T cell. T_{TD}: terminally differentiated T cell.

Based on the known role of TGF-β in the induction of CD103 in mouse models and T cell clones[20,21], we next assessed whether concurrent T cell activation and TGF-β receptor signaling was required for CD103 induction in PBMC:HGSC co-cultures (n≥3 donors). Induction of CD103 on PBMC was fully abrogated in the presence of TGF-β receptor I (TGFβR1) kinase inhibitor SB-431542 (Fig. 3G) without affecting T cell proliferation (Fig. 3H). To exclude an effect of selective depletion of CD8+ cells by TGFβR1 inhibition, we also analyzed the relative distribution of CD8 versus CD4 cells after treatment with either TGFβR1 kinase inhibitor alone, anti-CD3 agonistic antibody or the combination of both. While T cell activation with anti-CD3 agonist skewed the cell population towards a CD8+ phenotype, this change was not affected by treatment with TGFβR1 inhibitor (Supplementary Fig. S4C). Finally, to confirm a causal role for TGF-β in the induction of CD103 on peripheral CD8+ T cells, we activated T cells in the presence or absence of recombinant TGF-β (rTGF-β1). Treatment with rTGF-β1 did not affect T cell proliferation as assessed by CFSE dilution, but induced a significant upregulation of CD103 (Supplementary Fig. S4D and S4E). These data suggested that cancer antigen-specific circulating CD8+ T cells can upregulate CD103 after activation in the presence of HGSC cancer cells through a combination of TCR- and TGFβR1-signaling.

To demonstrate that CD103 is indeed induced on cancer antigen-specific T cells during an ongoing antitumor immune response against HGSC, we employed a cytomegalovirus (CMV) model system. OVCAR-3 HGSC cells were transfected with the pp65 protein of CMV. Activation and antitumor activity were then assessed using PBMC from a healthy CMV-seropositive donor. After 5 days of co-incubation, CD103 was induced on ~20% of all CD8+ cells and these CD103+ cells (but not CD103- cells) co-expressed classical markers of T cell activation such as CD137 and HLA-DR (Fig. 4A-C). As observed earlier (Fig. 3), PBMC co-cultured with wildtype OVCAR-3 cells in the absence of an activating signal did not induce CD103, nor did these cells upregulate CD137 and HLA-DR (Fig. 4A-C). Induction of CD103 and upregulation of CD137 and HLA-DR was abrogated by treatment with MHC class I blocking antibody W6/32, demonstrating antigen specificity (Fig. 4A-C). Of note, CD4+ T cells did not upregulate CD103 (Fig. 4A), nor CD137, HLA-DR, and OX40 (not shown). Concomitant to the induction of CD103, T cells in these co-cultures induced specific apoptosis in pp65+, but not wildtype, OVCAR-3 cells (Fig. 4D). Finally, isolation of CD103+ versus CD103- negative cells after 5 day co-culture revealed that the specific recognition and apoptotic capacity were restricted to the CD103+ cell population (Fig. 4E). Taken together, these data indicate that CD103 is induced on polyclonal and polyfunctional cancer antigen-specific CD8+ T cells in response to specific recognition of HGSC cells in the presence of TGF-β produced by the epithelium.

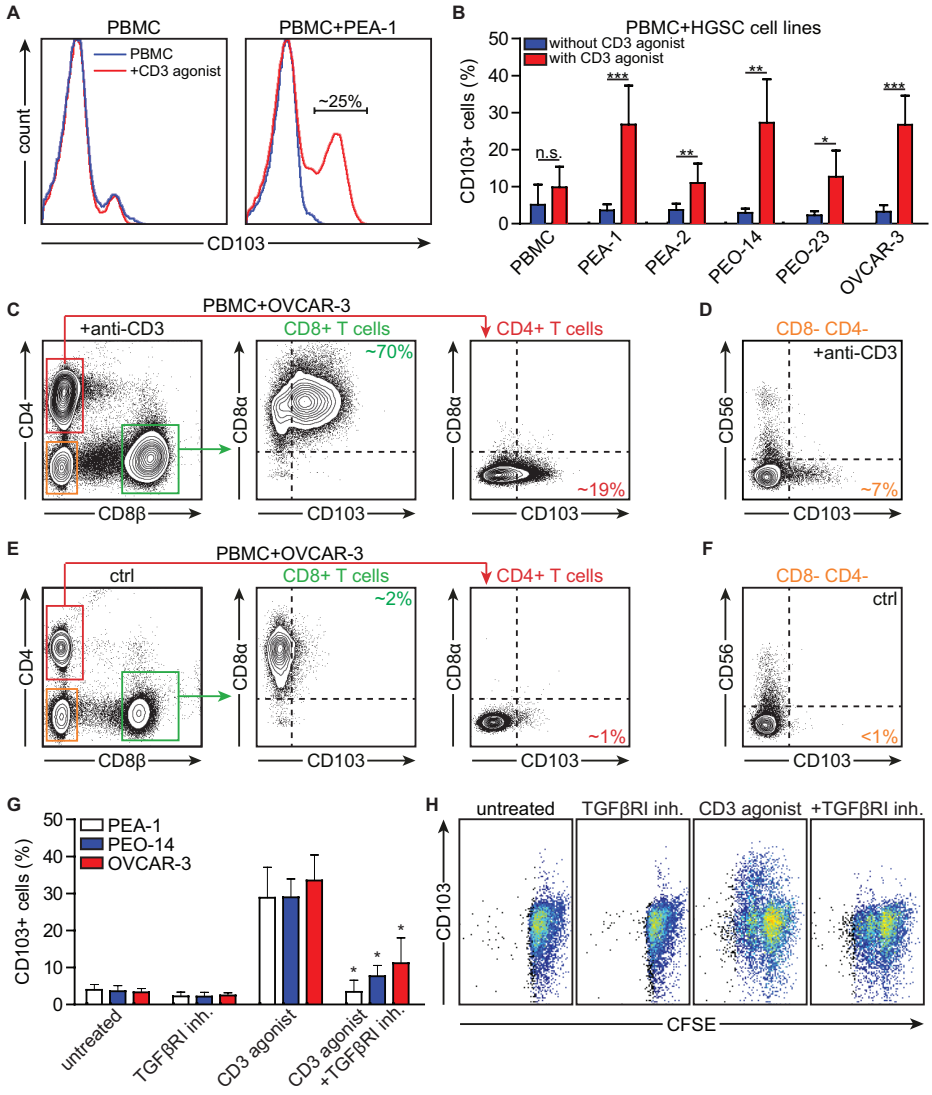

FIGURE 3. Activation in the presence of HGSC cell lines induces CD103 on peripheral blood CD8+ T cells through combined TCR and TGFβR1-signaling. PBMCs were isolated and cultured in the presence of HGSC cell lines. **A)** Histograms representing CD103 expression on PBMCs after incubation of PBMCs with anti-CD3 agonistic antibody (CD3 agonist) in the presence or absence of HGSC cell line PEA-1. **B)** Bar graph representing the percentage of CD103+ cells after incubation of PBMCs with HGSC cell lines (PEA-1, PEA-2, PEO-14, PEO-23, OVCAR-3) in the presence or absence of CD3 agonist. **C)** Representative flow cytometry images of CD103 expression on the CD8+ T cell and CD4+ T cell populations after incubation with OVCAR-3 and CD3 agonist. **D)** Representative flow cytometry image of CD103 expression on the CD8-CD4- T cell population after incubation with OVCAR-3 and CD3 agonist. **E)** Representative flow cytometry images of CD103 expression on the CD8+ T cell and CD4+ T cell populations after incubation with OVCAR-3 without CD3 agonist (control). **F)** Representative flow cytometry image of CD103 expression on the CD8-CD4- T cell population after incubation with OVCAR-3 without CD3 agonist (control). **G)** Bar graph representing the percentage CD103 expressing cells after incubation of PBMCs with HGSC cell lines (PEA-1, PEO-14, OVCAR-3) and TGFβR1 inhibitor and/or CD3 agonist as indicated. **H)** Representative images of CFSE dilution showing T cell proliferation after incubation of PBMCs with OVCAR-3 and TGFβR1 inhibitor and/or CD3 agonist as indicated, showing CD103 expression on the y axis. Differences were assessed by Mann-Whitney U or one-way ANOVA tests.

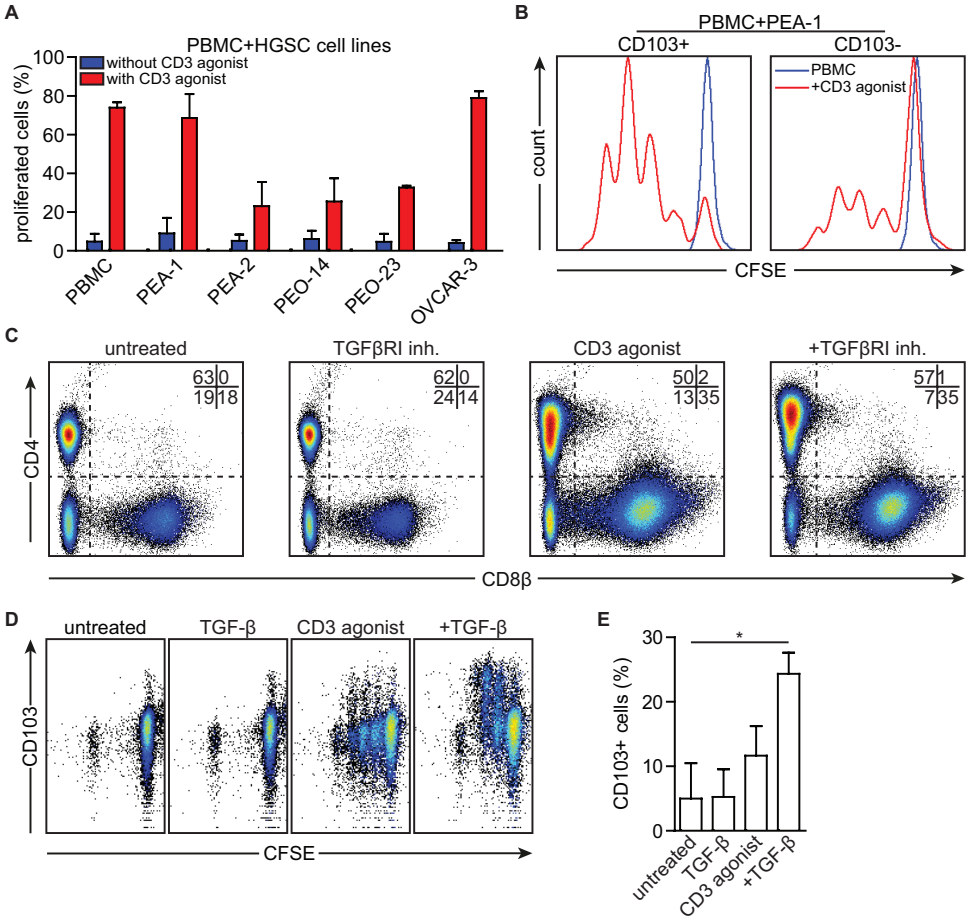

SUPPLEMENTARY FIGURE S4. Treatment with rTGF-β1 does not affect T cell proliferation but induces a significant upregulation of CD103 on T cells. Peripheral blood mononuclear cells (PBMCs) were isolated and cultured in the presence of HGSC cell lines. **A)** Bar graph representing the percentage of proliferating cells after incubation of PBMCs with HGSC cell lines (PEA-1, PEA-2, PEO-14, PEO-23, OVCAR-3) in the presence or absence of CD3 agonist. **B)** Representative histograms of T cell proliferation (CFSE dilution) after incubation of PBMCs with PEA-1 in the presence or absence of CD3 agonist within the CD103+ and the CD103- T cell population. **C)** Representative flow cytometry image of T cell phenotype after incubation of PBMCs with OVCAR-3 and TGFβR1 inhibitor and/or CD3 agonist as indicated. **D)** Representative images of CFSE dilution showing T cell proliferation after incubation of PBMCs with rTGF-β1 and/or CD3 agonist. **E)** Bar graph representing the percentage of CD103+ cells after incubation of PBMCs with rTGF-β1 and/or CD3 agonist. Differences were assessed by Mann-Whitney U or one-way ANOVA tests.

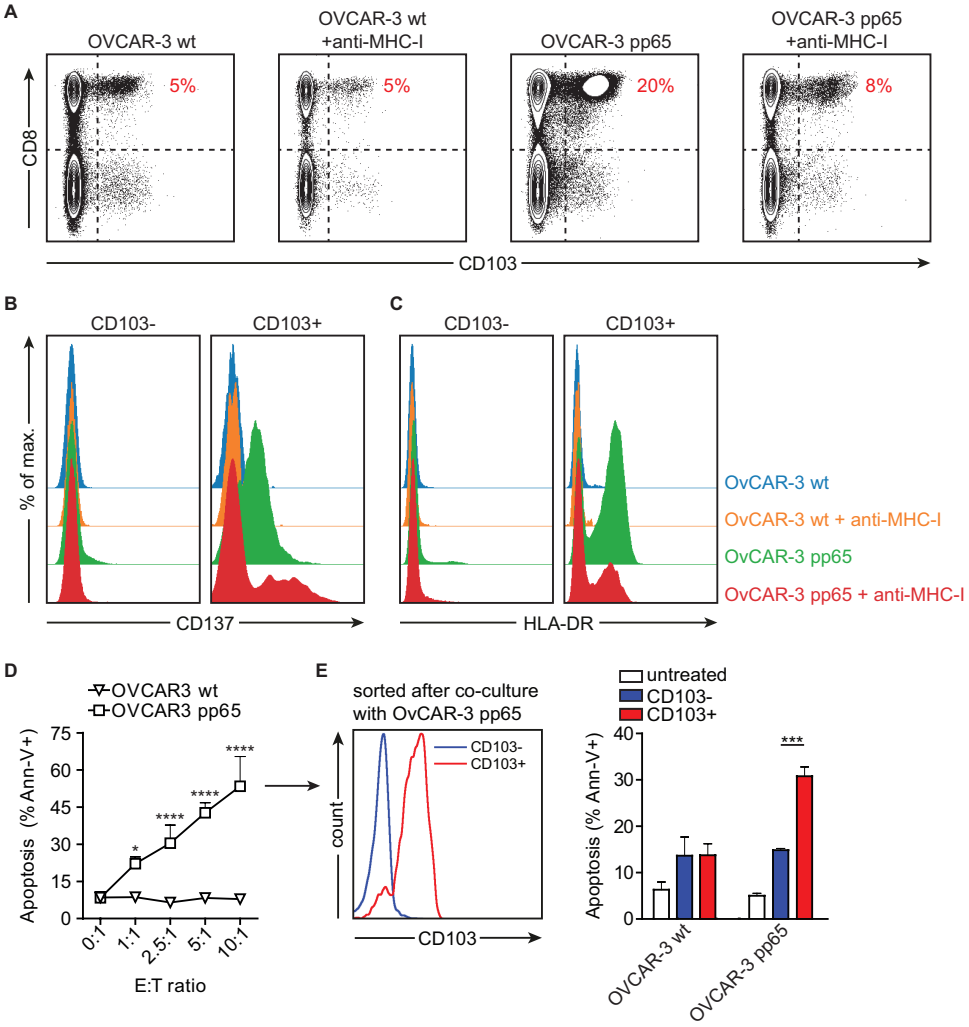

FIGURE 4. Activation in the presence of HGSC cell lines induces CD103 on CMV pp65-reactive CD8+ tumor-lytic T cells. PBMCs from a CMV seropositive donor were isolated and cultured in the presence of OVCAR-3 wildtype (OVCAR-3 wt) cells or OVCAR-3 cells transduced with CMV pp65 (OVCAR-3 pp65) for 5 days (n=3). **A)** Representative flow cytometry images of CD103 expression on the CD8+ T cell and CD4+ T cell populations after co-incubation for 5 days with OVCAR-3 wt or OVCAR-3 pp65 alone or in the presence of MHC class I blocking antibody W6/32. **B)** Histograms representing CD137 or **C)** HLA-DR expression on CD103+ and CD103- CD8+ PBMCs after co-incubation for 5 days with OVCAR-3 wt or OVCAR-3 pp65 alone or in the presence of MHC class I blocking antibody W6/32. **D)** Percentage of apoptotic OVCAR-3 wt or OVCAR-3 pp65 tumor cells after co-culture with PBMCs for 5 days. **E)** Histograms representing CD103 expression on sorted CD103- and CD103+ cells after 5 day co-incubation with OVCAR-3 pp65 cells (left), and percentage of apoptotic OVCAR-3 wt or OVCAR-3 pp65 tumor cells after co-culture with sorted CD103- or CD103+ cells for 48 hours (right). Differences were assessed by Mann-Whitney U or one-way ANOVA tests.

CD103+ TIL *in situ* are characterized by ongoing TCR- and TGFβR1-signaling

To confirm this proposed mode of action for the ontogeny of CD103+ TIL *in situ*, we first assessed whether CD103+ TIL in HGSC tumor tissue demonstrated signs of active TGF-β signaling.[22] Hereto, paraffin-embedded tissue of HGSC was probed by fluorescent microscopy for simultaneous expression of CD8, CD103 and nuclear pSMAD2/3, a hallmark of TGF-β signaling. HGSC tumor epithelial islets were characterized by a pronounced nuclear expression of pSMAD2/3 (Fig. 5A), a finding confirmed in a subsequent set of 37 HGSC patients by immunohistochemistry (Supplementary Fig. 5A). Moreover, CD8+ CD103+ TIL, but not CD8+ CD103- TIL localized almost exclusively to these pSMAD2/3+ tumor islets (Fig. 5A). Subsequent confocal analysis revealed that CD8+ CD103+ TIL were characterized by nuclear pSMAD2/3 expression, whereas CD8+ CD103- TIL were largely negative for pSMAD2/3 expression (Fig. 5B, 5C and Supplementary Fig. S5B-C). Of note, while a significant number of stromal cells in HGSC tumors expressed pSMAD2/3 in the nucleus, these cells were all negative for CD8 (Supplementary Fig. S5C), suggesting a non CTL-origin.

To assess TCR signaling, we determined the expression of the marker for recent T cell activation CD137 [23] in several HGSC digests (n=6). In almost all cases, CD137 was expressed on a significantly higher fraction of CD103+ cells than on CD103- cells (Fig. 5D, p=0.008). Taken together, our data suggest that CD103 expression on CD8+ TIL *in situ* is likely the result of concurrent TCR- and TGFβR1-signaling.

CD103+ HGSC TIL dominantly express checkpoint molecules PD-1 and CD27

Our data suggested CD8+ CD103+ T cells are an adaptive immune population infiltrating the epithelial bed of HGSC. Therefore, checkpoint molecules expressed on CD103+ cells may represent key targets for immunotherapy in HGSC. To assess this, we screened a series of HGSC digests (n≥3) for expression of clinically relevant antibody targets on CD8+ CD103+ and CD103- T cells. CD8+ CD103+TIL displayed a statistically significant higher percentage of PD-1+ cells when compared to their CD103- counterparts (Fig. 6A, p=0.04). In addition, expression of the pro-apoptotic molecule Fas was higher in CD103+ cells (Fig. 6A, p>0.05), in line with a recent report on a FasL-mediated endothelial barrier in epithelial islets in HGSC.[24] Immune checkpoint molecules TIM-3, LAG-3 and CTLA-4 could not be detected in HGSC digests (not shown). Expression of clinically relevant immune checkpoints from the tumor necrosis factor (TNF) family was largely restricted to expression of CD27, although no differences were observed between CD103+ and CD103- cells (Fig. 6A). Finally, as described above, CD103+, and to a significantly lesser extent, CD103- cells expressed the marker of recent T cell activation CD137 (Fig. 6A). To confirm the dominant co-expression of CD27 on CD103+ CD8+ TIL, we analyzed serial sections of our patient cohort (n=186; see also Fig. 1). As anticipated based on our flow cytometric analysis of CD27 expression, both epithelial CD27+ and stromal CD27+ cells could be observed

(Supplementary Fig. 6A). Epithelial CD27+ cells co-localized with CD103+ cells and epithelial CD8+ cells in the adjacent sections (Supplementary Fig. 6A). Analysis of the number of cells revealed a striking correlation between total CD103+ cells and epithelial CD8+ and epithelial CD27+ cells (Supplementary Fig. 6B). Taken together, these data identify PD-1, CD137 and CD27 as key targets for therapeutic reactivation of intraepithelial T cells in HGSC.

CD103+ HGSC TIL poorly expand during standard IL-2 culture for adoptive T cell therapy

We speculated that the prolonged contact of CD103+ CD8+ TIL with the cancer islets might render these cells less fit to expand on IL-2. Therefore, we assessed whether CD103+ TIL could be expanded from HGSC digests using a standard culture protocol of 6000 U/mL of IL-2 (n=6). After 7 days, CD103+ T cells were readily detected in IL-2 cultures and co-expressed CD8, but not CD4 (Fig. 6B). Similar to the HGSC digests, CD8+ CD103+ cells expressed CD137 and were negative for OX40, whereas CD4+ TIL expressed high levels of OX40 at the cell surface (Fig. 6B). Notably, prolonged IL-2 culture (3 weeks) resulted in a significant loss of CD103+ T cells from the TIL product (Fig. 6C). Indeed, analysis of 4 distinct TIL cultures revealed a predominant expansion of CD4+ and/or CD8+ CD103- cells over CD8+ CD103+ cells (Fig. 6D). In line with this, CD8+ CD103+ cells underwent less rounds of cellular proliferation during IL-2 culture compared to CD8+ CD103- and CD4+ cells (Fig. 6E). Taken together, these data highlight a defective expansion of intraepithelial CD8+ TIL in a clinically relevant IL-2 expansion culture.

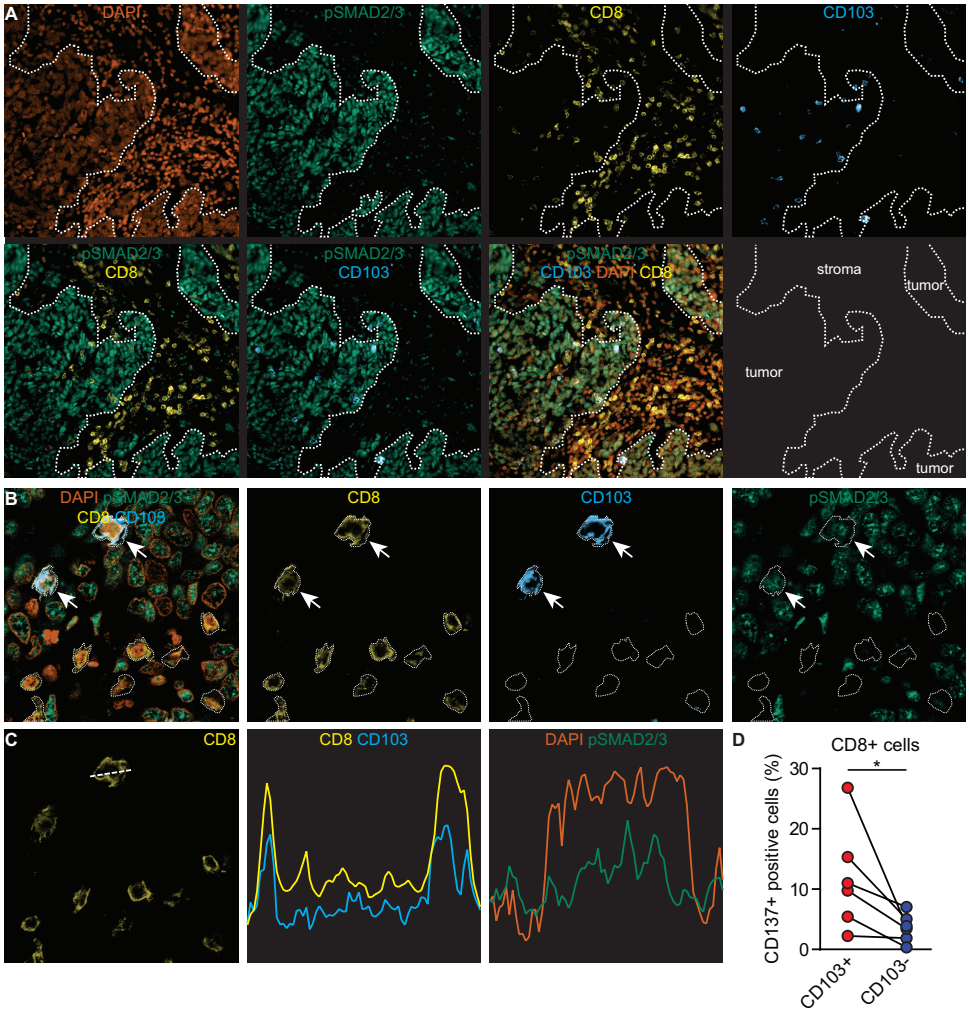

FIGURE 5. CD103+ TIL in situ are characterized by ongoing TCR and TGFβR1-signaling. A-C) FFPE tissue slides from HGSC patients were used for immunofluorescent staining. **A)** Representative single and multichannel images of tissue from a patient with HGSC stained for DNA (orange), pSMAD2/3 (green), anti-CD8 (yellow) and anti-CD103 (blue). **B)** Representative single and multichannel images of CD8+ CD103+ pSMAD2/3+ intraepithelial and CD8+ CD103- pSMAD2/3- stromal cells. CD8+CD103+ cells are depicted with an arrow. **C)** Representative image by confocal microscopy of a cross section of a CD8+ CD103+ T cell. CD8 and CD103 are expressed on the cell membrane whereas DAPI and pSmad2/3 are expressed within the nucleus. **D)** HGSC tumor tissue was subjected to enzymatic digestion and analyzed by flow cytometry. The percentage of CD137+ cells within the CD8+ CD103+ and CD8+ CD103- T cell populations is indicated. Differences were assessed by Mann-Whitney U tests.

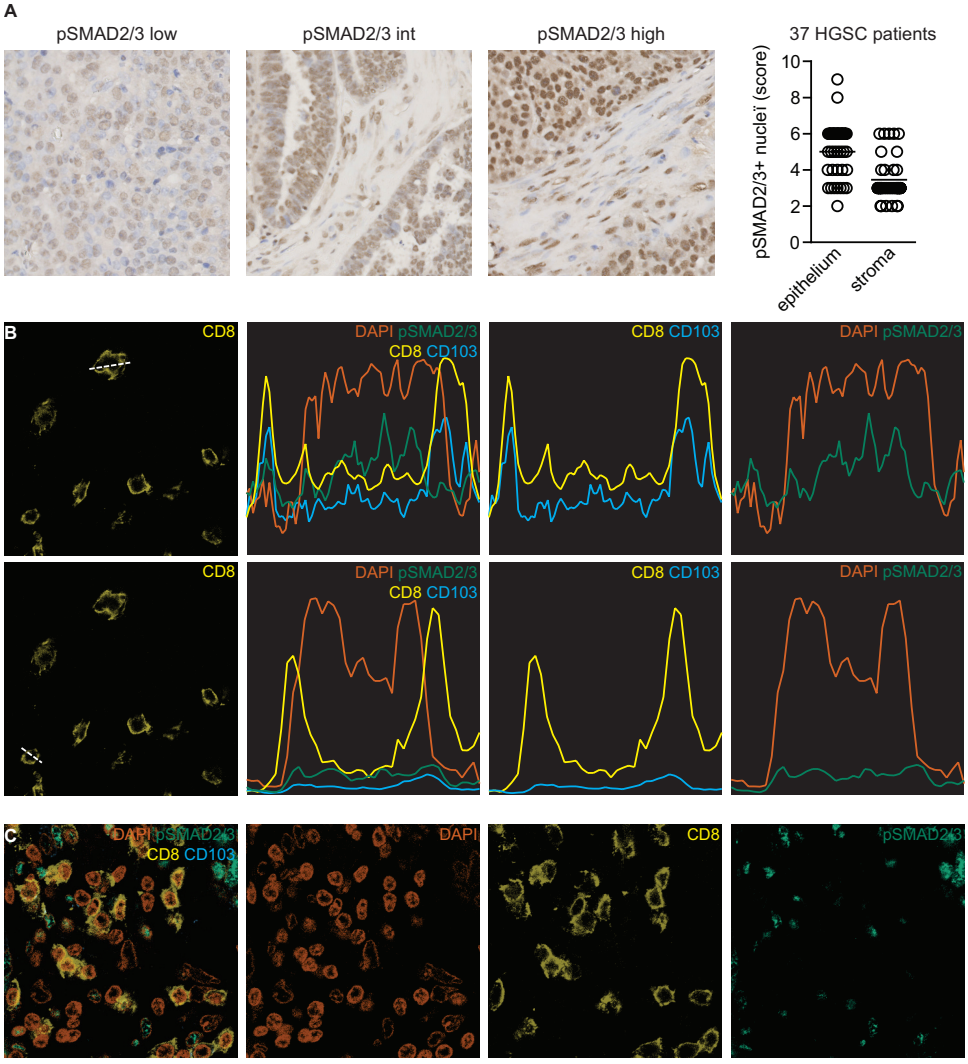

SUPPLEMENTARY FIGURE S5. CD103- CD8+ TIL are largely negative for pSMAD2/3 expression. A) HGSC tissue cores of 37 patients (3 cores per patient) were stained with anti-pSMAD2/3 antibody and scored for expression. **B/C)** Formalin-fixed paraffin-embedded (FFPE) tissue slides from HGSC patients were used for immunofluorescent staining. **B)** Representative images of cross sections of CD8+ T cells by confocal microscopy. Upper row shows an intraepithelial CD8+ CD103+ T cell with nuclear pSMAD2/3 expression. The lower row shows a stromal CD8+CD103- T cell where no pSMAD2/3 expression is observed in the nucleus. **C)** Representative single and multichannel images of tissue from a patient with HGSC stained for DNA (orange), pSMAD2/3 (green), anti-CD8 (yellow) and anti-CD103 (blue) antibodies.

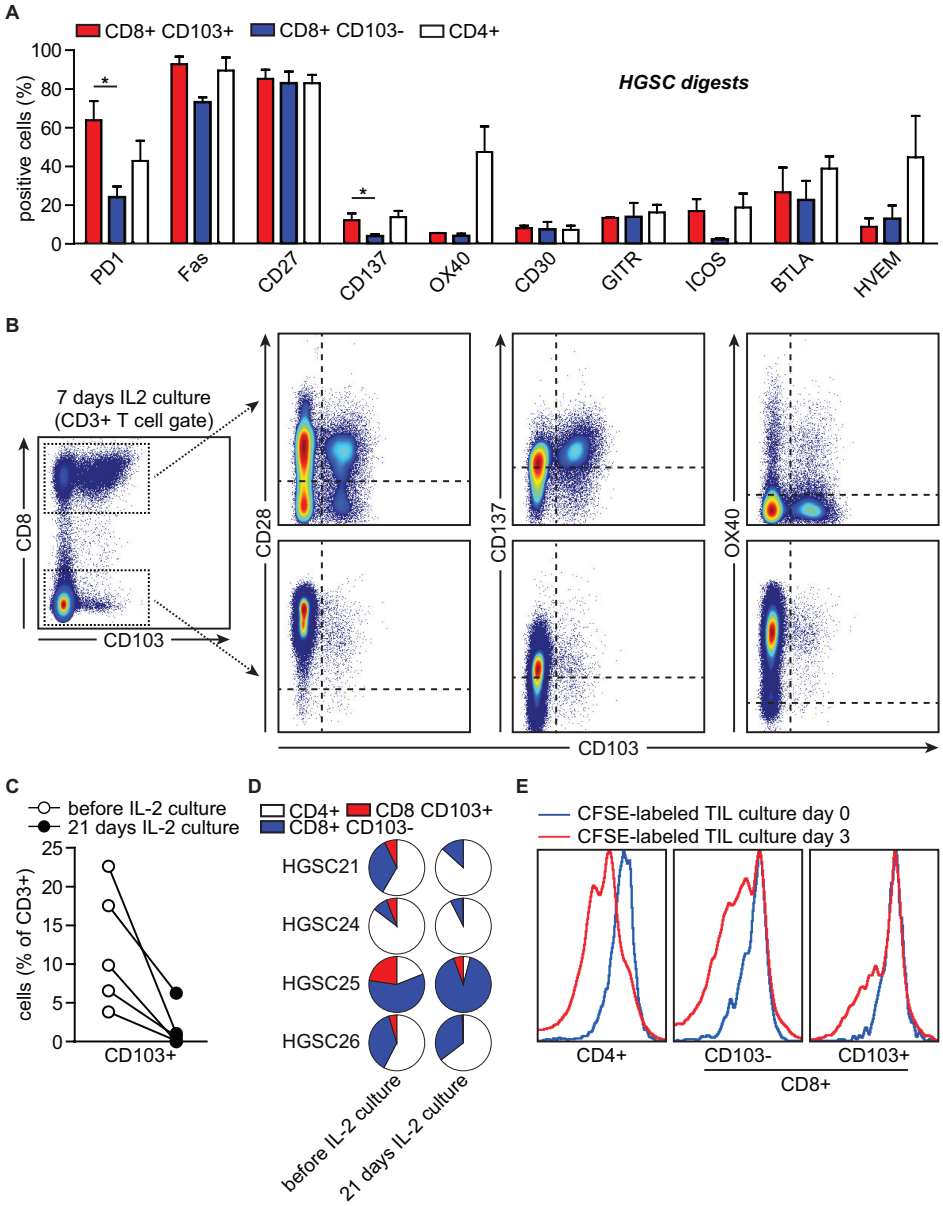

FIGURE 6. CD103+ TIL dominantly express checkpoint molecules PD-1 and CD27. HGSC tumor tissue was subjected to enzymatic digestion and analyzed by flow cytometry. **A)** Bar graph representing the percentage of cells positive for the indicated checkpoint molecules stratified by T cell population. **B)** Representative flow cytometry image of CD103 (x-axis) versus CD28, CD137 and OX40 (y-axis) (co-)expression within the CD8+ T cell (upper row) and the CD8- T cell population (lower row). **C)** Percentage of CD103 + cells within the CD3+ cell population after prolonged IL-2 culture (3 weeks). **D)** Pie charts representing percentage of indicated cell populations before and after prolonged IL-2 culture (3 weeks). TIL were derived from tumor digests (N=4). **E**) CFSE dilution showing proliferation of the indicated cell populations during IL-2 culture of TIL. Differences were assessed by Mann-Whitney U or one-way ANOVA.

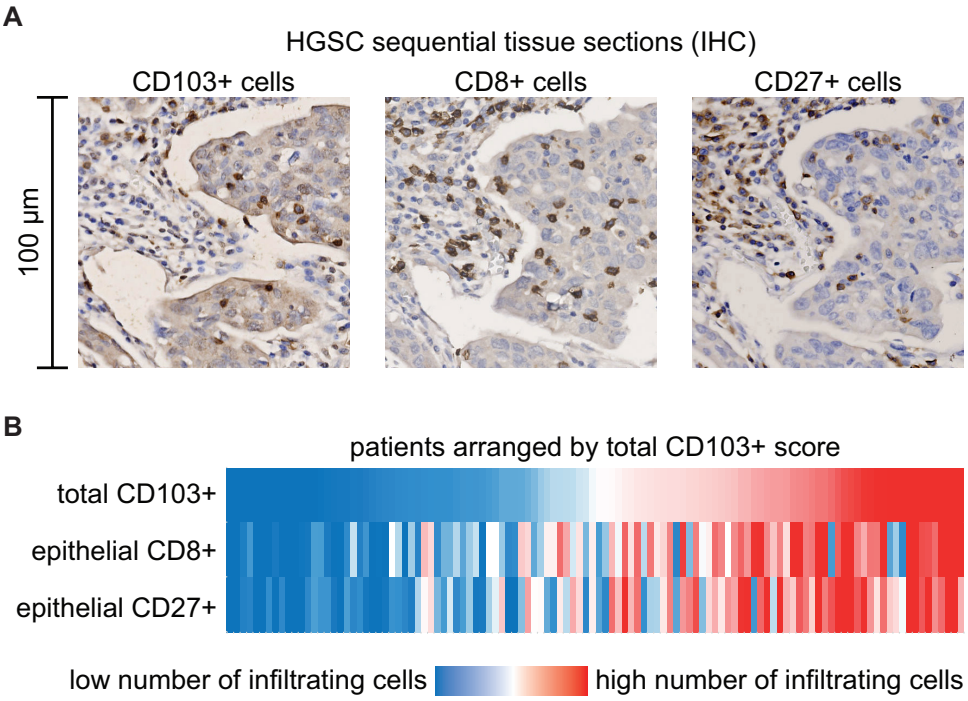

SUPPLEMENTARY FIGURE S6. CD103+ CD8+ TIL dominantly co-express checkpoint molecule CD27. A) Representative images of HGSC tissue cores with infiltration of CD103+, CD8+ or CD27+ cells. **B)** total CD103+, and epithelial CD8+ and CD27+ cells were quantified per patient (both cohorts). Patients were arranged from low to high total CD103+ cell infiltration and corresponding epithelial counts of CD8+ and CD27+ are displayed in a heatmap.

DISCUSSION

In the current study we demonstrate that CD103+ T cells in HGSC are classical TCRαβ+ CD8αβ+ T cells. These cells are generated as a consequence of contact between tumor-infiltrating CD8+ T cells and the epithelial micro-environment. In addition, we confirm the previously published prognostic benefit of total CD103+ TIL in HGSC, but demonstrate that this benefit is restricted to patients receiving primary cytoreductive surgery (PS). Our data further suggest that CD103+ TIL could be effectively targeted by dual PD-1/CD27 checkpoint modulation. Finally, we propose that novel expansion protocols for TIL from HGSC are likely required to maintain the CD103+ population for adoptive transfer.

Our data support the notion that CD103 defines CD8+ cells that are localized in the epithelial compartment of epithelium-derived tumors. Indeed, previous work in HGSC, non-small cell lung cancer (NSCLC), urothelial cell carcinoma of the bladder and endometrial cancer all suggest

CD103+ TIL infiltration is restricted to epithelial cancer islets.[7,16,25–27] However, our study also highlights key differences in the observed phenotypes for CD103+ TIL between malignancies. In NSCLC, CD103+ TIL were found to be of a homogeneous CD69+ CD62L– CD28– CD27+ CD45RA+ CD45RO+ CCR7– subtype.[16] By contrast, we recently found that CD103+ TIL in endometrial cancer were of a CD45RA-CD45RO+CCR7+/- phenotype.[27] Here, we demonstrate that in HGSC CD103+ TIL were homogeneously CD3+ CD56- TCRαβ+ CD8αβ+ CD4- CD45RO+, but heterogeneously expressed differentiation markers CCR7, CD27, and CD28. Furthermore, we demonstrate that almost all peripheral blood CD8+ T cells rapidly upregulate CD103 after activation in the presence of HGSC cancer cells in a TGF-β-dependent manner. These data suggest that CD103+ TIL are formed as a consequence of an adaptive immune response – comprising T cells at various stages of differentiation – instead of an expansion of T_{RM}. In line with this, short-term culture of tumor digests with IL-2 revealed a heterogeneous expression of CD28 on CD103+ and CD103- TIL.

Based on our data and several recent publications on T cell infiltration and migration in(to) ovarian tumors[7,11,28,29], we therefore propose a mode of action for the generation of CD103+ T cells. CD8+ T cells from the peripheral blood extravasate across the tumor vasculature and likely arrive in the small fibronectin/collagen-rich stromal areas that surround the cancer islets. This assumption is supported by the observation that the density of CD8+ TIL in stromal areas of most HGSC tumors is considerably higher than in the neighboring epithelial tissue, suggesting CD8+ T cell migration into cancer islets is a limiting factor (this paper and [28]). Herein, expression of e.g. FasL on the tumor vasculature is likely to play a role in limiting CD8+ T cell migration.[24] After extravasation, collagen density and fiber structure likely function as a barrier for effective CD8+ TIL migration from stromal areas into the epithelium of ovarian tumors.[28] In HGSC tumors where the collagen adopts a non-ring-like open structure, CD8+ TIL can cross the stromal barrier and engage epithelial HGSC cells.[28] At this point, cancer cell-reactive CD8+ T cells likely engage peptide-MHC class I molecules on the epithelial cancer cell and T cell receptor (TCR) signaling is triggered. Concurrently, epithelial cell-secreted TGF-β triggers TGF-β receptor signaling in the CD8+ T cell, resulting in upregulation of CD103. In line with this, we observed several CD103+ TIL in confocal analyses on the border of stromal and epithelial areas. These TIL showed signs of migration into the epithelium as evidenced by the characteristic elongation of activated T cells. If the T cell:cancer cell interaction results in release of e.g. IFN-γ, known immunosuppressive factors like PD-L1 are likely to be (transiently) upregulated, effectively shutting down the T cell. Reversing this immunosuppression by means of checkpoint inhibition and/or T cell agonistic antibodies is likely to reactivate the infiltrating CD103+ TIL and mediate cancer cell eradication.

Our data highlight three interesting immune-modulating targets to achieve this, namely PD-1, CD137 and CD27. Predominant co-expression of PD-1 on the CD103+ TIL in HGSC has previously been reported and may be a consequence of TCR signaling occurring more frequently/

exclusively in CD103+ TIL compared to CD103- TIL.[29] In line with this supposition, we further report that the marker for recent T cell activation CD137 was also expressed in a higher fraction of CD103+ TIL than in CD103- TIL. Interestingly, both PD-1 and CD137 have been reported to define the tumor-reactive T cell repertoire and our data show both markers are largely expressed within the CD103+, but not CD103- TIL populations.[23,30] In depth analysis of the TCR repertoire of both subpopulations therefore appears warranted. Further, combinatorial immunotherapeutic strategies that target PD-1, CD137 and/or CD27 are likely to provide meaningful clinical benefit to HGSC patients with a high number of CD103+ TIL. Several trials in this respect are ongoing and it will be interesting to see if CD103 can herein be employed as a treatment-response biomarker.

Another interesting aspect of our analysis of CD103+ TIL concerns their minimal capacity for expansion under standard IL-2 culture conditions. Several trials on adoptive T cell transfer in ovarian cancer have been conducted with minimal observed clinical benefit.[31,32] Our data provide a possible explanation by showing that the infusion product obtained after expansion is likely reduced in the intraepithelial (tumor-reactive) CD103+ TIL population and predominantly comprised of CD4+ and stromal CD8+ T cells. Of note, such a differential expansion of TIL subsets has previously been reported in the context of rapid TIL expansion for clinical infusion using artificial antigen presenting K562 cells (K562 aAPC).[33] aAPC that did not produce cytokines, or were transduced to secrete IL-2, preferentially expanded CD4+ cells, most of which were FoxP3+ Treg cells. By contrast, aAPC that secreted IL-21 promoted a significantly more expansion of CD8+ cells, while minimizing Treg expansion. Analogously, it is conceivable that the exposure to TGF-β primes CD8+ CD103+ TIL for differential responses to cytokines when compared to CD8+ CD103- TIL. Novel expansion protocols that incorporate alternative cytokines to IL-2 may therefore provide a way of expanding CD103+ TIL for therapy.

A caveat of our study is the lack of functional data on the anti-tumor effects of CD103+ and CD103- T cell populations in an autologous patient-derived xenograft (PDX) model. While we established PDX from several of the patients included in this study[34], we were unable to expand the low numbers of CD3+CD56-TCRαβ+CD8αβ+CD4-CD103+ cells obtained after isolation by fluorescence-activated cell sorting. Indeed, culture of isolated TIL in the presence of IL-2 resulted in expansion of sorted CD3+ CD56- TCRαβ+ CD4+ and CD3+ CD56- TCRαβ+ CD8αβ+ CD4- CD103- cells, but not CD3+ CD56- TCRαβ+ CD8αβ+ CD4- CD103+ cells in 10/10 samples (data not shown). These data are in line with our results on the loss of CD103+ TIL from IL-2 cultures as depicted in Figure 5.

Finally, we observed clear differences in the prognostic benefit of stromal and epithelial CD8+ and CD103+ cells in relation to the treatment regime (Supplementary Fig. 1). Stromal CD8+ T cells were of no prognostic benefit in any of the patient groups analyzed, nor were total CD8+ cells. By contrast, epithelial CD8+ cells and total CD103+ cells were of prognostic benefit only

in patients treated by primary surgery and adjuvant chemotherapy. Patients treated in the neo-adjuvant setting did not benefit from CD8+ or CD103+ cell infiltration. Why patients treated in the neo-adjuvant setting do not benefit from T cell infiltration remains unclear, but may be related to underlying differences in the biology of these cancers [35] or to changes in the tumor microenvironment induced by chemotherapy.[36]

In conclusion, our data indicate CD103+ TIL in HGSC are formed as the result of an adaptive anti-tumor immune response against HGSC. Combined checkpoint modulation that targets PD-1, CD137 and/or CD27 should be explored for treatment of HGSC patients with high numbers of CD103+ TIL.

MATERIALS AND METHODS

Patients and ethics

The patient cohort used for retrospective analysis of CD3, CD8 and CD103 infiltration has been reported previously.[12] In brief, patients with advanced stage (FIGO stage IIb) high-grade serous ovarian cancer were selected for analysis (N=186). 84 patients received primary surgery (PS) and 102 patients received neoadjuvant chemotherapy (NACT). All patient data was placed in an anonymous database, in which patient identity was protected by unique patient codes. According to Dutch law, no approval from our institutional review board was needed. Primary patient TIL used for prospective analysis of CD103+ TIL phenotype were isolated from fresh tumor samples obtained during cytoreductive surgery. Formalin-fixed paraffin-embedded (FFPE) tissue was available from several patients for matched analysis. This material was obtained from surgical tumor waste for which patients gave informed consent. No additional approval from our institutional review board was needed under Dutch law.

Immunohistochemistry

Preparation of sections, antigen retrieval and blocking was performed as described previously.[12] Sections were incubated with either rabbit-anti human CD103 mAb (anti-αEβ7-integrin, Abcam, Cambridge, UK, 1:200 in blocking buffer), mouse-anti human CD8 mAb (DAKO, Heverlee, Belgium, clone C8/144B, 1:25 in blocking buffer), mouse-anti human CD3 mAb (DAKO 1:25 in blocking buffer) or rabbit anti-human pSMAD2/3 (D27F4, Cell signaling, 1:50 in blocking buffer) overnight at 4°C. Slides were subsequently incubated with a peroxidase-labeled polymer (Envision+ anti-rabbit or anti-mouse; DAKO). For CD103, a Biotin Tyramide working solution was used according to the manufacturer's instructions (TSA Kit Perkin Elmer, Waltham, USA 1:50) and slides were incubated with streptavidin-HRP (TSA kit, Perkin Elmer, Waltham, USA 1:100). Specific signal for all staining was visualized by 3,3'diaminobenzidin (DAB). Slides were counterstained

with hematoxylin. For each core the percentage of tumor/stromal surface was estimated based on consecutive H&E slides using semi-quantitative estimation. The total number of cells that stained positive for CD103 was counted per core and corrected for the total surface area of the core (epithelium+stroma). For CD3+ and CD8+ cells, the intra-epithelial and stromal cells were counted separately and corrected for the surface area of each individual area. For epithelial counts patients were included if at least two cores contained >20% tumor epithelium. For stromal counts, patients were included if at least two of the cores contained >10% stroma and >20% tumor epithelium. For pSMAD2/3 staining, epithelial and stromal regions of individual cores were scored for no (0), low (1), intermediate (2) or high (3) expression and the sum of all 3 cores per patient used as the final score. For whole tumor sections, three individual 1 mm^2 regions of tumor epithelium were selected and counted. All slides were counted manually by two individuals that were blinded for clinicopathological data. The two individual scores were compared, and differences in counts of over 10% were reanalyzed until consensus was reached. Epithelial CD27+ cell counts were reported previously.[12]

Immunofluorescence

Preparation of sections, antigen retrieval and blocking was performed as described previously.[12] Sections were incubated overnight with rabbit-anti human CD103 mAb, washed and incubated with Envision-HRP anti-rabbit followed by fluorophore tyramide amplification diluents (TSA KIT Perkin Elmer, MA, USA 1:50) according to the manufacturer's instructions. Next, slides were incubated overnight at 4°C with mouse anti-human CD8 (DAKO, Heverlee, Belgium, clone C8/144B, 1:25 in blocking buffer) and rabbit anti-human pSMAD2/3 (D27F4, Cell signaling, 1:50 in blocking buffer). Sections were subsequently incubated with goat-anti-mouse Alexa Fluor 555 (Life Technologies, Eugene, OR, USA GαM-AF555, 1:150) and goat-anti-rabbit Alexa Fluor 488 (Life Technologies, Eugene, OR, USA 1:150). Nuclei were visualized with DAPI. Sections were embedded in prolong Gold anti-fade mounting medium (Life Technologies, Eugene, OR, USA) and scanned using a TissueFaxs imaging system (TissueGnostics, Vienna, Austria). Processed channels were merged using Adobe Photoshop. Analysis was performed using Fiji.[37]

Tumor digests and TIL cultures

Fresh tumor material was obtained from patients undergoing cytoreductive surgery (n=20). With a scalpel, tumor pieces of approximately 1 mm^3 were cut, and subjected to enzymatic digestion (RPMI supplemented with 1 mg/ml collagenase type IV (Life technologies) and 31 U/ml rhDNase (Pulmozyme, Genentech, California, USA)) for 30 minutes at 37°C or overnight at room temperature. Subsequently, the digestion medium containing remaining tumor pieces was filtered over a 70 µm cell strainer (Corning, Amsterdam, The Netherlands). For phenotypic analyses, cells were pelleted, washed, and cryopreserved until further use. For TIL culture, cells were pelleted, washed and cultured in AIM-V medium containing 5% pooled human AB serum

(Life Technologies) and 6000 IU/ml IL-2 (PROLEUKIN, Novartis). TIL cultures were routinely phenotyped using the antibodies described below. For proliferation assays, TIL cultures were labeled using the CellTrace™ CFSE Cell Proliferation Kit for flow cytometry (Life Technologies) according to the manufacturer's instructions.

Flow cytometric analysis

CD103+ TIL phenotype was characterized by multiparameter flow cytometry in combination with fluorescence-activated cell sorting (FACS). The Zombie Aqua Fixable Viability Kit (BioLegend, Uithoorn, The Netherlands) was used for live/dead staining according to the manufacturer's instructions. Antibodies used for analysis and cell sorting of CD103+ cells in HGSC tumor digests were CD3-BV421 (OKT3), CD103-FITC (ber-ACT8), CD56-PE (clone CMSSB) (all BD Biosciences, Ettenleur, The Netherlands), CD4-PerCP-CY5.5 (OKT4), CD8β-PE-Cy7 (clone SIDI8BEE), TCRαβ-APC (IP26) and CD8α-APC-eFluor780 (RPA-T8) (all eBioscience, Vienna, Austria). Flow cytometry and cell sorting was performed on a Beckman Coulter MoFlo Astrios (BD Biosciences). For analysis of T cell differentiation in HGSC digests a combination of CCR7-BV421 (clone 150503), CD103-FITC (ber-ACT8) (both BD Biosciences), CD27-APC (M-T271), CD45RO-PE-Cy7 (UCHL1), CD28-PerCP-Cy5.5 (CD28.2), CD3-PE (OKT3), CD8α-APC-eFluor780 (RPA-T8) (all eBioscience) and CD27-FITC (PeliCluster F) (Sanquin PeliCluster, Amsterdam, The Netherlands) were used. For analysis of expression of checkpoint molecules and costimulatory TNF family members in HGSC digests the following antibodies were used: CD134(OX40)-PE-Cy7 (ACT35), CD270(HVEM)-Alexa Fluor 647 (clone 94801), CD278(ICOS)-BV421 (DX29), CD272(BTLA)-APC (J168-540), CD30-PE (clone 550041) (all from BD Biosciences), CD357(GITR)-PE-Cy7 (eBioAITR), CD137-PE (4B4), PD1-APC (MIH4), CD95-PE-Cy7 (DX2), CD28-PerCP-Cy5.5 (CD28.2) (all from eBioscience) and CD27-FITC (PeliCluster F) (Sanquin PeliCluster). For analysis of T cell activation, HLA-DR-BV421 (G46-6) CD103-FITC (ber-ACT8) (both BD Biosciences), CD137-PE (4B4), CD3-PerCP-CY5.5 (OKT3), CD134(OX40)-PE-Cy7 (ACT35) and CD8α-APC-eFluor780 (RPA-T8) were used (all eBioscience). Flow cytometry was performed on a BD FACSVerse and samples were analyzed with Cytobank software (cytobank.org). For phenotyping of TIL cultures, the aforementioned antibodies were used in various combinations as indicated in the manuscript, acquired on a BD Accuri C6 flow cytometer (BD Biosciences) and analyzed using the accompanying software.

Coculture assays for induction of CD103

Freshly isolated PBMCs were activated with purified anti-CD3 monoclonal antibody OKT3 (1:1000, eBioscience) in the presence or absence of HGSC-cell lines PEA-1, PEA-2, PEO-14, PEO-23, OVCAR-3 (all routinely profiled using STR and mycoplasm screening assays). Cell lines were cultured using RPMI supplemented with 10% FCS, 1% Glutamine and 1% Sodium pyruvate for PEA-1, PEA-2, PEO-14 and PEO-23, and RPMI supplemented with 10% FCS for OVCAR-3. All co-culture experiments were performed in AIM-V medium supplemented with 5% pooled human

AB serum. Where indicated, cells were additionally incubated with 40 μM TGFβR1 inhibitor SB-431542 (Sigma-Aldrich, Zwijndrecht, The Netherlands) or recombinant TGFβ (Peprotech, Rocky Hill, United States). For proliferation assays, PBMC were labeled using the CellTrace™ CFSE Cell Proliferation Kit for flow cytometry (Life Technologies) according to the manufacturer's instructions. For analysis of antigen-specific immunity, OVCAR-3 cells were transfected with CMV pp65 protein using the pCMV6-pp65 Origene expression vector (VC101404-OR; Origene). Cells were cultured under G418 selection and used when >90% cells were pp65+ as assessed by antibody-based staining (IQ products clones C10/C11). PBMCs isolated from a CMV-seropositive donor (assessed by IgG antibodies to CMV) were co-cultured with pp65+ OVCAR-3 or wildtype OVCAR-3 cells for the indicated periods and effector-to-target (E:T) ratios and apoptosis assessed using Annexin-V staining (Immunotools). CD103+ cells induced after 5 days of co-culture were sorted using CD103-FITC (ber-ACT8) antibody and magnetic anti-mouse beads (Miltenyi Biotech) according to the manufacturer's instructions. Where indicated, cells were phenotyped using the antibody panel described above.

Statistics

All statistical analyses were performed using IBM SPSS version 22 (SPSS Inc., Chicago, USA) or Graphpad Prism. Survival analysis was performed using the Kaplan-Meier method with Log Rank test to test for differences between groups. Groups were stratified on the basis of the highest tertile. Differences in cell infiltration between 43 matched ovarian and omental primary tumor tissues were assessed by Wilcoxon signed ranks test, no differences were found and therefore primary ovarian and omental tissues were used in the analyses. To determine differences in cell populations between clinicopathological variables or between different TIL subsets, the Mann-Whitney U or one-way ANOVA test were used. Spearman's rank correlation coefficient was used to determine correlation between epithelial and stromal CD3+ and CD8+ TIL and total CD103+ TIL. All tests were performed two-sided, and p-values <0.05 were considered significant.

ACKNOWLEDGEMENTS

This work was supported by Dutch Cancer Society/Alpe d'Huzes grant UMCG 2014–6719 to MB and Jan Kornelis de Cock Stichting grants to FLK, MCAW, KLB and FAE. Part of the work has been performed at the UMCG Imaging and Microscopy Center (UMIC), which is sponsored by NWO-grants 40-00506-98-9021 and 175-010-2009-023.

The authors would like to thank Klaas Sjollema, Henk Moes, Geert Mesander, Tineke van der Sluis, Joan Vos and Niels Kouprie for their technical assistance.

REFERENCES

1. Jemal A, Siegel R, Xu J, Ward E. Cancer statistics, 2010. CA Cancer J Clin. 60:277–300.
2. Vaughan S, Coward JI, Bast RC, Berchuck A, Berek JS, Brenton JD, Coukos G, Crum CC, Drapkin R, Etemadmoghadam D, Friedlander M, Gabra H, Kaye SB, et al. Rethinking ovarian cancer: recommendations for improving outcomes. Nat Rev Cancer. 2011;11:719–25.
3. Hwang W-T, Adams SF, Tahirovic E, Hagemann IS, Coukos G. Prognostic significance of tumor-infiltrating T cells in ovarian cancer: a meta-analysis. Gynecol Oncol. 2012;124:192–8.
4. Vermeij R, de Bock GH, Leffers N, Ten Hoor KA, Schulze U, Hollema H, van der Burg SH, van der Zee AGJ, Daemen T, Nijman HW. Tumor-infiltrating cytotoxic T lymphocytes as independent prognostic factor in epithelial ovarian cancer with wilms tumor protein 1 overexpression. J Immunother. 34:516–23.
5. Leffers N, Gooden MJM, de Jong RA, Hoogeboom B-N, ten Hoor KA, Hollema H, Boezen HM, van der Zee AGJ, Daemen T, Nijman HW. Prognostic significance of tumor-infiltrating T-lymphocytes in primary and metastatic lesions of advanced stage ovarian cancer. Cancer Immunol Immunother. 2009;58:449–59.
6. Sato E, Olson SH, Ahn J, Bundy B, Nishikawa H, Qian F, Jungbluth AA, Frosina D, Gnjatic S, Ambrosone C, Kepner J, Odunsi T, Ritter G, et al. Intraepithelial CD8+ tumor-infiltrating lymphocytes and a high CD8+/regulatory T cell ratio are associated with favorable prognosis in ovarian cancer. Proc Natl Acad Sci U S A. 2005;102:18538–43.
7. Webb JR, Milne K, Watson P, Deleeuw RJ, Nelson BH. Tumor-infiltrating lymphocytes expressing the tissue resident memory marker CD103 are associated with increased survival in high-grade serous ovarian cancer. Clin Cancer Res. 2014;20:434–44.
8. D'Agostino PM, Kwak C, Vecchiarelli HA, Toth JG, Miller JM, Masheeb Z, McEwen BS, Bulloch K. Viral-induced encephalitis initiates distinct and functional CD103+ CD11b+ brain dendritic cell populations within the olfactory bulb. Proc Natl Acad Sci U S A. 2012;109:6175–80.
9. Woodberry T, Suscovich TJ, Henry LM, August M, Waring MT, Kaur A, Hess C, Kutok JL, Aster JC, Wang F, Scadden DT, Brander C. Alpha E beta 7 (CD103) expression identifies a highly active, tonsil-resident effector-memory CTL population. J Immunol. 2005;175:4355–62.
10. Laidlaw BJ, Zhang N, Marshall HD, Staron MM, Guan T, Hu Y, Cauley LS, Craft J, Kaech SM. CD4+ T cell help guides formation of CD103+ lung-resident memory CD8+ T cells during influenza viral infection. Immunity. 2014;41:633–45.
11. Bösmüller H-C, Wagner P, Peper JK, Schuster H, Pham DL, Greif K, Beschorner C, Rammensee H-G, Stevanović S, Fend F, Staebler A. Combined Immunoscore of CD103 and CD3 Identifies Long-Term Survivors in High-Grade Serous Ovarian Cancer. Int J Gynecol Cancer. 2016;
12. Wouters MCA, Komdeur FL, Workel HH, Klip HG, Plat A, Kooi NM, Wisman GBA, Mourits MJE, Arts HJG, Oonk MHM, Yigit R, de Jong S, Melief CJM, et al. Treatment Regimen, Surgical Outcome, and T-cell Differentiation Influence Prognostic Benefit of Tumor-Infiltrating Lymphocytes in High-Grade Serous Ovarian Cancer. Clin Cancer Res. 2016;22:714–24.
13. Franciszkiewicz K, Le Floc'h A, Boutet M, Vergnon I, Schmitt A, Mami-Chouaib F. CD103 or LFA-1 engagement at the immune synapse between cytotoxic T cells and tumor cells promotes maturation and regulates T-cell effector functions. Cancer Res. 2013;73:617–28.
14. Le Floc'h A, Jalil A, Vergnon I, Le Maux Chansac B, Lazar V, Bismuth G, Chouaib S, Mami-Chouaib F. Alpha E beta 7 integrin interaction with E-cadherin promotes antitumor CTL activity by triggering lytic granule polarization and exocytosis. J Exp Med. 2007;204:559–70.
15. Le Floc'h A, Jalil A, Franciszkiewicz K, Validire P, Vergnon I, Mami-Chouaib F. Minimal engagement of CD103 on cytotoxic T lymphocytes with an E-cadherin-Fc molecule triggers lytic granule polarization via a phospholipase Cgamma-dependent pathway. Cancer Res. 2011;71:328–38.
16. Djenidi F, Adam J, Goubar A, Durgeau A, Meurice G, de Montpréville V, Validire P, Besse B, Mami-Chouaib F. CD8+CD103+ tumor-infiltrating lymphocytes are tumor-specific tissue-resident

memory T cells and a prognostic factor for survival in lung cancer patients. J Immunol. 2015;194:3475–86.

17. Franciszkiewicz K, Le Floc'h A, Jalil A, Vigant F, Robert T, Vergnon I, Mackiewicz A, Benihoud K, Validire P, Chouaib S, Combadière C, Mami-Chouaib F. Intratumoral induction of CD103 triggers tumor-specific CTL function and CCR5-dependent T-cell retention. Cancer Res. 2009;69:6249–55.

18. Sheridan BS, Lefrançois L. Regional and mucosal memory T cells. Nat Immunol. 2011;12:485–91.

19. Mackay LK, Rahimpour A, Ma JZ, Collins N, Stock AT, Hafon M-L, Vega-Ramos J, Lauzurica P, Mueller SN, Stefanovic T, Tscharke DC, Heath WR, Inouye M, et al. The developmental pathway for CD103(+)CD8+ tissue-resident memory T cells of skin. Nat Immunol. 2013;14:1294–301.

20. Konkel JE, Maruyama T, Carpenter AC, Xiong Y, Zamarron BF, Hall BE, Kulkarni AB, Zhang P, Bosselut R, Chen W. Control of the development of CD8αα+ intestinal intraepithelial lymphocytes by TGF-β. Nat Immunol. 2011;12:312–9.

21. Mokrani M, Klibi J, Bluteau D, Bismuth G, Mami-Chouaib F. Smad and NFAT pathways cooperate to induce CD103 expression in human CD8 T lymphocytes. J Immunol. 2014;192:2471–9.

22. Massagué J, Blain SW, Lo RS. TGFbeta signaling in growth control, cancer, and heritable disorders. Cell. 2000;103:295–309.

23. Ye Q, Song D-G, Poussin M, Yamamoto T, Best A, Li C, Coukos G, Powell DJ. CD137 accurately identifies and enriches for naturally occurring tumor-reactive T cells in tumor. Clin Cancer Res. 2014;20:44–55.

24. Motz GT, Santoro SP, Wang L-P, Garrabrant T, Lastra RR, Hagemann IS, Lal P, Feldman MD, Benencia F, Coukos G. Tumor endothelium FasL establishes a selective immune barrier promoting tolerance in tumors. Nat Med. 2014;20:607–15.

25. Wang B, Wu S, Zeng H, Liu Z, Dong W, He W, Chen X, Dong X, Zheng L, Lin T, Huang J. CD103+ Tumor Infiltrating Lymphocytes Predict a Favorable Prognosis in Urothelial Cell Carcinoma of the Bladder. J Urol. 2015;194:556–62.

26. Boutet M, Gauthier L, Leclerc M, Gros G, De Montpreville V, Théret N, Donnadieu E, Mami-Chouaib F. TGF-β signaling intersects with CD103 integrin signaling to promote T lymphocyte accumulation and antitumor activity in the lung tumor microenvironment. Cancer Res. 2016;

27. Workel HH, Komdeur FL, Wouters MCA, Plat A, Klip HG, Eggink FA, Wisman GBA, Arts HJG, Oonk MHM, Mourits MJE, Yigit R, Versluis M, Duiker EW, et al. CD103 defines intraepithelial CD8+ PD1+ tumour-infiltrating lymphocytes of prognostic significance in endometrial adenocarcinoma. Eur J Cancer. 2016;60:1–11.

28. Bougherara H, Mansuet-Lupo A, Alifano M, Ngô C, Damotte D, Le Frère-Belda M-A, Donnadieu E, Peranzoni E. Real-Time Imaging of Resident T Cells in Human Lung and Ovarian Carcinomas Reveals How Different Tumor Microenvironments Control T Lymphocyte Migration. Front Immunol. 2015;6:500.

29. Webb JR, Milne K, Nelson BH. PD-1 and CD103 Are Widely Coexpressed on Prognostically Favorable Intraepithelial CD8 T Cells in Human Ovarian Cancer. Cancer Immunol Res. 2015;3:926–35.

30. Gros A, Robbins PF, Yao X, Li YF, Turcotte S, Tran E, Wunderlich JR, Mixon A, Farid S, Dudley ME, Hanada K-I, Almeida JR, Darko S, et al. PD-1 identifies the patient-specific $CD8^+$ tumor-reactive repertoire infiltrating human tumors. J Clin Invest. 2014;124:2246–59.

31. Kershaw MH, Westwood JA, Parker LL, Wang G, Eshhar Z, Mavroukakis SA, White DE, Wunderlich JR, Canevari S, Rogers-Freezer L, Chen CC, Yang JC, Rosenberg SA, et al. A phase I study on adoptive immunotherapy using gene-modified T cells for ovarian cancer. Clin Cancer Res. 2006;12:6106–15.

32. Freedman RS, Edwards CL, Kavanagh JJ, Kudelka AP, Katz RL, Carrasco CH, Atkinson EN, Scott W, Tomasovic B, Templin S. Intraperitoneal adoptive immunotherapy of ovarian carcinoma with tumor-infiltrating lymphocytes and low-dose recombinant interleukin-2: a pilot trial. J Immunother Emphasis Tumor Immunol. 1994;16:198–210.

33. Santegoets SJ a M, Turksma AW, Suhoski MM, Stam AGM, Albelda SM, Hooijberg E, Scheper RJ, van den Eertwegh AJM, Gerritsen WR, Powell DJ, June CH, de Gruijl TD. IL-21 promotes the expansion of CD27+ CD28+ tumor infiltrating lymphocytes with high cytotoxic potential and

low collateral expansion of regulatory T cells. J Transl Med. Journal of Translational Medicine; 2013;11:37.

34. Alkema NG, Tomar T, Duiker EW, Jan Meersma G, Klip H, van der Zee AGJ, Wisman GBA, de Jong S. Biobanking of patient and patient-derived xenograft ovarian tumour tissue: efficient preservation with low and high fetal calf serum based methods. Sci Rep. 2015;5:14495.

35. Riester M, Wei W, Waldron L, Culhane a. C, Trippa L, Oliva E, Kim S -h., Michor F, Huttenhower C, Parmigiani G, Birrer MJ. Risk Prediction for Late-Stage Ovarian Cancer by Meta-analysis of 1525 Patient Samples. JNCI J Natl Cancer Inst. 2014;106:dju048–dju048.

36. Böhm S, Montfort A, Pearce OMT, Topping J, Chakravarty P, Everitt GLA, Clear A, McDermott JR, Ennis D, Dowe T, Fitzpatrick A, Brockbank EC, Lawrence AC, et al. Neoadjuvant Chemotherapy Modulates the Immune Microenvironment in Metastases of Tubo-Ovarian High-Grade Serous Carcinoma. Clin Cancer Res. 2016;22:3025–36.

37. Schindelin J, Arganda-Carreras I, Frise E, Kaynig V, Longair M, Pietzsch T, Preibisch S, Rueden C, Saalfeld S, Schmid B, Tinevez J-Y, White DJ, Hartenstein V, et al. Fiji: an open-source platform for biological-image analysis. Nat Methods. 2012;9:676–82.

CD103 defines intraepithelial CD8+ PD1+ tumor-infiltrating lymphocytes of prognostic significance in endometrial adenocarcinoma

HH Workel*, FL Komdeur*, MCA Wouters, A Plat, HG Klip, FA Eggink, GBA Wisman, HJG Arts, MHM Oonk, MJE Mourits, R Yigit, M Versluis, EW Duiker, H Hollema, M de Bruyn, HW Nijman

*Authors contributed equally

Eur J Cancer. 2016 Jun;60:1-11

ABSTRACT

Introduction. Intraepithelial CD8+ tumor-infiltrating lymphocytes (TIL) are associated with a prolonged survival in endometrial cancer (EC). By contrast, stromal infiltration of CD8+ TIL does not confer prognostic benefit. A single marker to discriminate these populations would therefore be of interest for rapid assessment of the tumor immune contexture, *ex vivo* analysis of intraepithelial and stromal T cells on a functional level and/or adoptive T cell transfer. Here we determined whether CD103, the αE subunit of the αEβ7integrin, can be used to specifically discriminate the epithelial and stromal CD8+ TIL populations in EC.

Methods. CD103+ TIL were quantified in a cohort of 305 endometrial cancer patients by immunohistochemistry. Localization of CD103+ cells and co-expression of CD103 with CD3, CD8, CD16 and FoxP3 was assessed by immunofluorescence. Further phenotyping of CD103+ cells was performed by flow cytometry on primary endometrial tumor digests.

Results. CD8+CD103+ cells were preferentially located in endometrial tumor epithelium, whereas CD8+CD103- cells were located in stroma. CD103+ lymphocytes were predominantly CD3+CD8+ T cells and expressed PD1. The presence of a high CD103+ cell infiltration was associated with an improved prognosis in patients with endometrial adenocarcinoma (p=0.035). Moreover, this beneficial effect was particularly evident in high-risk adenocarcinoma patients (p=0.031).

Conclusions. Due to the restricted expression on intraepithelial CD8+ T cells, CD103 may be a suitable biomarker for rapid assessment of immune infiltration of epithelial cancers. Furthermore, this intraepithelial tumor-reactive subset might be an interesting T cell subset for adoptive T cell transfer and/or target for checkpoint inhibition therapy.

INTRODUCTION

Endometrial cancer (EC) is the most common gynecologic malignancy worldwide and the fourth most common malignancy afflicting women in developed countries.[1] Although the vast majority of patients are diagnosed in early stages, a subset of patients is at increased risk for disease-related relapse and mortality. Important prognostic factors to stratify these patients are tumor stage, grade, lymphovascular involvement, myometrial invasion, lymph node metastasis and tumor size.[2]

In addition to these clinicopathological characteristics, emerging evidence suggests that the immune system, in particular tumor-infiltrating T-lymphocytes (TIL), also plays an important role in the development and progression of endometrial cancer. Indeed, we and others have previously demonstrated an improved survival for patients with intraepithelial accumulation of CD8+ cytolytic TIL (CTL) in EC.[3-5] By contrast, stromal accumulation of CD8+ CTL was found to confer no prognostic benefit to EC patients.[3] Together, this suggests that the specific accumulation and retention of T cells within the epithelial compartment is likely a key component of a beneficial immune response in EC. However, markers that differentiate stromal and epithelial CD8+ TIL in EC have not been reported, hampering further *ex vivo* analysis of these two distinct populations.

Here, we hypothesized that CD103, the αE integrin subunit of the αEβ7 complex, could be used to discriminate epithelial from stromal T cells in EC. CD103/β7 binds to E-cadherin expressed on the surface of epithelial cells.[6,7] This interaction is thought to be responsible for retention of antigen-specific lymphocytes within epithelial tissues. Indeed, intraepithelial lymphocytes of the gut and lung are predominantly positive for CD103 while CD103 is expressed on less than 3% of healthy human peripheral blood lymphocytes.[8,9] Furthermore, the interaction of CD103/β7 with E-cadherin promotes CTL effector function[7,10] by promoting immunological synapse formation and subsequent polarization and release of lytic granules[8,10-12]. In line with this, CD103+ TIL have been linked to prolonged survival in non-small cell lung cancer (NSCLC), ovarian cancer and urothelial cell carcinoma of the bladder.[13-15]

In EC, a CD103+ TIL population has been identified previously, but the localization and prognostic influence of this subset has not yet been established.[5] Therefore, the aim of this study was to determine whether expression of CD103 defines the intraepithelial CD8+ CTL in EC and whether these CD103+ TIL are associated with prognosis.

RESULTS

CD103+ TIL are abundantly present in all prevalent endometrial cancer subtypes

Positive staining for CD103+ TIL was present in all histological subtypes analyzed, and CD103+ TIL count did not differ significantly between adenocarcinoma, clear cell and serous tumors (Figure 1A-B). However, to exclude possible confounding effects only adenocarcinoma patients were included for further analyses. Within this population, CD103+ cell infiltration did not correlate with low-, intermediate- and high-risk patient groups (Figure 1C), nor with FIGO stage, grade, treatment, lymphovascular space involvement (LVSI), myometrial invasion or distant metastasis (not shown). Finally, most tumors were infiltrated by low numbers of FoxP3+ Treg (Figure 1D and Supplementary Figure S1A), which associated with infiltration of CD103+ TIL ($p<0.001$, not shown).

CD103 demarcates intraepithelial CD8+ TIL in endometrial cancer

To determine whether CD103 was preferentially expressed on CD8+ TIL in epithelium, multicolor immunofluorescence was performed on full endometrial tumor slides using monoclonal antibodies recognizing CD8, CD103 and the stromal marker fibronectin. Stromal regions were abundant in both the periphery and core of the tumor (Figure 2A-B). CD8+ TIL were present in both the tumor epithelium and fibronectin-stained stromal areas, whereas CD103+ TIL appeared to distribute exclusively within the fibronectin-negative areas of the tumor (Figure 2C). Furthermore, the vast majority of CD103+ cells co-expressed CD8, suggesting a CD8+CD103+ T cell phenotype. Conversely, CD8+ TIL localized in the tumor stroma were negative for CD103 (Figure 2C-F).

Interestingly, while CD103+ cells where scarcely distributed in healthy endometrial tissue, few CD8+CD103+ cells were detected (Figure 3A-F). CD103+ cells in the healthy endometrium were also negative for CD3 and CD16, suggesting a non T cell origin (Figure 3G and H).

TABLE 1. Patient characteristics

	N=305	%
Hospital		
UMCG	305	100
Age		
<60 or 60	118	38,7
>60	187	61,3
Endometrioid		
Endometrioid	265	86,9
Non-endometrioid	40	13,1
Type		
Adenocarcinoma	253	83
Adenocanthoma	5	1,6
Adenosquamous	7	2,3
Clear-cell	17	5,6
Serous/papillary	14	4,6
Undifferentiated	5	1,6
Mixed	4	1,3
FIGO		
I	158	51,8
II	53	17,4
III	72	23,6
IV	22	7,2
Grade		
1	132	43,3
2	82	26,9
3	86	28,2
Undifferentiated	5	1,6
Risk of recurrence		
Low	21	6,9
Intermediate	110	36,1
High	174	57
Recurrence		
Yes	78	25,6
No	227	74,4
Surgery		
Abd. Uterus extirpation with adnexa	151	49,5
Abd.ut.ext.adn+pelv	81	26,6
Abd.ut.ext.adn.+pelv+aort	62	20,6
Otherwise treated	11	3,6
Chemotherapy		
Yes	9	3
No	296	97
Radiotherapy		
Yes	183	60
No	122	40

TABLE 1. (continued)

	N=305	%
Last check-up		
no evidence of disease	190	62,3
evidence of disease	19	6,2
death with, but not of disease	2	0,7
death of disease	55	18
death of other disease	39	12,8

FIGO - International Federation of Gynecology and Obstetrics. Abd.ut.ext.adn - abdominal uterus extirpation with adnexa. Pelv - pelvic lymph node dissection. Aort - para-aortal lymph node dissection

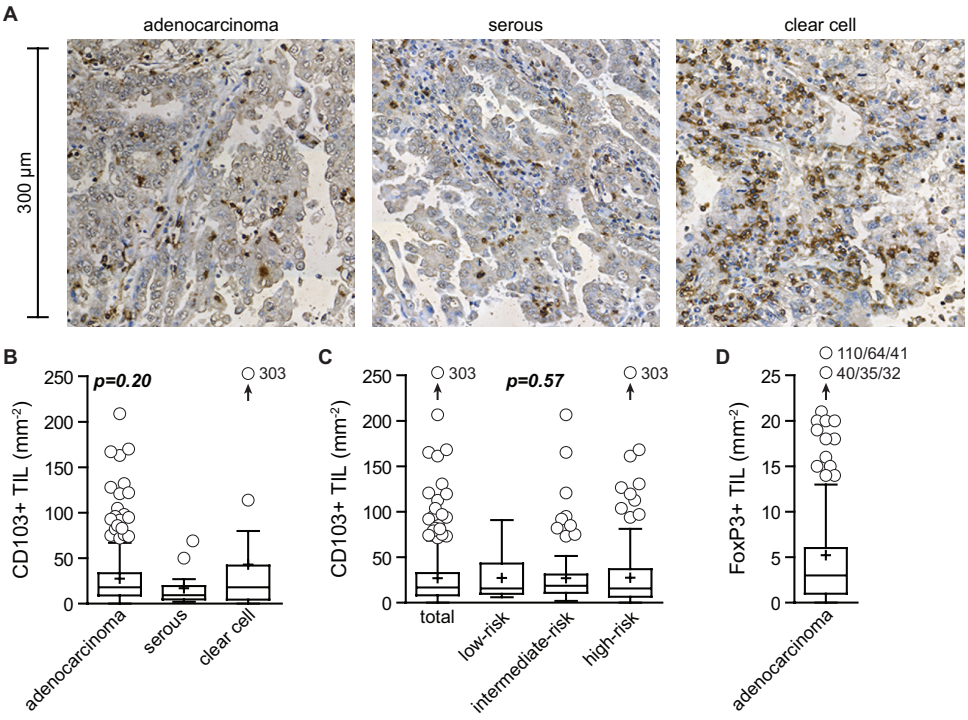

FIGURE 1. CD103+ TIL are abundantly present in all prevalent endometrial cancer subtypes. A) Representative images of tissue cores of adenocarcinoma, serous and clear cell endometrial cancer with infiltration of CD103+ cells. **B)** Box plots of CD103+ cell counts per 0.283 mm^2 tumor epithelium (recalculated for core surface area) in tissue from adenocarcinoma, serous and clear cell endometrial cancer. **C)** Box plots of CD103+ cell counts per 0.283 mm^2 tumor epithelium (recalculated for core surface area) in adenocarcinoma tissue stratified according to risk of disease recurrence. **D)** Intraepithelial FoxP3+ cell counts in patients with endometrial adenocarcinoma within 0.283 mm^2 tumor epithelium (recalculated for core surface area).

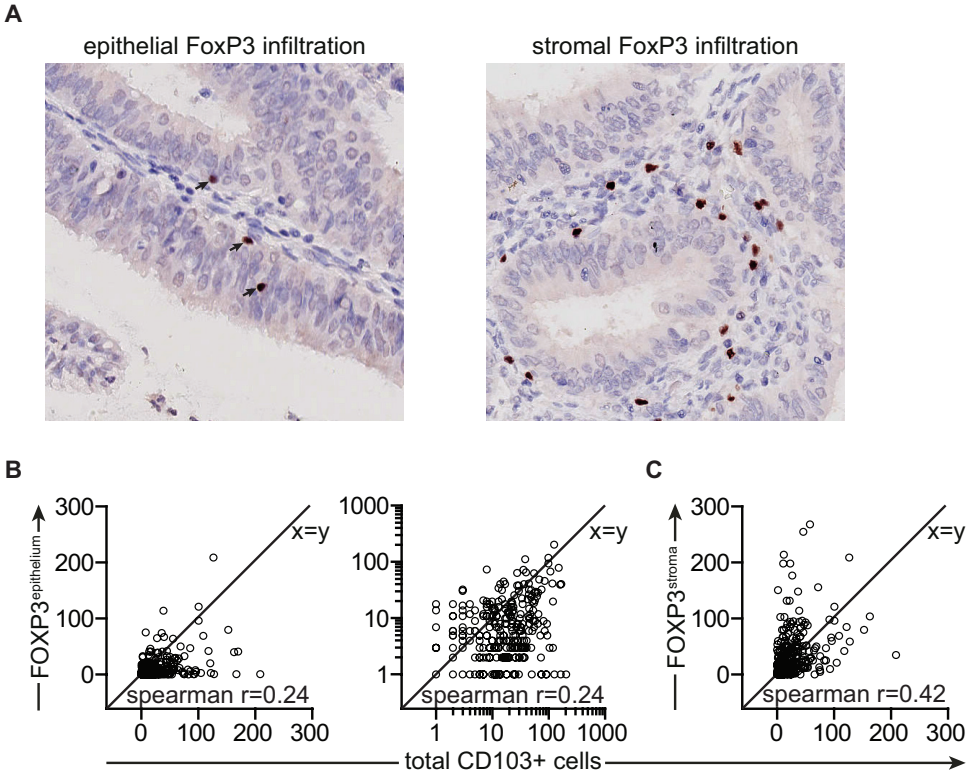

SUPPLEMENTARY FIGURE 1. A) Representative images of tissue cores infiltrated by FoxP3+ cells in the epithelial and stromal compartments. **B)** Correlation of total CD103+ cells per tumor core versus FoxP3+ cells in the tumor epithelium using either untransformed or log10-transformed values. Line inset represents a hypothetical perfect correlation on the x and y axis. **C)** Correlation of total CD103+ cells per tumor core versus FoxP3+ cells in the tumor stroma. Line inset represents a hypothetical perfect correlation on the x and y axis.

To validate these findings, we analyzed the correlation between CD103+ and CD8+ cells in the patient cohort. Total CD103+ TIL count was strongly correlated to the number of intraepithelial CD8+ TIL, a correlation particularly evident upon log10 transformation of the data (Figure 4A; spearman r=0.74, p<0.0001). By contrast, the number of stromal CD8+ TIL was significantly higher in almost all tumors when compared to the total number of CD103+ TIL, and stromal CD8 and total CD103 numbers correlated poorly (Figure 4B, spearman r=0.57). Since infiltration of CD103+ TIL was also associated with FoxP3+ Treg infiltration, we similarly assessed the correlation between epithelial and stromal FoxP3+ cells and total CD103+ cell count. Neither epithelial nor stromal FoxP3+ cell count correlated to CD103+ TIL (Supplementary Figure S1B and S1C). Further, in selected patients where infiltration by FoxP3+ cells into the epithelium was the highest (>15 cells/mm2; n=12/253 adenocarcinoma patients), only a minor subset of CD103+ cells co-expressed FoxP3 (Supplementary Figure S2).

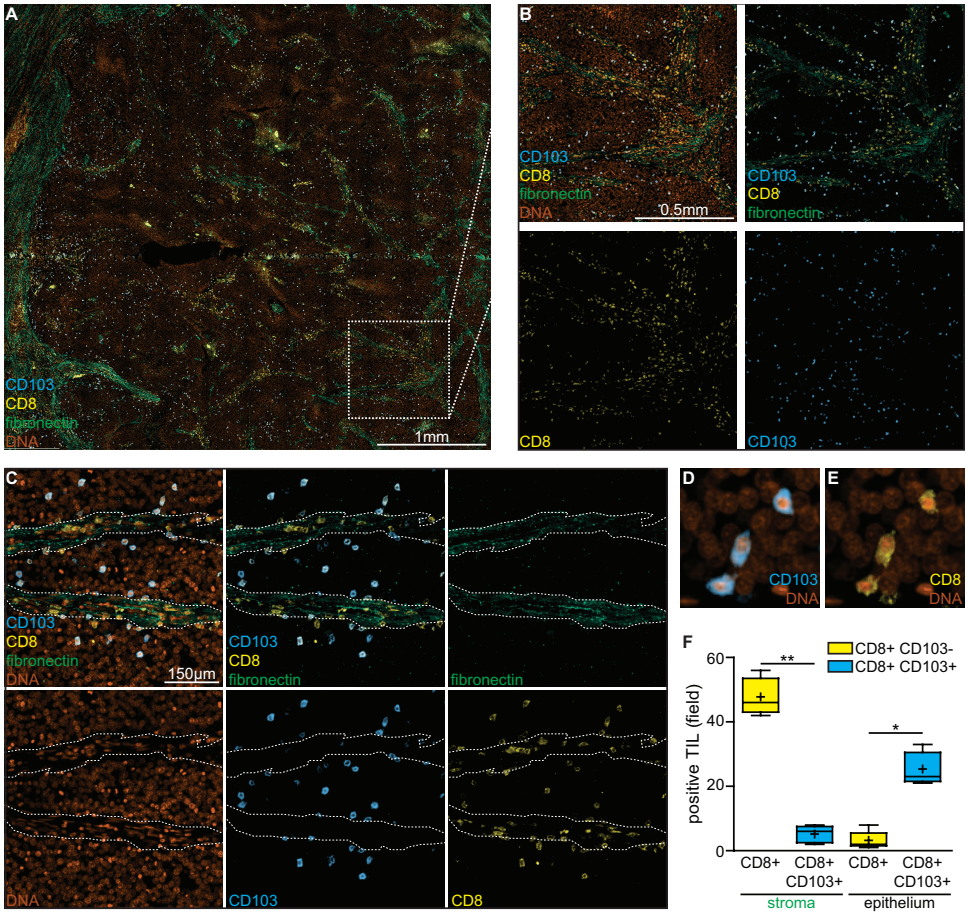

FIGURE 2. CD103 demarcates intraepithelial CD8+ TIL in endometrial cancer tissue. A) Representative image of tissue from a patient with endometrial adenocarcinoma stained with DAPI (DNA, orange), anti-CD8 (yellow), anti-CD103 (blue) and anti-fibronectin (green) antibodies. **B)** Representative images of CD8+ and CD103+ cells in the epithelial or stromal areas of 1 mm^2 of tumor tissue. **C-E)** Representative single and multichannel images of tumor areas used in quantification of TIL infiltration. **F)** Quantification of single CD8+ or CD8+ CD103+ cells in the stroma and epithelial areas of the tumor. Data represent cell counts from 3 independent regions (1mm^2) of 6 independent tumors. * $p<0.05$, ** $p<0.01$.

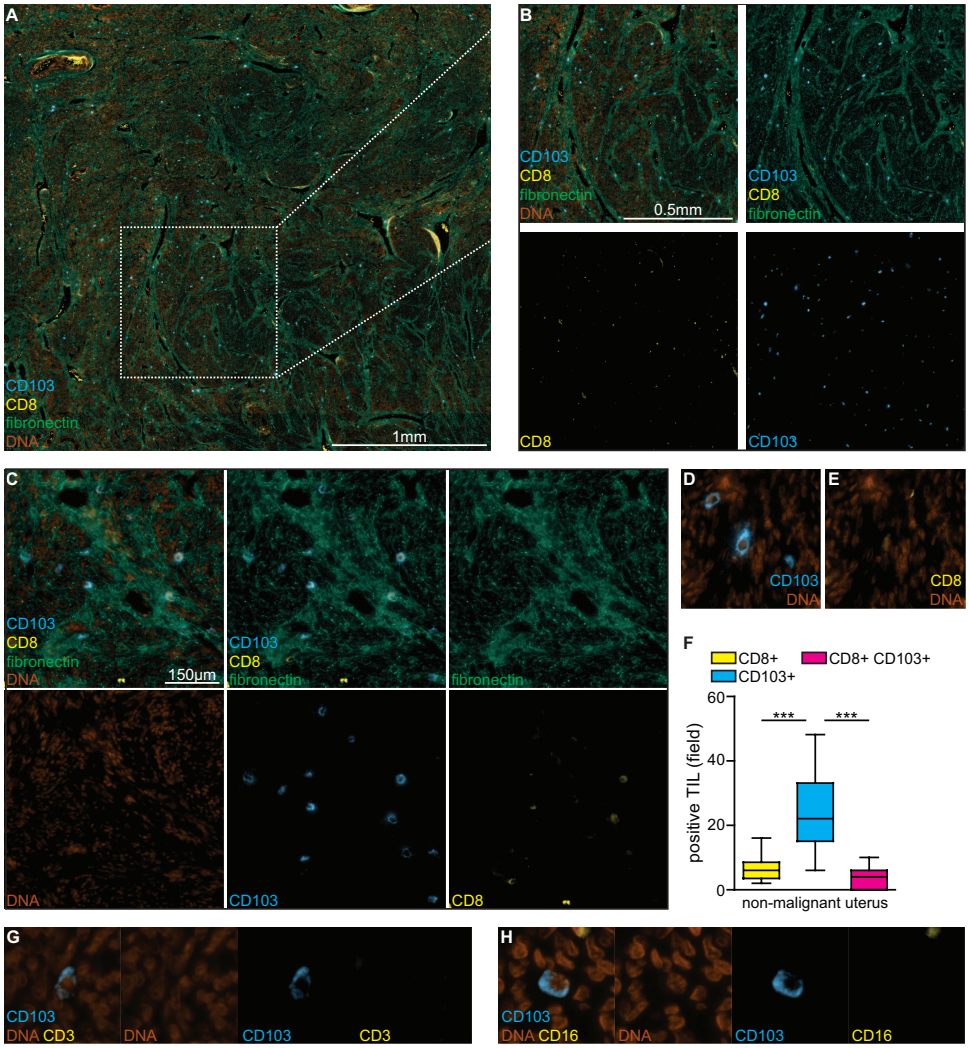

FIGURE 3. CD103+ cells in healthy uterus tissue are of non-T cell phenotype. A) Representative image of healthy endometrial tissue from a patient that underwent elective uterus extirpation as a result of uterine prolapse. Tissue was stained with DAPI (DNA, orange), anti-CD8 (yellow), anti-CD103 (blue) and anti-fibronectin (green) antibodies. **B)** Representative images of CD8+ and CD103+ cells in 1 mm^2 of endometrial tissue. **C-E)** Representative single and multichannel images of tumor areas used in quantification of TIL infiltration. **F)** Quantification of single CD8+ or CD103+ cells, and double CD8+CD103+ in healthy endometrial tissue. Data represent cell counts from 3 independent regions (1mm^2) of 6 healthy uteri. *** $p<0.001$. **G)** Representative image of healthy endometrial tissue stained with DAPI (DNA, orange), anti-CD3 (yellow), anti-CD103 (blue) and anti-fibronectin (green) antibodies. **H)** Representative image of healthy endometrial tissue stained with DAPI (DNA, orange), anti-CD16 (yellow), anti-CD103 (blue) and anti-fibronectin (green) antibodies.

Finally, to assess the phenotype of CD103+ cells, lymphocytes derived from freshly resected tumors from patients with endometrial adenocarcinoma were analyzed by flow cytometry. Within the isolated lymphocyte populations, CD3+CD8+ T cells demonstrated the highest percentage of CD103+ cells, although small populations of CD103+ cells could also be observed within the CD3-CD8+, CD3+CD8- and CD3-CD8- lymphocyte populations (Figure 4C). CD103+CD8+CD3+ TIL were characterized by a dominant expression of CD45RO, a heterogeneous expression of CCR7 and were largely negative for CD45RA, suggesting a central and effector memory phenotype (Figure 4D). Interestingly, CD103+CD8+CD3+ TIL predominantly co-expressed the marker for recent T cell activation CD137 (Figure 4E) and the T cell exhaustion marker PD-1 to a higher extent than observed in any other lymphocyte population (Figure 4F).

CD103+ TIL are associated with prolonged disease-specific and disease-free survival in endometrial adenocarcinoma patients

Adenocarcinoma patients (n=253) were selected to determine the prognostic effect of CD103+ TIL. 61 patients (24.1%) suffered a disease recurrence and 36 (14.2%) succumbed as a result of their disease during follow-up. Infiltration of CD103+ cells ranged from 0-209 TIL per core (0.283 mm^2). For survival analyses, patients were dichotomized on high or low/no infiltration, the cut-off was set at the highest tertile (cut-off 27.28 cells/mm^2) (Figure 5A). Disease-specific survival (DSS) analysis revealed a significant improvement of survival for patients with high CD103+ infiltration compared to patients with low or no infiltration (Figure 5B, p=0.035). Patients diagnosed with low- or intermediate-risk adenocarcinoma showed a non-significant difference in survival based on infiltration of CD103+ TIL (Figure 5C), likely due to the high survival rate already observed in this patient population. By contrast, a striking difference in survival was observed in patients diagnosed with high-risk adenocarcinoma (Figure 5D, p=0.031). Similar results were obtained when determining disease-free survival (DFS) (not shown).

To assess whether the prognostic benefit of infiltration by CD103+ TIL was modulated by immunosuppressive immune populations, we analyzed co-infiltration by FoxP3+ regulatory T cells (Treg). Numbers of intraepithelial FoxP3+ TIL in the adenocarcinoma population were low compared to the number of CD103+ TIL, ranging from 0-64 per 0.283 mm^2, and were similarly dichotomized based on the highest tertile (cut-off 5.00 cells/mm^2) (Figure 5E and Supplementary Figures S1 and S2). The presence or absence of FoxP3+ cells did not affect survival of EC patients, irrespective of their risk category (Figure 5F). However, the CD103/FoxP3 ratio proved to be a worse predictor of prognosis in high-risk adenocarcinoma patients than CD103 alone (Figure 5G, Figure 5H versus 5D). Finally, multivariate analysis of CD103 infiltration and clinicopathological factors revealed an independent association of CD103 with DSS and DFS (Table 2).

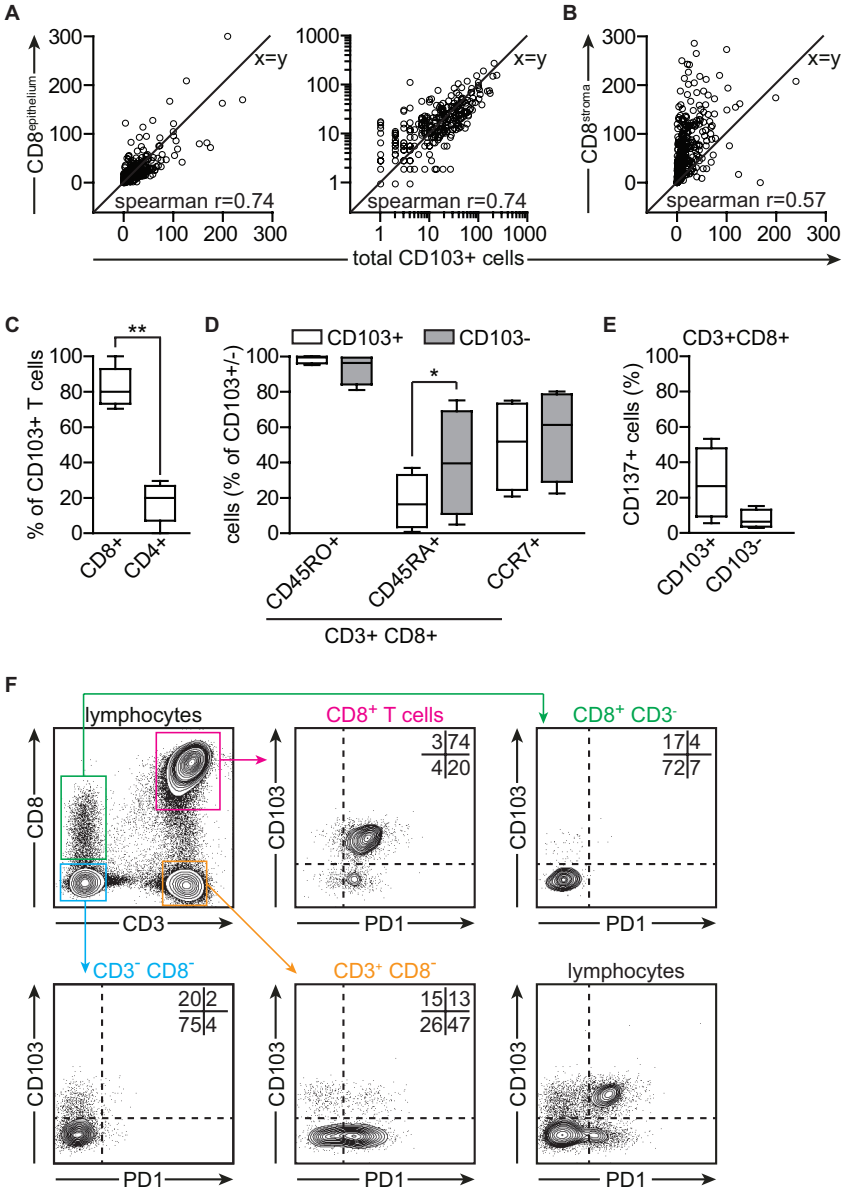

FIGURE 4. CD103 predominantly demarcates exhausted CD8+ TIL in dissociated endometrial cancers. A) Correlation of total CD103+ cells per tumor core versus CD8+ cells in the tumor epithelium using either untransformed or log10-transformed values. Line inset represents a hypothetical perfect correlation on the x and y axis. **B)** Correlation of total CD103+ cells per tumor core versus CD8+ cells in the tumor stroma. Line inset represents a hypothetical perfect correlation on the x and y axis. **C)** Box plots representing the percentage of CD8+ and CD4+ cells within the CD103+ T cell population isolated from primary endometrial cancer digests (n=5). **D)** Box plots representing the percentage of CD45RO+, CD45RA+ and CCR7+ cells within the CD103+ CD8+ T cell population isolated from primary endometrial cancer digests (n=5). **E)** Box plots representing the percentage of CD137+ cells within the CD103+ CD8+ T cell population isolated from primary endometrial cancer digests (n=5). * p<0.05, ** p<0.01. **F)** Representative flow cytometric plot of a primary EC tumor digest analyzed for expression of CD3, CD8, CD103 and PD1.

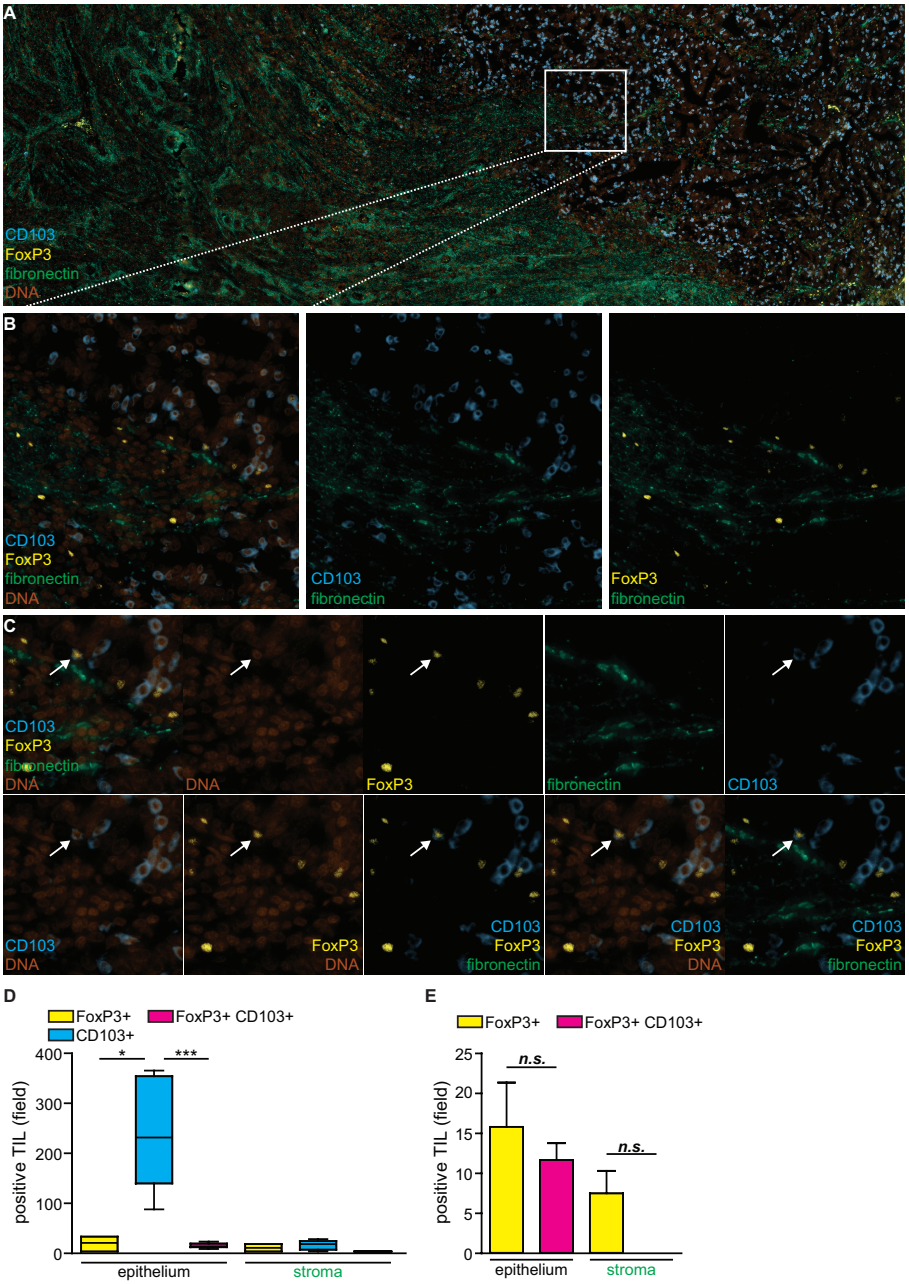

SUPPLEMENTARY FIGURE 2. A-C) Representative images of tissue from a patient with endometrial adenocarcinoma stained with DAPI (DNA, orange), anti-FoxP3 (yellow), anti-CD103 (blue) and anti-fibronectin (green) antibodies. **D)** Quantification of single FoxP3+, CD103+ or FoxP3+ CD103+ double-positive cells in the stroma and epithelial areas of the tumor. **E)** Quantification of single FoxP3+, or FoxP3+ CD103+ double-positive cells in the stroma and epithelial areas of the tumor. Data represent cell counts from 3 independent regions ($1mm^2$) of 12 independent tumors. * $p<0.05$, *** $p<0.001$.

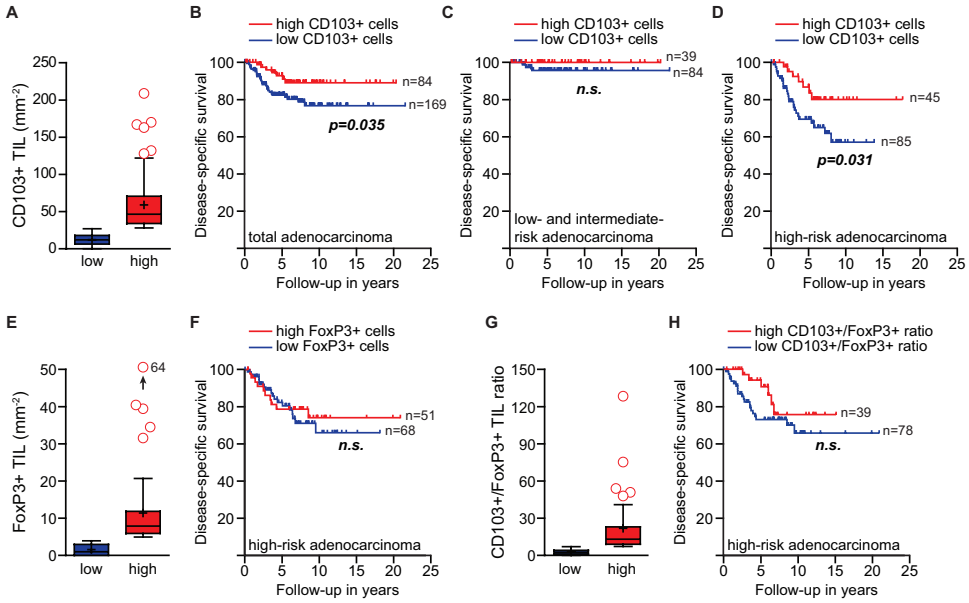

FIGURE 5. CD103+ TIL are strongly associated with survival in patients with endometrial adenocarcinoma. A) Box plots representing the distribution of CD103+ cells per patient within the dichotomized $CD103^{low}$ and $CD103^{high}$ groups. **B)** Disease-specific survival (DSS) of patients within the total adenocarcinoma population according to high or low infiltration of CD103+ cells (p=0.035). **C)** DSS of patients with low- and intermediate-risk adenocarcinoma with a high or low infiltration of CD103+ cells. **D)** DSS of patients with high-risk adenocarcinoma and either a high or low infiltration of CD103+ cells. **E)** Box plots representing the distribution of FoxP3+ cells per patient within the dichotomized $FoxP3^{low}$ and $FoxP3^{high}$ groups. **F)** DSS of patients with high-risk adenocarcinoma and a high or low infiltration of FoxP3+ cells. **G)** Box plots representing the ratio distribution of CD103+/FoxP3+ cells per patient within the dichotomized groups. **H)** DSS of patients with high-risk adenocarcinoma and a high or low ratio of CD103+/FoxP3+ cells.

TABLE 2. Cox regression survival analyses

	Univariate				Multivariate			
	HR	95% CI		p-value	HR	95% CI		p-value
Disease-free survival								
Age	1,302	0,775	2,187	0,319				
Grade	1,601	0,905	2,834	0,106				
Risk	3,731	2,053	6,781	<0.001	2,832	1,366	5,87	0,005
FIGO stage	2,707	1,635	4,483	<0.001	1,158	0,629	2,131	0,638
Myometrial invasion	2,284	1,377	3,789	0,001	1,108	0,627	1,958	0,725
LVSI	3,572	2,14	5,961	<0.001	2,555	1,455	4,486	0,001
Lymphe nodes	0,883	0,74	1,053	0,165				
Regulatory T cells	1125	0,644	1,967	0,679				
CD103+ T cells	0,825	0,707	0,961	0,014	0,808	0,691	0,944	0,007
CD8+ T cells	0,579	0,315	1,063	0,078				
Disease-specific survival								
Age	0,875	0,454	1,685	0,69				
Grade	1,504	0,707	3,199	0,29				
Risk	11,973	3,668	39,078	<0.001	4,939	1,311	18,606	0,018
FIGO stage	5,453	2,76	10,775	<0.001	1,768	0,797	3,92	0,161
Myometrial invasion	4,732	2,278	9,827	<0.001	2	0,874	4,577	0,101
LVSI	5,242	2,662	10,324	<0.001	2,423	1,151	5,097	0,02
Lymphe nodes	0,815	0,645	1,028	0,084				
Regulatory T cells	1,106	0,53	2,309	0,788				
CD103+ T cells	0,806	0,656	0,991	0,041	0,809	0,657	0,998	0,047
Disease-specific survival including CD8+ T cells								
Age	0,875	0,454	1,685	0,69				
Grade	1,504	0,707	3,199	0,29				
Risk	11,973	3,668	39,078	<0.001	3,762	0,959	14,76	0,057
FIGO stage	5,453	2,76	10,775	<0.001	2,095	0,858	5,119	0,105
Myometrial invasion	4,732	2,278	9,827	<0.001	1,604	0,679	3,787	0,281
LVSI	5,242	2,662	10,324	<0.001	2,518	1,118	5,669	0,026
Lymphe nodes	0,815	0,645	1,028	0,084				
Regulatory T cells	1,106	0,53	2,309	0,788				
CD103+ T cells	0,806	0,656	0,991	0,041	0,76	0,575	1,004	0,054
CD8+ T cells	0,313	0,12	0,815	0,017	0,557	0,201	1,542	0,26

FIGO - International Federation of Gynecology and Obstetrics
LVSI - lymphovascular space invasion

DISCUSSION

In the current study we demonstrate that CD103 is a potent marker to discriminate intraepithelial from stromal T cell populations in endometrial cancer (EC). Moreover, the total number of tumor-infiltrating CD103+ cells was an independent predictor of improved survival in high-risk endometrial adenocarcinoma patients. This differential effect of CD103 infiltration on survival in high and low risk patient groups was not confounded by differences in the number of infiltrating CD103+ cells, since all risk-groups were similarly infiltrated. Our results are in line with a growing body of evidence on the localization and prognostic influence of CD103+ TIL in epithelial malignancies. Indeed, CD103+ TIL have been linked to prolonged survival in ovarian cancer, non-small cell lung cancer (NSCLC) and urothelial cell carcinoma of the bladder.[13-16] Interestingly, our observation on the largely restricted expression of CD103 on CD8+ T cells matches the restricted expression observed in epithelial ovarian cancer and NSCLC. While not examined exhaustively, our data suggest that CD103+ CD8+ T cells from adenocarcinoma uterine tumors are predominantly of an antigen-experienced effector memory phenotype, a phenotype that has also been reported in other malignancies.[13]

In line with this, *ex vivo* analysis of endometrial adenocarcinomas revealed a dominant co-expression of PD1 on CD103+ CD8+ T cells, corresponding with a pattern that has been recently reported for ovarian cancer.[17] Nevertheless, within uterine adenocarcinomas, PD1 was also expressed at the cell surface of a similar fraction of stromal CD103- CD8+ T cells. This ubiquitous expression of PD1 on CD8+ TIL is consistent with the recently reported association between *CD8A* (CD8) and *PDCD1* (PD1) gene expression levels in immune-infiltrated microsatellite instable (MSI) and POLE gene-mutant endometrial cancers.[18] When compared to CD8+ TIL, significantly fewer CD4+ T cells expressed PD1 at the cell surface and CD4+ CD103+ TIL expressed PD1 to a similar extent as CD4+ CD103- TIL. Taken together, these data might suggest an intrinsic difference in the induction of PD1 expression on CD8+ and CD4+ cells rather than an expression difference based on epithelial localization.

Upregulation of CD103 has been mapped to simultaneous activation of the T cell receptor (TCR) and transforming growth factor beta (TGF-β) signaling pathways. Furthermore, studies using NSCLC cell lines indicate CD103 is involved in promoting immunological synapse formation and subsequent polarization and release of lytic granules.[8,10-12] As such, the dominant co-expression of PD1 on CD103+ cells reported here suggests CD103+ TIL may represent an exhausted reservoir of tumor-reactive and potentially tumor-lytic TIL that can be reactivated upon checkpoint inhibition with anti-PD1 antibodies.

In addition to this role as biomarker in checkpoint-based immunotherapy, CD103 could be used as a selection marker for use in adoptive T cell transfer protocols of epithelial malignancies.

Infusion of expanded TIL is associated with remarkable clinical benefit in a subset of melanoma patients[19], but has so far not been effectively translated to other non-hematological solid tumor entities. In part, this lack of efficacy might be explained by the bulk expansion of TIL from solid tumors that should invariably result in the simultaneous expansion of epithelial and stromal T cells. It is tempting to speculate that an up-front selection of epithelial, and therefore likely, tumor-reactive TIL would result in a superior infusion product for treatment of epithelial malignancies

Concluding, our findings indicate intraepithelial CD8+ TIL in endometrial cancer are demarcated by expression of CD103 and suggest these cells are induced and/or recruited as a consequence of tumor immune control. CD103+ TIL are associated with improved survival in EC patients and represent an interesting cell population for adoptive cell therapy in endometrial cancer and/or a potential biomarker for immune infiltration of epithelial cancers during checkpoint inhibition immunotherapy.

METHODS

Patient selection

305 anonymized patients treated for endometrial cancer between 1984 and 2004 in the University Medical Center Groningen (UCMG) were included in this study (Table 1). Tumors were classified and graded by a pathologist according to World Health Organization (WHO) criteria. Staging occurred according to International Federation of Gynecologic and Obstetrics (FIGO) guidelines of 2009. Follow-up was carried out until May 2010. For stratification into risk groups, patients were selected based on FIGO stage and grade. Low risk patients were characterized by FIGO 1A grade 1 and 2 endometrioid type, intermediate-risk by FIGO 1A grade 3 endometrioid type and FIGO 1B grade 1 and 2 endometrioid type, and high-risk patients were characterized by FIGO stage IB grade 3, FIGO stage II, III and IV and all non-endometrioid subtypes.[2] Patient data were retrieved from the institutional database into a new anonymous database.

Immunohistochemical analysis of CD103+ TIL infiltration

For analysis of the EC patient cohort, a tissue microarray (TMA) was constructed as described previously.[4] TMA sections were dewaxed and rehydrated, antigen retrieval was initiated (10mM citrate buffer, pH6) and endogenous peroxidase activity was blocked (0.45% H_2O_2solution). Sections were incubated in blocking buffer (1% human AB serum in 1% BSA/PBS solution), avidin/biotin block and rabbit-anti human CD103 mAb (anti-αEβ7-integrin, Abcam, Camebridge, UK, 1:200) before incubation at 4°C overnight. Subsequently, slides were incubated with peroxidase-labeled polymer (Envision+ anti-rabbit DAKO, Carpinteria, USA), Biotin Tyramide working solution

according to manufacturer's instructions (TSA Kit Perkin Elmer, Waltham, USA), streptavidin-HRP (TSA kit, Perkin Elmer,1:100), 3,3'diaminobenzidin (DAB) and hematoxylin. Positively stained CD103+ cells were counted per core and the percentage of tumor/stromal surface was estimated. Patients were included if at least two cores contained ≥20% tumor epithelium. All slides were counted manually by two individuals that were blinded for clinicopathological data. Inter-observer differences of over 10% were reanalyzed until consensus was reached. Cell count was re-calculated per 0.283 mm^2 (i.e. the surface of one core). FoxP3 and CD8 cell counts were previously reported.[4]

Immunofluorescent analysis of CD103+ TIL phenotype and localization

Preparation and antigen retrieval of full tumor slides was performed as described in immunohistochemistry. Sections were incubated with anti-CD103 mAb overnight at 4°C. Slides were incubated with Envision-HRP anti-rabbit and fluorophore tyramide stock solution according to manufacturer's instructions (TSA KIT Perkin Elmer,1:50). Next, biotinylated rabbit anti-fibronectin (Abcam, ab6584 1:50) and either mouse anti-human CD8 (DAKO, Heverlee, Belgium, clone C8/144B, 1:25), mouse anti-human CD3 (DAKO, 1:20), mouse anti-human CD16 (Genetex, 2H7,1:25), or mouse anti-human FoxP3 (Abcam, Ab20034, 1:50) were incubated overnight at 4°C. Sections were subsequently incubated with goat-anti-mouse Alexa Fluor 555 (Life Technologies, Eugene, Oregon, USA GαM-AF555, 1:150), streptavidin dylight 488 (Life Technologies, 1:150) and DAPI, and embedded in prolong Gold anti-fade mounting medium (Life Technologies). Sections were scanned using a TissueFaxs imaging system (TissueGnostics, Vienna, Austria). Processed channels were merged using Adobe Photoshop. On each slide 1 mm^2 of tumor epithelium was selected based on DAPI staining, and cells were counted manually.

Flow cytometric analysis of CD103+ TIL phenotype

Fresh tumor material was obtained from surgical waste of patients undergoing hysterectomy with salpingo-oophorectomy. Tumors were cut into pieces of approximately 0.5cm^3 and subjected to enzymatic digestion (RPMI supplemented with 1 mg/ml collagenase type IV (Life technologies) and 31 U/ml rhDNase (Pulmozyme, Genentech)) for 30 minutes at 37°C. The digests were filtered over a 70 µm cell strainer (Corning, Amsterdam, The Netherlands), cells were pelleted, washed, and cryopreserved until further use.

TIL phenotype was characterized by multiparameter flow cytometry. The Zombie Aqua Fixable Viability Kit was used for live/dead stain according to manufacturer's instructions (BioLegend, Uithoorn, The Netherlands). Antibodies used were CD3-PerCP-Cy5.5 (OKT3), CD8-APC-eFluor780 (RPA-T8), PD1-APC (MIH4), CD45RO-PE-Cy7, CD45RA-APC, CD137-PE, CD4-PerCP-Cy5.5 (all

eBioscience, Vienna, Austria), CCR7-BV421, CD3-BV421, CD103-FITC (333155) (all BD Biosciences, Ettenleur, The Netherlands). All flow cytometry was performed on FACSVerse (BD Biosciences) and samples were analyzed with Cytobank software (cytobank.org).

Statistics

Differences in cell count were determined by a Mann-Whitney U or a Kruskall-Wallis test. Disease-specific survival (DSS) and disease-free survival (DFS) were analyzed using a Kaplan-Meier function; differences in survival were assessed by log Rank test. DSS was defined as date of diagnosis to date of death due to disease. DFS was defined as date of diagnosis to date of recurrence or date of death of disease, in case no recurrence was reported previously. DFS was analyzed if patients had a complete remission three months after surgery. Significance was defined as a p-value of <0.05, all tests were performed two-sided. Statistics were performed using SPSS software version 22.0 (SPSS inc. Chicago, IL, USA) or GraphPad Prism (GraphPad Software inc. CA, USA).

Ethics

All patient identities were anonymized by unique patient codes. Primary patient tissue used was obtained from surgical waste. According to Dutch law no approval from our institutional review board was needed.

ACKNOWLEDGEMENTS

This work was supported by Dutch Cancer Society/Alpe d'Huzes grant UMCG 2014–6719 to MB and Jan Kornelis de Cock Stichting grants to FLK, MCAW and FAE. Part of the work has been performed at the UMCG Imaging and Microscopy Center (UMIC), which is sponsored by NWO-grants 40-00506-98-9021 and 175-010-2009-023.

The authors would like to thank Klaas Sjollema, Henk Moes, Geert Mesander and Roelof-Jan van der Lei for their technical assistance.

REFERENCES

1. Jemal A, Bray F, Center MM, Ferlay J, Ward E, Forman D. Global cancer statistics. CA Cancer J Clin. 2011 Mar-Apr;61(2):69-90.
2. Colombo N, Preti E, Landoni F, Carinelli S, Colombo A, Marini C, et al. Endometrial cancer: ESMO Clinical Practice Guidelines for diagnosis, treatment and follow-up. Ann Oncol. 2013;24 Suppl 6:vi33-8.
3. Kondratiev S, Sabo E, Yakirevich E, Lavie O, Resnick MB. Intratumoral CD8+ T lymphocytes as a prognostic factor of survival in endometrial carcinoma. Clin Cancer Res. 2004;10(13):4450-6.
4. de Jong RA, Leffers N, Boezen HM, ten Hoor KA, van der Zee AG, Hollema H, et al. Presence of tumor-infiltrating lymphocytes is an independent prognostic factor in type I and II endometrial cancer. Gynecol Oncol. 2009;114(1):105-10.
5. Chang WC, Li CH, Huang SC, Chang DY, Chou LY, Sheu BC. Clinical significance of regulatory T cells and CD8+ effector populations in patients with human endometrial carcinoma. Cancer. 2010;116(24):5777-88.
6. Karecla PI, Green SJ, Bowden SJ, Coadwell J, Kilshaw PJ. Identification of a binding site for integrin alphaEbeta7 in the N-terminal domain of E-cadherin. J Biol Chem. 1996;271(48):30909-15.
7. Cepek KL, Shaw SK, Parker CM, Russell GJ, Morrow JS, Rimm DL, et al. Adhesion between epithelial cells and T lymphocytes mediated by E-cadherin and the alpha E beta 7 integrin. Nature. 1994;372(6502):190-3.
8. Le Floc'h A, Jalil A, Vergnon I, Le Maux Chansac B, Lazar V, Bismuth G, et al. Alpha E beta 7 integrin interaction with E-cadherin promotes antitumor CTL activity by triggering lytic granule polarization and exocytosis. J Exp Med. 2007;204(3):559-70.
9. Cepek KL, Parker CM, Madara JL, Brenner MB. Integrin alpha E beta 7 mediates adhesion of T lymphocytes to epithelial cells. J Immunol. 1993;150(8 Pt 1):3459-70.
10. Franciszkiewicz K, Le Floc'h A, Jalil A, Vigant F, Robert T, Vergnon I, et al. Intratumoral induction of CD103 triggers tumor-specific CTL function and CCR5-dependent T-cell retention. Cancer Res. 2009;69(15):6249-55.
11. Le Floc'h A, Jalil A, Franciszkiewicz K, Validire P, Vergnon I, Mami-Chouaib F. Minimal engagement of CD103 on cytotoxic T lymphocytes with an E-cadherin-Fc molecule triggers lytic granule polarization via a phospholipase Cgamma-dependent pathway. Cancer Res. 2011;71(2):328-38.
12. Franciszkiewicz K, Le Floc'h A, Boutet M, Vergnon I, Schmitt A, Mami-Chouaib F. CD103 or LFA-1 engagement at the immune synapse between cytotoxic T cells and tumor cells promotes maturation and regulates T-cell effector functions. Cancer Res. 2013;73(2):617-28.
13. Djenidi F, Adam J, Goubar A, Durgeau A, Meurice G, de Montpreville V, et al. CD8+CD103+ Tumor-Infiltrating Lymphocytes Are Tumor-Specific Tissue-Resident Memory T Cells and a Prognostic Factor for Survival in Lung Cancer Patients. J Immunol. 2015;194(7):3475-86.
14. Webb JR, Milne K, Watson P, Deleeuw RJ, Nelson BH. Tumor-infiltrating lymphocytes expressing the tissue resident memory marker CD103 are associated with increased survival in high-grade serous ovarian cancer. Clin Cancer Res. 2014;20(2):434-44.
15. Wang B, Shaoxu W, Zeng H, Liu Z, Dong W, Wang H, et al. CD103 tumor-infiltrating lymphocytes predict a favorable prognosis in urothelial cell carcinoma of the bladder. J Urol. 2015.
16. Webb JR, Wick DA, Nielsen JS, Tran E, Milne K, McMurtrie E, et al. Profound elevation of CD8+ T cells expressing the intraepithelial lymphocyte marker CD103 (alphaE/beta7 Integrin) in high-grade serous ovarian cancer. Gynecol Oncol. 2010 Sep;118(3):228-36.
17. Webb JR, Milne K, Nelson BH. PD-1 and CD103 are widely co-expressed on prognostically favorable intraepithelial CD8 T cells in human ovarian cancer. Cancer Immunol Res. 2015.
18. van Gool IC, Eggink FA, Freeman-Mills L, Stelloo E, Marchi E, de Bruyn M, et al. POLE proofreading mutations elicit an anti-tumor immune response in endometrial cancer. Clin Cancer Res. 2015.

19. Rosenberg SA, Yang JC, Sherry RM, Kammula US, Hughes MS, Phan GQ, et al. Durable complete responses in heavily pretreated patients with metastatic melanoma using T-cell transfer immunotherapy. Clin Cancer Res. 2011;17(13):4550-7.

CD103+ tumor-infiltrating lymphocytes are tumor-reactive intraepithelial CD8+ T cells associated with prognostic benefit and therapy response in cervical cancer

FL Komdeur*, TM Prins*, S van de Wall, A Plat, GBA Wisman, H Hollema, T Daemen, DN Church, M de Bruyn, HW Nijman

*Authors contributed equally

Oncoimmunology. 2017 Jul 24;6(9):e1338230

ABSTRACT

Human papilloma virus (HPV)-induced cervical cancer constitutively expresses viral E6/E7 oncoproteins and is an excellent target for T cell-based immunotherapy. However, not all tumor-infiltrating T cells confer equal benefit to patients, with epithelial T cells being superior to stromal T cells.

To assess whether the epithelial T cell biomarker CD103 could specifically discriminate the beneficial antitumor T cells, association of CD103 with clinicopathological variables and outcome was analyzed in the TCGA cervical cancer dataset (n=304) and by immunohistochemistry (IHC) in an independent cohort (n=460). Localization of CD103+ cells in the tumor was assessed by immunofluorescence. Furthermore, use of CD103 as a response biomarker was assessed in an *in vivo* E6/E7+ tumor model.

Our results show that CD103 gene expression was strongly correlated with cytotoxic T cell markers (e.g. CD8/GZMB/PD1) in the TCGA series. In line with this, CD103+ cells in the IHC series co-expressed CD8 and were preferentially located in cervical tumor epithelium. High CD103+ cell infiltration was strongly associated with an improved prognosis in both series, and appeared to be a better predictor of outcome than CD8. Interestingly, the prognostic benefit of CD103 in both series seemed limited to patients receiving radiotherapy. In a preclinical mouse model, HPV E6/E7-targeted therapeutic vaccination in combination with radiotherapy increased the intratumoral number of CD103+ CD8+ T cells, providing a potential mechanistic basis for our results.

In conclusion, CD103 is a promising marker for rapid assessment of tumor-reactive T cell infiltration of cervical cancers and a promising response biomarker for E6/E7-targeted immunotherapy.

INTRODUCTION

Cervical cancer is the most common gynecologic malignancy and the second most common malignancy afflicting women worldwide (globcan). The development of cervical cancer is largely dependent on persistent human papilloma virus (HPV) infections, with HPV16 and 18 being the dominant subtypes.[1,2] As a virally-induced cancer, control of cervical cancer development appears at least partly mediated by the immune system,[3–5] and multiple studies have demonstrated a clear benefit of T cell infiltration on survival in cervical cancer patients.[6–9]

The malignant transformation of cervical epithelial cells by HPVs involves integration of viral oncogenes, such as HPV E6 and E7, into the cellular DNA. Subsequent expression of these HPV E6 and E7 proteins inhibits the tumor suppressors p53 and pRb, respectively, resulting in a loss of cell cycle control, proliferation and malignant transformation. Importantly, sustained expression of E6 and/or E7 is required for maintaining a malignant cellular phenotype in this setting.[10] E6/E7 therefore represent bona fide cancer-specific antigens that can be targeted for cancer immunotherapy. Indeed, T cell-based therapies targeting E6/E7 have met with clinical success in early trials.[11–21] As readout for therapeutic efficacy of these approaches, systemic immune monitoring in the blood is usually employed alone, or in combination with monitoring of CD8+ T cell tumor infiltration. Herein, a distinction is frequently made between CD8+ TIL that infiltrate the epithelial cancer nests or TIL that infiltrate the surrounding stroma. This distinction is based on the known need for contact between TIL and cancer cells for efficient induction of cell death, and the observed stronger association of epithelial TIL compared to stromal TIL with regards to patient prognosis.[22] However, this approach relies on distinguishing epithelial from stromal regions, a non-trivial feat in many tumors. The identification of a biomarker for identifying tumor-reactive cells would therefore be of substantial benefit.

Recently, we and others have demonstrated that CD103, also known as the αE integrin subunit, delineates prognostically favorable intraepithelial CD8+ tumor-infiltrating lymphocytes (TIL) in endometrial, ovarian, lung and bladder cancer.[23–27] In contrast to the prognostic benefit observed for CD8+ TIL,[28,29] this survival benefit was also evident when quantifying the total number of CD103+ TIL present within the tumor.[23–27] This finding is in line with the proposed restricted expression of CD103 on CD8+ TIL that have infiltrated the tumor epithelium.

The aim of this study was therefore to determine whether expression of CD103 defines the intraepithelial CD8+ TIL in cervical cancer and whether CD103+ TIL are associated with improved prognosis. Further, we explored the mechanistic basis of our findings in a preclinical mouse model and determined whether CD103 infiltration could be used as a response biomarker for therapeutic HPV16 E6/E7-targeted immunotherapy.

RESULTS

Expression of CD103 is an independent prognostic factor in cervical cancer and strongly associated with an immune signature

To investigate the utility of CD103 as a biomarker of an anti-tumor T cell response in cervical cancer, we first analyzed expression of CD103 (ITGAE) mRNA in The Cancer Genome Atlas (TCGA) cervical cancer dataset. CD103 gene expression was strongly correlated with the expression of T cell markers (CD3, CD2), exhaustion molecules (PD1, TIGIT), antigen-presenting molecules (HLA-DR, -DQ) and B cell markers (CD19) suggesting that increased CD103 expression defines a group of immunologically "hot" tumors in this cervical cancer cohort (Figure 1A). High CD103 expression (>median) was associated with younger patient age (49.9 vs. 46.5 years, *P*=0.03, t-test) and squamous histology (P=0.026, Fisher exact test), though no association with disease stage, tumor differentiation or treatment use was observed (Supplementary Table 1). Notably, CD103 expression greater than the median was associated with significantly improved cancer-specific survival both in univariable analysis (Figure 1B; HR=0.56, 95%CI=0.34-0.92, P=0.02) and after adjusting for disease stage in multivariable analysis (HR=0.55, 95%CI=0.32-0.94, P=0.03) (Supplementary Table 2). By contrast, increased expression of CD8A was not significantly associated with cancer-specific survival in this population (Supplementary Table 2).

SUPPLEMENTARY TABLE 1. Correlation of CD103 expression with other clinicopathological variables in the TCGA cohort.

Variables N=460	CD103 low	CD103 high	P value
Age (mean)	50	46,2	0,021
Stage			
<1b2	45	51	0,37
≥1b2	88	78	
Radio(chemo)therapy			
No	54	57	0,72
Yes	92	88	
Histology			
Pure squamous	116	130	0,022
Adenocarcinoma	30	15	
Tumour grade			
G1/2	80	67	0,11
G3	51	65	

LVI not analyzed as only documented in 150 cases. T size not analyzed as only available in 171 cases. Precise disease stage could be assigned in 273 cases. This table only includes cases used for survival analysis.

Exploratory analysis according to treatment modality (surgery vs. radio(chemo)therapy) suggested that the prognostic benefit of increased CD103 expression was observed in patients treated with radiotherapy, but not in patients treated with surgery alone (Figure 1C (p=0.015) and 1D (p=0.47), respectively).

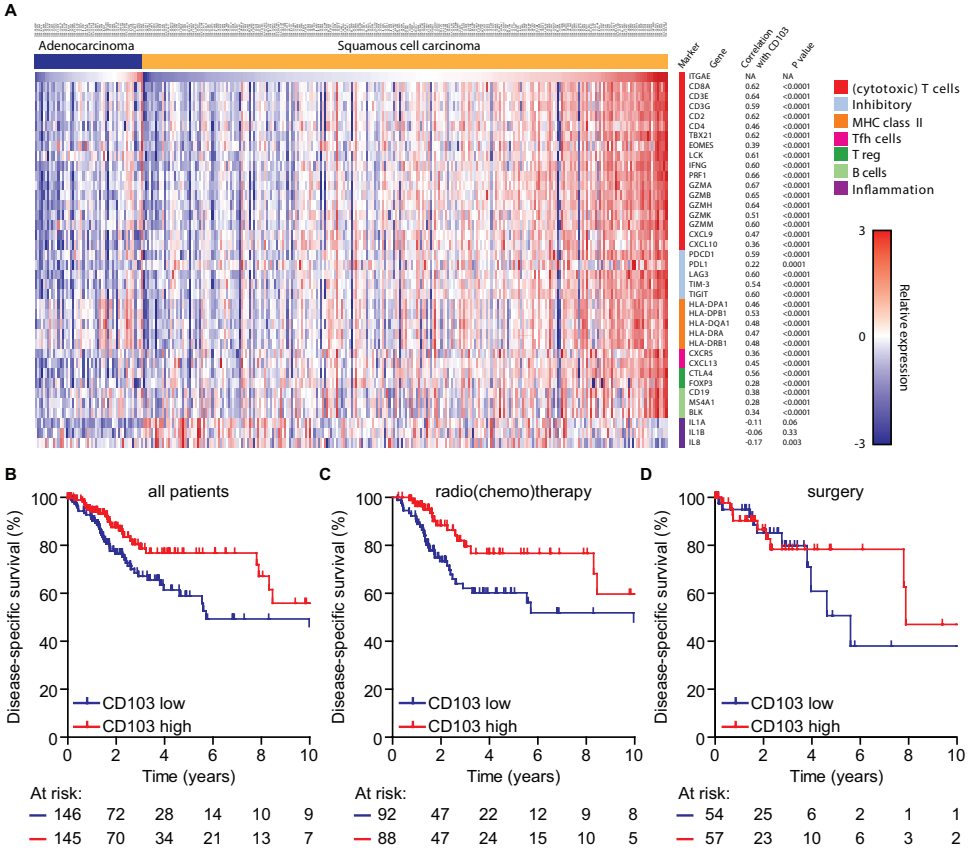

FIGURE 1. CD103-associated immune responses and clinical outcome in TCGA cervical cancers. A) Heatmap showing expression of immunologic genes according to tumor histology and ordered by CD103 (ITGAE) expression. RSEM-normalized RNAseq expression data were log2 transformed, mean centered and assigned unit variance. For each gene, the correlation with CD103 expression was calculated by spearman rho. **B-D)** Kaplan–Meier curves demonstrating cancer survival of patients in the TCGA series dichotomized by median CD103 (ITGAE) expression for the total cohort (B) and according to radiotherapy treatment (C,D) (note that survival data were not available for 13 cases). Comparison between groups was made by the two-sided log-rank test.

SUPPLEMENTARY TABLE 2. Univariable and multivariable cancer-specific survival analysis of TCGA cohort

	Disease specific survival (DSS)					
	Univariate		Multivariate [a]		Multivariate [b]	
Variable	HR	p-value	HR	p-value	HR	p-value
Age (continues)	1.01	0,26				
Stage ≥1b2	1,78	0,049	1,71	0,067	1,68	0,08
Radio(chemo)therapy	1,06	0,84				
Poor differentiation	0,87	0,62				
Tumour histology (AC vs SCC)	0,91	0,8				
CD103+ (>median) [a]	0,56	0,022	0,55	0,03		
CD103+ (continuous) [b]	0,62	0,007			0,65	0,023

Cox regression analysis for disease-specific survival AC: Adenocarcinoma SCC: Squamous Cell Carcinoma
Corresponding results for multivariable-adjusted analysis of CD8A expression are:
(a) HR=0.60, 95%CI=0.35-1.01, P=0.055
(b) HR=0.87, 95%CI=0.76-0.99, P=0.032

CD103+ TIL are associated with prolonged disease-specific and disease-free survival in cervical cancer patients

To validate our findings from the TCGA dataset, we analyzed infiltration of CD103+ cells by immunohistochemistry (IHC) in an independent cohort of 630 cervical cancer patients. Patients were included for quantification of CD103+ TIL if the tissue microarray (TMA) used contained at least two cores with a minimum of 20% tumor. Representative tumor cores were available from 460 patients. Patient and tumor characteristics did not differ between analyzed and excluded patients (data not shown). Table 1 shows the patient and tumor characteristics of the patients eligible for CD103 quantification. Of the 460 included patients, 123 were treated with surgery alone and 337 were treated with radio(chemo)therapy (R(C)T) (alone or in combination with surgery). The surgery cohort consisted of patients diagnosed with Fédération Internationale de Gynécologie Obstétrique (FIGO) stages IB1-IIA. The R(C)T cohort consisted of patients diagnosed with FIGO stages IB1-IVA. The majority of patients in the surgery cohort were diagnosed with FIGO IB1 (n=86; 69.9%) and the majority of patients in the R(C)T cohort were diagnosed with FIGO stage IIB (n=112; 33.2%). Of the surgery and R(C)T cohort, 64.2% (n=79) and 78.9% (n=266) of tumors were squamous cell carcinomas (SCC) and 17.9% (n=22) and 13.1% (n=44) were adenocarcinomas (AC), respectively. The median follow-up time was 5.12 years with a maximum of 21.31 years. Positive staining for CD103+ TIL was equally present in SCC, AC and other subtypes (Supplementary Figure S1A). Interestingly, the median infiltration of CD103+ cells in patients that received radio(chemo)therapy was significantly lower than for patients that received surgery alone (Table 1; median surgery 55 vs. 24 R(C)T; p<0.0001).

Further, within the R(C)T cohort, patients with a higher FIGO stage were characterized by a lower number of CD103+ cells (Table 1; median 38 in IB1 vs. 20 in IIB and 11 in IIIB; $p<0.05$ and $p<0.01$, respectively). Likewise, adenocarcinomas in the R(C)T cohort were infiltrated less than squamous cell carcinomas (Table 1; median 25 vs. 13; $p<0.05$). To analyze survival, patients were dichotomized based on high or low/no infiltration and the cohorts treated with either surgery or radio(chemo)therapy were analyzed together or separately. The cut-off was determined based on median CD103+TIL infiltration of the total cohort and was 29 cells/mm^2. Disease-specific survival (DSS) analysis based on infiltration of CD103+ cells revealed a significant improved survival in the total cohort (Figure 2A; $p<0.0001$), a nonsignificant improvement of survival in the cohort treated with surgery only (Figure 2B; $p=0.9947$) and a significant improvement of survival in the radio(chemo)therapy cohort (Figure 2C; $p=0.0032$). Similar results were obtained when determining disease-free survival (Figure 2D-E; $p=0.0004$ for the total cohort, $p=0.7350$ for surgery alone, and $p=0.0072$ for R(C)T). In analysis of the total cohort, additional prognostic factors were stage (HR=4.19, $p<0.001$), use of radio(chemo)therapy (HR=1.49, $p<0.001$) and tumor diameter (HR=2.9; $p<0.001$) (Supplementary Table 3). In multivariate analysis, stage (HR=2.43, $p<0.006$), use of radio(chemo)therapy (HR=1.30, $p<0.001$) and CD103+ cells (HR=0.67, $p<0.027$) were independent prognostic factors (Supplementary Table 3).

CD103 demarcates intraepithelial CD8+ TIL in cervical cancer

To investigate the localization and the phenotype of CD103+ TIL in cervical cancer, 18 tumors containing high levels of CD103+ TIL were selected, and tumor sections were stained for CD3, CD8, FoxP3, NKp46, fibronectin, DAPI, and CD103. For each section, cell infiltration was quantified for at least 3 independent regions. When examining the localization of the TIL we noticed different patterns of stromal infiltration into the epithelial areas previously classified as 'pushing' tumors and 'desmoplastic' tumors.[30] Due to their distinctive nature, both types of tumors were subsequently analyzed separately (Figure 3A).

Fluorescent staining of the pushing tumor type (n=12) showed that CD103+ TIL were preferentially localized within the tumor epithelium and not within the tumor stroma (Figure 3A). Furthermore, these intraepithelial CD103+ TIL largely co-expressed CD8 (Figure 3B). A subset of CD103+ TIL in the pushing tumor type did not express CD8 (Figure 3C-D). Further analysis of these CD8- CD103+ TIL showed that these cells did express CD3 and could therefore represent CD4+ regulatory T cells (Treg) or natural Killer T cells (NKT) (Supplementary Figure 2). Interestingly, the CD3+ CD8- CD103+ TIL did not express NKP46 or FoxP3 (Supplementary Figures 3 and 4, respectively) suggesting a CD3+ CD4+ non-Treg phenotype.

TABLE 1. Patient characteristics of the IHC cohort

Variables N=460	Surgery n (%)	CD103 median (range)	(chemo-) RT n (%)	CD103 median (range)	Total n (%)	CD103 median (range)
Patients	123 (26.7)	55 (1-367)	337 (73.3)	24 (0-256)****	460 (100)	29 (0-367)
Age at diagnosis (in years)						
Median	41.2		50.7		47.7	
Range	(24.4-84.7)		(20.6-92.0)		(20.6-92.0)	
FIGO stage						
IA2	0 (0)		0 (0)		0 (0)	
IB1	86 (69.9)	52 (1-367)	77 (22.8)	38 (0-256)	163 (35.4)	50 (0-367)
IB2	20 (16.3)	83 (7-286)	50 (14.8)	23 (2-204)	70 (15.2)	31 (2-286)
IIA	17 (13.8)	80 (10-203)	60 (17.8)	23 (0-215)	77 (16.7)	29 (0-215)
IIB	0 (0)		112 (33.2)	20 (1-150)	121 (24.3)	20 (1-150)
IIIA	0 (0)		4 (1.2)	16 (5-34)	4 (0.9)	16 (5-34)
IIIB	0 (0)		28 (8.3)	11 (0-115)	28 (6.1)	11 (0-115)
IVA	0 (0)		6 (21.8)	16 (5-43)	6 (1.3)	16 (5-43)
Histology						
Squamous cell carcinoma	79 (64.2)	82 (7-367)	266 (78.9)	25 (1-215)	345 (75.0)	30 (1-367)
Adenocarcinoma	22 (17.9)	53 (6-246)	44 (13.1)	13 (0-256)	66 (14.3)	16 (0-256)
Other	22 (17.9)	33 (1-186)	27 (8.0)	36 (4-199)	49 (10.7)	36 (1-286)
Grade of differentiation						
Good/moderate	69 (56.1)	55 (1-367)	190 (56.4)	24 (0-215)	259 (56.3)	29 (0-367)
Poor/undifferentiated	51 (41.5)	83 (3-303)	129 (38.3)	26 (0-256)	180 (39.1)	33 (0-304)
Unknown	3 (2.4)	52 (6-53)	18 (5.3)	14 (3-120)	21 (4.6)	16 (3-120)
Lymphangioinvasion						
No	74 (60.2)	56 (5-367)	173 (51.3)	22 (0-216)	247 (53.7)	28 (3-367)
Yes	49 (39.8)	55 (1-304)	105 (31.2)	35 (2-256)	154 (33.5)	38 (1-304)
Unknown	0 (0)		59 (17.5)	16 (0-128)	59 (12.8)	16 (0-128)
Tumor diameter						
0-4 cm	97 (78.9)	52 (1-367)	118 (35.0)	36 (0-256)	215 (46.7)	40 (0-367)
≥ 4 cm	26 (21.1)	86 (6-286)	203 (60.2)	18 (0-204)	229 (49.9)	22 (0-286)
Unknown	0 (0)		16 (4.7)	33 (3-128)	16 (3.5)	33 (3-128)
Treatment						
WM	123 (100)	55 (1-367)				
WM+ post operative RT			83 (24.6)	42 (2-256)		
WM+ Post operative RCT			14 (4.2))	33 (2-84)		
Primary RT			115 (34.1)	22 (0-198)		
Primary RCT			125 (37.1)	16 (0-133)		
Follow-up (in years)						
Median	5.62		4.81		5.12	
Range	(0.53-16.93)		(0.14-21.31)		(0.14-21.31)	
Result last follow-up						
No evidence of disease	109 (88.6)	77 (3-367)	168 (49.9)	29 (0-216)	227 (60.2)	38 (0-367)
Evidence of disease	2 (1.6)	92 (1-184)	2 (0.6)	52 (3-102)	4 (0.9)	52 (1-184)
Death of other disease	0 (0)		33 (9.8)	24 (0-215)	33 (7.2)	24 (0-215)
Death of disease	12 (9.8)	42 (7-170)	134 (39.8)	15 (0-256)	146 (31.7)	17 (0-256)

Abbreviations: FIGO: International Federation of Gynecologists and Obstetricians
WM: Wertheim Meigs RT: Radiotherapy RCT: Radio-chemotherapy

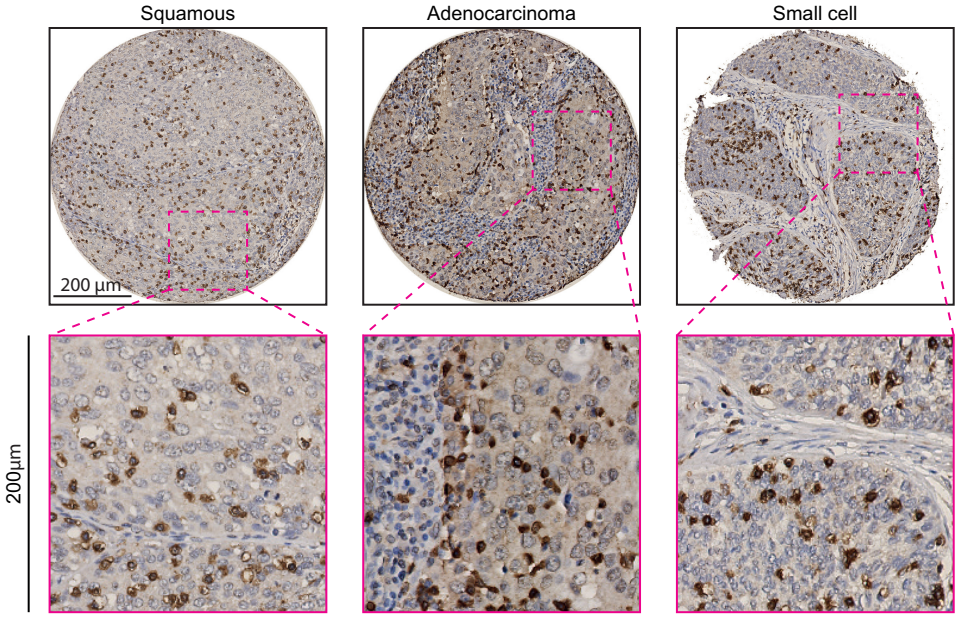

SUPPLEMENTARY FIGURE 1. CD103+ TIL are abundantly present in cervical cancer subtypes. Representative images of tissue cores of squamous, adenocarcinoma and small cell cervical cancer with infiltration of CD103+ cells.

Within the desmoplastic tumor type (n=6), a distinct selection of stromal versus epithelial areas could not be made (Figure 3A-B). Nevertheless, the desmoplastic tumors contained an even higher percentage of CD8+ CD103+TIL (Figure 3D). By contrast, single CD8+ or CD103+ cells could barely be detected in these tumors. In healthy cervical tissue, no CD8+ CD103+ cells were detected (Figure 3A), but epithelial CD8+ CD103- cells and a small number of stromal CD8- CD103+ cells were found. Untransformed stromal cervical tissue surrounding the pushing tumor types were frequently rich in CD8- CD103- cells that expressed NKp46 (data not shown). Taken together, these data demonstrate that CD103+ cells in cervical cancer tissue are predominantly CD8+ T cells, with a minor fraction of CD4+ non-Treg cells. By contrast, CD103+ T cells are largely absent from untransformed epithelium and stroma. In tumor-adjacent stroma, mainly CD103- NK cells are present.

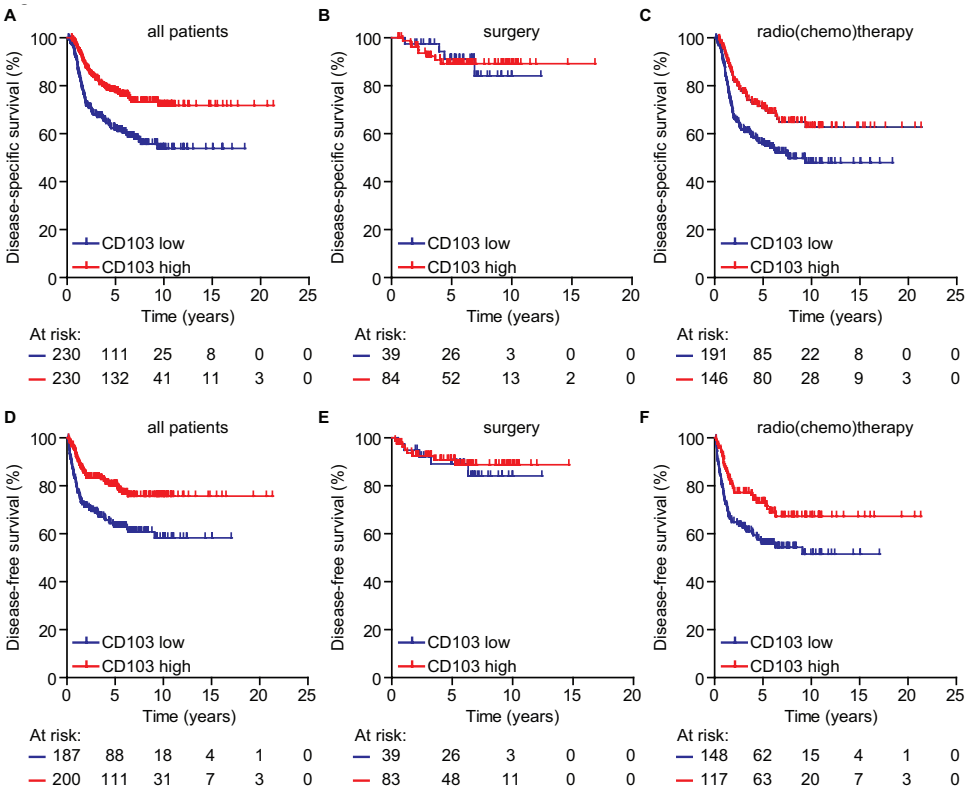

FIGURE 2. CD103+ TIL are strongly associated with survival in patients with cervical cancer. A) Disease-specific survival (DSS) of patients within the total cohort according to high or low infiltration of CD103+ cells ($p<0.0001$). **B)** DSS of patients treated with surgery alone with a high or low infiltration of CD103+ cells. **C)** DSS of patients treated with radio(chemo)therapy and either a high or low infiltration of CD103+ cells. **D)** Disease-free survival (DFS) of patients within the total cohort according to high or low infiltration of CD103+ cells ($p=0.0004$). **E)** DFS of patients treated with surgery alone with a high or low infiltration of CD103+ cells. **F)** DFS of patients treated with radio(chemo)therapy and either a high or low infiltration of CD103+ cells. Comparison between groups was made by the two-sided log-rank test.

SUPPLEMENTARY TABLE 3. Univariable and multivariable cancer-specific survival analysis of IHC cohort

	Disease specific survival (DSS)					
	Univariate		Multivariate [a]		Multivariate [b]	
Variable	HR	p-value	HR	p-value	HR	p-value
Age	1.01	0.051				
Stage ≥1b2	4.19	<0.001	2.43	0.006	2.35	0.008
Radio(chemo)therapy	1.49	<0.001	1.30	0.001	1.27	0.003
Lymphangioinvasion	1.09	0.640				
Tumor diameter ≥4 cm	2.90	<0.001	1.18	0.503	1.20	0.459
Poor differentiation	1.32	0.099				
Tumour histology		0.157				
AC vs SCC	0.66	0.054				
AC vs other	0.73	0.317				
Other vs SCC	1.10	0.718				
CD103+ (>median) [a]	0.52	<0.001	0.67	0.027		
CD103+ (continuous) [b]	0.99	<0.001			0.99	0.024

Cox regression analysis for disease-specific survival AC: Adenocarcinoma SCC: Squamous Cell Carcinoma

CD103+ TIL *in situ* are characterized by ongoing TGFbR1-signaling

We and others have demonstrated that CD103 is upregulated on T cells following concomitant T cell and transforming growth factor (TGF)-β receptor (TGFβR) signaling.[31–35] Indeed, CD103+, but not CD103-, TIL in high-grade serous ovarian cancer are characterized by nuclear phosphorylated mothers against decapentaplegic homolog 2 and 3 (pSMAD2/3) expression, a hallmark of TGF-β signaling. To confirm signs of active TGF-β signaling in CD103+ TIL from SCC, paraffin-embedded tissue was probed by fluorescent microscopy for simultaneous expression of CD8, CD103 and nuclear pSMAD2/3. SCC tumor islets, the surrounding stroma cells, and CD103- and CD103+ TIL were all characterized by a pronounced nuclear expression of pSMAD2/3 (Figure 4) suggesting TGFβR1-signaling is highly active in the cervical cancer microenvironment, but not restricted to CD103+ TIL. In healthy cervical tissue, pSMAD2/3 signaling was also abundant in epithelial, stromal, CD8+ and CD103+ cells (Supplementary Figure 5).

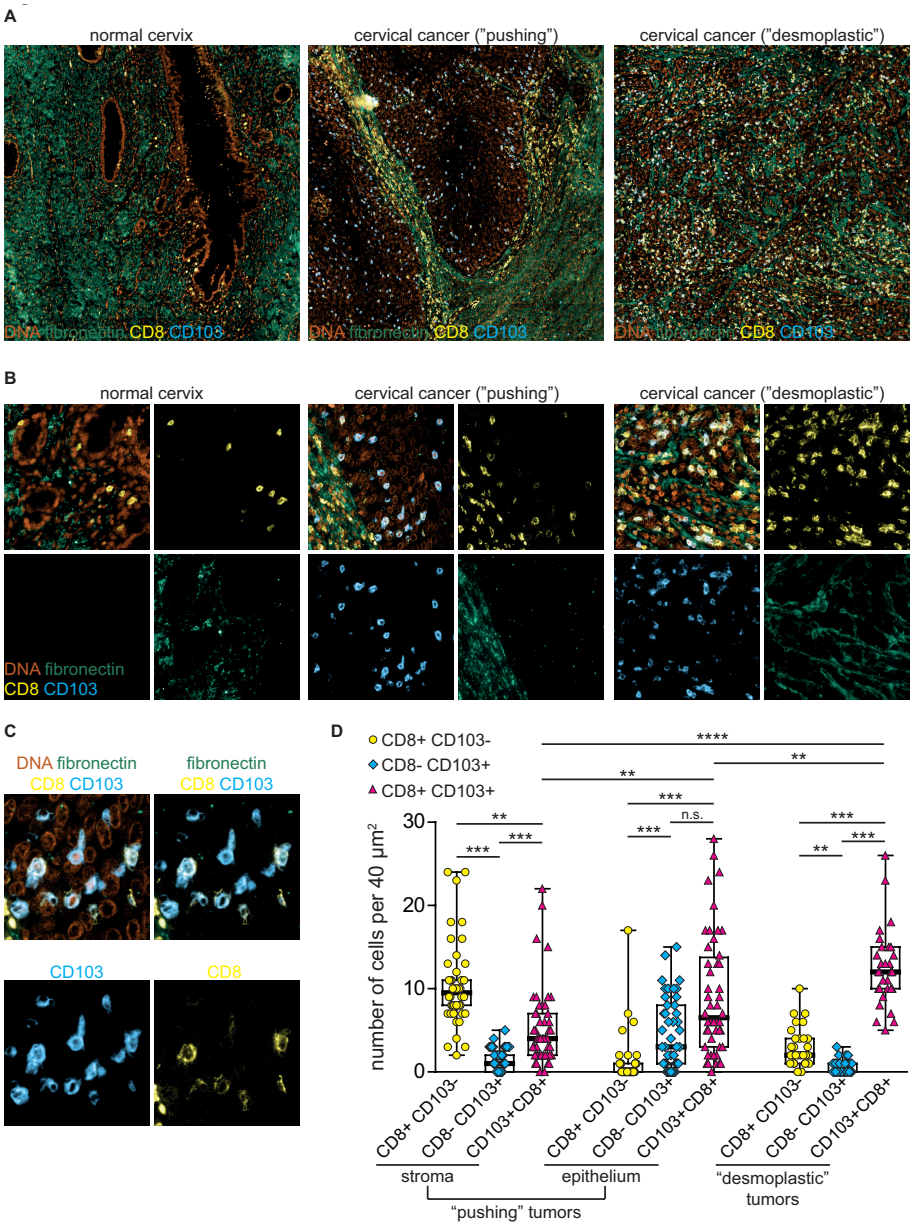

FIGURE 3. CD103 demarcates intraepithelial CD8+ TIL in cervical cancer tissue. A) Representative image of tissue from a normal cervix, from a patient with cervical cancer of the "pushing" type and of a patient with cervical cancer of the "desmoplastic" type stained with DAPI (DNA, orange), anti-CD8 (yellow), anti-CD103 (blue) and anti-fibronectin (green) antibodies. **B)** Representative images of CD8+ and CD103+ cells in the epithelial or stromal areas of 40 µm² of tumor tissue. **C)** Representative single and multichannel images of tumor areas showing co-expression of CD8 and CD103. **D)** Quantification of single CD8+, single CD103+ or CD8+ CD103+ double-positive cells in the stroma and epithelial areas of the "pushing" tumors or total of the "desmoplastic" tumors. Each data point represents a cell count from a 40µm² independent region of 18 independent tumors (3-6 in total per tumor section). Groups were compared by ANOVA using a Dunns post-test. * $p<0.05$, ** $p<0.01$, *** $p<0.001$.

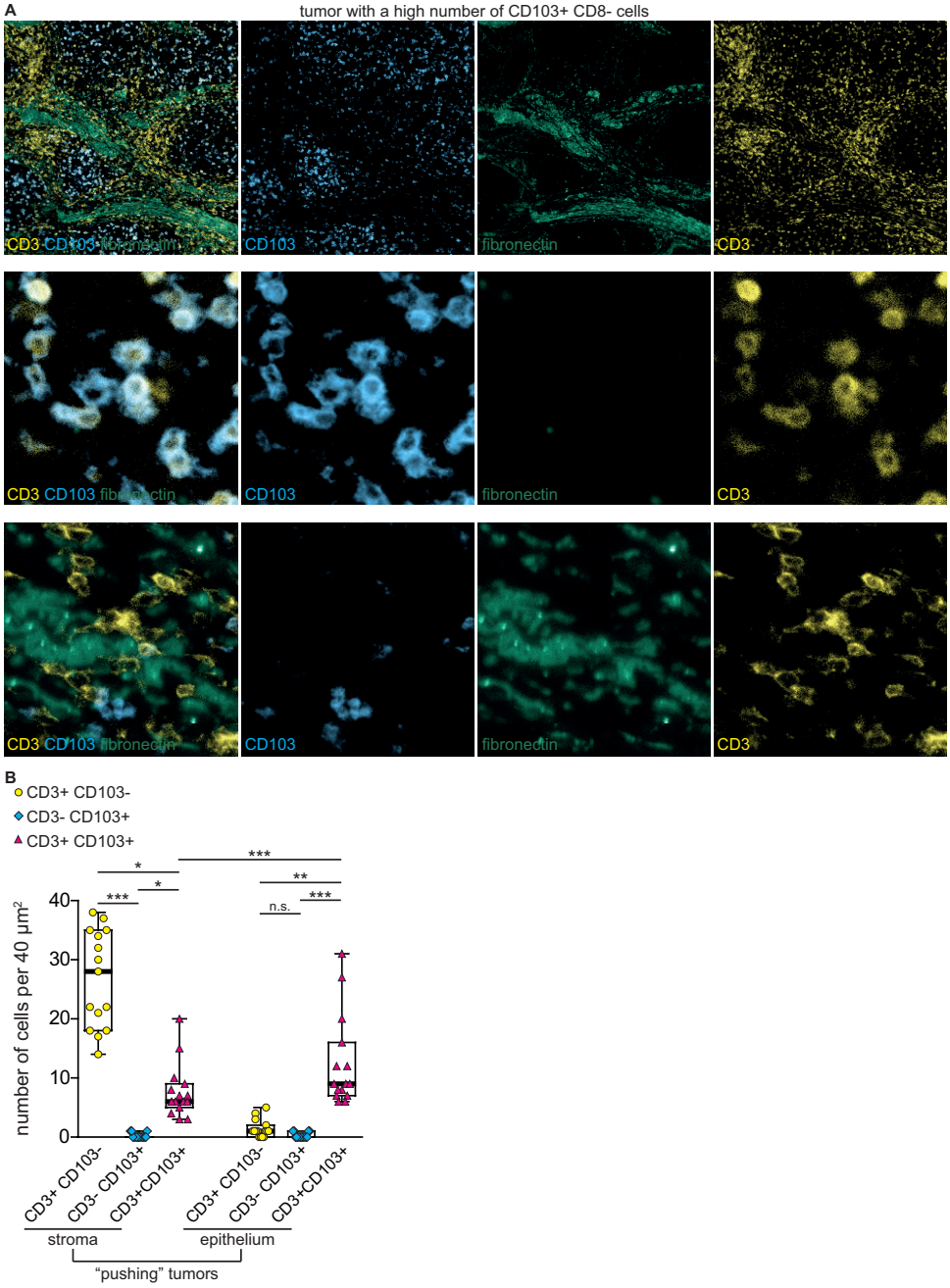

SUPPLEMENTARY FIGURE 2. CD103+ TIL in cervical cancer express CD3. A) Representative images and **B)** quantification of tissue from patients with cervical cancer stained with DAPI (DNA, orange), anti-CD3 (yellow), anti-CD103 (blue) and anti-fibronectin (green) antibodies. Each data point represents a cell count from a 40µm² independent region of 5 pre-selected tumors based on CD103 infiltration (3 areas were counted in total per tumor section). Groups were compared by ANOVA using a Dunns post-test. * $p<0.05$, ** $p<0.01$, *** $p<0.001$.

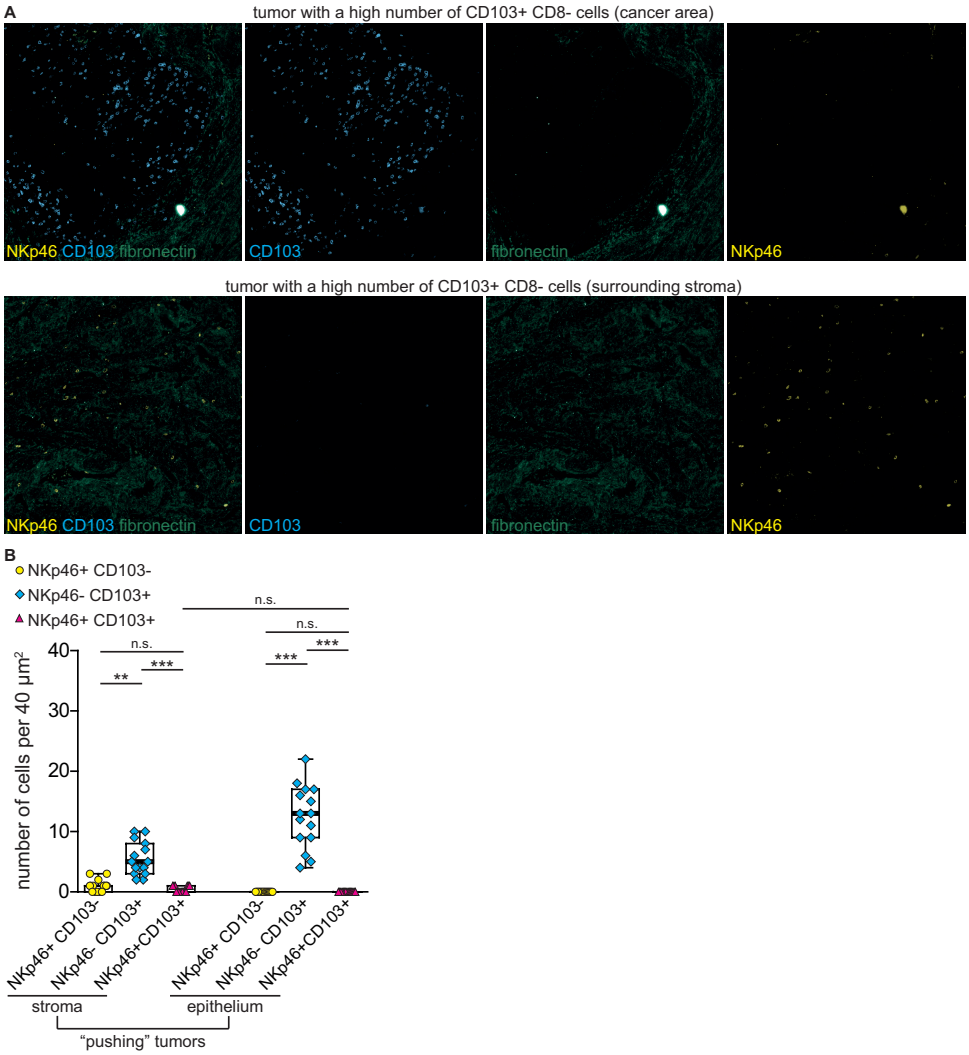

SUPPLEMENTARY FIGURE 3. CD103+ TIL in cervical cancer do not express NKp46. A) Representative images and **B)** quantification of tissue from patients with cervical cancer stained with DAPI (DNA, orange), anti-NKp46 (yellow), anti-CD103 (blue) and anti-fibronectin (green) antibodies. Each data point represents a cell count from a 40µm^2 independent region of 5 pre-selected tumors based on CD103 infiltration (3 areas were counted in total per tumor section). Groups were compared by ANOVA using a Dunns post-test. * $p<0.05$, ** $p<0.01$, *** $p<0.001$.

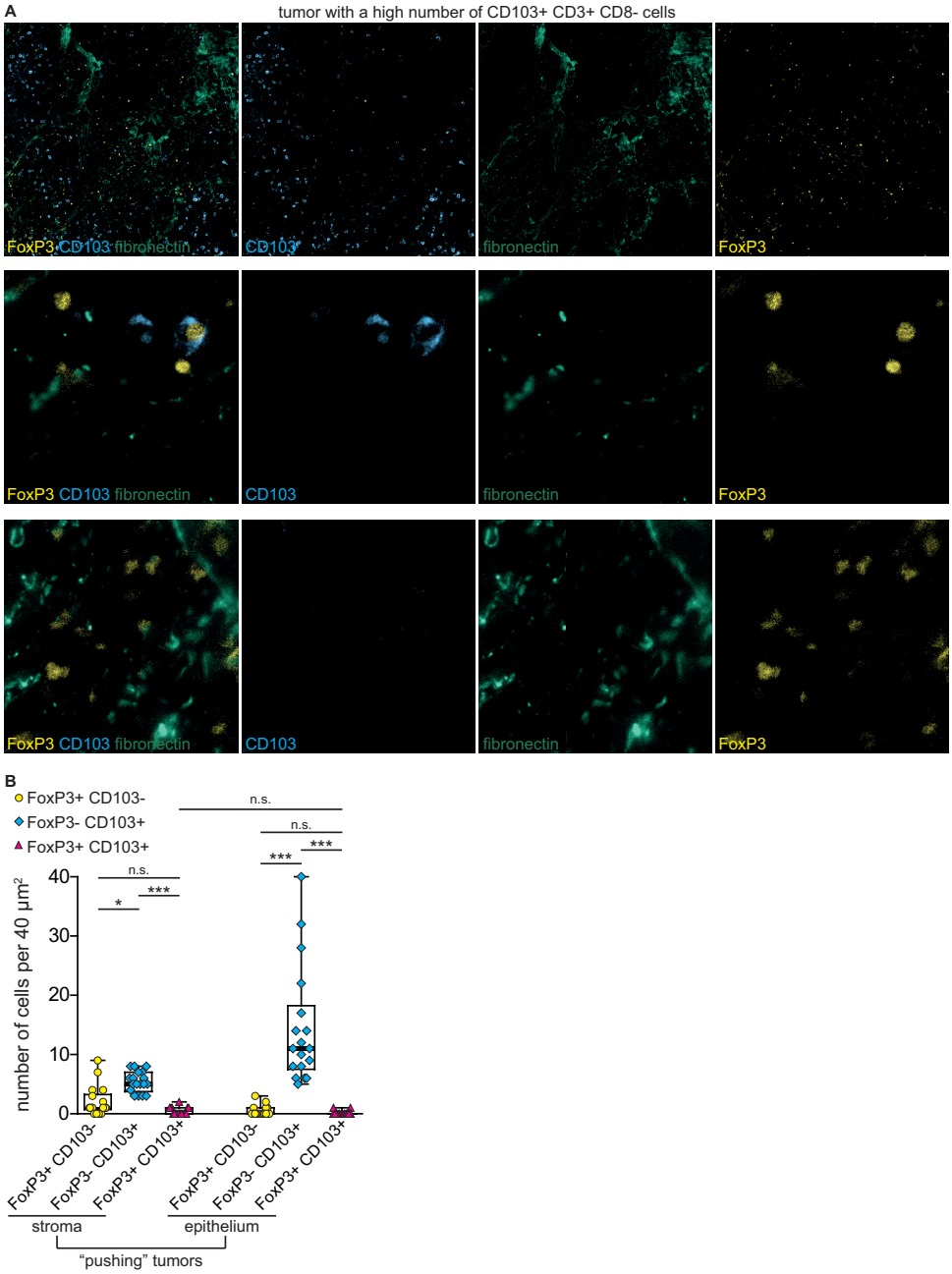

SUPPLEMENTARY FIGURE 4. CD103+ TIL in cervical cancer tissue minimally express FoxP3. A) Representative images and **B)** quantification of tissue from patients with cervical cancer stained with DAPI (DNA, orange), anti-FoxP3 (yellow), anti-CD103 (blue) and anti-fibronectin (green) antibodies. Each data point represents a cell count from a 40µm² independent region of 5 pre-selected tumors based on CD103 infiltration (3 areas were counted in total per tumor section). Groups were compared by ANOVA using a Dunns post-test. * $p<0.05$, ** $p<0.01$, *** $p<0.001$.

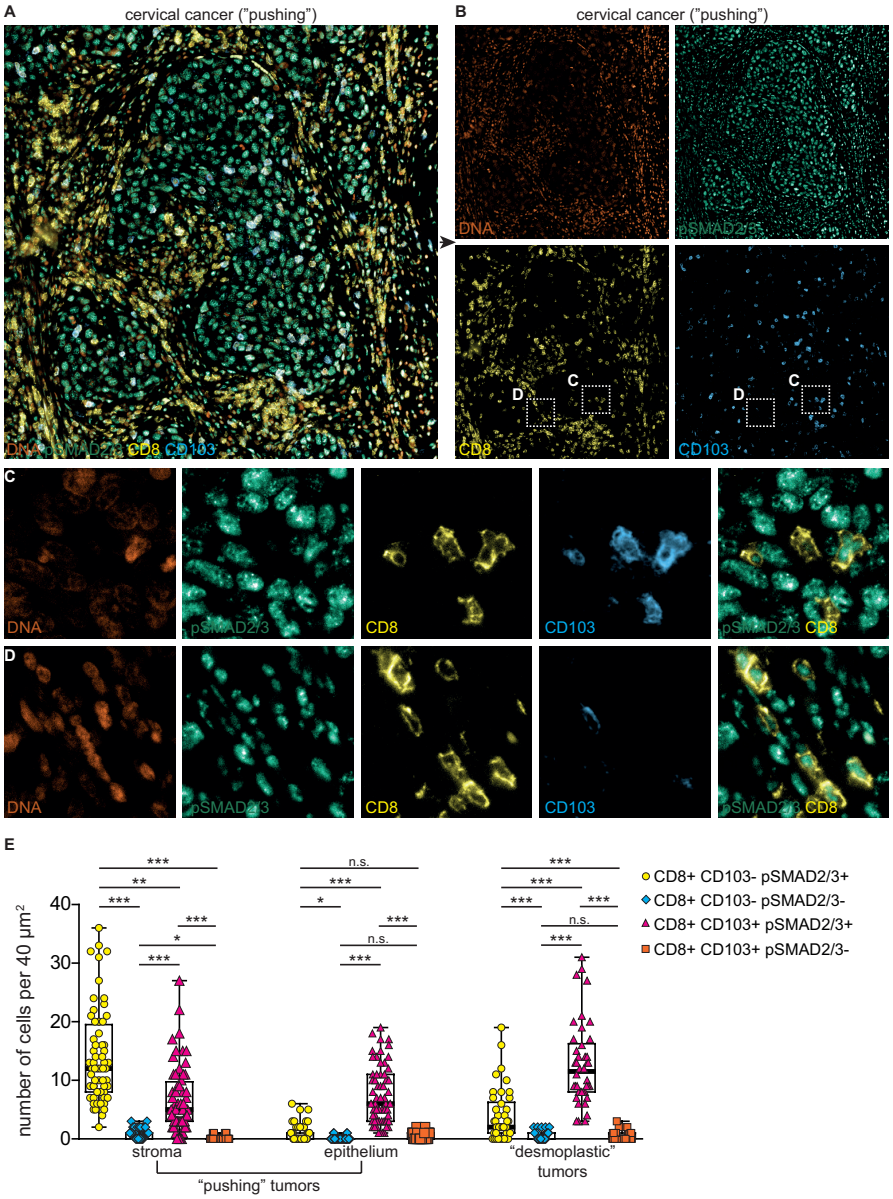

FIGURE 4. TGF-β signaling is abundant in cervical cancer tissue. A) Representative image of tissue from a patient with cervical cancer of the "pushing" type stained with DAPI (DNA, orange), anti-CD8 (yellow), anti-CD103 (blue) and anti-pSMAD2/3 (green) antibodies. **B)** Representative single and multichannel images of the tumor area from A showing predominant localization of CD8+ cells in the pSMAD2/3+ stromal region and CD8+ CD103+ cells in the pSMAD2/3+ epithelial region. Insets represent areas magnified in panels C and D. **C-D)** Representative images of CD8+ and CD103+ cells in magnified epithelial (C) or stromal areas (D) of tumor tissue as indicated by insets in B. **E)** Quantification of CD8+, CD103+ and/or pSMAD2/3+ cells in the stroma and epithelial areas of the "pushing" tumors or total of the "desmoplastic" tumors. Each data point represents a cell count from a 40µm² independent region of 18 independent tumors (3-6 in total per tumor section). Groups were compared by ANOVA using a Dunns post-test. * $p<0.05$, ** $p<0.01$, *** $p<0.001$.

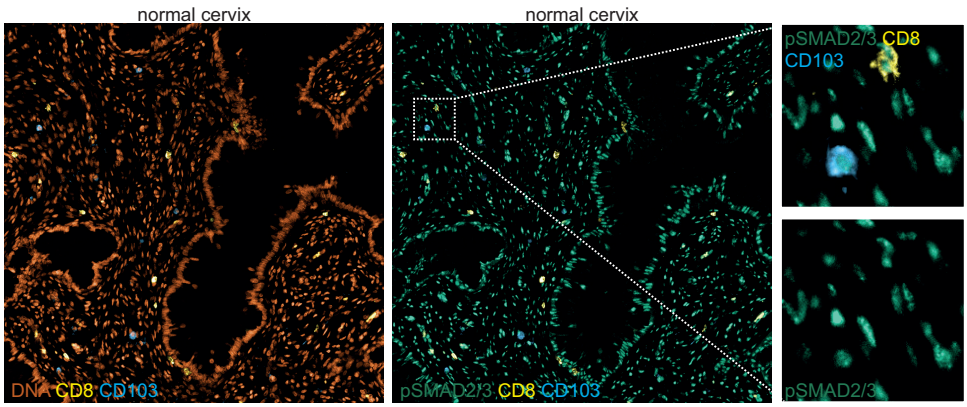

SUPPLEMENTARY FIGURE 5. TGF-β signaling in untransformed cervical cancer tissue. Representative image of normal cervical tissue stained with DAPI (DNA, orange), anti-CD8 (yellow), anti-CD103 (blue) and anti-pSMAD2/3 (green) antibodies.

Anti-tumor therapeutic efficacy is mediated by recruitment of CD103+ TIL *in vivo*

Finally, to determine whether CD103 could also be used as a response biomarker for immunotherapy targeting E6 and E7, we used the E6/E7-transformed TC1 mouse model.[36] TC-1 cells are derived from primary epithelial cells of C57BL/6 mice co-transformed with HPV-16 E6 and E7 and c-Ha-ras oncogenes. These cells form tumors composed largely of epithelial cells after subcutaneous injection and should therefore induce CD103 on infiltrating CD8+ T cells. Based on the differential prognostic effects of radiotherapy observed in both the TCGA and IHC series, we also assessed whether radiotherapy synergized with E6/E7-specific antitumor immune responses *in vivo* using our previously published experimental setup[36] (Figure 5A). In brief, female C57BL/6 mice were challenged with TC1 tumors and treated with a suboptimal immunization regimen of $5x10^6$ i.u. semliki forest virus (SFV)eE6,7 immunization 14 days after tumor inoculation with or without radiation. At this dose, immunization alone is insufficient at inducing tumor eradication and synergizes with ionizing radiation. After 22 days mice were sacrificed, tumors were measured and digested.

For flow cytometric analysis, TC1 Tumor digests were gated on lymphocyte singlets and subsequently on DAPI- live cells (Figure 5B). Within the TC1 tumor digests, untreated mice showed ~10% CD8+ CD103+ cells (Figure 5C-D). Therapeutic SFVeE6/E7 vaccination increased the intratumoral number of CD8+ CD103+ T cells to ~25%, an effect that further synergized with concomitant irradiation to ~60% (representative plots in Figure 5C). Irradiation alone resulted in a ~10% CD8+ CD103+ T cell infiltration (Figures 5C-D). Within all treatment groups, and independent of the number of infiltrating cells, CD103+ cells were almost exclusively CD8+ T cells (Figure 5C). As expected, the percentage of infiltrating CD8+ CD103+ T cells across all

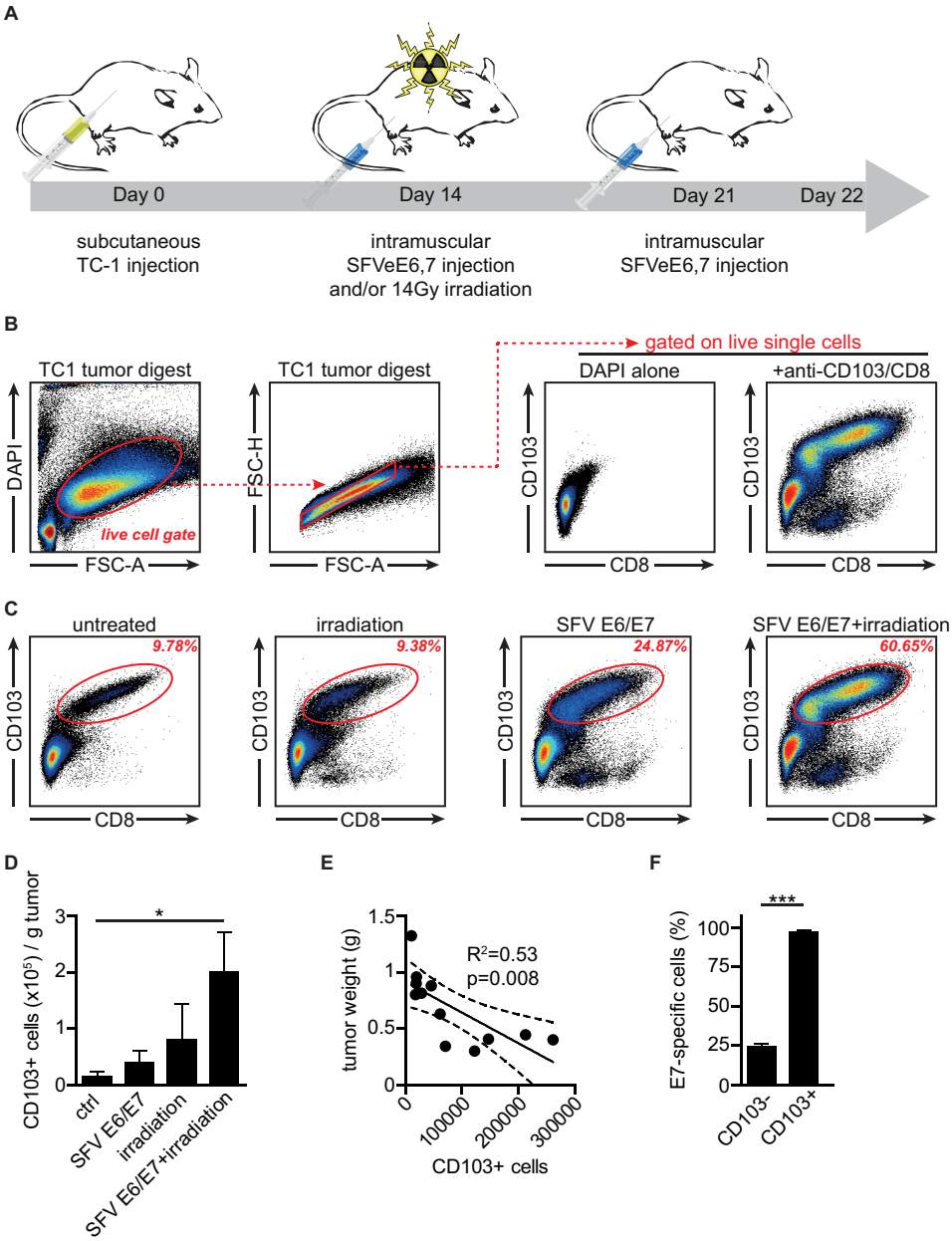

FIGURE 5. Combination immunotherapy targeting HPV E6 and E7 induces accumulation of CD103+ cells *in vivo*. A) Schematic depiction of the TC1 mouse model. **B)** Representative flow cytometric plot of a TC1 tumor digest analyzed for expression of CD103 and CD8 within the DAPI-negative live cell population. **C)** Representative flow cytometric plots of TC1 tumor digests from untreated mice or mice treated with irradiation, a low dose of SFV E6/E7 vaccine, or both analyzed for expression of CD8 and CD103 within the DAPI-negative live cell population. **D)** Bar graphs representing the absolute number of CD103+ cells per gram of tumor of the experimental groups (n=3-6). **E)** Scatter plots representing the number of CD103+ cells per gram of tumor across all groups (n=3-6). **F)** Percentage of E7-specific CD8+ T cells across all treatment groups. * $p<0.05$.

treatment groups was negatively correlated to tumor weight (Figure 5E; R^2=0.53 p=0.008). Finally, analysis of E7-reactive T cells using E7 H-2Kb dextramer staining revealed E7-specificity to be largely restricted to the CD103+ T cell population (Figure 5F).

DISCUSSION

In the present study we demonstrate that infiltrating CD103+ T cells are a prognostic factor for survival in cervical cancer patients. By gene expression analysis on tumor samples from cervical cancer patients available within the TCGA dataset, we showed that expression of *ITGAE*, the gene encoding for CD103, correlates with significantly improved survival. This prognostic benefit of CD103-expressing T cells was confirmed in an independent cohort of 460 cervical cancer patients by immunohistochemical analysis of CD103+ TIL in FFPE-tumor cores. Furthermore, we show that CD103 is a marker for intraepithelial CD8+ T cells in cervical cancer. Finally, we demonstrate that CD103 holds considerable promise as both a predictive and response biomarker for radiotherapy and/or E6/E7-targeted immunotherapy.

Our results in the cervical cancer cohorts are in line with earlier findings on the localization and prognostic influence of CD103+ TIL in endometrial, ovarian, bladder and lung cancer. However, in contrast to other malignancies, infiltration of cervical cancers was related to the type of treatment patients received and the stage of disease. Patients that were treated with radio(chemo)therapy alone or in combination with surgery had fewer infiltrating CD103+ TIL compared to patients that qualified for surgical treatment alone. Moreover, within the radio(chemo)therapy group, patients that presented with a higher stage of disease were characterized by even lower numbers of CD103+ TIL when compared to patients with lower FIGO stages. This strongly suggests an interference of T cells and tumor cells where an equilibrium is reached in the early stages of disease, whereas larger tumors have escaped immune control by T cells and advanced stages of the disease are able to develop.[37] As a result, patients with immunological 'hot' tumors generally present with an early stage of disease, whereas patients with immunological 'cold' tumors show a more aggressive disease with indications for primary (locally advanced disease) or adjuvant radio(chemo)therapy treatment (e.g. positive resection margins after surgery or positive lymph nodes).

In addition to the reduced number of infiltrating cells in clinically more aggressive cancers, analysis of the TCGA cervical cancer data set shows that *ITGAE* expression is not only strongly associated with the common T cell genes such as CD8A, but more importantly also with T cell activation and exhaustion markers such as CD137, CTLA4, PD1, and PDL1. This suggests that these patients may be candidates for additional adjuvant therapy with immune checkpoint inhibitors such as antibodies targeting CTLA-4 (ipilimumab) or PD-1 (nivolumab/pembroluzimab). In patients

with melanoma and non-small cell lung cancer in particular, immune checkpoint inhibitors have met with considerable clinical success. In these malignancies, responses to immune checkpoint inhibitors have been strongly linked to the presence of neo-antigens in cancer cells (particularly those expressed across lesions) that provide a true tumor-specific target for T cells for which tolerance has likely not been established.[38,39] In cervical cancer, the constitutive expression and the viral nature of E6/E7 oncoproteins in malignant cells is likely to provide a similar strong and non-tolerant target for T cell recognition that may be exploited with immune checkpoint inhibitors.

One caveat herein may be the poor infiltration of these tumors by immune cells. Indeed, as discussed above, aggressive tumors at higher stages of the disease show relatively poor infiltration by CD103+ TIL that may preclude effective responses to checkpoint inhibition. In one melanoma trial, a high number of preexisting T cells was a determinant for subsequent responses to therapy with anti-PD1 antibody pembroluzimab. In the absence of a strong T cell response, additional therapeutic strategies may therefore be required to pre-condition these patients for therapy with checkpoint inhibitors.[40] One promising approach is the use of therapeutic vaccins targeting the E6/E7 oncoproteins. Indeed, several clinical trials have demonstrated promising results in CIN and cervical cancer patients treated with therapeutic E6/E7 targeted vaccines.[11,16,18,19,41] In one study using a therapeutic DNA vaccine, seven out of nine CIN3 patients showed complete regression and viral clearance within 36 weeks of follow up.[16] In a randomized, double-blind, placebo-controlled trial in CIN2/3 patients, 49.5% of the DNA vaccine recipients showed regression of the disease versus 30.6% in the control group.[11] These promising results may eventually lead to a change in treatment strategy for CIN 2/3, in which therapeutic vaccination could represents a non-surgical option.

In this work, we similarly demonstrate that an E6/E7-targeted SFV vaccine can induce accumulation of CD103+ T cells in tumors *in vivo*, an effect that synergized with radiotherapy. SFV E6/E7 vaccination therefore not only promotes systemic immune responses, but T cells induced by this vaccination effectively penetrate the tumor lesion and engage the epithelial cells present, resulting in CD103 upregulation. Importantly, all infiltrating cells in this model were CD8+, in line with the phenotype observed in the human setting.

With regards to this phenotype and ontogeny of CD103+ TIL in human tumors the literature remains diverse. In the gut, CD103 has been described to be expressed on Intra-epithelial Lymphocytes (IEL), characterized by a CD8αα+ phenotype.[42,43] In NSCLC the phenotype of CD103+ TIL has been described as tissue-resident memory T cells (characterized by a CD69+ CD62L− CD28− CD27+ CD45RA+ CD45RO+ CCR7- phenotype).[24] In endometrial cancer CD103+ TIL were of heterogenous memory phenotypes,[34] and in HGSC, CD103+TIL were classical CD3+ CD56- TCRab+ CD8ab+ CD4- T cells, also with heterogeneous differentiation status.[35] While

we demonstrate dominant CD8 co-expression in cervical cancer, the precise differentiation status has not been investigated. We hypothesize that, as the cervix functions as a barrier against pathogens, CD103 tissue-resident memory T cells may also be present. However, in the context of tumor specific (E6/E7-directed) immune responses, the majority of CD103+ TIL are likely recruited as a result of an adaptive immune response. Within cervical cancer tumor slides, we also show that CD103+ CD8- TIL expressed CD3 but were negative for NkP46 and FoxP3, suggesting a CD4 but not a NKT cell nor a Treg origin.

Interestingly, when analyzing the fluorescent images of the tumor tissue we noticed different patterns of stromal infiltration into the epithelial areas, namely a pushing and desmoplastic type.[30] The pushing tumor type was characterized by a distinct separation of epithelial and stromal areas. Whereas in the desmoplastic tumor type, a separation between stromal versus epithelial areas could not be made. The desmoplastic tumor type has been described in literature as a more invasive tumor, but the exact consequences of this remains unclear. Interestingly, we observed that the desmoplastic tumors contained an even higher percentage of CD8+ CD103+TIL when compared to the pushing type. This might suggest that the desmoplastic tumors are more accessible to infiltration of CD8+ T cells which then engage the epithelial tumor cells and upregulate CD103 after T cell receptor (TCR) activation.

In line with this hypothesis, our data strongly suggests that upregulation of CD103 in cervical cancer is mainly the result of TCR signaling upon cancer cell contact. It has been well established that ITGAE (CD103) expression is induced by dual TCR and TGFβR1 activation.[32,33,44] In HGSC, we have further shown that CD103+, but not CD103-, TIL are characterized by nuclear pSMAD2/3 expression, a hallmark of TGF-β signaling.[35] In contrast to HGSC tissue, the total tumor micro environment in cervical cancer tissue was rich in pSMAD2/3 expression and no differences in expression between epithelial and stromal areas were observed. This TGF-β rich microenvironment might be explained by the E6/E7-dependent ontogeny of cervical cancer. HPV-16 E6 and E7 oncoproteins have been shown to directly regulate the TGF-beta1 promoter in cervical tumor cells through a specific DNA sequence motif in the TGF-beta1 core promoter.[45] It is thought the upregulation of TGF-beta facilitates the development of cervical neoplasia after E6/E7 integration by promoting genomic instability in the infected epithelial cells.[46] As a consequence, the immune environment is rich in TGF-beta expression likely rendering T cell contact with the cancer cell as the key determinant of CD103 induction. CD103 may therefore represent an excellent biomarker for tumor-reactive T cells in cervical cancers that could be quantified in a rapid manner without having to account for epithelial versus stromal compartments. It is tempting to speculate that the same may therefore hold true for other types of HPV-mediated cancers, such as head and neck squamous cell carcinoma (HNSCC). Indeed, TGF-beta is overexpressed in ~80% of HNSCC cases [47] and likely produced by both cancer cells,

stroma, and/or infiltration immune cells (reviewed in Yang et al.[48]) It will be interesting to assess whether differences exist between CD103+ cells infiltration in HPV-positive versus HPV-negative HNSCC tumors, as has been reported for CD8+ cells.[49]

This use of CD103 as an easy-to-use biomarker for assessing immune responses against cervical cancer is supported by our *in vivo* data that demonstrate increased infiltration of TC1 tumors by CD103+ CD8+ cells upon treatment with a synergizing combination of HPV E6/E7 vaccination and radiotherapy. Indeed, an inverse correlation exists between the number of CD103+ cells in the tumor digest and the size of the tumor. With the clinical advent of therapeutic E6/E7-based vaccination strategies, CD103 may be incorporated both for patient selection and for monitoring early therapy responses in the tumor by biopsy. Of note, clues for synergistic effects on tumor control for radiation and E6/E7-targeted therapy in the human setting were also found in this study. In particular, the prognostic benefit of CD103+ cell infiltration in both the TCGA and IHC datasets were found within the group of patients that received adjuvant radio(chemo) therapy within 6 months of surgical intervention, but not in patients that received surgery alone. Assuming infiltrating T cells in most patients react against E6/E7 proteins to a certain extent, it is tempting to speculate that the pre-existing immune responses are augmented by the radiotherapy, similar to what was observed in the animal model. Future studies on clinical vaccination in combination with radiotherapy therefore appear warranted in this patient population.

Taken together, we demonstrate here for the first time that CD103 is a suitable marker for rapid unbiased assessment of prognostically beneficial CD8+ T cell infiltration of cervical cancers and might be used as a response biomarker for E6/E7-targeted immunotherapy alone or in combination with radiotherapy.

METHODS

TCGA data and analysis

TCGA RSEM normalized[50] RNAseq and clinical data were downloaded from FireBrowse (http://firebrowse.org) on August 22nd, 2016. After removal of normal tissue controls and technical duplicates, 304 cervical cancer cases were informative for this study. RNAseq data were log2 transformed prior to further analysis. The expression of CD103 (*ITGAE*) relative to that of other immune markers[51] was visualized by means of a heatmap using GENE-E (Broad Institute). For analysis of CD103 expression with clinicopathological variables and patient survival, cases were dichotomized according to median CD103 expression. Analyses of clinical outcome excluded 13 patients for whom survival data were not available. For the exploratory analyses of the relationship

between CD103 expression, radiotherapy treatment and clinical outcome, we excluded cases in which radiotherapy was given ≥6 months after diagnosis, to avoid misclassification of patients irradiated after disease recurrence.

Patient selection for the immunohistochemical series

Clinicopathological characteristics of cervical cancer patients treated within the University Medical Center Groningen were prospectively stored in a database since January 1980. As described by Maduro et al,[52] a separate anonymized database was retrieved containing all patients with stage IA2-IVA cervical cancer. Patients were treated between January 1980 and December 2004 with either surgery or radiotherapy depending on stage of disease and/or results of surgical outcome. We categorized patients into two groups based on their treatment modality, namely surgery or radio(chemo)therapy. The treatment modality was considered surgery in those patients in whom a radical hysterectomy combined with pelvic lymph node dissection was performed (first choice of treatment in early stage disease). The treatment modality was considered radio(chemo) therapy (first choice of treatment in locally advanced disease) if patients received radiotherapy or radio-chemotherapy, even if a surgical procedure was performed, as is the case in e.g. patients where positive nodes are detected after primary hysterectomy/lymph node dissection. Patients were selected if sufficient formalin-fixed, paraffin-embedded (FFPE) tissue was available for tissue microarray (TMA) construction. For the construction of the TMA, only pretreatment biopsies were used. Follow up data was collected up to April 2012. According to Dutch law, no approval from our institutional review board was needed.

Tissue microarray (TMA) construction

From the patients meeting the inclusion criteria, a TMA was constructed as described previously.[53] In brief, cancer nests were determined by a gynecologic pathologist based on H&E staining. Triplicate 1mm^2 cores were randomly selected from cancer nests and placed in a recipient paraffin block by a tissue microarrayer (Beecher instruments). After insertion of cores, recipient blocks were placed at 37°C for 15 minutes in order to maximize tissue adhesion to the wax. The paraffin block was sliced into 4µm sections and placed on APES-coated slides (Starfrost).

Immunohistochemical analysis of CD103+ TIL infiltration

TMA sections were dewaxed in xylene and rehydrated using degraded concentrations of ethanol to distilled water. Antigen retrieval was initiated using a preheated 10mM citrate buffer (pH6), endogenous peroxidase activity was blocked by submerging of sections in a 0.45% H_2O_2 solution. Sections were incubated in a blocking buffer (1% human AB serum in 1% BSA/PBS solution), followed by an avidin/biotin block. Afterwards, sections were incubated with rabbit-anti human CD103 mAb (anti-αEβ7-integrin, Abcam, ab129202, 1:200 in blocking buffer) and incubated at 4°C overnight. Slides were incubated with a peroxidase-labeled polymer (Envision+ anti-rabbit

Dako) and a Biotin Tyramide working solution according to the manufacturer's instructions (TSA Kit Perkin Elmer, NEL700A001KT). Subsequently, slides were incubated with streptavidin-HRP (dilution: 1:100) (TSA kit, Perkin Elmer) and specific signal visualized by 3,3'diaminobenzidin (DAB). Slides were counterstained with hematoxylin.

The total number of positively stained CD103+ cells was counted per core and the percentage of tumor/stromal surface was estimated. Patients were included if at least two cores contained >20% tumor epithelium. All slides were counted manually by two individuals that were blinded for clinicopathological data. The two individual scores were compared and differences in counts of over 10% were reanalyzed until consensus was reached. Cell count was re-calculated per 1 mm^2 (i.e. the surface of one core).

Immunofluorescent analysis of CD103+ TIL localization and phenotype

Preparation, antigen retrieval and incubation with primary CD103 antibody of full tumor slides was performed as described in immunohistochemistry (IHC). Sections were subsequently incubated with Envision-HRP anti-rabbit followed by fluorophore tyramide stock solution:amplification diluents (TSA KIT Perkin Elmer,1:50) according to the manufacturer's instructions. Slides were incubated overnight at 4°C with either biotinylated rabbit anti-fibronectin (Abcam, ab6584 1:50 in blocking buffer) or rabbit anti-phospho-SMAD2/3 Mab (cell signaling, Ser 465/467 #3101, 1:50 in blocking buffer), and either mouse anti-human CD8 (DAKO, clone C8/144B, M710301-2, 1:25 in blocking buffer), anti-NKp46 (R&D Systems, ab1850, 1:25 in blocking buffer), anti-CD3 (Abcam, ab11089, 1:25 in blocking buffer) or anti-FoxP3 (Abcam, ab20034, 1:50 in blocking buffer) antibodies. Sections were subsequently incubated with goat-anti-mouse Alexa Fluor 555 (Life Technologies, Eugene,1:150) and streptavidin dylight 488 (Life Technologies, 1:150) Nuclei were visualized with DAPI. Sections were embedded in prolong Diamond anti-fade mounting medium (Life Technologies, Eugene) and scanned using a TissueFaxs imaging system (TissueGnostics). Processed channels were merged using Adobe Photoshop. On each slide three to six representative epithelial and three to six stromal areas of 40 μm^2 were selected based on DAPI staining. Within each area, single-positive (CD103-CD8+ or CD103+CD8-) cells as well as double-positive (CD103+CD8+) cells were counted manually.

Mice

Specified pathogen-free female C57BL/6 mice were used at 8 to 12 weeks of age at the onset of the experiment. They were purchased from Harlan CPB (Zeist, The Netherlands) and kept according to institute guidelines. All animal experiments were approved by the local Animal Experimentation Ethical Committee.

Tumor inoculation, local tumor irradiation and rSFV immunization

TC-1 cells were a kind gift from Dr. Cornelis J. Melief and Dr. Rienk Offringa (Leiden University Medical Center, The Netherlands). The TC-1 cell line was generated from C57Bl/6 primary lung epithelial cells with a retroviral vector expressing HPV16 E6E7. All cells were cultured as described before.[54] Mice were inoculated subcutaneously in the neck with 2×10^4 TC-1 cells suspended in 0.2 mL Hank's Balanced Salt Solution (Invitrogen,). Fourteen days after injection of TC-1, mice were locally irradiated with 14Gy and/or semliki forest virus (SFV)eE6,7 immunization. Radiation was performed using X-RAD 320 Biological Irradiator (Precision X-Ray) with a delivery rate of 1.64 Gy/min. Immunization was performed intramuscularly with a dose of $5x10^6$ i.u. of SFVeE6,7 and boosted twice with a one-week interval (day 14 and 21) as a suboptimal immunization regimen. Control mice were injected intramuscularly with PBS. Tumors were isolated 22 days after TC-1 inoculation.

Tumor digestion and flow cytometry analysis

Tumors isolated from mice were processed as previous described[51]. In brief, pre-warmed Collagenase A (Roche) solution was used for digestion and tumors were homogenized using the gentle MACStm Dissociator (Miltenyi Biotec). Tumors cells were further stained with PeCy7-anti-CD8 (eBioscience, clone 53-6.7, 25-5273-41) and FITC-anti-CD103 (BD Biosciences, clone 2E7, 333155). For the dextramer staining, cell suspensions were first washed twice in FACS buffer (PBS containing 0.5% bovine serum albumin) and stained with PE-H-2D^b $E7_{49-57}$ dextramers (Immudex, Copenhagen, Denmark) for 10 min at room temperature. Subsequently, the cells were stained with PE-Cy7-anti-CD8a Ab and FITC-anti-CD103 Ab. To exclude dead cells, cells were stained with Zombie Violet™ (Biolegend, 423113).

Statistics

Differences in cell count were determined by a Mann-Whitney U, Kruskall-Wallis, ANOVA or t-test. Disease-specific survival (DSS) and disease-free survival (DFS) were analyzed using a Kaplan-Meier function; differences in survival were assessed by log Rank test. DSS was defined as date of diagnosis to date of death due to disease. DFS was defined as date of diagnosis to date of recurrence or date of death of disease, in case no recurrence was reported previously. Differences in DSS and DFS according to clinicopathologic characteristics and to infiltration of CD103+ TIL were analyzed using the Cox regression analyses. Variables with a p-value <0.05 in the univariate analyses were included in the multivariate analyses. Significance was defined as a p-value of <0.05, all tests were performed two-sided. Statistics were performed using SPSS software version 22.0 (SPSS inc.), Stata (StataCorp,) or GraphPad Prism (GraphPad Software inc.).

ACKNOWLEDGEMENTS

This work was supported by Dutch Cancer Society/Alpe d'Huzes grant UMG 2014–6719 to MB and a Jan Kornelis de Cock Stichting grant to FLK. DNC is supported by a Clinician Scientist Award from the Academy of Medical Sciences / Health Foundation, and has received funding from the Oxford Cancer Centre, University of Oxford. Part of the work has been performed at the UMCG Imaging and Microscopy Center (UMIC), which is sponsored by NWO-grants 40-00506-98-9021 and 175-010-2009-023.

The authors would like to thank Klaas Sjollema for his technical assistance.

Disclose statement: HW Nijman and T Daemen have a financial ownership interest in ViciniVax and may financially benefit if the company is successful in marketing its product related to this research. The terms of this arrangement have been reviewed and approved by the University of Groningen.

REFERENCES

1. Kjaer SK, van den Brule AJC, Paull G, Svare EI, Sherman ME, Thomsen BL, Suntum M, Bock JE, Poll PA, Meijer CJLM. Type specific persistence of high risk human papillomavirus (HPV) as indicator of high grade cervical squamous intraepithelial lesions in young women: population based prospective follow up study. BMJ [Internet] 2002 [cited 2015 Oct 8]; 325:572.
2. Remmink AJ, Walboomers JM, Helmerhorst TJ, Voorhorst FJ, Rozendaal L, Risse EK, Meijer CJ, Kenemans P. The presence of persistent high-risk HPV genotypes in dysplastic cervical lesions is associated with progressive disease: natural history up to 36 months. Int J Cancer [Internet] 1995 [cited 2015 Aug 26]; 61:306–11.
3. Kalinski P, Mailliard RB, Giermasz A, Zeh HJ, Basse P, Bartlett DL, Kirkwood JM, Lotze MT, Herberman RB. Natural killer-dendritic cell cross-talk in cancer immunotherapy. Expert Opin Biol Ther [Internet] 2005 [cited 2016 Jan 11]; 5:1303–15.
4. Blankenstein T, Qin Z. The role of IFN-gamma in tumor transplantation immunity and inhibition of chemical carcinogenesis. Curr Opin Immunol [Internet] 2003 [cited 2016 Jan 11]; 15:148–54.
5. Mellman I, Coukos G, Dranoff G. Cancer immunotherapy comes of age. Nature [Internet] 2011 [cited 2014 Jul 9]; 480:480–9.
6. Gorter A, Prins F, van Diepen M, Punt S, van der Burg SH. The tumor area occupied by Tbet+ cells in deeply invading cervical cancer predicts clinical outcome. J Transl Med [Internet] 2015 [cited 2016 Sep 14]; 13:295.
7. de Vos van Steenwijk PJ, Ramwadhdoebe TH, Goedemans R, Doorduijn EM, van Ham JJ, Gorter A, van Hall T, Kuijjer ML, van Poelgeest MIE, van der Burg SH, et al. Tumor-infiltrating CD14-positive myeloid cells and CD8-positive T-cells prolong survival in patients with cervical carcinoma. Int J cancer [Internet] 2013 [cited 2016 Sep 14]; 133:2884–94.
8. Sasagawa T, Takagi H, Makinoda S. Immune responses against human papillomavirus (HPV) infection and evasion of host defense in cervical cancer. J Infect Chemother [Internet] 2012 [cited 2016 Jan 11]; 18:807–15.
9. Steele JC, Mann CH, Rookes S, Rollason T, Murphy D, Freeth MG, Gallimore PH, Roberts S. T-cell responses to human papillomavirus type 16 among women with different grades of cervical neoplasia. Br J Cancer [Internet] 2005 [cited 2016 Jan 11]; 93:248–59.
10. Nasseri M, Gage JR, Lorincz A, Wettstein FO. Human papillomavirus type 16 immortalized cervical keratinocytes contain transcripts encoding E6, E7, and E2 initiated at the P97 promoter and express high levels of E7. Virology [Internet] 1991 [cited 2016 Jan 11]; 184:131–40.
11. Trimble CL, Morrow MP, Kraynyak KA, Shen X, Dallas M, Yan J, Edwards L, Parker RL, Denny L, Giffear M, et al. Safety, efficacy, and immunogenicity of VGX-3100, a therapeutic synthetic DNA vaccine targeting human papillomavirus 16 and 18 E6 and E7 proteins for cervical intraepithelial neoplasia 2/3: a randomised, double-blind, placebo-controlled phase 2b trial. Lancet (London, England) [Internet] 2015 [cited 2015 Sep 22];
12. Stevanović S, Draper LM, Langhan MM, Campbell TE, Kwong ML, Wunderlich JR, Dudley ME, Yang JC, Sherry RM, Kammula US, et al. Complete regression of metastatic cervical cancer after treatment with human papillomavirus-targeted tumor-infiltrating T cells. J Clin Oncol [Internet] 2015 [cited 2015 Sep 9]; 33:1543–50.
13. Maldonado L, Teague JE, Morrow MP, Jotova I, Wu TC, Wang C, Desmarais C, Boyer JD, Tycko B, Robins HS, et al. Intramuscular therapeutic vaccination targeting HPV16 induces T cell responses that localize in mucosal lesions. Sci Transl Med [Internet] 2014 [cited 2015 Jul 4]; 6:221ra13.
14. Kawana K, Adachi K, Kojima S, Taguchi A, Tomio K, Yamashita A, Nishida H, Nagasaka K, Arimoto T, Yokoyama T, et al. Oral vaccination against HPV E7 for treatment of cervical intraepithelial neoplasia grade 3 (CIN3) elicits E7-specific mucosal immunity in the cervix of CIN3 patients. Vaccine [Internet] 2014 [cited 2015 Sep 16]; 32:6233–9.
15. Rosales R, López-Contreras M, Rosales C, Magallanes-Molina J-R, Gonzalez-Vergara R, Arroyo-Cazarez JM, Ricardez-Arenas A, Del Follo-Valencia A, Padilla-Arriaga S, Guerrero MV, et al. Regression of human papillomavirus

intraepithelial lesions is induced by MVA E2 therapeutic vaccine. Hum Gene Ther [Internet] 2014 [cited 2015 Sep 16]; 25:1035–49.

16. Kim TJ, Jin H-T, Hur S-Y, Yang HG, Seo YB, Hong SR, Lee C-W, Kim S, Woo J-W, Park KS, et al. Clearance of persistent HPV infection and cervical lesion by therapeutic DNA vaccine in CIN3 patients. Nat Commun [Internet] 2014 [cited 2015 Jul 21]; 5:5317.

17. Trimble CL, Peng S, Kos F, Gravitt P, Viscidi R, Sugar E, Pardoll D, Wu TC. A phase I trial of a human papillomavirus DNA vaccine for HPV16+ cervical intraepithelial neoplasia 2/3. Clin Cancer Res [Internet] 2009 [cited 2015 Sep 15]; 15:361–7.

18. de Vos van Steenwijk PJ, Ramwadhdoebe TH, Löwik MJG, van der Minne CE, Berends-van der Meer DMA, Fathers LM, Valentijn ARPM, Oostendorp J, Fleuren GJ, Hellebrekers BWJ, et al. A placebo-controlled randomized HPV16 synthetic long-peptide vaccination study in women with high-grade cervical squamous intraepithelial lesions. Cancer Immunol Immunother [Internet] 2012 [cited 2015 Sep 15]; 61:1485–92.

19. van Poelgeest MIE, Welters MJP, van Esch EMG, Stynenbosch LFM, Kerpershoek G, van Persijn van Meerten EL, van den Hende M, Löwik MJG, Berends-van der Meer DMA, Fathers LM, et al. HPV16 synthetic long peptide (HPV16-SLP) vaccination therapy of patients with advanced or recurrent HPV16-induced gynecological carcinoma, a phase II trial. J Transl Med [Internet] 2013 [cited 2015 Sep 15]; 11:88.

20. Kenter GG, Welters MJP, Valentijn ARPM, Lowik MJG, Berends-van der Meer DMA, Vloon APG, Drijfhout JW, Wafelman AR, Oostendorp J, Fleuren GJ, et al. Phase I immunotherapeutic trial with long peptides spanning the E6 and E7 sequences of high-risk human papillomavirus 16 in end-stage cervical cancer patients shows low toxicity and robust immunogenicity. Clin Cancer Res [Internet] 2008 [cited 2015 Jul 4]; 14:169–77.

21. Borysiewicz LK, Fiander A, Nimako M, Man S, Wilkinson GW, Westmoreland D, Evans AS, Adams M, Stacey SN, Boursnell ME, et al. A recombinant vaccinia virus encoding human papillomavirus types 16 and 18, E6 and E7 proteins as immunotherapy for cervical cancer. Lancet (London, England) [Internet] 1996 [cited 2015 Oct 8]; 347:1523–7.

22. Piersma SJ, Jordanova ES, van Poelgeest MIE, Kwappenberg KMC, van der Hulst JM, Drijfhout JW, Melief CJM, Kenter GG, Fleuren GJ, Offringa R, et al. High number of intraepithelial CD8+ tumor-infiltrating lymphocytes is associated with the absence of lymph node metastases in patients with large early-stage cervical cancer. Cancer Res [Internet] 2007 [cited 2016 Sep 14]; 67:354–61.

23. Wang B, Wu S, Zeng H, Liu Z, Dong W, He W, Chen X, Dong X, Zheng L, Lin T, et al. CD103+ Tumor Infiltrating Lymphocytes Predict a Favorable Prognosis in Urothelial Cell Carcinoma of the Bladder. J Urol [Internet] 2015 [cited 2016 Mar 22]; 194:556–62.

24. Djenidi F, Adam J, Goubar A, Durgeau A, Meurice G, de Montpréville V, Validire P, Besse B, Mami-Chouaib F. CD8+CD103+ tumor-infiltrating lymphocytes are tumor-specific tissue-resident memory T cells and a prognostic factor for survival in lung cancer patients. J Immunol [Internet] 2015 [cited 2016 Mar 22]; 194:3475–86.

25. Workel HH, Komdeur FL, Wouters MCA, Plat A, Klip HG, Eggink FA, Wisman GBA, Arts HJG, Oonk MHM, Mourits MJE, et al. CD103 defines intraepithelial CD8+ PD1+ tumour-infiltrating lymphocytes of prognostic significance in endometrial adenocarcinoma. Eur J Cancer 2016; 60:1–11.

26. Webb JR, Milne K, Nelson BH. PD-1 and CD103 Are Widely Coexpressed on Prognostically Favorable Intraepithelial CD8 T Cells in Human Ovarian Cancer. Cancer Immunol Res [Internet] 2015; 3:926–35.

27. Webb JR, Milne K, Watson P, Deleeuw RJ, Nelson BH. Tumor-infiltrating lymphocytes expressing the tissue resident memory marker CD103 are associated with increased survival in high-grade serous ovarian cancer. Clin Cancer Res [Internet] 2014 [cited 2016 Mar 22]; 20:434–44.

28. Chao HT, Wang PH, Tseng JY, Lai CR, Chiang SC, Yuan CC. Lymphocyte-infiltrated FIGO Stage IIB squamous cell carcinoma of the cervix is a prominent factor for disease-free survival. Eur J Gynaecol Oncol [Internet] 1999 [cited 2016 Sep 14]; 20:136–40.

29. Bethwaite PB, Holloway LJ, Thornton A, Delahunt B. Infiltration by immunocompetent cells in early

stage invasive carcinoma of the uterine cervix: a prognostic study. Pathology [Internet] 1996 [cited 2016 Sep 14]; 28:321–7.

30. Ronnett BM. Endocervical adenocarcinoma: selected diagnostic challenges. Mod Pathol [Internet] 2016; 29 Suppl 1:S12-28.

31. Massagué J, Blain SW, Lo RS. TGFbeta signaling in growth control, cancer, and heritable disorders. Cell [Internet] 2000 [cited 2016 Mar 22]; 103:295–309.

32. Mokrani M, Klibi J, Bluteau D, Bismuth G, Mami-Chouaib F. Smad and NFAT pathways cooperate to induce CD103 expression in human CD8 T lymphocytes. J Immunol [Internet] 2014 [cited 2016 Mar 22]; 192:2471–9.

33. Boutet M, Gauthier L, Leclerc M, Gros G, De Montpreville V, Théret N, Donnadieu E, Mami-Chouaib F. TGF-β signaling intersects with CD103 integrin signaling to promote T lymphocyte accumulation and antitumor activity in the lung tumor microenvironment. Cancer Res [Internet] 2016 [cited 2016 Mar 22].

34. Workel HH, Komdeur FL, Wouters MCA, Plat A, Klip HG, Eggink FA, Wisman GBA, Arts HJG, Oonk MHM, Mourits MJE, et al. CD103 defines intraepithelial CD8+ PD1+ tumour-infiltrating lymphocytes of prognostic significance in endometrial adenocarcinoma. Eur J Cancer [Internet] 2016 [cited 2016 Apr 4]; 60:1–11.

35. Komdeur FL, Wouters MCA, Workel HH, Tijans AM, Terwindt ALJ, Brunekreeft KL, Plat A, Klip HG, Eggink FA, Leffers N, et al. CD103+ intraepithelial T cells in high-grade serous ovarian cancer are phenotypically diverse TCRαβ+ CD8αβ+ T cells that can be targeted for cancer immunotherapy. Oncotarget [Internet] 2016 [cited 2016 Sep 23];

36. Draghiciu O, Boerma A, Hoogeboom BN, Nijman HW, Daemen T. A rationally designed combined treatment with an alphavirus-based cancer vaccine, sunitinib and low-dose tumor irradiation completely blocks tumor development. Oncoimmunology [Internet] 2015 [cited 2017 Mar 30]; 4:e1029699.

37. Dunn GP, Old LJ, Schreiber RD. The immunobiology of cancer immunosurveillance and immunoediting. Immunity [Internet] 2004 [cited 2016 Sep 14]; 21:137–48.

38. Van Allen EM, Miao D, Schilling B, Shukla SA, Blank C, Zimmer L, Sucker A, Hillen U, Geukes Foppen MH, Goldinger SM, et al. Genomic correlates of response to CTLA-4 blockade in metastatic melanoma. Science [Internet] 2015 [cited 2016 Sep 15]; 350:207–11.

39. McGranahan N, Furness AJS, Rosenthal R, Ramskov S, Lyngaa R, Saini SK, Jamal-Hanjani M, Wilson GA, Birkbak NJ, Hiley CT, et al. Clonal neoantigens elicit T cell immunoreactivity and sensitivity to immune checkpoint blockade. Science [Internet] 2016 [cited 2016 Sep 15]; 351:1463–9.

40. Tumeh PC, Harview CL, Yearley JH, Shintaku IP, Taylor EJM, Robert L, Chmielowski B, Spasic M, Henry G, Ciobanu V, et al. PD-1 blockade induces responses by inhibiting adaptive immune resistance. Nature [Internet] 2014 [cited 2016 Sep 16]; 515:568–71.

41. de Vos van Steenwijk PJ, van Poelgeest MIE, Ramwadhdoebe TH, Löwik MJG, Berends-van der Meer DMA, van der Minne CE, Loof NM, Stynenbosch LFM, Fathers LM, Valentijn ARPM, et al. The long-term immune response after HPV16 peptide vaccination in women with low-grade pre-malignant disorders of the uterine cervix: a placebo-controlled phase II study. Cancer Immunol Immunother [Internet] 2014 [cited 2015 Jul 21]; 63:147–60.

42. Woo JC, Roccabianca P, van Stijn A, Moore PF. Characterization of a feline homologue of the alphaE integrin subunit (CD103) reveals high specificity for intra-epithelial lymphocytes. Vet Immunol Immunopathol [Internet] 2002 [cited 2016 Sep 14]; 85:9–22.

43. Konkel JE, Maruyama T, Carpenter AC, Xiong Y, Zamarron BF, Hall BE, Kulkarni AB, Zhang P, Bosselut R, Chen W. Control of the development of CD8αα+ intestinal intraepithelial lymphocytes by TGF-β. Nat Immunol [Internet] 2011 [cited 2016 Mar 22]; 12:312–9.

44. Mackay LK, Rahimpour A, Ma JZ, Collins N, Stock AT, Hafon M-L, Vega-Ramos J, Lauzurica P, Mueller SN, Stefanovic T, et al. The developmental pathway for CD103(+)CD8+ tissue-resident memory T cells of skin. Nat Immunol [Internet] 2013 [cited 2016 Mar 22]; 14:1294–301.

45. Peralta-Zaragoza O, Bermúdez-Morales V, Gutiérrez-Xicotencatl L, Alcocer-González J, Recillas-Targa F, Madrid-Marina V. E6 and E7 oncoproteins from human papillomavirus type 16 induce activation of human transforming

growth factor beta1 promoter throughout Sp1 recognition sequence. Viral Immunol [Internet] 2006 [cited 2016 Sep 15]; 19:468–80.

46. Deng W, Tsao SW, Kwok YK, Wong E, Huang XR, Liu S, Tsang CM, Ngan HYS, Cheung ANY, Lan HY, et al. Transforming growth factor beta1 promotes chromosomal instability in human papillomavirus 16 E6E7-infected cervical epithelial cells. Cancer Res [Internet] 2008 [cited 2016 Sep 15]; 68:7200–9.

47. Lu S-L, Reh D, Li AG, Woods J, Corless CL, Kulesz-Martin M, Wang X-J. Overexpression of Transforming Growth Factor 1 in Head and Neck Epithelia Results in Inflammation, Angiogenesis, and Epithelial Hyperproliferation. Cancer Res [Internet] 2004 [cited 2017 Mar 30]; 64:4405–10.

48. Yang L, Moses HL. Transforming Growth Factor : Tumor Suppressor or Promoter? Are Host Immune Cells the Answer? Cancer Res [Internet] 2008 [cited 2017 Mar 30]; 68:9107–11.

49. Partlová S, Bouček J, Kloudová K, Lukešová E, Zábrodský M, Grega M, Fučíková J, Truxová I, Tachezy R, Špíšek R, et al. Distinct patterns of intratumoral immune cell infiltrates in patients with HPV-associated compared to non-virally induced head and neck squamous cell carcinoma. Oncoimmunology [Internet] 2015 [cited 2017 Mar 30]; 4:e965570.

50. Li B, Dewey CN. RSEM: accurate transcript quantification from RNA-Seq data with or without a reference genome. BMC Bioinformatics [Internet] 2011 [cited 2016 Sep 14]; 12:323.

51. van Gool IC, Eggink FA, Freeman-Mills L, Stelloo E, Marchi E, de Bruyn M, Palles C, Nout RA, de Kroon CD, Osse EM, et al. POLE Proofreading Mutations Elicit an Antitumor Immune Response in Endometrial Cancer. Clin Cancer Res [Internet] 2015 [cited 2016 Sep 23]; 21:3347–55.

52. Maduro JH, Noordhuis MG, ten Hoor KA, Pras E, Arts HJG, Eijsink JJH, Hollema H, Mom CH, de Jong S, de Vries EGE, et al. The prognostic value of TRAIL and its death receptors in cervical cancer. Int J Radiat Oncol Biol Phys [Internet] 2009 [cited 2016 Sep 14]; 75:203–11.

53. Noordhuis MG, Eijsink JJH, Ten Hoor KA, Roossink F, Hollema H, Arts HJG, Pras E, Maduro JH, Reyners AKL, de Bock GH, et al. Expression of epidermal growth factor receptor (EGFR) and activated EGFR predict poor response to (chemo)radiation and survival in cervical cancer. Clin Cancer Res [Internet] 2009 [cited 2016 Sep 14]; 15:7389–97.

54. Daemen T, Riezebos-Brilman A, Regts J, Dontje B, van der Zee A, Wilschut J. Superior therapeutic efficacy of alphavirus-mediated immunization against human papilloma virus type 16 antigens in a murine tumour model: effects of the route of immunization. Antivir Ther [Internet] 2004 [cited 2015 Oct 14]; 9:733–42.

Treatment regimen, surgical outcome and T cell differentiation influence prognostic benefit of tumor-infiltrating lymphocytes in high grade serous ovarian cancer

MCA Wouters*, FL Komdeur*, HH Workel, HG Klip, A Plat, NM Kooi, GBA Wisman, MJE Mourits, HJG Arts, MHM Oonk[1], R Yigit, S de Jong, CJM Melief ,H Hollema, EW Duiker, T Daemen, M de Bruyn, HW Nijman

*Authors contributed equally

Clin Cancer Res. 2016 Feb 1;22(3):714-24

ABSTRACT

Purpose. Tumor-infiltrating lymphocytes (TIL) are associated with a better prognosis in high grade serous ovarian cancer (HGSC). However, it is largely unknown how this prognostic benefit of TIL relates to current standard treatment of surgical resection and (neo-)adjuvant chemotherapy. To address this outstanding issue, we compared TIL infiltration in a unique cohort of advanced stage HGSC cancer patients primarily treated with either surgery or neo-adjuvant chemotherapy.

Experimental Design. Tissue Microarray (TMA) slides containing samples of 171 patients were analyzed for CD8+ TIL by immunohistochemistry. Freshly isolated CD8+ TIL subsets were characterized by flow cytometry based on differentiation, activation and exhaustion markers. Relevant T cell subsets (CD27+) were validated using immunohistochemistry and immunofluorescence.

Results. A prognostic benefit for patients with high intratumoral CD8+ TIL was observed if primary surgery had resulted in a complete cytoreduction (no residual tissue). By contrast, optimal (< 1 cm of residual tumor) or incomplete cytoreduction fully abrogated the prognostic effect of CD8+ TIL. Subsequent analysis of primary TIL by flow cytometry and immunofluorescence identified CD27 as a key marker for a less-differentiated, yet antigen-experienced and potentially tumor-reactive CD8+ TIL subset. In line with this, CD27+ TIL was associated with an improved prognosis even in incompletely-cytoreduced patients. Neither CD8+ nor CD27+ cell infiltration was of prognostic benefit in patients treated with neo-adjuvant chemotherapy.

Conclusions. Our findings indicate that treatment regimen, surgical result and the differentiation of TIL should all be taken into account when studying immune factors in HGSC or, by extension, selecting patients for immunotherapy trials.

INTRODUCTION

Epithelial ovarian cancer (EOC) is the most deadly gynecological malignancy with an overall 5-year survival of 38-40% [1]. EOC is a heterogeneous disease with multiple histological subtypes, of which high grade serous carcinoma (HGSC) is the most common [2]. The poor prognosis of the disease is largely due to diagnosis at advanced stage and therapy-resistant disease relapses that occur in the majority of patients following initial treatment consisting of cytoreductive surgery and platinum-containing chemotherapy [2]. Nevertheless, a subset of HGSC patients appears to remain disease-free for prolonged periods of time. To date, several factors have been identified to define this subset of patients.

Arguably the strongest prognostic factor is the amount of residual tumor tissue after surgery [3]. Indeed, patients in which a complete resection, leaving no residual macroscopic lesions, is achieved have an approximately 1.6-fold longer survival than patients with remaining macroscopic disease [4]. As such, neo-adjuvant chemotherapy (NACT) is increasingly considered as the treatment option of choice in patients in whom the chances of up-front complete cytoreduction are minimal (e.g. patients with stage IIIC/IV disease with widespread tumor dissemination) or as an effort to reduce morbidity due to aggressive primary cytoreductive surgery (PS). NACT may reduce tumor load before cytoreductive interval surgery, increasing the likelihood of completely resected tumors [5], as well as reduce perioperative morbidity and mortality in this group of patients.

A second major factor in determining the prognosis of HGSC is the presence of tumor-infiltrating lymphocytes (TIL). Infiltration of CD3+ T cells, and particularly CD8+ cytotoxic T cells (CTL) is associated with a better prognosis for HGSC patients [6,7]. Moreover, the ratio between CTL and immune-inhibitory cells (FoxP3+ regulatory T cells, CD33+ myeloid-derived suppressor cells (MDSC)), the activation status of T cells (CD45RO), and their cytolytic activity (measured by TIA-1/Granzyme B expression) are all predictive for survival [8–10]. Despite these well-established prognostic roles of both surgical outcome and TIL, the relationship between both factors has remained largely unknown. Indeed, most studies on the prognostic value of TIL in ovarian carcinomas used heterogeneous patient populations including various subtypes of EOC, early and advanced stages and different grades and included patients treated with various chemotherapeutic regimens. In addition, many studies use different outcome measures for the result of cytoreductive surgery, further complicating analysis.

Next to this effect of surgical outcome on the prognostic value of TIL, neo-adjuvant chemotherapeutic treatment might also alter TIL infiltration and function and therefore the overall effectiveness of a (pre-existing) immune response. Indeed, platinum-based NACT in patients with breast cancer can increase TIL infiltrate [11] and levels of TIL before treatment are

reportedly predictive for the subsequent response to chemotherapy [12–14] as well as response to Trastuzumab, a monoclonal antibody targeted against HER2 [15]. While no association of TIL infiltrate and (neo-)adjuvant chemotherapy has been described in HGSC, a single study found that patients with high TIL were more likely to be completely cytoreduced, potentially due to a better tumor control by the immune system [6].

To address the effects of cytoreductive surgery and neo-adjuvant chemotherapy on the prognostic role of CD8+ TIL, patient cohorts therefore need to be highly standardized in terms of treatment schedule, stage, grade and outcome of cytoreductive surgery. Here, we generated two such cohorts of advanced stage HGSC patients treated with identical chemotherapy, but with primary treatment being either PS or NACT.

We show here that the prognostic benefit of CD8+ TIL is restricted to patients in whom a complete cytoreductive surgery was achieved (no residual tumor) and is not demonstrable in patients in which up-front complete cytoreduction was considered to be unattainable (NACT patients). Interestingly, we also found that patients performed better when the tumor was infiltrated by less-differentiated, CD8+ T cells, despite the presence of a residual macroscopic tumor after cytoreduction. Taken together, our findings indicate that treatment regimen, surgical result and the differentiation of TIL should all be taken into account when studying immune factors in HGSC or, by extension, selecting HGSC patients for immunotherapy trials.

RESULTS

Primary surgery and neo-adjuvant chemotherapy cohort

From a total of 265 patients, tissue in FFPE blocks obtained at primary or interval surgery was available to construct the TMA. Two cohorts were created on the basis of treatment strategy, a primary surgery (PS) (n=134) and a neo-adjuvant chemotherapy (NACT) (n=121) cohort. From 15 patients tissue from a recurrence and from 5 patients tissue from both primary and interval surgery were included on the TMA. Patients diagnosed with high grade (grade III and undifferentiated), advanced stage (FIGO ≥ IIB) serous ovarian carcinoma were selected for analysis in the current study (n=171), recurrences were excluded (Table 1). The five patients of which both primary and interval tissue was available, were analyzed in the cohort of their primary treatment, which was for all 5 NACT.

For the PS cohort 87 patients were included, who received 6 cycles of platinum-based chemotherapeutic treatment after surgery. Five patients did not receive chemotherapy, either because they received palliative treatment and refused additional chemotherapy, or died due to surgical complications. Surgical cytoreduction resulted in 39 (44.8%) patients with no residual

macroscopic lesions. The mean age was 64.1 years (standard deviation (SD)=11.3) and median duration of follow-up was 31.0 months (interquartile range (IQR): 40). Analysis of the disease-specific survival (DSS) of these patients showed a better prognosis for patients who had no residual macroscopic lesions as compared to optimal (≤1 cm residual tumor tissue; p=0.036) and suboptimal (>1 cm remaining tumor nodules; p<0.001) cytoreduced tumors (Supplementary Fig. S1A), confirming the value of complete cytoreduction. Age was also a prognostic parameter in this cohort, older patients (cut-off 59 years of age) had a worse prognosis (p=0.002, Supplementary Fig. S1B).

TABLE 1. Clinicopathological characteristics

	PS TMA cohort (N=87)		NACT TMA cohort (N=84)		Fresh tumor digests (N=9)	
Age						
mean (SD)	64.1 (11.3)		64.4 (8.6)		61.0 (7.4)	
Disease-specific survival (months) median (95% CI)	34.0 (26.6-41.4)		24.0 (20.4-27.6)		-	
	N	**%**	**N**	**%**	**N**	**%**
FIGO stage						
IIB	3	3.4	0	0.0	0	0.0
IIC	5	5.7	0	0.0	1	11.1
IIIA	2	2.3	0	0.0.	0	0.0
IIIB	6	6.9	2	2.4	0	0.0
IIIC	56	64.4	64	76.2	5	55.6
IV	15	17.2	18	21.4	3	33.3
Surgical cytoreduction						
No residual tissue	39	44.8	27	32.1	5	55.6
≤1cm residual tissue	15	17.2	39	46.4	0	0
>1cm residual tissue	33	37.9	18	21.3	4	44.4
Age						
<59	27	31.0	20	23.8	4	44.4
≥59	60	69.0	64	76.2	5	55.6
Chemotherapy						
No chemotherapy	5	5.7	0	0.0	0	0.0
Platinum-based	82	94.3	84	100.0	9	100.0

FIGO: International Federation of Gynaecology and Obstetrics. PS: primary surgery. NACT: neo-adjuvant chemotherapy treatment. TMA: Tissue Micro-Array. SD: standard deviation. CI: confidence interval.

In the NACT cohort, all 84 included patients received 3 cycles of platinum-based chemotherapy before and 3 cycles following surgical cytoreduction. Complete cytoreduction was achieved at interval surgery in 27 of the 84 patients (32.1%). The mean age of patients in this cohort was 64.4 years (SD: 8.6) and median duration of follow-up was 22.0 months (IQR: 24.5). DSS was significantly shorter in patients in this cohort in comparison to the PS cohort (median DSS 24.0 vs. 34.0

months, p=0.042, Table 1). For DSS analysis concerning residual tumor tissue after surgery, the same trend could be observed as in the PS cohort, though the difference in DSS between non-macroscopic disease and optimal cytoreduction was not significantly different (p=0.073), while the difference between no residual tumor and >1 cm tumors was (p<0.001, Supplementary Fig. S1C). Age was not a significant prognostic marker in this cohort (**Supplementary Fig. S1D**).

CD8+ TIL are predictive for DSS only in completely cytoreduced patients

In these two cohorts of advanced stage HGSC patients treated with identical chemotherapeutics, we first validated the previously published observation that CD8+ TIL are associated with prognosis in HGSC. TMA slides were analyzed for the infiltration of CD8+ CTL in the tumor epithelium. In the PS cohort, 87.9% of the samples had infiltrating CD8+ cells with a median infiltration of 21.31 cells/mm^2 tumor (IQR: 69.78) (Fig. 1A; 1B). Prognostic characteristics were analyzed for differences in CD8+ cell count in order to determine whether these factors influence intratumoral CTL infiltration. Age (p=0.215), FIGO stage (p=0.172), or surgical cytoreductive outcome (p=0.194) did not show differences in total CD8+ count.

In the NACT cohort, tumors obtained at interval surgery were infiltrated with CD8+ cells in 96.2% of patients with a median infiltration of 35.00 cells/mm^2 (IQR: 81.76) (Fig. 1B). There were no differences in number of cells within patient groups regarding age (p=0.856), FIGO stage (p=0.564), or surgical result (p=0.535). Comparing the two cohorts revealed that the infiltration of CD8+ TIL did not seem to be affected by the received neo-adjuvant chemotherapeutic treatment (Fig. 1B; p=0.084).

For subsequent survival data analysis, patients were dichotomized based on the group of patients with the highest infiltration of cells (highest tertile) vs. the group with low or no infiltration. DSS analysis based on infiltration of CD8+ cells revealed a non-significant improvement of survival (p=0.052) in the PS cohort for the group with high infiltration compared to patients with low or no infiltration (Fig. 1C). In the NACT cohort, no differences in survival were detected between the groups with either a high or a low infiltration of CD8+ (Fig. 1D, p=0.992).

Since the result of cytoreductive surgery is a major predictor for prognosis and determines the course of disease, we next analyzed the prognostic benefit of CD8+ TIL in relation to primary surgical outcome. Patients were categorized based on patients that had no residual macroscopic lesions after surgery and those with residual macroscopic disease. Within the group without residual tissue, a clear survival benefit was observed for patients who had a high infiltration of CD8+ T cells (Fig. 1E, p=0.028), suggesting a role of CD8+ in tumor immunosurveillance. By contrast, no survival benefit of CD8+ T cell infiltration was detected in the group of patients that received an incomplete cytoreduction. No difference was found in total number of infiltrating CD8+ TIL in completely resected tumors as compared to tumors of patients with remaining

tumor tissue (Fig. 1F), suggesting that the number of TIL present does not affect surgical outcome in these patients. Concluding, a survival benefit of infiltration with CD8+ TIL is present only in patients that had a complete tumor resection at time of primary surgery.

CD27 is expressed on CD8+ TIL of HGSC in situ

Interestingly, in adoptive cell transfer (ACT) studies, undifferentiated T cells provide greater control over established large tumor masses, with terminally differentiated T cells providing only poor tumor control [16]. Therefore, we wondered whether less-differentiated T cells were equally associated with better tumor control in HGSC patients in which complete cytoreduction could not be achieved. Hereto, we analyzed expression of the differentiation marker CD27, known to be a key marker associated with improved outcome in ACT. First, to assess co-expression of CD27 on CD8+ TIL, whole slides from 10 patients with a high infiltration of CD8+ cells (95.9-2555.0 cells/mm^2) were selected from the TMA dataset and stained for CD27 and CD8 using immunofluorescence. First, we determined if tumor regions could be differentiated from stromal regions by using DAPI nuclear staining. Tumor slides were stained with anti-EpCAM and anti-fibronectin antibodies, followed by DAPI staining of the nuclei. By means of DAPI, tumor islands were selected and checked for expression of EpCAM and fibronectin, showing that indeed the differentiation between tumor islands (EpCAM^{pos}) and stromal regions (fibronectin^{pos}) could be made (data not shown). Figure 2A shows a representative image for the double staining of CD8 and CD27, with the background staining of DAPI. Within the tumor islands, both CD8 and CD27 positive cells could be detected which were either single or double-positive (Fig. 2B, 2C). While CD8+CD27+ cells were the dominant subtype, clear differences were detected in the percentages of CD8+CD27- and CD8+CD27+ cells/mm^2 tumor epithelium within this group of patients (Fig. 2D). Thus CD27 is expressed on CD8+ TIL in HGSC, with variability in infiltration between patients.

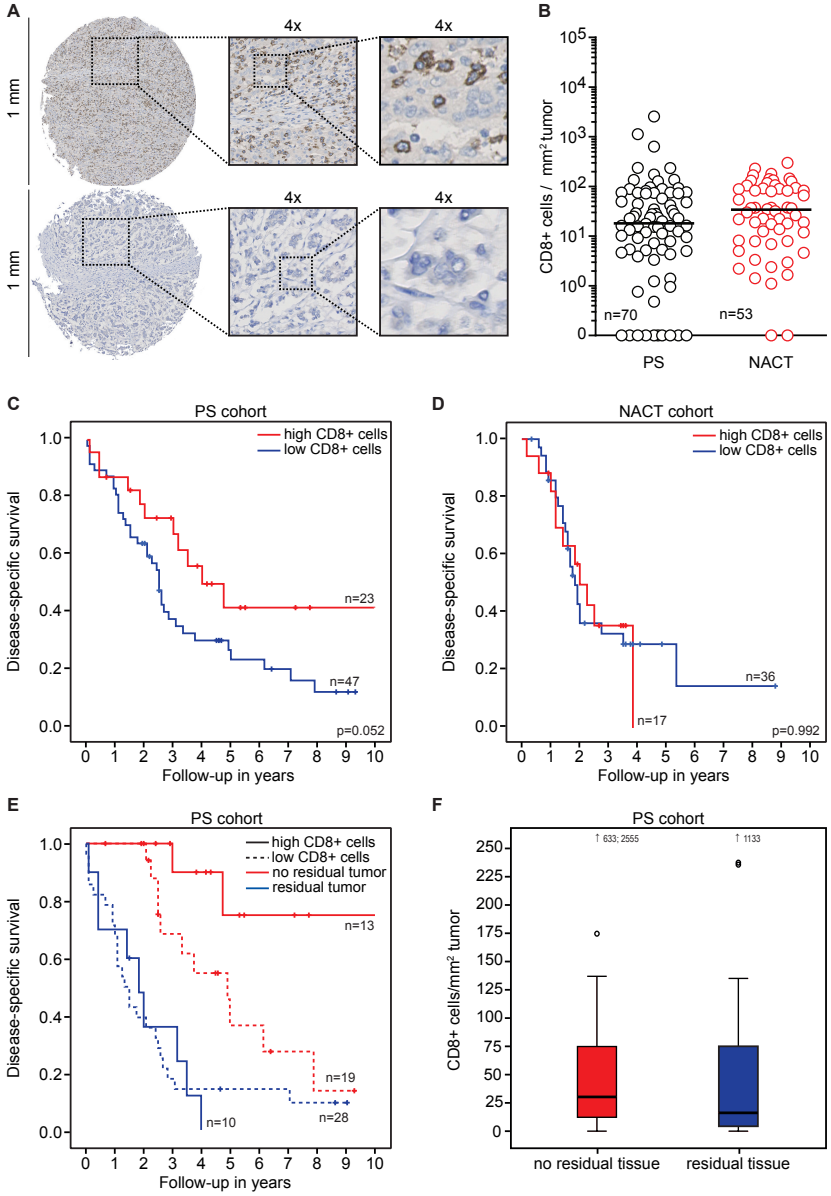

FIGURE 1. CD8+ tumor-infiltrating T cells associate with improved prognosis in completely cytoreduced patients only. A) Representative images of a 1 mm tissue core with high infiltration of CD8+ cells (top) and without CD8+ cells (bottom). Insets indicate magnification at 4x and 16x. **B**) Total CD8+ cell counts within 1 mm^2 tumor epithelium per patient in tissue from the primary surgery cohort (PS) and from the neo-adjuvant chemotherapy cohort (NACT). **C)** Disease-specific survival (DSS) of patients in the primary surgery cohort with a high or low infiltration of CD8+ cells in the tumor epithelium (p=0.052). **D)** DSS of patients in the neo-adjuvant chemotherapy cohort with a high or low infiltration of CD8+ cells in the tumor epithelium (p=0.992). **E)** DSS of patients in which cytoreductive surgery was complete (no residual tumor tissue) or incomplete (residual tumor tissue) and that displayed either as having a high or low infiltration of CD8+ cells in the tumor epithelium (complete: p=0.028; incomplete: p=0.897). **F)** Numbers of infiltrating CD8+ cells in patients in which cytoreductive surgery was complete or incomplete.

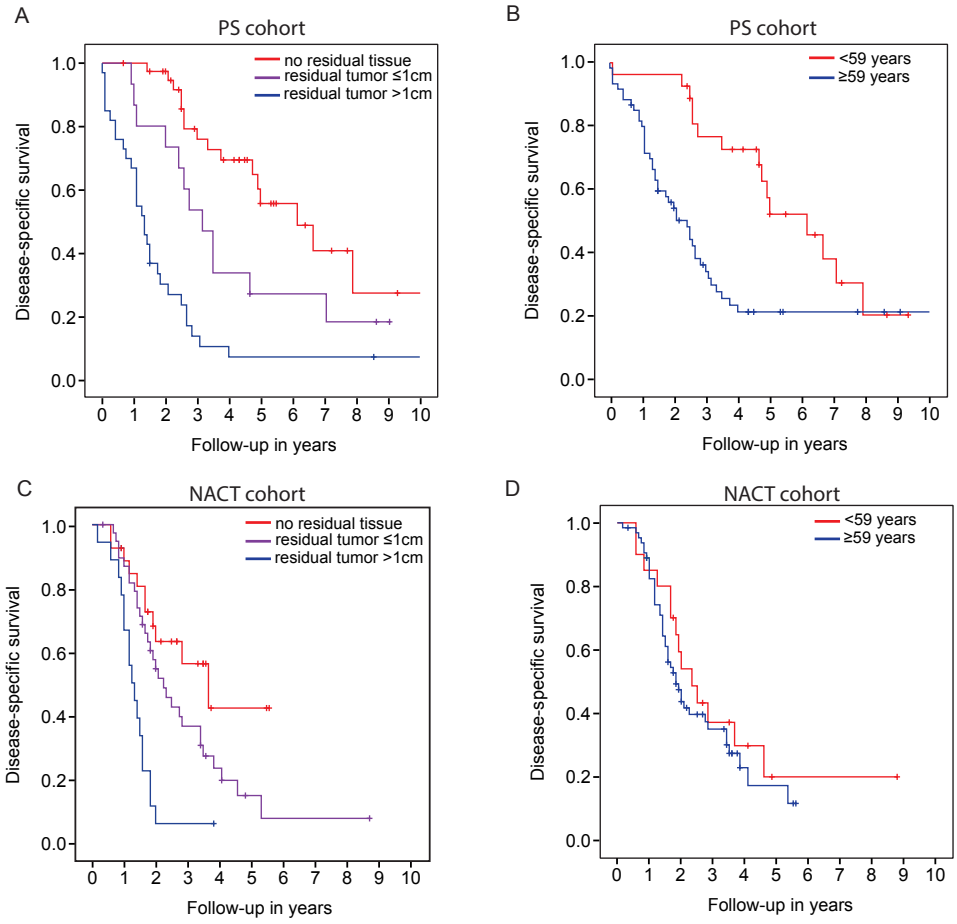

SUPPLEMENTARY FIGURE S1. Disease-specific survival (DSS) analyses by Kaplan Meier method of cohort treated with primary surgery (PS) and cohort treated with neo-adjuvant chemotherapy (NACT). A) DSS depicted for patients in PS cohort split on surgical outcome. B) Age is a predictor for survival in the PS cohort. C) Prognostic effect of surgical outcome in the NACT cohort. D) Age is not a predictor of survival in the NACT cohort.

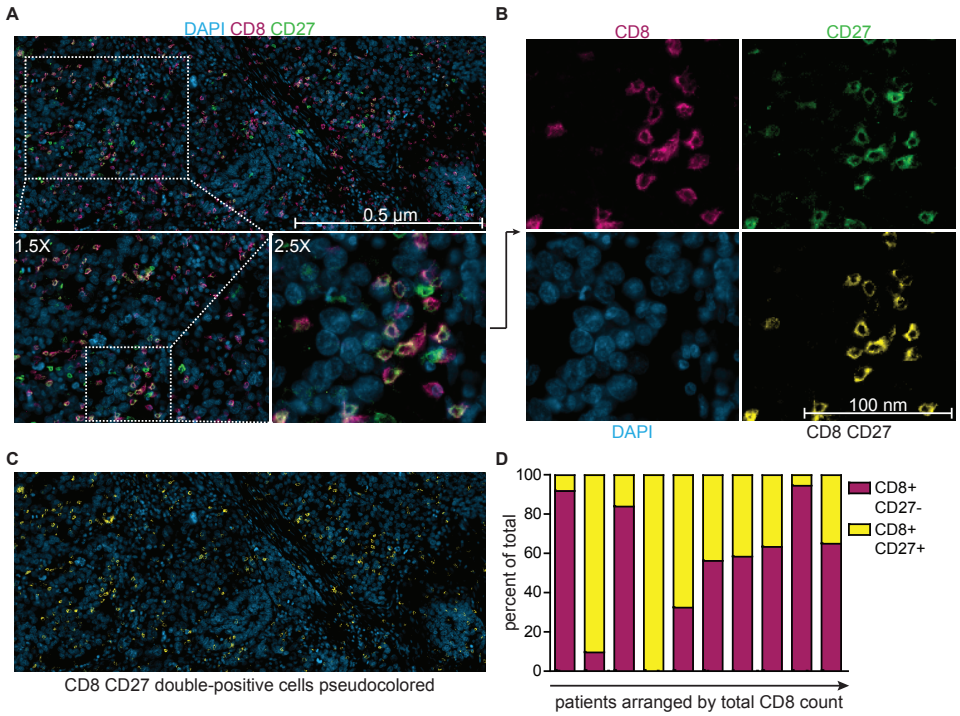

FIGURE 2. CD27 is expressed on CD8+ T cells *in situ*. **A**) Image of a highly infiltrated tumor (full slide) with CD8 in magenta, CD27 in green and DAPI nuclear staining in blue. Magnification 1.5x and 2.5x. **B**) Single stains for CD8, CD27 and DAPI, as well as double staining for CD8 and CD27. Inset represents the indicated area of panel A. **C**) CD8 and CD27 double positive cells pseudo colored in yellow, with DAPI nuclear staining in blue. **D**) Bar graph representing the total percentage of CD8 and CD27 single positive and CD8CD27 double positive cells of all counted cells within 1 mm^2 of tumor epithelium. Each bar represents 1 patient, from left to right in order of total CD8 count.

CD27+ TIL represent a less-differentiated antigen-experienced subset of CD8+ T cells

To further analyze the phenotype of CD8+ and CD27+ infiltrating cells, TIL were isolated from fresh tumor tissue (N=9, Table 1) and analyzed by flow cytometry. The gating strategy for live CD8+CD27+ cells is depicted in Figure 3A. First, we compared TIL populations isolated from fresh tumor tissue to fluorescent staining results of full slides. The percentages of CD27+ cells within the CD8+ subpopulation found were comparable for samples analyzed by either of the two techniques, confirming the reproducibility of the used methods of analysis (Fig. 3B; p=0.440). Within the population of CD8+ TIL, we then compared the CD27+ with the CD27- cells for differentiation markers. Here, no differences were found in expression of CD45RO (Fig. 3C; p=0.421), but CCR7 was predominantly expressed in the CD27+ group (Fig. 3D; p=0.042). Indeed, most of the CD27+CD8+ cells were double positive for CD45RO and CCR7 (Fig. 3E), confirming the less- differentiated, yet antigen-experienced phenotype of these TIL. CD8+CD27- cells had relatively comparable levels of CD45RO+ cells positive or negative for CCR7, suggesting

this cell subset represents a further differentiated phenotype compared to the CD8+CD27+ population (Fig. 3F). PD1 was expressed on most of the CD8+ TIL (Fig. 3G) with no difference within the subsets with or without CD27 expression (p=0.095). On the other hand, the marker for recent T cell activation CD137, was found to be expressed on a significantly higher percentage of CD27+CD8+ cells in comparison to the CD8+CD27- population (Fig. 3H; p=0.008). Conversely, within the total CD8+CD137+ population, most cells were CD27+PD1+, which was a significantly higher percentage compared to the CD8+CD137- subpopulation (Fig 3I, p=0.016). Comparing the subsets with or without expression of CCR7 within the CD8+CD27+ population, showed that there was no difference in the percentage of CD137+PD1+ cells (Fig. 3J; p=0.440). Taken together, CD27+ TIL represent a less-differentiated, potentially activated, antigen-experienced subset of CD8+ T cells.

CD27 infiltration in HGSC is not different between the PS and NACT cohort

Based on the flow cytometry results, we hypothesized the CD27 subset of TIL to resemble less-differentiated TIL which are therefore better capable of immune control of the tumor, presumably due to a greater expansion potential [17]. In order to further analyze this, expression of this marker was determined in both the PS and the NACT cohort. In the PS cohort 85.5% out of a total of 76 patients demonstrated CD27+ cell infiltration. Median cell count was 13.94 cells per mm^2 of tumor epithelium (IQR: 30.92), revealing lower total cell counts compared to CD8+ (Fig. 4A; 4B vs. 1B). Infiltration was not influenced by any of the prognostic factors age (p=0.832), stage (p=0.161), or surgery status (p=0.749).

In the NACT cohort the same trend could be observed. In comparison to CD8, a lower percentage of patients had CD27 infiltration (86.4%) and the total number of cells in these tumors was lower (median: 10.83, IQR: 30.25) (Fig. 4B vs. 1B). There were no differences in amount of cells within patient groups regarding age (p=0.965), FIGO stage (p=0.773), or surgical result (p=0.902). In order to determine whether the chemotherapy had influenced the infiltration of CD27+ TIL, we compared cell numbers between the two datasets and found no differences between the two cohorts (Fig. 4B, p=0.891). Thus, in the majority of patients in both cohorts infiltration of CD27+ cells was detected, with higher numbers of CD8 as compared to CD27, which was not influenced by any clinicopathological factors or neo-adjuvant chemotherapy.

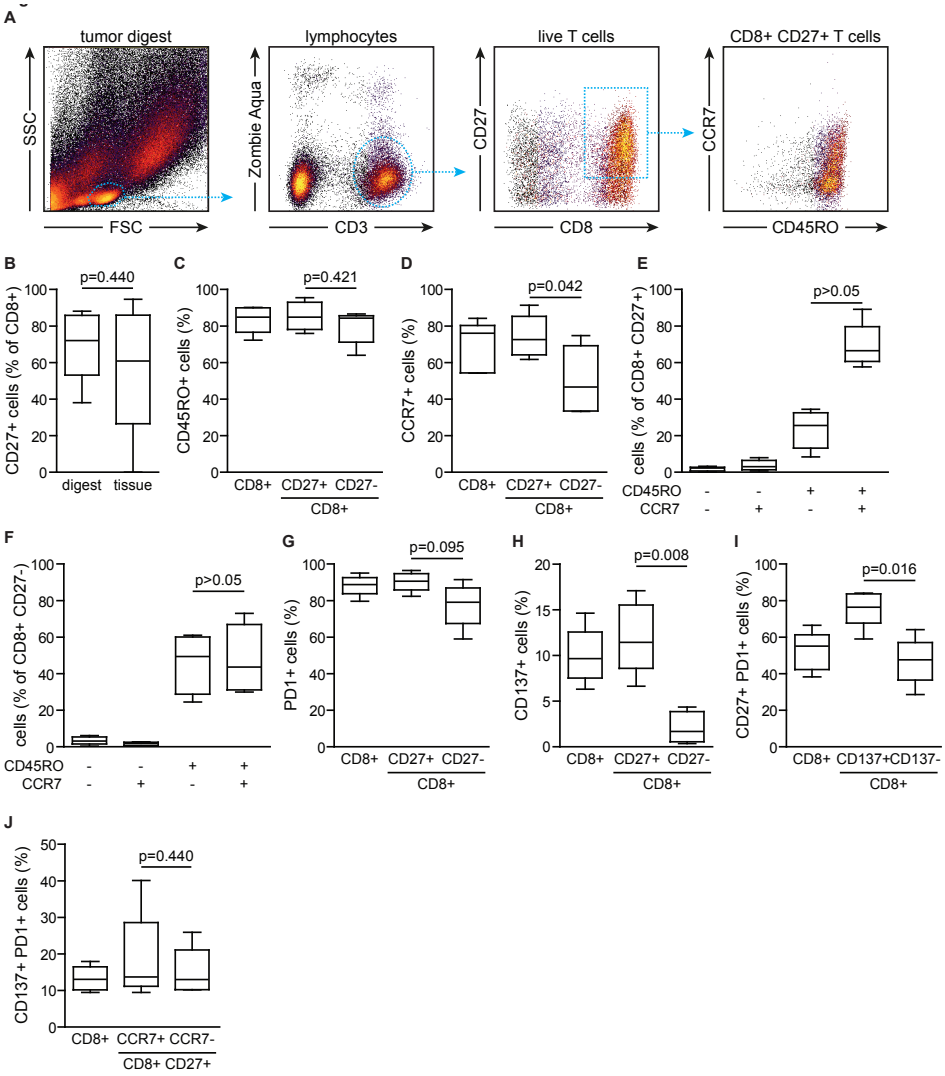

FIGURE 3. CD27 is predominantly expressed on antigen-experienced, recently activated CD8+ T cells. Ovarian tumor tissue was subjected to enzymatic digestion and analyzed by flow cytometry. **A)** Gating strategy for live CD8+CD27+ TIL. **B)** Comparison of the total percentage of CD27+ cells within the CD8+ population in tumor digest vs tissue slides (immunofluorescence; **Fig. 2**). **C)** Percentage of CD45RO+ cells on the total CD8+ population or the indicated CD8+CD27+ and CD8+CD27- populations. **D)** CCR7 expression on the total CD8+ population or the indicated CD8+CD27+ and CD8+CD27- populations. **E)** CD45RO and CCR7 expression on CD27+CD8+ TIL. **F)** CD45RO and CCR7 expression on CD27+CD8+ TIL. **G)** PD1 expression on the total CD8+ population or the indicated CD8+CD27+ and CD8+CD27- populations. **H)** CD137 expression on the total CD8+ population or the indicated CD8+CD27+ and CD8+CD27- populations. **I)** Expression of CD27 and PD1 on the indicated CD8/CD137+ subpopulations. **J)** Expression of CD137+/PD1+ on the indicated CCR7+/- CD8+CD27+ subpopulations.

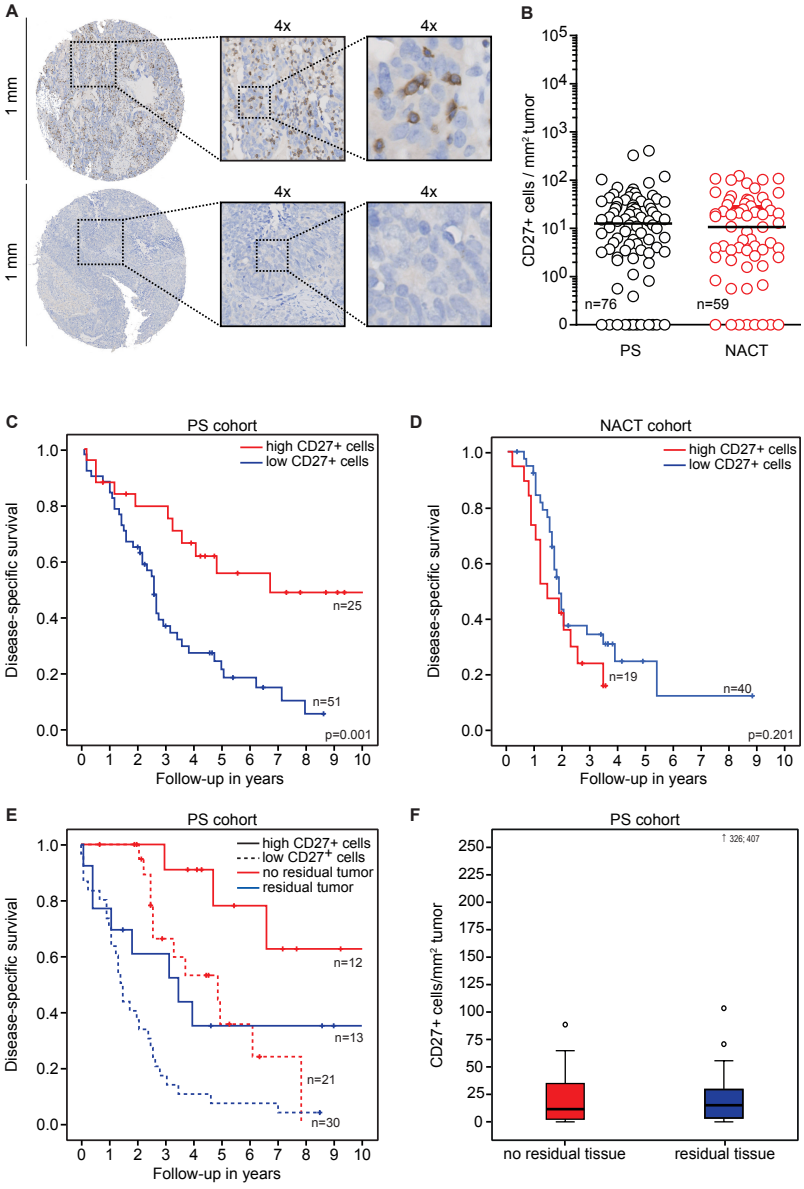

FIGURE 4. CD27+ TIL are strongly associated with survival in both completely and incompletely-cytoreduced HGSC patients. **A)** Representative images of a 1 mm tissue core of a highly infiltrated tissue (top) and one with low infiltration (bottom) of CD27+ cells. Insets indicate magnification at 4x and 16x **B)** Total CD27+ cell counts per mm² tumor tissue for patients in the primary surgery (PS) and neo-adjuvant chemotherapy (NACT) cohort. **C)** Disease-specific survival (DSS) of patients in the PS cohort with a high or low infiltration of CD27+ cells in the tumor epithelium (p=0.001). **D)** DSS of patients in the NACT cohort with a high or low infiltration of CD27+ cells in the tumor epithelium (p=0.201). **E)** DSS of patients in which cytoreductive surgery was complete (no residual tumor tissue) or incomplete (residual tumor tissue) and that displayed as either a high or low infiltration of CD27+ cells in the tumor epithelium (complete: p=0.011, incomplete: p=0.017). **F)** Numbers of CD27+ infiltrating cells in patients in which cytoreductive surgery was complete or incomplete.

CD27+ TIL are strongly associated with survival in the PS cohort

To determine the prognostic value of CD27+ TIL infiltration, patients were subdivided based on cut-off for the highest tertile of CD27 cell counts. In the PS cohort, DSS analysis based on CD27 expression showed a clear survival benefit for the highly infiltrated group (p=0.001, Fig. 4C). In the NACT cohort, no differences in survival could be detected within the groups with a high or low infiltration of CD27+ (cut-off highest tertile) (Fig. 4D).

If indeed CD27+ TIL show better tumor control, it is to be expected that these cells show prognostic value in completely resected tumors as well as in patients who had remaining tumor tissue following surgery. To determine whether CD27+ cells can compensate for incomplete removal of the tumor, we again analyzed groups based on surgical outcome in the PS cohort. Indeed, a clear survival benefit could not only be observed in patients without residual disease (p=0.011), but also in the group of patients which were incompletely cytoreduced (p=0.017; Fig. 4E). The survival benefit in the incomplete group can be attributed completely to the optimally cytoreduced patients (≤1 cm; p=0.021), while no benefit was observed in the patients that had >1 cm of residual tumor after surgery (p=0.369) (Supplementary Fig. 2).

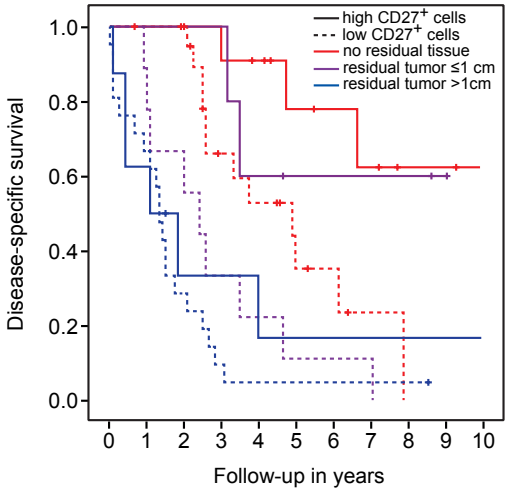

SUPPLEMENTARY FIGURE S2. Disease-specific survival (DSS) analyses by Kaplan Meier method of the primary surgery (PS) cohort for high and low infiltration of CD27+ cells. CD27 infiltration in the tumor epithelium is a prognostic factor in patients in which the surgical cytoreduction resulted in residual tissue of maximum 1 cm. Groups were created on basis of surgical outcome; red line shows patients that had no residual tumor after surgery, the violet lines depict patients that had residual tumors of {less than or equal to}1 cm, blue line represents patients with >1cm of residual tumor.

To confirm the value of CD27 over CD8 as a marker for prognosis in HGSC, we performed a multivariate cox regression analysis (Table 2), including all variables shown to be associated with survival in univariate analyses (FIGO stage, surgery result and age). In this model, only surgical result (hazard risk (HR): 1.50, 95%CI: 1.24-1.80) and CD27+ cell infiltration (HR: 0.23, 95%CI: 0.10-0.56) proved to be of prognostic value.

Taken together, the CD27+ TIL subset is more strongly associated with a favorable prognosis compared to the CD8+ TIL in HGSC patients, due to survival benefit in both patients with residual macroscopic disease and patients with no residual macroscopic disease. Whereas CD8+ TIL provide survival benefit only in patients where no macroscopic disease is present after cytoreductive surgery.

TABLE 2. Multivariate Cox regression analyses of disease-specific survival in primary surgery cohort

	HR	p-value	95% CI
FIGO stage	1.39	0.24	0.80-2.42
Surgical result (residual tissue)	1.50	<0.001	1.24-1.80
Age (>59 years)	1.92	0.123	0.84-4.41
CD8 (highest tertile)	1.44	0.385	0.63-3.30
CD27 (highest tertile)	0.23	0.001	0.10-0.56

FIGO: International Federation of Gynecology and Obstetrics. HR: hazard risk. CI: confidence interval

DISCUSSION

In the present study we demonstrate that the prognostic value of TIL in advanced stage HGSC is variable for patients primarily treated with surgery or neo-adjuvant chemotherapy. Furthermore, the differentiation status of infiltrating CD8+ T cells, as determined by CD27 expression, proved to be associated with a survival benefit superior to that observed for the overall CD8+ TIL population. This differential impact of various T cell subsets is related to surgical result of primary surgery. The less-differentiated CD27+ TIL were found to have a prognostic benefit even in patients with residual tumor tissue after surgery.

TIL have long been known to be associated with a favorable prognosis in EOC, with ratios between subtypes of cells, their activation status and cytolytic activity as determining factors [8,9]. We analyzed two patient cohorts of advanced stage HGSC treated with either surgery or neo-adjuvant chemotherapy as the primary treatment modality. Patient selection for the latter treatment is based on tumor dissemination, comorbidity and performance status. Therefore,

not surprisingly, the patients in the NACT cohort showed a worse prognosis in general. Also, when studying parameters that were of clear prognostic value in the PS cohort, namely residual tissue after surgery and age, the effect on prognosis was less clear or not present at all in the NACT group. This may in part explain why the effect of infiltrating CD8+ or CD27+ cells was also not associated with a survival benefit in this group. Whether this is due to the response of T cells to chemotherapy cannot be excluded, although total cell counts of these cell populations do not indicate a difference in infiltration. This is in line with the observation in mice that high dose carboplatin or paclitaxel treatment does not affect the amount of circulating T cells, nor the number of ovalbumin-specific T cells after vaccination [18]. Further studies will have to reveal whether functional differences are present in the TIL of tumors treated with these agents. Also, it is of interest whether response to chemotherapy can be predicted by TIL infiltrate as is the case in breast cancer [12–14].

In both cohorts, the most pronounced indicator of survival is the result of cytoreductive surgery, with a more distinct effect in the primary surgery cohort, consistent with observations by Rosen et al. [19]. In line with the immune tumor control hypothesis, one would expect that the influence of TIL infiltration on prognosis is affected by the amount of residual tumor tissue after surgery. Indeed, our data indicate that CD8+ TIL are of prognostic benefit only when maximum tumor cytoreduction can be achieved. Less-differentiated CD27+ TIL were able to compensate for incomplete surgical resection of the tumor, but only to a limited extent (residual tumor mass <1 cm). These data clearly indicate that the level of cytoreduction should be taken into account when studying immunomodulating effects. Of note, surgical outcome may not be a predictor of survival itself, but rather a reflection of the underlying tumor biology. Indeed, it was recently shown that a specific gene expression signature correlates with surgical outcome in ovarian cancer [20]. In our cohort, this may have led to a selection bias for the NACT cohort, since patients were selected for NACT if chance of up-front complete cytoreduction in primary surgery was minimal, thus these patients possibly differ in expression of key genes. Therefore, the lack of prognostic effect of infiltrating CD8 and CD27 cells in the NACT cohort could potentially be due to a difference in tumor biology. It will be of interest to determine whether patients with the two profiles show contrasting prognostic effects of immune infiltrates, and if so, whether a combined immune and cytoreduction gene signature can be identified for the stratification of patients or as a selection criterion for patients likely to respond to immunotherapy.

Our first in-human analysis of intraepithelial CD27+ TIL suggests these cells to represent a more potent tumor-controlling subset of CD8+ TIL in HGSC. These observations are in line with recent adoptive cell transfer (ACT) studies in melanoma. In particular, CD27+ TIL were found to persist longer after ACT and had a higher reactivity upon re-administration [21], presumably due to a greater expansion potential in response to antigen exposure [17]. Not surprisingly, the proportion of CD8+CD27+ cells within the transferred TIL was therefore strongly associated with tumor

regression in patients [22]. Furthermore, introduction of a CD27 intracellular signaling domain to chimeric antigen receptor (CAR) T cells led to longer persistence after infusion and improved efficacy in an ovarian cancer xenograft mouse model [23]. This matches our results showing longer survival in patients that have infiltrating CD27+ cells in their tumors. Interestingly, while CD27 is constitutively expressed on naive T cells, further upregulation is induced upon activation via TCR signaling, while loss of CD27 occurs in more terminal stages of differentiation. Therefore, the CD8+CD27+ subpopulation found within tumors might represent a more activated, tumor-reactive subset of cells. Indeed, when compared to the CD27- CTL, CD27+ CTL demonstrated a significantly higher percentage of cells expressing CD137, the recently-described marker for tumor-reactive T cells in HGSC [24]. Conversely, CD137+ CTL were predominantly (>80%) double-positive for CD27 and PD-1. In addition to this increased capacity for tumor recognition, CD27+ CTL also expressed CD45RO and CCR7, indicating that these cells are indeed antigen-experienced, but not yet terminally differentiated [25].

Our results suggest CD27 as an interesting target for immunotherapy in HGSC, in which stimulation of T cells via CD27 signaling might evoke anti-tumor responses in patients. A first humanized anti-CD27 antibody (1F5) was well-tolerated in non-human primates and was explored for the treatment of hematological malignancies overexpressing CD27 [26]. Treatment with the 1F5 antibody further inhibited growth of CD27+ human lymphoma cells in SCID mice and, in a human CD27-transgenic mouse model, led to an increase in antigen-specific CTL with concomitant anti-tumor activity [27]. The 1F5 antibody is currently in phase I trial for the treatment of hematological malignancies and solid tumors. Based on the co-expression of CD27 and PD1 on TIL, combining agonistic CD27 antibody with a checkpoint blockade targeting the PD1/PD-L1 axis might be of further interest, since preclinical studies have shown a synergistic effect of combinatorial antibody treatment [28].

Currently, also other treatment strategies for HGSC are being explored including strategies targeting angiogenesis (e.g. Bevacizumab) and poly(ADP-ribose) polymerase (PARP) inhibitors in tumors with alterations in the homologous recombination repair pathway. Whether supplementation of these strategies to current PS or NACT treatment regimens may affect the surgical outcome and overall prognosis of patients remains to be determined. Furthermore, effect it may have on the immune infiltrate and potential synergism with immunotherapy is of interest [29]. Exploration of these ideas can help to stratify patients with respect to different treatment modalities to predict the patients who might benefit most from immunotherapy.

In conclusion, the methodology of interpreting TIL infiltrates in tissue of HGSC and the cut-off values for positive samples need to be standardized before it can be considered as a prognostic

marker or serve as a selective marker for treatment strategies. Here we showed that the treatment regimen, surgical outcome, and the differentiation status of TIL should also be taken into account.

METHODS

Patient selection

An anonymized database was created containing information on clinicopathological characteristics and follow-up of patients diagnosed with serous ovarian cancer at the University Medical Center Groningen (Groningen, The Netherlands) between January 2000 and December 2012. Patients were staged according to International Federation of Gynecology and Obstetrics (FIGO) criteria, and graded by a gynecologic pathologist based on World Health Organization (WHO) guidelines. Patients were selected if sufficient formalin-fixed paraffin-embedded (ffpe) tissue was available for TMA construction. Tissue was obtained either from primary cytoreductive surgery (PS cohort) or from interval surgery (NACT cohort). Patients that underwent PS subsequently received six cycles of platinum-based chemotherapeutic regimen often combined with paclitaxel. Patients that were selected for NACT first received three cycles of chemotherapy, followed by interval surgery and three more cycles of chemotherapy. Follow-up was calculated from date of initial treatment (either surgery or neo-adjuvant chemotherapy) and was last updated in April 2014.

Ethical review

Patient data were retrieved from the institutional database into a new anonymous database, in which patient identity was protected by unique patient codes. According to Dutch law no approval from our institutional review board was needed. Primary patient TIL were isolated from surgical tumor waste for which no approval from our institutional review board was needed according to Dutch law.

Tissue MicroArray (TMA)

From 265 HGSC patients FFPE tissue was available for the construction of a tissue microarray (TMA). A gynecologic pathologist confirmed the presence of tumor tissue on H&E slides and selected representative locations with tumor tissue. Triplicate cores with a diameter of 1 mm were taken from each paraffin-embedded tissue block and placed in a recipient block by using a tissue microarrayer (Beecher instruments, Silver Spring, USA). An asymmetrical grid was chosen with a 14x9 layout. Both normal and tumor tissue were included as orientation cores and controls. The seventh column from the fourth row onwards, and the fourth row from the seventh column onwards were left empty as a points of reference for grid layout. From each

TMA block, 4 µm sections were cut and applied to APES-coated slides (Starfrost, Braunschweig, Germany). Core-loss was on average 9.0% (PS cohort) and 10.6% (NACT cohort). The presence of tumor in the arrayed samples was confirmed by H&E staining.

Immunohistochemistry and multicolor immunofluorescence

TMA slides were stained with mouse anti-human CD8 antibody (DAKO, Heverlee, Belgium; clone: C8/144B, 1:25 in blocking buffer (1% BSA/PBS with 1% human AB serum)) or rabbit anti-human CD27 antibody (Abcam, Cambridge, UK; clone: EPR8569, 1:150 in blocking buffer) by use of immunohistochemistry using standard methods (Supplementary methods). Furthermore, on the basis of the highest infiltration of CD8+ cells, 10 patients were selected from the TMA dataset and full tumor tissue slides were retrieved for analysis of CD8 and CD27 costaining by use of multicolor immunofluorescence. Antibody binding was visualized with goat anti-rabbit Alexa Fluor-488 and goat anti-mouse Alexa Fluor-555 (1:150, Life Technologies, Bleiswijk, The Netherlands). Counterstaining was done by 4',6-diamidino-2-phenylindole (DAPI).

Isolation of TIL from fresh tumor tissue

Fresh tumor material was obtained for the isolation of TIL from patients undergoing cytoreductive surgery. With a scalpel, tumor pieces of approximately 0.5 cm^3 were cut, and subjected to digestion in digestion medium (RPMI supplemented with 1 mg/ml collagenase type IV (Life technologies) and 31 U/ml rhDNase (Pulmozyme, Genentech, California, USA) for 30 minutes at 37°C. Subsequently, the digestion medium containing remaining tumor pieces was filtered over a 70 µm cell strainer (Corning, Amsterdam, The Netherlands) and cells were pelleted, washed, and cryopreserved until further use.

Multi-parameter flow cytometry

From the digested tumor samples TIL were phenotyped by multiparameter flow cytometry. The Zombie Aqua Fixable Viability Kit was used for live/dead stain according to manufacturer's instructions (BioLegend, Uithoorn, The Netherlands). Antibodies used were CD3-PerCP-Cy5.5 (OKT3), CD8-APC-eFluor780 (RPA-T8), CD45RO-PE-Cy7 (UCHL1), CD137-PE (4B4-1), and PD1-APC (MIH4) (all eBioscience, Vienna, Austria), CCR7-BV421 (150503) (BD Biosciences, Etten-Leur, The Netherlands), and CD27-FITC (9F4) (Sanquin, Amsterdam, The Netherlands). All flow cytometry was performed on a FACSVerse (BD Biosciences) and samples were analyzed with Cytobank software (cytobank.org).

Image acquisition and analysis

Scoring of TMA samples was performed if cores had at least 20% tumor epithelium present, and if at least two cores per patient were analyzable. All CD8+ or CD27+ stained cells localized

in tumor epithelium in each core were counted manually by two individuals that were blinded for patient characteristics. The two individual scores were compared and differences in counts of >10% were reanalyzed until consensus was reached. Cell counts were represented as total number of cells per mm^2 of tumor epithelium. H&E slides were used for comparison in cases tumor/stroma regions were not clearly definable.

Immunofluorescent slides were scanned using a TissueFaxs imaging system (TissueGnostics, Vienna, Austria). Processed channels were merged using Adobe Photoshop. On each slide an area of 1 mm^2 of tumor epithelium was selected based on DAPI staining, and cells were counted manually.

Statistical analysis

All statistical analyses were performed using IBM SPSS version 22 (SPSS Inc., Chicago, USA) or Graphpad Prism. Disease-specific survival (DSS) was defined as the time period from date of surgery or first chemotherapeutic treatment until death due to ovarian cancer or last follow-up and was analyzed by using Kaplan-Meier method, with Log Rank test to determine differences between groups. Variables that were significantly associated with DSS in univariate analyses were entered into a multivariate analysis using the Cox proportional hazards model. Differences in cell infiltration between 43 matched ovarian and omental primary tumor tissues were assessed by Wilcoxon signed ranks test, no differences were found and therefore primary ovarian and omental tissues were both used in the analyses. To determine differences in cell populations between clinicopathological variables or between different TIL subsets, the Mann Whitney U or one-way ANOVA test were used. P-values <0.05 were considered significant, and all tests were performed two-sided.

SUPPLEMENTARY METHODS

Immunohistochemistry

TMA slides were stained with anti-CD8 and anti-CD27 antibodies. After deparaffinization and rehydration, slides were subjected to heat-induced epitope retrieval (HIER) by microwaving the slides in a citrate buffer (10 mM citrate, pH 6.0) for 15 minutes. After cooling down, endogenous peroxidase was blocked 30 minutes in a 0.3% H_2O_2 solution. Slides were then incubated with either mouse anti-human CD8 antibody (DAKO, Heverlee, Belgium; clone: C8/144B, 1:25 in blocking buffer (1% BSA/PBS with 1% human AB serum)) or rabbit anti-human CD27 antibody (Abcam, Cambridge, UK; clone: EPR8569, 1:150 in blocking buffer) overnight at 4°C. The next

day slides were incubated with either anti-mouse or anti-rabbit Envision secondary antibodies (K4007, K4011; DAKO). Antibody binding was visualized with 3,3'-diaminobenzidine (DAB) and slides were counterstained with hematoxylin.

Multi-color immunofluorescence

On the basis of the highest infiltration with CD8+ cells, 10 patients were selected from the TMA dataset and full tumor tissue slides were retrieved for further analysis. Slides were deparaffinized, rehydrated, and HIER was performed in a citrate buffer (10 mM citrate, pH 6.0). After cooling, endogenous peroxidase was blocked 30 minutes in a 0.3% H_2O_2 solution. Slides were then incubated overnight with mouse anti-human CD8 (DAKO, clone C8/144B, 1:25) and rabbit anti-human CD27 (Abcam, clone EPR8569, 1:150). These were visualized with goat anti-rabbit Alexa Fluor-488 and goat anti-mouse Alexa Fluor-555 (1:150, Life Technologies, Bleiswijk, The Netherlands). Counterstaining was done by 4',6-diamidino-2-phenylindole (DAPI). Slides were mounted in Prolong Gold (Life Technologies) and stored in the dark at RT.

In order to differentiate tumor from stromal regions, slides were stained as described above, with a rabbit polyclonal antibody to Fibronectin (1:50, Abcam) and mouse anti-human EPCAM antibody (clone: AUA1, 1:50, Abcam).

Multi-parameter flow cytometry

From the digested tumor samples TIL were phenotyped by multiparameter flow cytometry. The Zombie Aqua Fixable Viability Kit was used for live/dead stain according to manufacturer's instructions (BioLegend, Uithoorn, The Netherlands). Antibodies used were CD3-PerCP-Cy5.5 (OKT3), CD8-APC-eFluor780 (RPA-T8), CD45RO-PE-Cy7 (UCHL1), CD137-PE (4B4-1), and PD1-APC (MIH4) (all eBioscience, Vienna, Austria), CCR7-BV421 (150503) (BD Biosciences, Etten-Leur, The Netherlands), and CD27-FITC (9F4) (Sanquin, Amsterdam, The Netherlands). All flow cytometry was performed on a FACSVerse (BD Biosciences) and samples were analyzed with Cytobank software (cytobank.org).

ACKNOWLEDGEMENTS

This work was supported by Dutch Cancer Society/Alpe d'Huzes grant UMG 2014–6719 to MB and Jan Kornelis de Cock Stichting grants to MCAW and FLK. Part of the work has been performed at the UMCG Imaging and Microscopy Center (UMIC), which is sponsored by NWO-grants 40-00506-98-9021 and 175-010-2009-023.

The authors would like to thank Klaas Sjollema, Henk Moes, Geert Mesander, Roelof-Jan van der Lei, Tineke van der Sluis, Joan Vos and Niels Kouprie for their technical assistance.

REFERENCES

1. Allemani C, Weir HK, Carreira H, Harewood R, Spika D, Wang X-S, et al. Global surveillance of cancer survival 1995–2009: analysis of individual data for 25 676 887 patients from 279 population-based registries in 67 countries (CONCORD-2). Lancet. 2015;385:997–1010.
2. Vaughan S, Coward JI, Bast RC, Berchuck A, Berek JS, Brenton JD, et al. Rethinking ovarian cancer: recommendations for improving outcomes. Nat Rev Cancer. 2011;11:719–25.
3. Winter WE, Maxwell GL, Tian C, Sundborg MJ, Rose GS, Rose PG, et al. Tumor residual after surgical cytoreduction in prediction of clinical outcome in stage IV epithelial ovarian cancer: a Gynecologic Oncology Group Study. J Clin Oncol. 2008;26:83–9.
4. Bristow RE, Tomacruz RS, Armstrong DK, Trimble EL, Montz FJ. Survival effect of maximal cytoreductive surgery for advanced ovarian carcinoma during the platinum era: a meta-analysis. J Clin Oncol. 2002;20:1248–59.
5. Vergote I, Tropé CG, Amant F, Kristensen GB, Ehlen T, Johnson N, et al. Neoadjuvant chemotherapy or primary surgery in stage IIIC or IV ovarian cancer. N Engl J Med. 2010;363:943–53.
6. Zhang L, Conejo-Garcia JR, Katsaros D, Gimotty PA, Massobrio M, Regnani G, et al. Intratumoral T cells, recurrence, and survival in epithelial ovarian cancer. N Engl J Med. 2003;348:203–13.
7. Sato E, Olson SH, Ahn J, Bundy B, Nishikawa H, Qian F, et al. Intraepithelial CD8+ tumor-infiltrating lymphocytes and a high CD8+/regulatory T cell ratio are associated with favorable prognosis in ovarian cancer. Proc Natl Acad Sci U S A. 2005;102:18538–43.
8. Milne K, Köbel M, Kalloger SE, Barnes RO, Gao D, Gilks CB, et al. Systematic analysis of immune infiltrates in high-grade serous ovarian cancer reveals CD20, FoxP3 and TIA-1 as positive prognostic factors. PLoS One. 2009;4:e6412.
9. Leffers N, Gooden MJM, de Jong RA, Hoogeboom B-N, ten Hoor KA, Hollema H, et al. Prognostic significance of tumor-infiltrating T-lymphocytes in primary and metastatic lesions of advanced stage ovarian cancer. Cancer Immunol Immunother. 2009;58:449–59.
10. Cui TX, Kryczek I, Zhao L, Zhao E, Kuick R, Roh MH, et al. Myeloid-derived suppressor cells enhance stemness of cancer cells by inducing microRNA101 and suppressing the corepressor CtBP2. Immunity. 2013;39:611–21.
11. Demaria S, Volm MD, Shapiro RL, Yee HT, Oratz R, Formenti SC, et al. Development of Tumor-infiltrating Lymphocytes in Breast Cancer after Neoadjuvant Paclitaxel Chemotherapy. Clin Cancer Res. 2001;7:3025–30.
12. Denkert C, Loibl S, Noske A, Roller M, Müller BM, Komor M, et al. Tumor-associated lymphocytes as an independent predictor of response to neoadjuvant chemotherapy in breast cancer. J Clin Oncol. 2010;28:105–13.
13. Ono M, Tsuda H, Shimizu C, Yamamoto S, Shibata T, Yamamoto H, et al. Tumor-infiltrating lymphocytes are correlated with response to neoadjuvant chemotherapy in triple-negative breast cancer. Breast Cancer Res Treat. 2012;132:793–805.
14. West NR, Milne K, Truong PT, Macpherson N, Nelson BH, Watson PH. Tumor-infiltrating lymphocytes predict response to anthracycline-based chemotherapy in estrogen receptor-negative breast cancer. Breast Cancer Res. 2011;13:R126.
15. Loi S, Michiels S, Salgado R, Sirtaine N, Jose V, Fumagalli D, et al. Tumor infiltrating lymphocytes are prognostic in triple negative breast cancer and predictive for trastuzumab benefit in early breast cancer: results from the FinHER trial. Ann Oncol. 2014;25:1544–50.
16. Besser MJ, Shapira-Frommer R, Treves AJ, Zippel D, Itzhaki O, Hershkovitz L, et al. Clinical responses in a phase II study using adoptive transfer of short-term cultured tumor infiltration lymphocytes in metastatic melanoma patients. Clin Cancer Res. 2010;16:2646–55.
17. Gattinoni L, Klebanoff CA, Palmer DC, Wrzesinski C, Kerstann K, Yu Z, et al. Acquisition of full effector function in vitro paradoxically impairs the in vivo antitumor efficacy of adoptively transferred CD8+ T cells. J Clin Invest. 2005;115:1616–26.
18. Diaz Y, Tundidor Y, Lopez A, Leon K. Concomitant combination of active immunotherapy and

carboplatin- or paclitaxel-based chemotherapy improves anti-tumor response. Cancer Immunol Immunother. 2013;62:455–69.

19. Rosen B, Laframboise S, Ferguson S, Dodge J, Bernardini M, Murphy J, et al. The impacts of neoadjuvant chemotherapy and of debulking surgery on survival from advanced ovarian cancer. Gynecol Oncol. 2014;134:462–7.

20. Riester M, Wei W, Waldron L, Culhane AC, Trippa L, Oliva E, et al. Risk prediction for late-stage ovarian cancer by meta-analysis of 1525 patient samples. J Natl Cancer Inst. 2014;106.

21. Huang J, Khong HT, Dudley ME, El-Gamil M, Li YF, Rosenberg SA, et al. Survival, persistence, and progressive differentiation of adoptively transferred tumor-reactive T cells associated with tumor regression. J Immunother. 2005;28:258–67.

22. Rosenberg SA, Yang JC, Sherry RM, Kammula US, Hughes MS, Phan GQ, et al. Durable Complete Responses in Heavily Pretreated Patients with Metastatic Melanoma Using T-Cell Transfer Immunotherapy. Clin Cancer Res. 2011;17:4550–7.

23. Song D-G, Ye Q, Poussin M, Harms GM, Figini M, Powell DJ. CD27 costimulation augments the survival and antitumor activity of redirected human T cells in vivo. Blood. 2012;119:696–706.

24. Ye Q, Song D-G, Poussin M, Yamamoto T, Best A, Li C, et al. CD137 accurately identifies and enriches for naturally occurring tumor-reactive T cells in tumor. Clin Cancer Res. 2014;20:44–55.

25. Restifo NP, Gattinoni L. Lineage relationship of effector and memory T cells. Curr Opin Immunol. 2013;25:556–63.

26. Vitale LA, He L-Z, Thomas LJ, Widger J, Weidlick J, Crocker A, et al. Development of a human monoclonal antibody for potential therapy of CD27-expressing lymphoma and leukemia. Clin Cancer Res. 2012;18:3812–21.

27. He L-Z, Prostak N, Thomas LJ, Vitale L, Weidlick J, Crocker A, et al. Agonist anti-human CD27 monoclonal antibody induces T cell activation and tumor immunity in human CD27-transgenic mice. J Immunol. 2013;191:4174–83.

28. Buchan SL, Manzo T, Flutter B, Rogel A, Edwards N, Zhang L, et al. OX40- and CD27-Mediated Costimulation Synergizes with Anti-PD-L1 Blockade by Forcing Exhausted CD8+ T Cells To Exit Quiescence. J Immunol. 2015;194:125–33.

29. Kandalaft LE, Powell DJ, Chiang CL, Tanyi J, Kim S, Bosch M, et al. Autologous lysate-pulsed dendritic cell vaccination followed by adoptive transfer of vaccine-primed ex vivo co-stimulated T cells in recurrent ovarian cancer. Oncoimmunology. 2013;2:e22664.

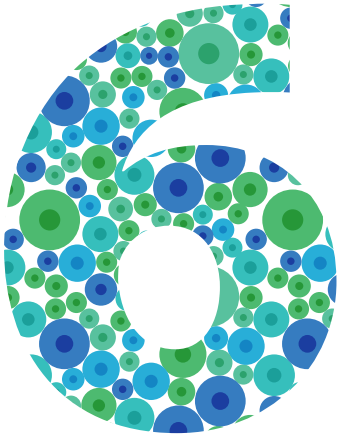

Size matters: survival benefit conferred by intratumoral T cells is dependent on surgical outcome, treatment sequence and T cell differentiation

MCA Wouters, FL Komdeur, M de Bruyn, HW Nijman

Oncoimmunology. 2016 Jan 4;5(5):e1122863

ABSTRACT

Outcome of cytoreductive surgery, treatment sequence and the differentiation status of T cells are key factors to take into account when studying the prognostic value of tumor-infiltrating lymphocytes in high grade serous ovarian cancer.

AUTHOR'S VIEW

It has become absolutely clear that the immune system exerts control over cancer growth and can even mediate tumor regression. Indeed, patients with so-called immunologically "hot" tumors - highly infiltrated with immune cells - generally have a better prognosis than patients with immunologically "cold" tumors. However, how conventional treatment affects this prognostic benefit of the immune system has remained underexplored[1–3]. Recently, we addressed this question in a unique cohort of high-grade serous ovarian cancer (HGSC) patients.

HGSC patients included in our cohort were highly similar in terms of clinicopathological characteristics and were treated with an identical combination of cytoreductive surgery and platinum-based chemotherapy, in the adjuvant or neo-adjuvant setting. The outcome of primary and interval cytoreductive surgery (adjuvant and neo-adjuvant treatment, respectively) was standardized and registered as complete (no residual tissue), optimal (<1cm residual tissue) or incomplete (>1 cm residual tissue) in line with international agreements. Interestingly, we observed that only those patients that had no residual macroscopic tumor lesions following primary surgery benefitted from high infiltration of CD8+ tumor-infiltrating lymphocytes (TIL). By contrast, CD8+ TIL infiltration in patients treated in the neo-adjuvant setting did not predict a better prognosis, even in patients in whom cytoreductive surgery was complete. These striking differences may in part be explained by the selection of patients for a given treatment regimen. Patients with a small chance of complete surgical cytoreduction at start of treatment - based in large part on considerable tumor dissemination - are more likely to receive neo-adjuvant chemotherapy. In this patient group, anti-tumor immunity may therefore be insufficient to constrain aggressive tumor growth even after complete cytoreduction. Patients with immunologically "hot" tumors treated in the neo-adjuvant setting might therefore especially benefit from checkpoint inhibition to augment the existing anti-tumor immunity. Alternatively, one could speculate that these aggressive tumors reflect a distinct subset of HGSC with an underlying biology less conducive to immune-mediated tumor control. In line with this hypothesis, a specific gene expression signature was recently found to correlate with surgical outcome in ovarian cancer[4].

We also observed no overall differences in median T cell infiltration in tissue obtained during primary or interval surgery, suggesting that chemotherapy does not exert a major effect on the absolute number of T cells infiltrating the tumor. A key next step would be to validate this finding by determining whether changes in TIL infiltration occur in individual patients during chemotherapeutic treatment using matched pre- and post-chemotherapy samples. One consideration herein remains that lesions available after chemotherapy may differ from lesions

eradicated by chemotherapy and may therefore differ in key genomic/immunologic factors. Indeed, heterogeneity in both cancer cells and tumor microenvironment has frequently been reported between lesions.

In contrast to what we observed for the total CD8+ TIL population, a CD27+ subset of CD8+ TIL was not only predictive for better outcome in patients in whom complete removal of the tumor during primary surgery was achieved, but was also of prognostic benefit in patients with remaining macroscopic lesions[5]. This CD27+ subset of TIL largely consisted of CD45RO+CCR7+ central memory and CD45RO+CCR7- effector memory T cell populations and were highly enriched for PD-1 and CD137 expression, a phenotype consistent with a naïve-like antigen-experienced tumor-reactive T cell subset[6,7]. The association of this phenotype with tumor control is in line with results from various adoptive cell transfer studies in humans and mice where a high ratio of less-differentiated CD27+CD28+ cells in transferred TIL was strongly correlated with anti-tumor immune activity[8]. Together, these data suggest T cell differentiation is a critical component of immune control *in situ*, but also in the therapeutic setting.

Finally, the finding that the co-stimulatory molecule CD27 is abundantly expressed in HGSC and is highly predictive for prognosis suggests CD27 to be an attractive target for therapeutic immunomodulation. In preclinical models, CD27 agonistic antibodies have proven highly effective and a fully humanized CD27 monoclonal antibody is undergoing clinical development with patients currently being enrolled for trials[9,10]. Based on the strong co-stimulatory effect of this antibody, activation of TIL, IFN-γ production and concomitant upregulation of PD-L1 on tumor and immune cells in the tumor micro-environment is to be expected. This combined with our work and that of others demonstrating that most intratumoral T cells in HGSC express PD-1, provides rationale for a combination strategy with checkpoint blockade targeting the PD-1/PD-L1 axis.

To conclude, outcome of surgical intervention and treatment with adjuvant or neo-adjuvant chemotherapy highly influence the prognostic value of TIL in HGSC. A naïve-like, less-differentiated CD27+ subtype of TIL can partly compensate for incomplete surgical removal of tumor and might be predictive for an immunologically "hot" tumor.

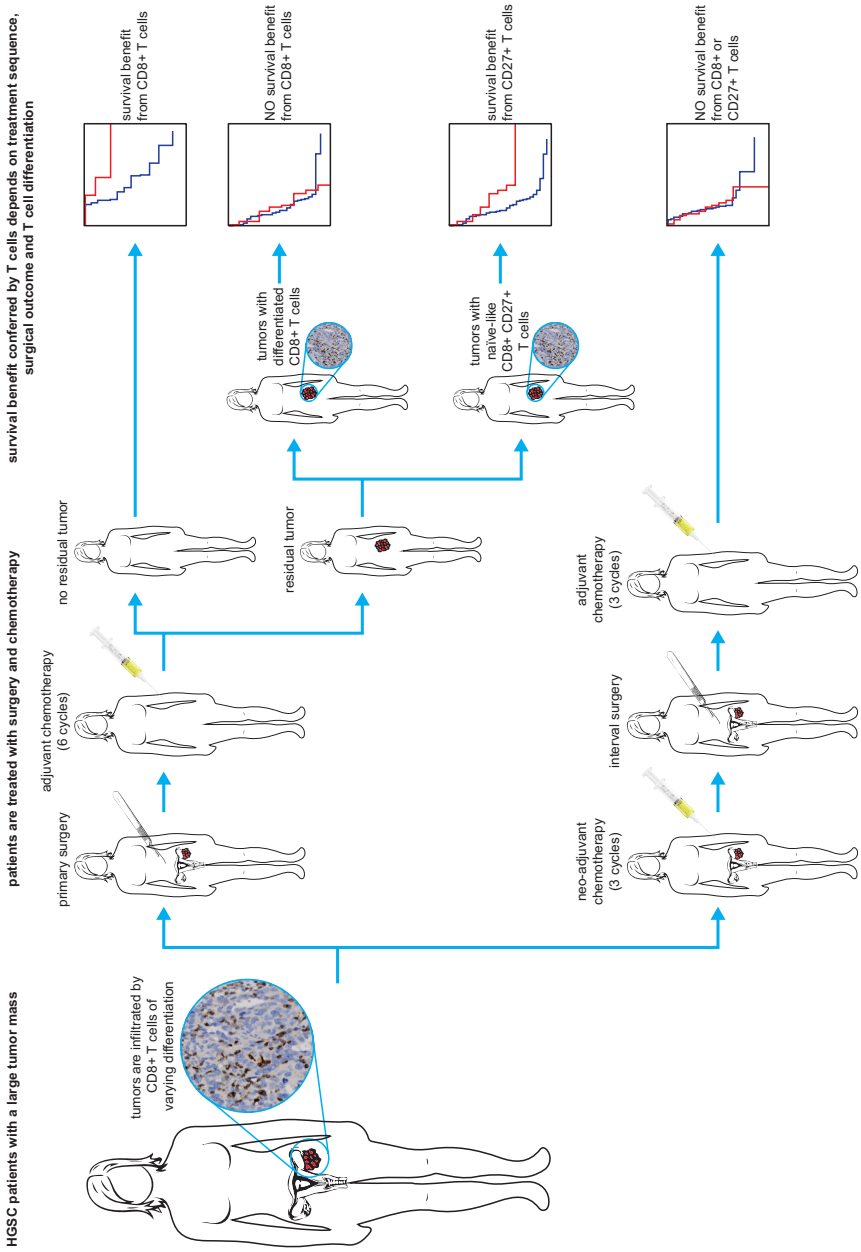

FIGURE 1. Surgical result and treatment regimen affect prognostic benefit conferred by tumor-infiltrating lymphocytes. CD8+ TIL confer a prognostic benefit only in HGSC patients whom received a complete surgical cytoreduction, whereas the CD27+ TIL subset also confers a prognostic benefit in patients with residual tumor after surgery. Patients treated with neo-adjuvant chemotherapy do not benefit from infiltration by CD8+ nor CD27+ TIL.

REFERENCES

1. Zhang L, Conejo-Garcia JR, Katsaros D, Gimotty PA, Massobrio M, Regnani G, Makrigiannakis A, Gray H, Schlienger K, Liebman MN, et al. Intratumoral T cells, recurrence, and survival in epithelial ovarian cancer. N Engl J Med 2003; 348:203–13.

2. Leffers N, Gooden MJM, de Jong RA, Hoogeboom B-N, ten Hoor KA, Hollema H, Boezen HM, van der Zee AGJ, Daemen T, Nijman HW. Prognostic significance of tumor-infiltrating T-lymphocytes in primary and metastatic lesions of advanced stage ovarian cancer. Cancer Immunol Immunother 2009; 58:449–59.

3. Vergote I, Tropé CG, Amant F, Kristensen GB, Ehlen T, Johnson N, Verheijen RHM, van der Burg MEL, Lacave AJ, Panici PB, et al. Neoadjuvant chemotherapy or primary surgery in stage IIIC or IV ovarian cancer. N Engl J Med 2010; 363:943–53.

4. Riester M, Wei W, Waldron L, Culhane AC, Trippa L, Oliva E, Kim S-H, Michor F, Huttenhower C, Parmigiani G, et al. Risk prediction for late-stage ovarian cancer by meta-analysis of 1525 patient samples. J Natl Cancer Inst 2014; 106:dju048.

5. Wouters MCA, Komdeur FL, Workel HH, Klip HG, Plat A, Kooi NM, Wisman GBA, Mourits MJE, Arts HJG, Oonk MHM, et al. Treatment regimen, surgical outcome and T cell differentiation influence prognostic benefit of tumor-infiltrating lymphocytes in high grade serous ovarian cancer. Clin Cancer Res 2015;

6. Ye Q, Song D-G, Poussin M, Yamamoto T, Best A, Li C, Coukos G, Powell DJ. CD137 accurately identifies and enriches for naturally occurring tumor-reactive T cells in tumor. Clin Cancer Res 2014; 20:44–55.

7. Restifo NP, Gattinoni L. Lineage relationship of effector and memory T cells. Curr Opin Immunol 2013; 25:556–63.

8. Rosenberg SA, Yang JC, Sherry RM, Kammula US, Hughes MS, Phan GQ, Citrin DE, Restifo NP, Robbins PF, Wunderlich JR, et al. Durable Complete Responses in Heavily Pretreated Patients with Metastatic Melanoma Using T-Cell Transfer Immunotherapy. Clin Cancer Res 2011; 17:4550–7.

9. Vitale LA, He L-Z, Thomas LJ, Widger J, Weidlick J, Crocker A, O'Neill T, Storey J, Glennie MJ, Grote DM, et al. Development of a human monoclonal antibody for potential therapy of CD27-expressing lymphoma and leukemia. Clin Cancer Res 2012; 18:3812–21.

10. He L-Z, Prostak N, Thomas LJ, Vitale L, Weidlick J, Crocker A, Pilsmaker CD, Round SM, Tutt A, Glennie MJ, et al. Agonist anti-human CD27 monoclonal antibody induces T cell activation and tumor immunity in human CD27-transgenic mice. J Immunol 2013; 191:4174–83.

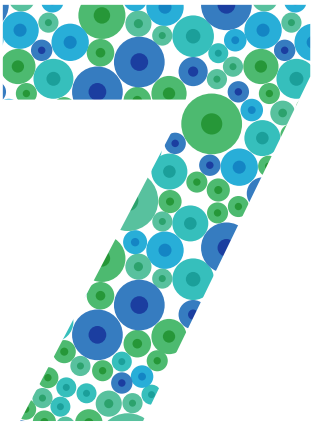

Carboplatin-paclitaxel chemotherapy selectively depletes circulating myeloid cells in high-grade serous ovarian cancer patients

FL Komdeur*, FA Eggink*, KL Brunekreeft, A Plat, EJ Propper, HH Workel, N Leffers, M de Bruyn, HW Nijman

*Authors contributed equally

Submitted

ABSTRACT

High-grade serous ovarian cancer (HGSOC) is the most lethal gynecological malignancy with limited therapeutic options. While trials exploring immunotherapy in HGSOC are promising, clinical efficacy remains restricted to a small percentage of patients. Several lines of evidence suggest that this low response rate might be improved by incorporating immunotherapy into standard-of-care chemotherapy for HGSOC, consisting of carboplatin and paclitaxel. To address whether this approach might be feasible, we analysed the systemic effects of first line carboplatin/paclitaxel chemotherapy on 35 immune markers in HGSOC patients pre-, mid- and post-chemotherapy. HGSOC patients had baseline immune profiles consistent with their advanced age, including a high relative ratio of myeloid to lymphocyte cells, but did not differ significantly from age-matched controls. A significant decrease in the relative abundance of the myeloid compartment of HGSOC patients was observed during carboplatin/paclitaxel treatment, which rebounded slightly after completion of chemotherapy. Depletion was uniform across all major myeloid subsets. No changes were observed in the relative abundance of other immune cell subsets, and T cell proliferation was not negatively affected by carboplatin/paclitaxel. Our data suggest carboplatin/paclitaxel chemotherapy might potentiate immunotherapy in the neo-adjuvant treatment of HGSOC through depletion of myeloid cells.

INTRODUCTION

High-grade serous ovarian cancer (HGSOC) is the most lethal gynecological malignancy and the fifth leading cause of cancer death in women. Almost all HGSOC patients present with advanced stage of disease and relapse rates are high with a 5-year survival of only 35%.[1] This poor prognosis for women with HGSOC has not improved in decades and new therapies are urgently needed. A promising new approach for the treatment of HGSOC may be immunotherapy.

Indeed, the immune system plays an important role in the development and control of HGSOC, and the number of intraepithelial CD8+ T cells in particular is associated with prolonged survival.[2–4] In addition, differentiation, exhaustion and other functional parameters of these intraepithelial CD8+ T cells have all been associated with prognosis, as has the presence of regulatory T cells, macrophages, B cells, myeloid-derived suppressor cells and others.[5–9] As in many tumor types, the immune checkpoint programmed death 1 (PD-1) and its ligand PD-L1 are also associated with prognosis, although controversy on the direction of this effect remains.[10–14] Nevertheless, initial trials using blocking antibodies (immune checkpoint blockade; ICB) targeting PD-1 or PD-L1 have demonstrated clinical effect in HGSOC patients, albeit in a small percentage of patients.[15] One potential strategy to increase the efficacy of immunotherapy, including ICB, is to combine treatment with other modalities, such as chemotherapy.

In HGSOC, a combination of carboplatin and paclitaxel chemotherapy is the standard of care for treatment of patients with advanced disease worldwide. Carboplatin and paclitaxel are DNA intercalating and cell cycle inhibitors, respectively, used frequently in combination for the treatment of ovarian, endometrial, lung and breast cancers. For HGSOC patients, carboplatin/paclitaxel is administered in 6 cycles of 3 weeks and combined with cytoreductive surgery performed either prior to chemotherapy, or at the interval (i.e. after 3 cycles of chemotherapy; see also supplementary Figure 1A and 1B). Previously, we demonstrated that the number and differentiation of tumor-infiltrating lymphocytes (TIL) did not differ between tumours that were carboplatin/paclitaxel-naïve when compared with tumours isolated after 3 cycles of chemotherapy.[16,17] Further, Lo et al. recently demonstrated that TIL+ tumours even showed an increase in the number of TIL after carboplatin/paclitaxel chemotherapy, whereas TIL- tumours did not, suggesting carboplatin/paclitaxel augments existing anti-tumour immunity.[18] However, little longitudinal data exists on the systemic immune cell status of HGSOC patients undergoing carboplatin/paclitaxel chemotherapy.

In this study, we analysed the effects of carboplatin/paclitaxel chemotherapy on the immune cell composition of HGSOC patients by evaluating 35 immune cell markers pre-, mid- and post-chemotherapy.

RESULTS

Carboplatin/paclitaxel chemotherapy selectively depletes myeloid cells from the circulation

A total of 75 patients with suspected ovarian cancer participated in the study. HGSOC was diagnosed in 18 of these patients. Consecutive pre- and post-chemotherapy samples were available in 7 patients (Table 1). First, we performed unbiased analyses of changes in the immune cell composition of the peripheral blood of HGSOC patients during carboplatin/paclitaxel chemotherapy. Hereto, PBMCs from HGSOC patients were isolated before chemotherapy, after 3 cycles of chemotherapy, and/or after completion of all 6 cycles of chemotherapy. PBMCs were screened by flow cytometry using validated antibodies against 35 major immune cell markers (supplementary table 1) in combinations of 8 distinct flow cytometry panels (supplementary table 2). After manual gating on live single cells of myeloid/lymphocyte size and density (supplementary Figure 1C), a previously described unsupervised clustering algorithm for identifying differences between different treatment groups in high-dimensional flow cytometry data (CITRUS) was used for analysis of each flow cytometry panel separately, totalling 8 analyses of up to 7 markers per analysis.[19]

Initial assessment of T cell differentiation (Figure 1A; panel 1, supplementary table 2) revealed no significant changes in T cell prevalence or differentiation during chemotherapy. However, a significant change was observed in the non-lymphocytic subset of $CD95^{high}$ / $CD4^{int}$ / FSC^{high} / SSC^{high} cell clusters, consistent with a myeloid cell population (Figure 1B and 1C). A significant relative decrease of clusters I and II was observed after 3 cycles of chemotherapy which rebounded slightly after 6 cycles of chemotherapy (Figure 1D). Back-gating and overlay of the identified cell clusters onto the total dataset similarly revealed these cells to be of myeloid cell size and density, with a specific loss from the total leukocyte population during chemotherapy treatment (exemplified for one patient in Figure 1D). Further, manual assessment of the data using standard gating strategies revealed a similar and significant relative depletion of myeloid cells compared to lymphocytes during chemotherapy (Figure 1E and supplementary Figure 1D). Of note, comparing age-matched patients with a benign ovarian tumour to HGSOC patients revealed no significant differences in the relative myeloid cell fraction (supplementary Figure 1E), nor did any other CITRUS analysis comparing baseline HGSOC samples to age-matched controls. Together, these data suggest that the relative expansion of the myeloid cells in the HGSOC population is due to cancer-unrelated patient-specific changes. Indeed, baseline percentages of myeloid cells varied extensively between individuals with HGSOC and benign tumours (Figure 1F and Supplementary Figure 1E).

TABLE 1. Patient characteristics

Age (years)	Stage (FIGO)	Grade	Histology	CA125 level	Primary treatment	Residual disease (cm)	Follow up status	DSS (months)	PFS (Months)
62	IIIc	grade III	serous	215	PS	0	ED	48	41
72	IIIc	grade III	serous	1771	PS	0	NED	39	39
60	IIc	grade II	serous with clearcell component	238	PS	0	NED	34	34
59	IIIc	grade III	serous	17776	NACT	0	NED	31	31
64	IIIc	grade III	serous	1287	PS	0	ED	26	18
52	IIIc	grade III	serous	470	PS	0	NED	11	11
75	IIIc	grade III	serous	432	NACT	0	ED	12	12

PS: primary cytoreductive surgery; followed by 6 cycles carboplatin/paclitaxel chemotherapy. chemotherapy.
NACT: neoadjuvant chemotherapy; 3 cycles carboplatin/paclitaxel chemotherapy followed by cytoreductive surgery and 3 additional cycles of carboplatin/paclitaxel
NED: no evidence of disease. ED: evidence of disease DSS: disease specific survival. PFS: progression free survival

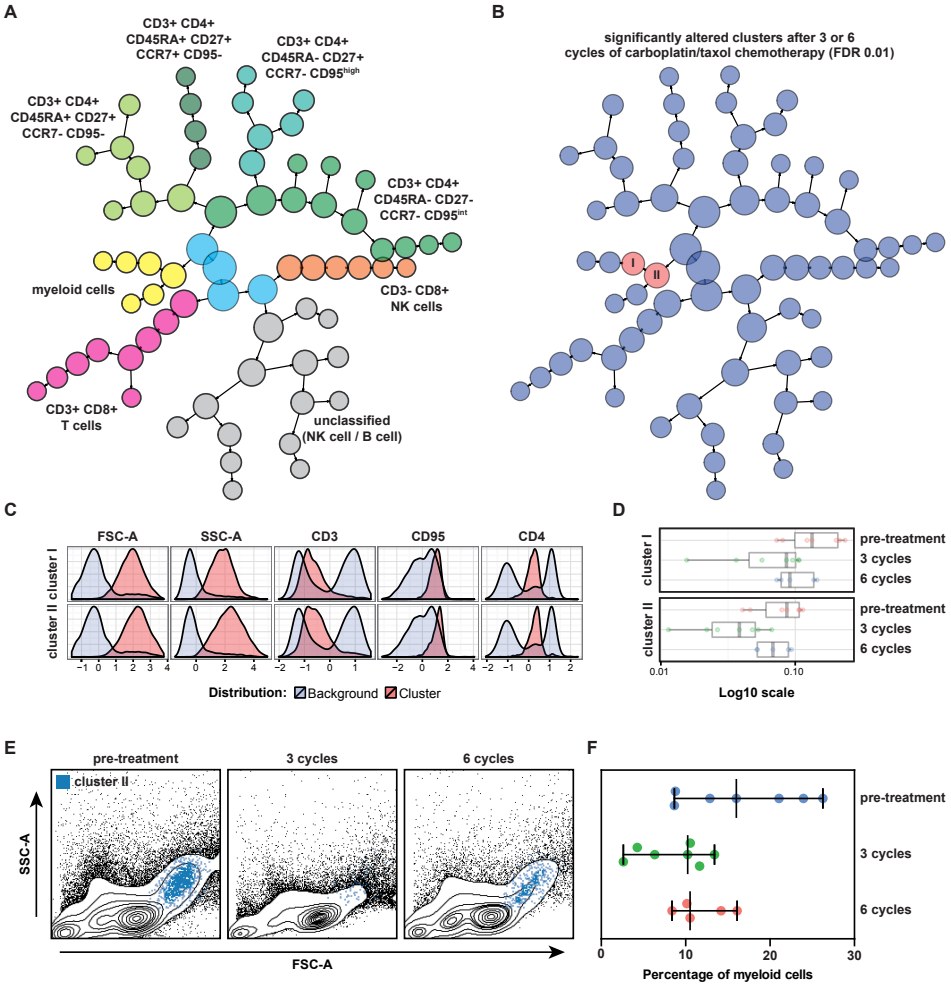

FIGURE 1. Carboplatin/paclitaxel selectively depletes myeloid cells from the circulation. Unsupervised hierarchical clustering of PBMCs was performed using CITRUS based on FSC and SSC light scatter characteristics, and expression of CD3, CD4, CD8, CD45RA, CCR7, CD27 and CD95 (panel 1, supplementary table 2). **A)** Identified clusters were assigned to specific immune cell subsets and pseudocolored based on expression of CD3, CD4, CD8, CD45RA, CCR7, CD27 and CD95. **B)** Clusters significantly altered between pre-, mid- and post-chemotherapy samples are highlighted in red (I and II) **C)** Phenotype of significantly altered cluster I and II and **D)** prevalence of cluster I and II at the indicated time-points. **E)** Events from cluster I and II were exported and overlaid on the total dataset of the individual patients and time-points to confirm the phenotype (illustrated for 1 patient). **F)** Manual gating and quantification of myeloid cells based on FSC and SSC light scatter characteristics.

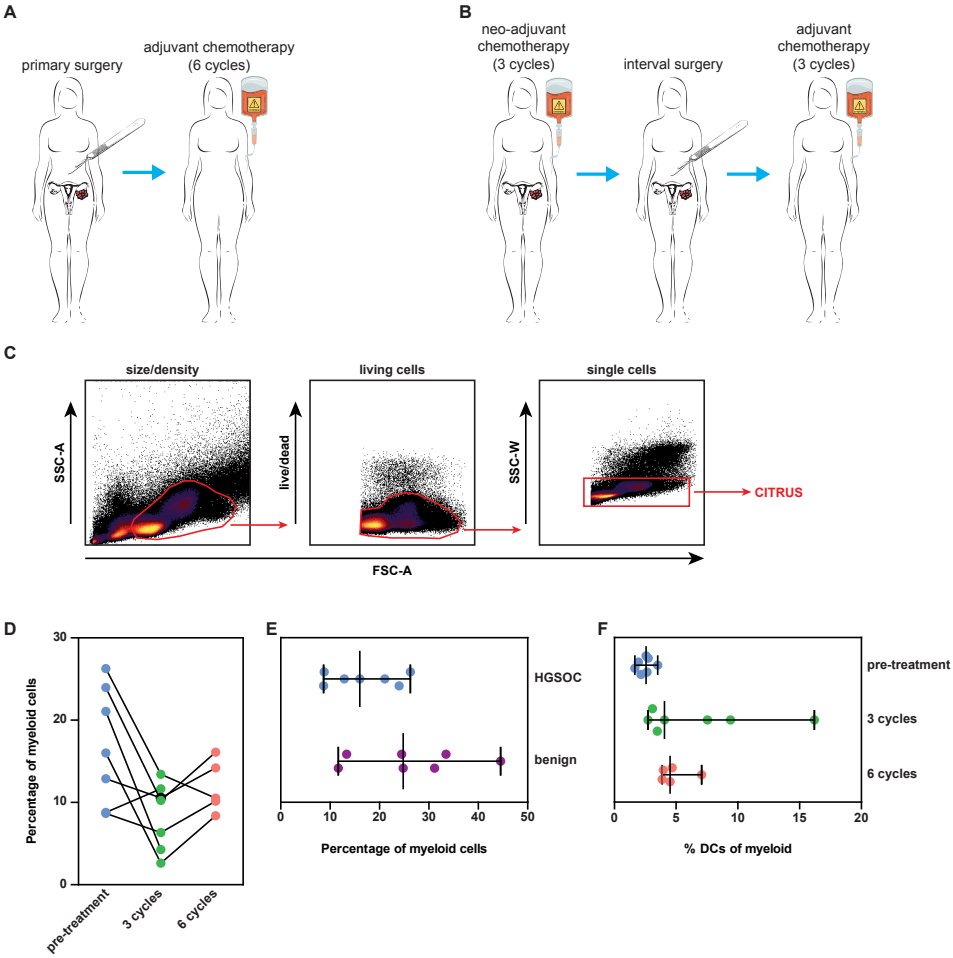

SUPPLEMENTARY FIGURE 1. Carboplatin/paclitaxel selectively depletes myeloid cells from the circulation. A-B) Treatment scheme for high-grade serous ovarian cancer patients included in this study. **C)** Gating strategy used for preselecting events for analysis by CITRUS. **D)** Manual gating and quantification of myeloid cells based on FSC and SSC light scatter characteristics for each individual patients per time point. **E)** Manual gating and quantification of myeloid cells based on FSC and SSC light scatter characteristics comparing HGSOC and age-matched control with benign ovarian tumours. **F)** Percentage of Lineage-negative HLA-DR+ cells as a fraction of the total myeloid population at the indicated time-points.

Carboplatin/paclitaxel chemotherapy depletes cells evenly across all major myeloid subpopulations

In line with the above, analysis of major myeloid cell populations using a myeloid-directed antibody panel (panel 2; supplementary table 2) also revealed a significant decrease in the percentage of circulating myeloid cells after carboplatin/paclitaxel chemotherapy (Figure 2A). This change was present only in a root cluster, but not linked to specific myeloid subsets (Figure 2A). In line with this, the identified clusters showed a remarkably homogenous phenotype of $CD14^{+}$ / $CD11b^{+}$ / $CD11c^{+}$ /$CD33^{+}$ / HLA-DR^{+} / FSC^{high} /SSC^{high}, consistent with circulating monocytes (Figure 2B). The relative depletion of myeloid cells observed using these myeloid markers was similar as that observed when analysing T cell differentiation markers as described above, indicating the use of "basic" FSC and SSC characteristics may already be sufficient to assess the carboplatin/paclitaxel-induced myeloid cell depletion (Figure 2C).

To confirm that carboplatin/paclitaxel did not have a specific and negative effect on circulating antigen-presenting dendritic cell subsets (DCs), we also analysed major DC markers (supplementary table 1 and 2) using CITRUS and visualized the distribution of the subsets using t-Distributed Stochastic Neighbour Embedding (t-SNE) followed by manual gating for all patients and time-points (exemplified in Figure 2D). No differences were observed in DC abundance by CITRUS. In a single patient, we observed a marked expansion of CD11c+ CD1c- mDCs after 6 cycles of chemotherapy (Figure 2D and 2E), but most other effects observed were minimal and similarly heterogeneous (Figure 2E), in line with the initial CITRUS analysis. Thus, DC subsets were not specifically depleted by chemotherapy in these patients, slightly shifting the relative ratio of DC over monocyte in favour of DCs (supplementary Figure 1F).

Carboplatin/paclitaxel chemotherapy in HGSOC has minimal effects on T cell phenotype and function

Finally, we assessed how carboplatin/paclitaxel chemotherapy affects T cell phenotype and function using a combination of T cell activation, differentiation and exhaustion markers specific for both CD4 and CD8 T cells (panel 6, supplementary table 2). In addition, we assessed markers previously associated with improved prognosis and/or response to immunotherapy in other malignancies (panels 4-7, supplementary table 2). In line with the initial unsupervised analysis, no consistent changes in T cell markers were observed across all patients and time-points analysed for either CD4 (Figure 3A) or CD8 cells (Figure 3B).

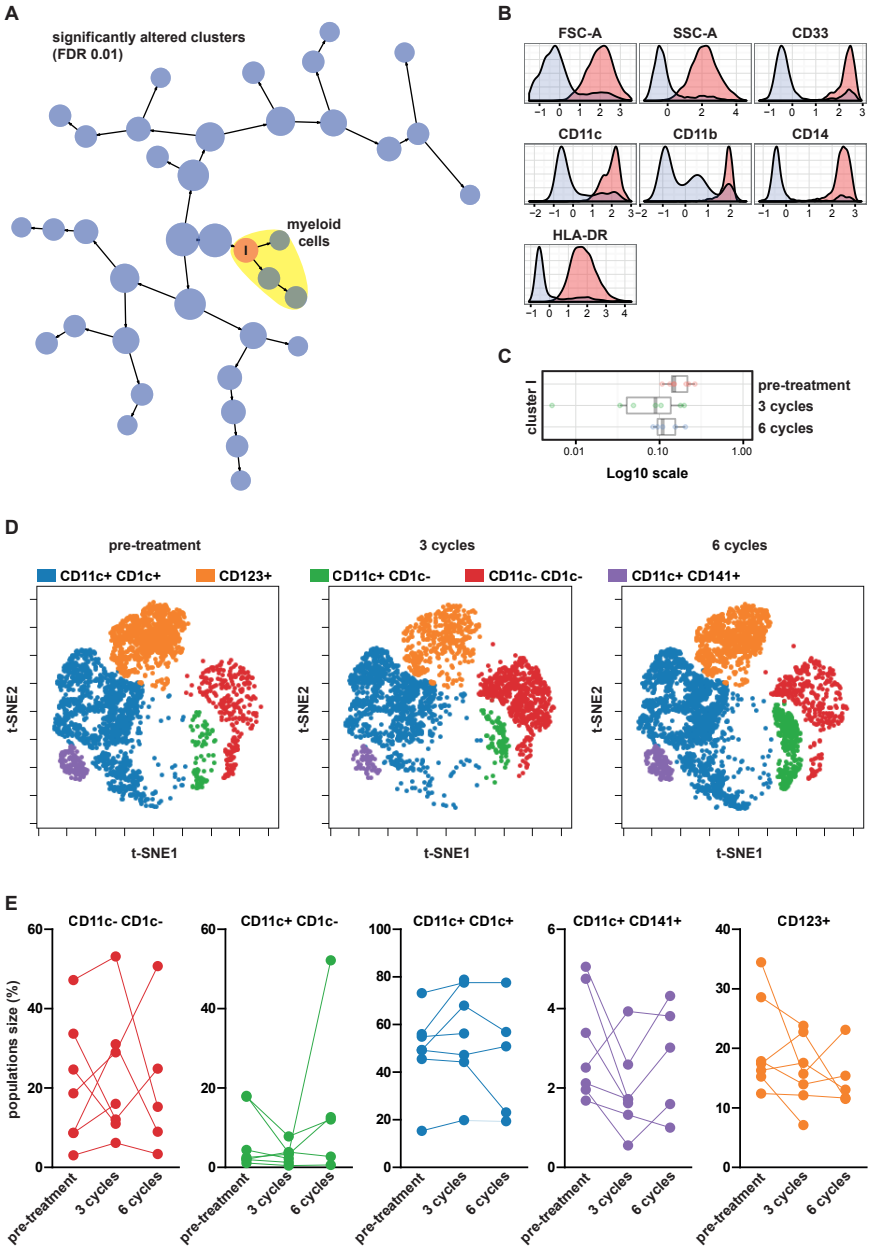

FIGURE 2. Carboplatin/paclitaxel depletes myeloid cells evenly across all major subpopulations. Unsupervised hierarchical clustering of PBMCs was performed using CITRUS based on FSC and SSC light scatter characteristics, and expression of CD33, CD14, CD11c, CD11b and HLA-DR (panel 2, supplementary table 2). **A)** Clusters significantly altered between pre-, mid- and post-chemotherapy samples are highlighted in red (I) **B)** Phenotype of significantly altered cluster I and **C)** prevalence of cluster I at the indicated time-points. **D)** PBMCs were gated based on a Lineage-negative HLA-DR+ phenotype and DC subpopulations identified using t-Distributed Stochastic Neighbour Embedding (t-SNE) on the basis of CD11c, CD123, CD141 and CD1c expression. **E)** Quantification of the identified DC populations for individual patients and time-points.

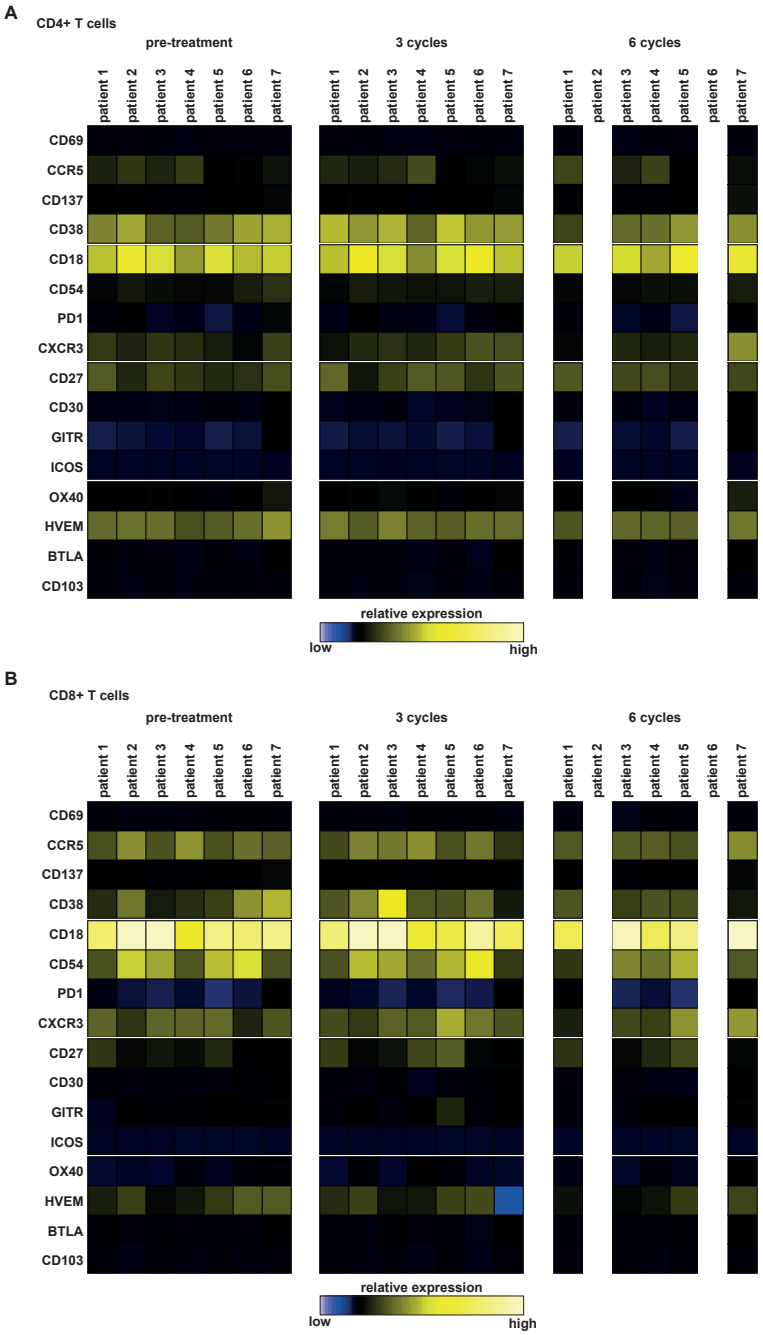

FIGURE 3. Carboplatin/paclitaxel has minimal effects on T cell phenotype. A) CD4 and **B)** CD8+ T cells were identified based on expression of CD3 and CD4 or CD8 and expression of the indicated markers assessed in each of the two cell populations using mean fluorescent intensity (panels 4-7, supplementary table 2).

Moreover, carboplatin/paclitaxel chemotherapy did not affect the proliferation of T cells as determined by Ki67 staining (Figure 4A; panel 8, supplementary table 2), the relative expression of key transcription factors EOMES and Tbet (Figure 4B), nor the activation and expansion of T cells in response to stimulation with anti-CD3/anti-CD28 beads in combination with low dose IL-2 (Figure 4C). Lastly, the proportion of regulatory FoxP3+ T cells and their proliferative capacity was also not affected in this patient cohort (Figure 4A). Taken together, our data suggests T cell phenotype and function remain unaffected by the administration of carboplatin/paclitaxel chemotherapy in HGSOC patients.

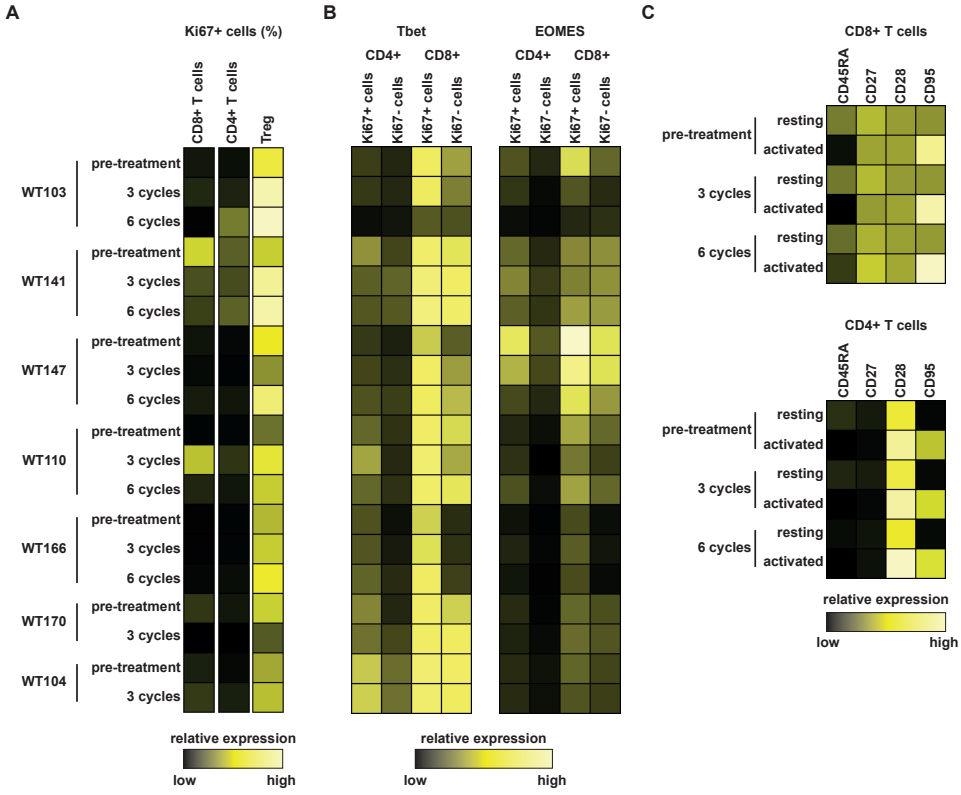

FIGURE 4. Carboplatin/paclitaxel has minimal effects on T cell activity. A-B) CD4 and CD8+ T cells were identified based on expression of CD3 and CD4 or CD8 and expression of Ki67, Tbet and/or EOMES assessed using mean fluorescent intensity as indicated (panel 8, supplementary table 2). **C)** PBMCs from one of the patients at 3 individual time-points were stimulated *ex vivo* using anti-CD3/anti-CD28 beads in the presence of 100 U/mL IL-2 and T cell activation and differentiation markers assessed as indicated. **D)** Percentage of FoxP3+ CD4+ cells for all patients at all time-points.

DISCUSSION

In the current study we demonstrate that carboplatin/paclitaxel chemotherapy specifically depletes myeloid cells from the circulation of HGSOC patients. Depletion does not appear to affect any major myeloid subset in particular and shifted the relative ratio of DCs to total myeloid cells in favour of DCs. In addition, we establish that carboplatin/paclitaxel chemotherapy does not affect T cell phenotype, activation or differentiation in HGSOC patients at the indicated time-points.

Our data is in line with a report on the effect of carboplatin/paclitaxel treatment in cervical cancer patients.[20] In that study, Welters et al. described an expansion of myeloid cells in advanced cervical cancer patients compared to healthy controls, which normalized after carboplatin/paclitaxel chemotherapy. This effect was also associated with increased T cell reactivity to recall antigens. Interestingly, the baseline magnitude of myeloid cell expansion appears to be more pronounced in cervical cancer, with some patients having almost 70% of myeloid cells at baseline, and a median of ~50% compared to a median of ~16% observed in our patients. This difference in magnitude may also explain why Welters et al. observed an increase in circulating myeloid cells compared to healthy donors while this difference did not reach statistical significance in our set. Despite these differences, the magnitude and timing of the observed decrease in myeloid cells are remarkably consistent between cervical and HGSOC patients with a more pronounced depletion during chemotherapy that rebounds somewhat after conclusion of all 6 cycles. Since the depletion of myeloid cells in cervical cancer patients also enhanced the proliferative HPV16-specific T cell responses after a therapeutic vaccination, this suggests a rationale for combining carboplatin/paclitaxel with e.g. immune checkpoint inhibitors or tumour antigen-specific vaccination in the neo-adjuvant treatment setting of HGSOC.[21]

There are a number of potential explanations for the decreased number of myeloid cells during chemotherapy Firstly, carboplatin/paclitaxel has a well-established toxicity profile that includes a decreased leukocyte output from the bone marrow resulting in leukopenia in some patients.[22] Indeed, some, but not all, of the patients included in our analysis displayed leukopenia during treatment (data not shown), although we did not observe a direct correlation with the magnitude or timing of myeloid cell depletion and leukopenia. Nevertheless, the half-life of myeloid cells in circulation (1-3 days) would render them more sensitive to depletion by reduced bone-marrow output when compared to e.g. lymphocytes with an estimated half-life of between 1 month and 8 years depending on the subset.[23–25] Alternatively, the decreased tumour burden after chemotherapy and/or cytoreductive surgery may reduce the release of cancer-produced factors from the tumour that induced the initial myeloid expansion. Indeed, release of IL-6 and/or IL-10 from ovarian cancer cells has been linked to reduced HLA-DR levels on circulating $CD14^+$ monocytes and acquisition of myeloid-derived suppressor cell (MDSC) function.[26] Nevertheless,

while we have previously detected such a $CD14^+$ HLA-DR^{low} population in HGSOC tumours (unpublished data), we did not observe this MDSC population in the circulation here. Further, our data on age-matched controls suggests the expansion of myeloid cells in these patients may be independent of tumour-derived factors. Finally, the combination of carboplatin/paclitaxel may have direct effects on the myeloid cell populations. While the cytotoxic effects of carboplatin/paclitaxel on myeloid cells has not been described as particularly higher than those observed in lymphocytes, auto- and/or paracrine effects have been described to skew monocyte differentiation and/or migration, potentially through IL-6- and PGE2-dependent mechanisms.[27]

Importantly, we observed no deleterious effects of carboplatin/paclitaxel on differentiation, activation and/or proliferation of T cells, confirming previous reports that certain chemotherapeutic regimes can be effectively combined with T cell-targeting immunotherapy.[20,21,28] Indeed, combined carboplatin/paclitaxel with immune checkpoint inhibitors in the neo-adjuvant treatment of breast cancer appears well tolerated and efficacious.[28]

In conclusion, our data suggests carboplatin/paclitaxel chemotherapy fosters a permissive environment for immunotherapeutic intervention in the neo-adjuvant treatment setting of HGSOC by depleting myeloid cells without affecting T cells. These findings have direct implications for the design of immunotherapy trials in HGSOC patients.

MATERIALS AND METHODS

Patients and ethics

PBMCs from HGSOC patients were isolated before carboplatin/paclitaxel chemotherapy, 1-3 weeks after 3 cycles of chemotherapy, and 4-6 weeks after completion of all 6 cycles of chemotherapy. PBMCs were isolated by ficoll density centrifugation using lymphoprep according to the manufacturer's instructions. As a control, PBMCs were isolated from age-matched patients with a benign ovarian tumour. According to Dutch law, approval from our institutional review board was obtained. Subsequently, all patients gave written informed consent and data was collected in an anonymous database in which patient identity was protected by unique patient codes.

Flow cytometric analysis

PBMCs were characterized by multiparameter flow cytometry. The Zombie Aqua Fixable Viability Kit (BioLegend, Uithoorn, The Netherlands) was used for live/dead staining according to the manufacturer's instructions. Antibodies used for analysis are described in supplementary table 1. Specific combinations used for cytometry panels are described in supplementary table 2.

SUPPLEMENTARY TABLE 1. Antibodies used

Antigen	Clone	Fluorophore	Vendor	Catalog no. (on 12-12-2017)
Lineage (CD3, CD14, CD16, CD19, CD20, CD56)	MφP9, NCAM16.2, 3G8, SK7, L27, SJ25C1	FITC	BD Biosciences	340546
CD1c	L161	PE-Cy7	ThermoFisher Scientific (eBioscience)	25-0015-41
CD3	OKT3	PerCP-Cy5.5	ThermoFisher Scientific (eBioscience)	45-0037-42
CD3	OKT3	PE	BD Biosciences	16-0037-81
CD3	UCHT1	BV421	BD Biosciences	562427/562427
CD4	OKT4	PerCP-Cy5.5	ThermoFisher Scientific (eBioscience)	45-0048-42
CD8a	RPA-T8	APC-eFlour 780	ThermoFisher Scientific (eBioscience)	47-0088-42
CD11b	ICRF44	PE	ThermoFisher Scientific (eBioscience)	12-0118-41
CD11c	BU15	APC-eFlour 780	ThermoFisher Scientific (eBioscience)	47-0128-41
CD14	61D3	APC	ThermoFisher Scientific (eBioscience)	17-0149-42
CD18	6.7	FITC	ThermoFisher Scientific (eBioscience)	11-0189-42
CD27	9F4	FITC	Sanquin	M1764
CD28	CD28.2	PerCP-Cy5.5	ThermoFisher Scientific (eBioscience)	45-0289-41
CD30	BerH8	PE	BD Biosciences	550041
CD33	WM53	PE-Cy7	ThermoFisher Scientific (eBioscience)	25-0338-42
CD38	HB7	PE-Cy7	ThermoFisher Scientific (eBioscience)	25-0388-41
CD45RA	HI100	APC	ThermoFisher Scientific (eBioscience)	17-0458-42/41
CD54	HA58	APC	ThermoFisher Scientific (eBioscience)	17-0549-41
CD69	FN50	FITC	ThermoFisher Scientific (eBioscience)	11-0699-41
CD95	DX2	PE-Cy7	BD Biosciences	561636
CD103	BerACT8	FITC	BD Biosciences	561677
CD123	7G3	PerCP-Cy5.5	BD Biosciences	560904
CD134 (OX40)	ACT35	PE-Cy7	BD Biosciences	563663
CD137	4B4	PE	ThermoFisher Scientific (eBioscience)	12-1379-42
CD141	1A4	PE	BD Biosciences	559781
CD183 (CXCR3)	CEW33D	PE-Cy7	ThermoFisher Scientific (eBioscience)	25-1839-42
CD195 (CCR5)	NP-6G4	APC	ThermoFisher Scientific (eBioscience)	17-1956-41
CD197 (CCR7)	150503	BV421	BD Biosciences	562555
CD270 (HVEM)	94801	Alexa Fluor 647	BD Biosciences	564411
CD272 (BTLA)	J168-540	APC	BD Biosciences	564800
CD278 (ICOS)	DX29	BV421	BD Biosciences	562901
CD274 (PD1)	MIH4	PE	ThermoFisher Scientific (eBioscience)	12-9969-41
CD357 (GITR)	eBioAITR	PE-Cy7	ThermoFisher Scientific (eBioscience)	25-5875-41
HLA-DR	G46-6	BV421	BD Biosciences	562804
T-bet	eBio4B10	eFluor 660	ThermoFisher Scientific (eBioscience)	55-5825-80
Eomesodermin	WD1928	PE-Cy7	ThermoFisher Scientific (eBioscience)	25-4877-41
FOXP3	236A/E7	FITC	ThermoFisher Scientific (eBioscience)	11-4777-41

When indicated, PBMCs were pre-activated prior to phenotyping using anti-CD3/anti-CD28 beads (Life Technologies) and 100 U/mL IL-2. Flow cytometry was performed on a BD FACSVerse (BD Biosciences) and samples were analysed with Premium Cytobank software (cytobank.org). Each cytometry panel indicated in supplementary table 2 was analysed separately by CITRUS comparing baseline PBMCs to PBMCs after 3 and 6 cycles of chemotherapy (3 time points total). For analysis by CITRUS, the following parameters were used: 95000 total events were clustered at 5000 sampled events per file. Minimum cluster size was set at 2.3% with an FDR of 1%. Where indicated, additional t-SNE analysis was performed to visualize the data. For analysis by t-SNE, the viSNE function was used with the following parameters: ~60.000 total events were sampled using proportional sampling from across all files. ViSNE was run using 1000 iterations, a perplexity of 30 and theta of 0.5.

SUPPLEMENTARY TABLE 2. Antibody panels used

Panel 1	Panel 2	Panel 3	Panel 4	Panel 5	Panel 6	Panel 7	Panel 8
CD3	HLA-DR	HLA-DR	CD3	CD3	CD3	CD3	CD3
CD8a	CD11b	Lineage	CD8a	CD8a	CD8a	CD8a	CD8a
CD4	CD33	CD141	CD4	CD4	CD27	CD4	CD4
CD45RA	CD14	CD123	CD69	CD18	CD30	CD30	FOXP3
CD27	CD11c	CD1c	CCR5	CD54	GITR	OX40	Eomesodermin
CCR7		CD11c	CD137	PD1	ICOS	HVEM	Tbet
CD95			CD38	CXCR3	BTLA	CD103	Ki-67

Statistics

All statistical analyses were performed using built-in cytobank analysis (CITRUS), or Graphpad Prism for data obtained by manual gating. For data that was gated manually, all tests were performed by two-sided non-parametric t-tests or Friedman with Dunn's post-test, and p-values <0.05 were considered significant.

ACKNOWLEDGEMENTS

This work was supported by Dutch Cancer Society/Alped'Huzes grant UMCG 2014–6719 to MB, Jan Kornelis de Cock Stichting grants to FLK, KLB and FAE, Dutch Cancer Society grant RuG2012-5557 to NL and a UMCG Mandema Stipend to NL.

The authors would like to thank Henk Moes and Geert Mesander for their technical assistance.

REFERENCES

1. Vaughan S, Coward JI, Bast RC, Berchuck A, Berek JS, Brenton JD, Coukos G, Crum CC, Drapkin R, Etemadmoghadam D, Friedlander M, Gabra H, Kaye SB, Lord CJ, et al. Rethinking ovarian cancer: recommendations for improving outcomes. Nat Publ Gr [Internet]. 2011 [cited 2017 Aug 8];11.

2. Leffers N, Gooden MJM, de Jong RA, Hoogeboom B-N, ten Hoor KA, Hollema H, Boezen HM, van der Zee AGJ, Daemen T, Nijman HW. Prognostic significance of tumor-infiltrating T-lymphocytes in primary and metastatic lesions of advanced stage ovarian cancer. Cancer Immunol Immunother [Internet]. 2009 [cited 2016 Mar 22];58:449–59.

3. Vermeij R, de Bock GH, Leffers N, Ten Hoor KA, Schulze U, Hollema H, van der Burg SH, van der Zee AGJ, Daemen T, Nijman HW. Tumor-infiltrating cytotoxic T lymphocytes as independent prognostic factor in epithelial ovarian cancer with wilms tumor protein 1 overexpression. J Immunother [Internet]. [cited 2016 Mar 22];34:516–23.

4. Hwang W-T, Adams SF, Tahirovic E, Hagemann IS, Coukos G. Prognostic significance of tumor-infiltrating T cells in ovarian cancer: a meta-analysis. Gynecol Oncol [Internet]. 2012 [cited 2016 Mar 22];124:192–8. Available from: http://www.ncbi.nlm.nih.gov/pubmed/22040834

5. Barnes TA, Amir E. HYPE or HOPE: the prognostic value of infiltrating immune cells in cancer. Br J Cancer [Internet]. 2017 [cited 2017 Aug 8];

6. Nelson BH. The impact of T-cell immunity on ovarian cancer outcomes. Immunol Rev [Internet]. 2008;222:101–16.

7. Sato E, Olson SH, Ahn J, Bundy B, Nishikawa H, Qian F, Jungbluth AA, Frosina D, Gnjatic S, Ambrosone C, Kepner J, Odunsi T, Ritter G, Lele S, et al. Intraepithelial CD8+ tumor-infiltrating lymphocytes and a high CD8+/regulatory T cell ratio are associated with favorable prognosis in ovarian cancer. Proc Natl Acad Sci U S A [Internet]. 2005 [cited 2015 Jan 18];102:18538–43.

8. Wouters MCA, Komdeur FL, Workel HH, Klip HG, Plat A, Kooi NM, Wisman GBA, Mourits MJE, Arts HJG, Oonk MHM, Yigit R, de Jong S, Melief CJM, Hollema H, et al. Treatment Regimen, Surgical Outcome, and T-cell Differentiation Influence Prognostic Benefit of Tumor-Infiltrating Lymphocytes in High-Grade Serous Ovarian Cancer. Clin Cancer Res [Internet]. 2016 [cited 2016 Dec 1];22:714–24.

9. Wouters MCA, Komdeur FL, de Bruyn M, Nijman HW. Size matters: Survival benefit conferred by intratumoral T cells is dependent on surgical outcome, treatment sequence and T cell differentiation. Oncoimmunology [Internet]. 2016 [cited 2016 Dec 1];5:e1122863.

10. Tumeh PC, Harview CL, Yearley JH, Shintaku IP, Taylor EJM, Robert L, Chmielowski B, Spasic M, Henry G, Ciobanu V, West AN, Carmona M, Kivork C, Seja E, et al. PD-1 blockade induces responses by inhibiting adaptive immune resistance. Nature [Internet]. 2014 [cited 2014 Nov 26];515:568–71.

11. Karyampudi L, Lamichhane P, Krempski J, Kalli KR, Behrens MD, Vargas DM, Hartmann LC, Janco JMT, Dong H, Hedin KE, Dietz a. B, Goode EL, Knutson KL. PD-1 blunts the function of ovarian tumor-infiltrating dendritic cells by inactivating NF-KappaB. Cancer Res [Internet]. 2015.

12. Landskron J, Helland Ø, Torgersen KM, Aandahl EM, Gjertsen BT, Bjørge L, Taskén K. Activated regulatory and memory T-cells accumulate in malignant ascites from ovarian carcinoma patients. Cancer Immunol Immunother [Internet]. 2015;64:337–47.

13. Teng MWL, Ngiow SF, Ribas a., Smyth MJ. Classifying Cancers Based on T-cell Infiltration and PD-L1. Cancer Res [Internet]. 2015;75:2139–45.

14. Khagi Y, Kurzrock R, Patel SP. Next generation predictive biomarkers for immune checkpoint inhibition. Cancer Metastasis Rev [Internet]. Springer US; 2017 [cited 2017 Aug 17];36:179–90.

15. Wang D, Guo L, Wu X. Checkpoint inhibitors in immunotherapy of ovarian cancer. Tumor Biol [Internet]. 2014;36:33–9.

16. Wouters MCA, Komdeur FL, Workel HH, Klip HG, Plat A, Kooi NM, Wisman GBA, Mourits MJE, Arts HJG, Oonk MHM, Yigit R, de Jong S, Melief CJM, Hollema H, et al. Treatment Regimen, Surgical Outcome, and T-cell Differentiation Influence Prognostic Benefit of Tumor-Infiltrating

Lymphocytes in High-Grade Serous Ovarian Cancer. Clin Cancer Res [Internet]. 2016 [cited 2016 Mar 22];22:714–24.

17. Komdeur FL, Wouters MCA, Workel HH, Tijans AM, Terwindt ALJ, Brunekreeft KL, Plat A, Klip HG, Eggink FA, Leffers N, Helfrich W, Samplonius DF, Bremer E, Wisman GBA, et al. CD103+ intraepithelial T cells in high-grade serous ovarian cancer are phenotypically diverse TCRαβ+ CD8αβ+ T cells that can be targeted for cancer immunotherapy. Oncotarget [Internet]. 2016 [cited 2016 Dec 1].

18. Lo CS, Sanii S, Kroeger DR, Milne K, Talhouk A, Chiu DS, Rahimi K, Shaw PA, Clarke BA, Nelson BH. Neoadjuvant Chemotherapy of Ovarian Cancer Results in Three Patterns of Tumor-Infiltrating Lymphocyte Response with Distinct Implications for Immunotherapy. Clin Cancer Res [Internet]. 2017 [cited 2018 Jan 21];23:925–34.

19. Bruggner R V, Bodenmiller B, Dill DL, Tibshirani RJ, Nolan GP. Automated identification of stratifying signatures in cellular subpopulations. Proc Natl Acad Sci U S A [Internet]. National Academy of Sciences; 2014 [cited 2017 Mar 21];111:E2770-7.

20. Welters MJ, Van Der Sluis TC, Van Meir H, Loof NM, Van Ham VJ, Van Duikeren S, Santegoets SJ, Arens R, De Kam ML, Cohen AF, Van Poelgeest MI, Kenter GG, Kroep JR, Burggraaf J, et al. Vaccination during myeloid cell depletion by cancer chemotherapy fosters robust T cell responses.

21. Komdeur FL, Prins TM, van de Wall S, Plat A, Wisman GBA, Hollema H, Daemen T, Church DN, de Bruyn M, Nijman HW. CD103+ tumor-infiltrating lymphocytes are tumor-reactive intraepithelial CD8+ T cells associated with prognostic benefit and therapy response in cervical cancer. Oncoimmunology. 2017;

22. Yoshihama T, Nomura H, Iwasa N, Kataoka F, Hashimoto S, Nanki Y, Hirano T, Makabe T, Sakai K, Yamagami W, Hirasawa A, Aoki D. Efficacy and safety of dose-dense paclitaxel plus carboplatin as neoadjuvant chemotherapy for advanced ovarian, fallopian tube or peritoneal cancer. Jpn J Clin Oncol [Internet]. 2017 [cited 2018 Jan 21];47:1019–23.

23. Summers C, Rankin SM, Condliffe AM, Singh N, Peters AM, Chilvers ER. Neutrophil kinetics in health and disease. Trends Immunol [Internet]. Elsevier; 2010 [cited 2018 Jan 22];31:318–24.

24. Yang J, Zhang L, Yu C, Yang X-F, Wang H. Monocyte and macrophage differentiation: circulation inflammatory monocyte as biomarker for inflammatory diseases. Biomark Res [Internet]. BioMed Central; 2014 [cited 2018 Jan 22];2:1.

25. Farber DL, Yudanin NA, Restifo NP. Human memory T cells: generation, compartmentalization and homeostasis. Nat Rev Immunol [Internet]. NIH Public Access; 2014 [cited 2018 Jan 22];14:24–35.

26. Wu L, Deng Z, Peng Y, Han L, Liu J, Wang L, Li B, Zhao J, Jiao S, Wei H, Wu L, Deng Z, Peng Y, Han L, et al. Ascites-derived IL-6 and IL-10 synergistically expand CD14+HLA-DR low myeloid-derived suppressor cells in ovarian cancer patients. Oncotarget [Internet]. Impact Journals; 2017 [cited 2018 Jan 21];8:76843–56.

27. Dijkgraaf EM, Heusinkveld M, Tummers B, Vogelpoel LTC, Goedemans R, Jha V, Nortier JWR, Welters MJP, Kroep JR, van der Burg SH. Chemotherapy alters monocyte differentiation to favor generation of cancer-supporting M2 macrophages in the tumor microenvironment. Cancer Res [Internet]. 2013 [cited 2018 Jan 21];73:2480–92.

28. Polk A, Svane I-M, Andersson M, Nielsen D. Checkpoint inhibitors in breast cancer – Current status. Cancer Treat Rev [Internet]. 2018 [cited 2018 Jan 21];63:122–34.

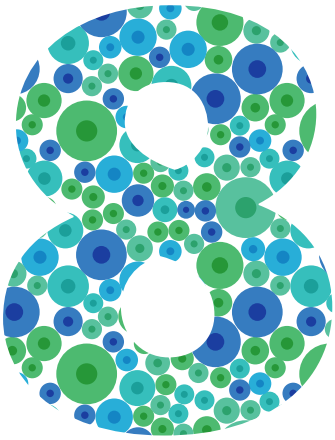

Immune modulating effects and safety of Vvax001, a therapeutic Semliki Forest Virus based cancer vaccine, in patients with a history of (pre) malignant cervical lesions: Study protocol

FL Komdeur, S van de Wall, R Yigit, A Singh, M de Bruyn, A Boerma, BN Hoogeboom, E Schuuring, JWG Kosterink, A Jorritsma-Smit, T Daemen and HW Nijman

ABSTRACT

Background: Currently, high-grade premalignant lesions of the cervix are treated with large loop excision of the transformation zone (LLETZ). This procedure has potential complications, and does not necessarily eradicate the underlying HPV infection, causative agent for (pre) malignant neoplasia of the cervix. Therefore, therapeutic vaccination is a potential non-invasive alternative for the treatment of these premalignant cervical lesions. We developed a new therapeutic vaccine, called Vvax001. Vvax001 aims at inducing long-lasting immune responses against HPV16-infected cells. In preclinical studies, Vvax001 was shown to be an effective and well-tolerated treatment for HPV16-induced tumors. These preclinical results supported the application for a first-in-human phase I clinical trial. The aim of this study is to assess the immunological activity, safety and tolerability of Vvax001 in human.

Methods: In this first-in-human phase 1 clinical trial, four dose levels of Vvax001 will be tested. Vvax001 is a therapeutic viral vector vaccine consisting of replication-incompetent Semliki Forest Virus (rSFV) replicon particles encoding the HPV16 derived tumor antigens E6 and E7. Patients will receive three consecutive vaccinations, with an interval of 3 weeks. Cohorts of 3 patients will be treated per dose level.

Discussion: Based on preclinical results, Vvax001 represents a promising therapeutic vaccine for the treatment of (pre)malignant lesions of the cervix caused by HPV16. All results on immunogenicity and tolerability of Vvax001 in human are expected to be available mid-2018.

Trials registration: NCT03141463; NL56680.000.16

BACKGROUND

Human Papillomavirus (HPV) is the causative agent for cervical cancer[1], the second most common cause of cancer death among women worldwide.[2,3] In addition, persistent infection with high-risk HPV types has been linked to the development of other genital cancers in men and women such as anal cancer, vulvar cancer and penile cancer, but also in the development of oropharyngeal cancer.[4,5] Overall, HPV is therefore estimated to be responsible for ~5% of the worldwide cancer burden. Of all HPV subtypes, HPV16 is most commonly associated with (pre) malignant disease of the cervix. [6]

The risk of developing malignancies after an HPV infection is largely due to the capacity of high-risk HPVs to transform epithelial cells by integrating DNA encoding the viral early proteins E6 and E7 into the host cell genome. This integration leads to constitutive overexpression of E6 and E7 proteins, mediating transformation of the infected cells through premalignant conditions towards a malignant phenotype.[7,8]

The premalignant condition of cervical cancer is called cervical intraepithelial neoplasia (CIN) and, due to population-based screening programs, most patients are diagnosed at this stage of the disease. Currently, high-grade CIN lesions are treated with surgical excision, a so-called large loop excision of the transformation zone (LLETZ). This procedure has potential complications, such as bleeding, infection, cervical stenosis and preterm birth, probably due to cervical insufficiency.[9–11] Above all, surgical excision does not necessarily eradicate the underlying HPV infection. Therefore, there is a need for novel non-invasive therapeutic approaches.

Since the continued production of E6 and E7 is required for the maintenance of the transformed phenotype, E6 and E7 in fact represent tumor-specific antigens in HPV-associated carcinoma and premalignant HPV-transformed cells.[7,8] Therefore, E6 and E7 are potential targets for immunotherapeutic intervention strategies involving induction or stimulation of cytotoxic T lymphocyte (CTL) activity against HPV-transformed cells.[4]

Here, we report the study protocol of our first-in-human clinical trial using Vvax001, a therapeutic viral vector vaccine consisting of recombinant Semliki Forest Virus replicon particles (rSFV) encoding the HPV16 derived tumor antigens E6 and E7 (Vvax001; rSFVeE6,7). Remarkably, the strong booster effect of rSFV makes Vvax001 a viral vector vaccination strategy with exquisite potency.[12] In line with this, we previously demonstrated that immunization of mice with rSFVeE6,7 induces strong CTL activity and eradication of established HPV-transformed tumors.[13–19] In this phase I study, immunogenicity, safety and tolerability of Vvax001 will be evaluated.

METHODS

Investigational product

The therapeutic vaccine Vvax001 is a rSFV vector encoding a fusion protein of HPV-16 E6 and E7 (*rSFVeE6,7*). A translational enhancer has been inserted upstream of the gene encoding the E6,7 fusion protein to increase recombinant gene expression. Vvax001 induces production of a fusion protein of HPV-16 E6 and E7 in the cytoplasm of infected cells.[16,20] Between 48 and 72 hours after infection, infected cells die. Dying cells, containing large amounts of the E6,7 fusion protein or fragments hereof, are taken up by dendritic cells, which present the E6,7 antigens to CTL thereby resulting in the induction of an immune response against HPV-infected tumor cells and consequently regression/eradication of the tumor.[21]

Design

In this phase I immunization study, four dose levels of Vvax001 will be tested. Patients will receive three consecutive vaccinations, with an interval of 3 weeks. Cohorts of 3 patients will be treated per dose level. Although no limiting toxicities are anticipated based on previous experience with similar viral vector vaccines, enrollment of subsequent patients will proceed with a minimum interval of 48 hours. In this phase I trial, there will be no restriction based on HPV-status in order to expedite accrual, given that immune responses are anticipated irrespective of HPV-status.

Results will be analyzed and the optimal dose will be determined based on level of systemic cellular immune response and by monitoring limiting toxicity.

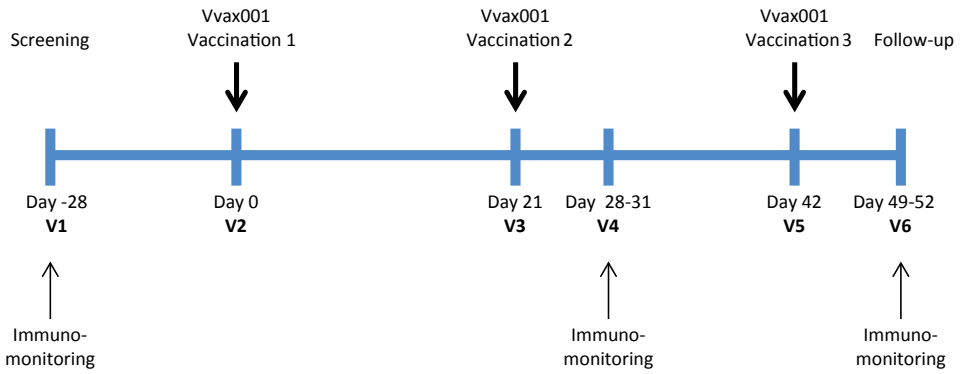

FIGURE 1. Phase I trial design. Bold arrows represent the VVAX001 immunizations at day 0, 21 and 42. Thin arrows represent the peripheral blood mononuclear cells (PBMC) collection for immunomonitoring at baseline, day 28-31 and day 49-52.

Participants

The study population consists of adult female patients with a history of cervical intraepithelial neoplasia (CIN) II and III, and patients with a history of cervical cancer, both minimally 12 weeks after completion of treatment. Patients will be accrued from the outpatient clinic of the University Medical center Groningen (UMCG).

Additional inclusion criteria are: Adequate bone marrow functions; HIV- and HBV-negative; patients of child-bearing potential should test negative using a serum pregnancy test and agree to utilize effective contraception during the entire treatment and follow-up period of the study; written informed consent according to local guidelines.

A potential subject who meets any of the following criteria will be excluded from participation in this study: Prior treatment with immunotherapeutic agents against HPV; history of an autoimmune disease or other systemic intercurrent disease that might affect the immunocompetence of the patient; current or prior use of high dose immunosuppressive therapy (4 weeks before start of the study); participation in a study with another investigational drug within 30 days prior to the enrolment in this study.

Intervention

Patients will receive three consecutive vaccinations of Vvax001, with an interval of 3 weeks. Each dose will be given as two injections; 1 injection in each leg. The injections will be administered intramuscularly in the upper legs, preferably in the m. vastus lateralis. Patient evaluation will be performed before, during and after vaccination, including history, physical examination and toxicity scoring using common toxicity criteria grades. Biochemistry will be performed at baseline, prior to each vaccination, and at follow up including full blood count, urea, electrolytes and liver function tests. Urine dipstick, ECG, HIV and HBV tests will be performed at baseline. In case of child bearing potential, a pregnancy test will be performed prior to each vaccination. Peripheral blood mononuclear cells (PBMC) and serum will be collected at baseline, 7-10 days after the second vaccination, and 7-10 days after the third vaccination, to monitor HPV-specific immune responses and anti-SFV antibodies.

Outcome

The main study endpoint is the immunogenicity of Vvax001. HPV-16 E6,7-specific T cell immune responses as measured by IFN-γ-ELISPOT. The secondary parameters are side effects/ adverse events related to Vvax001. Toxicity will be graded according to the NCI Common Terminology Criteria for Adverse Events (CTCAE) Version 4.0.

Immunomonitoring

In order to assess the systemic changes in immunity induced by vaccination, venous blood samples obtained at baseline, and 7-10 days after the second and third vaccination, will be examined by using peripheral blood mononuclear cells (PBMCs). PBMCs will be tested for: *i.* Antigen-specific responses by IFN-γ-ELISPOT; *ii.* Proliferation (Ki67+ T cells) and cytokine production (e.g. IFNγ, TNFα, IL-4, IL-5, IL-10, and IL-2); *iii.* Intracellular cytokine production (by CD4+ and/or CD8+) after one round of in vitro stimulation; *iv.* Phenotypic analysis by flowcytometry. Serum will be tested for antibodies against SFV by Elisa. The IFN-γ-ELISPOT (*i*) is the parameter for the primary immunogenicity endpoint. The other immunomonitoring parameters are exploratory.

Sample size

Cohorts of 3 patients will be treated per dose level using a standard 3+3 dose escalation design. Four dose levels of Vvax001 will be tested. A minimum total of 12 subjects will be included. In case dose limiting toxicity occurs, a maximum of 24 patients will be included.

Statistical analysis

There will be 3-6 subjects per dose level, 12-24 subjects in total. Descriptive statistics will be used to summarise the data. In order for patients to be included in the evaluation of the HPV-16 E6,7-specific T cell responses (IFN-γ-ELISPOT) they have to fulfil all of the below listed criteria: Patients should have received at least two doses of Vvax001; The pre-vaccination blood sample should have sufficient numbers of PBMCs (i.e. $10x10^6$); The patients should have given at least one blood sample after the second vaccination (at visit 4 or 6) and this blood sample should have sufficient numbers of PBMCs (i.e. $10x10^6$). All patients receiving at least one dose of Vvax001 will be included in the evaluation of safety.

DISCUSSION

Within this Phase I first-in-human clinical study, Vvax001, a therapeutic viral vector vaccine consisting of a replication-incompetent Semliki Forest Virus (rSFV) encoding the HPV16 derived tumor antigens E6 and E7, will be evaluated for immunogenicity and tolerability. Preclinical studies revealed exquisite efficacy by demonstrating that immunization of mice induced strong CTL activity and eradication of established HPV-transformed tumors.[13–19] These preclinical results have led to the development of a clinical batch, named Vvax001, and the initiation of this Phase I clinical trial.

Although prophylactic vaccines have been successful in the prevention of HPV infections, they are not capable of curing pre-existing HPV-infections and HPV-related diseases.[22] In addition,

current vaccine rates hover at about only 50% of the young adult population.[23] Therefore, there remains a need for therapeutic vaccination for the treatment of pre-existing as well as new HPV-infections and HPV-related diseases.

Thus far, various immunotherapeutic strategies, including therapeutic vaccination strategies, have been explored in early phase clinical trials. These immunotherapeutic strategies aim to stimulate CTL activity against HPV-transformed cells and thereby target HPV-related (pre) malignancies. Vaccination with therapeutic HPV16 overlapping synthetic long peptides (HPV16-SLP) resulted in regression of HPV16-induced premalignant lesions of the vulva.[24–26] Furthermore, HPV16-SLP vaccination in patients with advanced or recurrent HPV16-related cervical cancer partly installed specific T cell reactivity, although no clinical effect was observed on tumor growth.[27] Therapeutic vaccination using a DNA-vaccine showed clearance of HPV infection and regression of CIN3 lesions in 7 out of 9 patients.[28] In addition, pembrolizumab (anti-PD1 antibody) treatment resulted in a 20% response rate in patients with HPV-related head and neck squamous cell carcinoma (HNSCC),[29–32] and adoptive cellular transfer therapy using HPV-targeted tumor-infiltrating T cells resulted in complete regression of disease in metastatic cervical cancer.[33]

In contrast to the above described SLP- and DNA-based vaccines, Vvax001 is a therapeutic vaccine based on a viral vector. Viral vector vaccines, and Vvax001 in particular, have specific advantages over other vaccination platforms. First, cells are very efficiently infected after which large amounts of the encoded antigens are produced. This enhanced presentation of tumor antigens to the immune system leads to an increase in the frequency of CTL that target tumor cells expressing the tumor antigen(s) encoded in the vaccine vector. Secondly, the virus infection leads to a 'danger'-signal by the infected cells and the subsequent accumulation and activation of dendritic cells.[34,35] Due to this pro-inflammatory environment produced by the expression of viral proteins, no adjuvant is needed to enhance delivery of the tumor antigens. On the contrary, a disadvantage of some vectors is the development of host-induced neutralizing antibodies to the vector itself, thus limiting its continued use.[34] However, preclinical studies with rSFV revealed that neither SFV-specific antibodies nor T cells directed against rSFV-infected cells affect the boosting activity of this vector system. In line with this, the strong booster effect of rSFV makes Vvax001 a viral vector vaccination strategy with exquisite potency.[12]

We previously demonstrated that immunization of mice with rSFVeE6,7 induces strong CTL activity and eradication of established HPV-transformed tumors. Furthermore, mice that underwent a second tumor-challenge, 6 months after initial immunization with rSFVeE6,7, were protected for tumor outgrowth.[13–19] These results implicate that vaccination with rSFVe6,7 induces long-term immune memory and that therapeutic vaccination might also protect for recurrence of (pre)malignant cervical lesions.

Within this phase I first-in-human clinical study, Vvax001 will be evaluated for immunogenicity and tolerability. When successfully completed, Vvax001 will be evaluated in a phase II clinical trial for clinical efficacy in terms of HPV clearance and regression of high-grade CIN lesions. Once Vvax001 is proven to be well tolerated, immunogenic and therapeutically effective in these phase I and II clinical trials, SFV can be further expanded as an immunization platform. This could be for the treatment of other HPV types, for the treatment of other HPV-related malignancies such as head and neck squamous cell carcinoma, or against a variety of other cancer antigens, including e.g. neo-antigens.

In conclusion, based on preclinical results, Vvax001 represents a promising therapeutic vaccine for the treatment of (pre)malignant lesions of the cervix caused by HPV16. The clinical results on immunogenicity and tolerability of Vvax001 in human are expected to be available mid-2018.

CONFLICT OF INTEREST

Toos Daemen and Hans Nijman are stock holders/founders of ViciniVax BV, a spin-off company of the UMCG, developing therapeutic cancer vaccines.

ACKNOWLEDGEMENTS

This study was supported by the Dutch Cancer Society: project grant RUG 2008-4066 and two grants from the National Cancer Control Program (NPK) RUG 2009-4579 and RUG 2011-5156. In addition, funding was provided by the European Fund for Regional Development (EFRO), project number 068/073 'Drug Delivery and targeting' and ViciniVax BV.

REFERENCES

1. Schiffman, M., Castle, P. E., Jeronimo, J., Rodriguez, A. C. & Wacholder, S. Human papillomavirus and cervical cancer. *Lancet (London, England)* 370, 890–907 (2007).
2. Einstein, M. H. *et al.* Clinician's guide to human papillomavirus immunology: knowns and unknowns. *Lancet Infect. Dis.* 9, 347–356 (2009).
3. Parkin, D. M. & Bray, F. Chapter 2: The burden of HPV-related cancers. *Vaccine* 24, S11–S25 (2006).
4. zur Hausen, H. Papillomaviruses and cancer: from basic studies to clinical application. *Nat. Rev. Cancer* 2, 342–50 (2002).
5. Zur Hausen, H. The search for infectious causes of human cancers: where and why. *Virology* 392, 1–10 (2009).
6. Tota, J. E., Chevarie-Davis, M., Richardson, L. A., deVries, M. & Franco, E. L. Epidemiology and burden of HPV infection and related diseases: Implications for prevention strategies. *Prev. Med. (Baltim).* 53, S12–S21 (2011).
7. Nasseri, M., Gage, J. R., Lorincz, A. & Wettstein, F. O. Human papillomavirus type 16 immortalized cervical keratinocytes contain transcripts encoding E6, E7, and E2 initiated at the P97 promoter and express high levels of E7. *Virology* 184, 131–40 (1991).
8. Howley, P. M. Role of the human papillomaviruses in human cancer. *Cancer Res.* 51, 5019s–5022s (1991).
9. Kyrgiou, M. *et al.* Obstetric outcomes after conservative treatment for intraepithelial or early invasive cervical lesions: systematic review and meta-analysis. *Lancet* 367, 489–498 (2006).
10. Arbyn, M. *et al.* Perinatal mortality and other severe adverse pregnancy outcomes associated with treatment of cervical intraepithelial neoplasia: meta-analysis. *BMJ* 337, a1284–a1284 (2008).
11. Crane, J. M. G. Pregnancy outcome after loop electrosurgical excision procedure: a systematic review. *Obstet. Gynecol.* 102, 1058–62 (2003).
12. de Mare, A. *et al.* Viral vector-based prime-boost immunization regimens: a possible involvement of T-cell competition. *Gene Ther.* 15, 393–403 (2008).
13. Daemen, T. *et al.* Eradication of established HPV16-transformed tumours after immunisation with recombinant Semliki Forest virus expressing a fusion protein of E6 and E7. *Vaccine* 21, 1082–8 (2003).
14. Riezebos-Brilman, A. *et al.* A comparative study on the immunotherapeutic efficacy of recombinant Semliki Forest virus and adenovirus vector systems in a murine model for cervical cancer. *Gene Ther.* 14, 1695–704 (2007).
15. Riezebos-Brilman, A. *et al.* Induction of human papilloma virus E6/E7-specific cytotoxic T-lymphocyte activity in immune-tolerant, E6/E7-transgenic mice. *Gene Ther.* 12, 1410–1414 (2005).
16. Daemen, T., Regts, J., Holtrop, M. & Wilschut, J. Immunization strategy against cervical cancer involving an alphavirus vector expressing high levels of a stable fusion protein of human papillomavirus 16 E6 and E7. *Gene Ther.* 9, 85–94 (2002).
17. Daemen, T. *et al.* Genetic immunization against cervical carcinoma: induction of cytotoxic T lymphocyte activity with a recombinant alphavirus vector expressing human papillomavirus type 16 E6 and E7. *Gene Ther.* 7, 1859–66 (2000).
18. Daemen, T., Regts, J., Holtrop, M. & Wilschut, J. Immunization strategy against cervical cancer involving an alphavirus vector expressing high levels of a stable fusion protein of human papillomavirus 16 E6 and E7. *Gene Ther.* 9, 85–94 (2002).
19. Daemen, T. *et al.* Eradication of established HPV16-transformed tumours after immunisation with recombinant Semliki Forest virus expressing a fusion protein of E6 and E7. *Vaccine* 21, 1082–8 (2003).
20. Daemen, T. *et al.* Superior therapeutic efficacy of alphavirus-mediated immunization against human papilloma virus type 16 antigens in a murine tumour model: effects of the route of immunization. *Antivir. Ther.* 9, 733–42 (2004).
21. Huckriede, A. *et al.* Induction of cytotoxic T lymphocyte activity by immunization with recombinant Semliki Forest virus: indications for cross-priming. *Vaccine* 22, 1104–13 (2004).

22. Harper, D. M. & DeMars, L. R. HPV vaccines – A review of the first decade. *Gynecol. Oncol.* 146, 196–204 (2017).

23. van Lier EAOP, Giesbers H, Drijfhout IH, de Hoogh PAAM, de M. H. *Vaccinatiegraad Rijksvaccinatieprogramma Nederland*. (2012).

24. Welters, M. J. P. *et al.* Success or failure of vaccination for HPV16-positive vulvar lesions correlates with kinetics and phenotype of induced T-cell responses. *Proc. Natl. Acad. Sci. U. S. A.* 107, 11895–9 (2010).

25. van Poelgeest, M. I. E. *et al.* Vaccination against Oncoproteins of HPV16 for Noninvasive Vulvar/ Vaginal Lesions: Lesion Clearance Is Related to the Strength of the T-Cell Response. *Clin. Cancer Res.* 22, 2342–50 (2016).

26. Kenter, G. G. *et al.* Vaccination against HPV-16 oncoproteins for vulvar intraepithelial neoplasia. *N. Engl. J. Med.* 361, 1838–47 (2009).

27. E van Poelgeest, M. I. *et al.* HPV16 synthetic long peptide (HPV16-SLP) vaccination therapy of patients with advanced or recurrent HPV16-induced gynecological carcinoma, a phase II trial. *J. Transl. Med.* 11, 1 (2013).

28. Kim, T. J. *et al.* Clearance of persistent HPV infection and cervical lesion by therapeutic DNA vaccine in CIN3 patients. *Nat. Commun.* 5, 5317 (2014).

29. Larkins, E. *et al.* U.S. Food and Drug Administration Approval Summary: Pembrolizumab for the Treatment of Recurrent or Metastatic Head and Neck Squamous Cell Carcinoma with Disease Progression on or After Platinum-Containing Chemotherapy. *Oncologist* theoncologist.2016-0496 (2017). doi:10.1634/ theoncologist.2016-0496

30. Bauml, J. *et al.* Pembrolizumab for Platinum- and Cetuximab-Refractory Head and Neck Cancer: Results From a Single-Arm, Phase II Study. *J. Clin. Oncol.* 35, 1542–1549 (2017).

31. Chow, L. Q. M. *et al.* Antitumor Activity of Pembrolizumab in Biomarker-Unselected Patients With Recurrent and/or Metastatic Head and Neck Squamous Cell Carcinoma: Results From the Phase Ib KEYNOTE-012 Expansion Cohort. *J. Clin. Oncol.* 34, 3838–3845 (2016).

32. Seiwert, T. Y. *et al.* Safety and clinical activity of pembrolizumab for treatment of recurrent or metastatic squamous cell carcinoma of the head and neck (KEYNOTE-012): an open-label, multicentre, phase 1b trial. *Lancet Oncol.* 17, 956–965 (2016).

33. Stevanović, S. *et al.* Complete Regression of Metastatic Cervical Cancer After Treatment With Human Papillomavirus–Targeted Tumor-Infiltrating T Cells. *J. Clin. Oncol.* 33, 1543–1550 (2015).

34. Larocca, C. & Schlom, J. Viral vector-based therapeutic cancer vaccines. *Cancer J.* 17, 359–71 (2011).

35. Lundstrom, K. Alphavirus-based vaccines. *Viruses* 6, 2392–415 (2014).

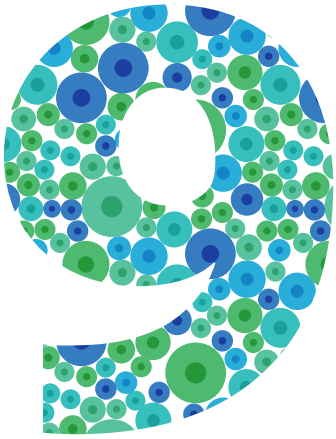

Summary and Discussion

SUMMARY

The immune system plays a crucial role in the recognition and elimination of (pre)malignant cells. Immune T cells in particular are highly skilled at surveying the body and distinguishing (pre)malignant from normal cells for elimination. When these immune T cells infiltrate the tumor microenvironment they are referred to as tumor-infiltrating lymphocytes (TIL). In line with their cancer-killing role, TIL have a pronounced effect on the survival of patients across malignancies. Moreover, it has also become abundantly clear that TIL can be targeted by cancer immunotherapy to induce lasting clinical benefit. In this thesis, we explored several aspects of TIL biology, including localization and differentiation, with the ultimate aim of developing novel therapeutic interventions to eradicate cancer.

Tumor-infiltrating lymphocytes

Tumor-infiltrating lymphocytes (TIL) are an important biomarker for improved prognosis and response to immune checkpoint blockade (ICB) therapy in several malignancies.[1] However, not all TIL subsets contribute equally to the eradication of cancer cells. CD8-positive cytotoxic T lymphocytes (CTL) are generally known as the tumor-killing subset, and the presence of these CD8-positive CTL contributes to an improved prognosis of cancer patients. On the contrary, regulatory T cells (Treg), characterized by CD4 and FoxP3 expression, have been described as an immune suppressive subset. As such, the presence of this suppressive subset does not confer prognostic benefit. In addition to the phenotype of TIL, the localization within the tumor microenvironment also appears to influence their prognostic benefit.

In **chapter 2** we first examined the prognostic effect of CD8-positive CTL localization in high-grade serous ovarian cancer (HGSC). We observed a strong prognostic benefit for patients from TIL that localize within the epithelial cancer islets of HGSC, in contrast to TIL localized in the connective tissue of the tumor. Distinguishing epithelial regions from stromal regions is based on histological assessment and could be a somewhat arbitrary process. A single marker to discriminate intraepithelial from stromal TIL populations is therefore of interest. Webb et al. showed that the epithelial and stromal CTL populations in HGSC can be discriminated by expression of CD103.[2] In **chapter 2,** we first confirmed that CD103 is indeed a marker for the intraepithelial T cell population in HGSC. In line with this, we showed that the total number of CD103-positive TIL, irrespective of localization, was associated with improved prognosis in HGSC. In addition, we elucidated the mechanism underlying induction of CD103 on CD8-positive CTL and demonstrate that CD103-positive TIL comprise the cancer cell-reactive subset.

To see whether CD103 could be used as a pan-cancer biomarker for intraepithelial TIL, we investigated the localization and prognostic role of CD103-positive T cells in endometrial cancer and cervical cancer (**chapter 3 and 4**)**.** We confirmed that CD103 performed consistently across

gynecological malignancies as a prognostic biomarker. In addition to the prognostic value of TIL, the presence of TIL has also been described as a predictive and/or response biomarker for therapeutic efficacy of immunotherapy. We therefore investigated in **chapter 4** whether CD103 also demonstrates promise as a response biomarker in an animal model of cervical cancer treated with therapeutic vaccination and/or immuno-radiotherapy.

Along with the number and localization of TIL, their differentiation status is also an important prognostic factor.[3] In brief, naive T cells circulate through secondary lymphoid organs, which maximizes their opportunity for encountering an antigen presenting cell (APC) and subsequent activation. These naïve T cells are characterized by expression of CD45RA, CCR7, CD28 and CD27. Upon activation, these naïve T cells progressively lose many of these markers and, upon chronic antigen stimulation (e.g. in the context of cancer) acquire a so-called exhausted phenotype wherein they are in the end no longer able to exert tumor control. In line with this, in **chapters 5 and 6** we identified that less differentiated "younger" CD27+ TIL in the cancer cell epithelium were of greater prognostic benefit to patients than "older" more differentiated TIL In HGSC.

Effects of standard treatment on local and systemic immunity

As immunotherapy by itself is insufficient for most patients, it is often proposed as combination therapy in addition to conventional treatments such as chemotherapy. As chemotherapy is known for its effects on dividing cells, chemotherapy might also affect tumor-reactive immune cell subsets. To this end, we describe in **chapters 2, 5-7** whether, and at which time point, immunotherapy might best be combined with conventional chemotherapy. The effects of Carboplatin/Paclitaxel containing chemotherapy on peripheral blood immune cell subsets was investigated in a cohort of ovarian cancer patients. No systemic changes in the proportion of T cell subsets were observed during the course of Carboplatin/Paclitaxel chemotherapy. In line with this, we observed equal levels of tumor-infiltrating T cells in tumors of patients obtained during primary debulking surgery (PDS) versus tumors of patients that were pretreated with neoadjuvant Carboplatin/Paclitaxel chemotherapy (NACT). Interestingly, while we did not observe systemic or local immune modulating effects of chemotherapy on the T cell subsets, we identified a pronounced depletion of circulating myeloid cells during treatment with Carboplatin/Paclitaxel in ovarian cancer patients. Surprisingly, unpublished work by our group has so far revealed no such differences in infiltrating myeloid cells in the tumors of PDS treated patients versus NACT treated patients. Nevertheless, myeloid cells have been proposed to suppress the immune response even outside of the tumor microenvironment, thus highlighting a possible route for immunotherapy in ovarian cancer patients during the systemic depletion of these myeloid cells by standard-of-care chemotherapy.

Immunotherapy in cervical neoplasia and cervical cancer

As persistent infection with human papillomavirus (HPV) has been established as the causative agent for cervical cancer, all HPV infected cells are thought to express the viral oncoproteins E6 and E7. The oncoproteins E6 and E7 are therefore bona fide targets for immunotherapy in the form of therapeutic vaccination. E6/E7-targeted therapeutic vaccination aims to activate the immune system of the host against E6 and E7 expressing (pre)malignant cells. Indeed, in an animal model for cervical cancer described in **chapter 4**, therapeutic vaccination using a Semliki forest virus (SFV)-based vaccine targeting the oncogenes E6 and E7 induced HPV-specific immune responses and infiltration of tumor-reactive CD103-positive TIL into the tumor. In an effort to translate these findings into the clinic, a clinical batch of SFV-based therapeutic vaccine, named Vvax001, was evaluated for immunogenicity and tolerability in a phase first-in-human clinical study described in **chapter 8**. Taken together, the data described in this thesis contributes to our understanding of the tumor immune biology of gynecological malignancies and may help guide therapeutic intervention in the near future.

DISCUSSION

This thesis contains both translational studies and clinical studies. First the translational results **from the bench** will be discussed. Second, the immediate clinical implications of our work will be discussed and taken **to the bedside**….

From bench….

Tumor-infiltrating lymphocytes

In this thesis, we establish the prognostic value of localization and differentiation of TIL in high-grade serous ovarian cancer, endometrial adenocarcinoma, and cervical cancer. The presence of TIL has been widely described to be associated with improved prognosis across several malignancies[1], including breast cancer[4], colorectal cancer[5–7], ovarian cancer[8–11], non-small cell lung cancer[12], melanoma[13,14], renal cell cancers[15], head and neck cancer[16]. However, there are many different TIL subsets and not all subsets contribute equally to an improved prognosis. CD103, the αE integrin subunit, has been described as a marker for prognostically favorable intraepithelial CD8-positive CTL in ovarian cancer, lung cancer, bladder cancer and, more recently, breast cancer.[2,17–22] Within this thesis, we confirmed the prognostic benefit of CD103-positive TIL in ovarian cancer and extended this observation to endometrial cancer and cervical cancer.

We furthermore determined the ontogeny of CD103-positive TIL in HGSC, and were the first to demonstrate that CD103-positive TIL represent adaptive immune cells that are formed as part

of an ongoing anti-cancer immune response. Interestingly, we found that CD103 expression is induced by dual T cell-receptor- and TGF-β-receptor-signaling. TGF-β is generally known as an immunosuppressive molecule. However, our results indicate that TGF-β also plays an important role in T cell retention via binding of CD103 to E-cadherin on the tumor epithelium. This interaction of CD103-positive CTL in the tumor is important for the lysis of cancer cells as engagement of CD103 on CTL with E-cadherin triggers lytic granule polarization and cancer cell death.[23,24] Until now, TGF-β secretion by tumor cells was only thought to paralyze infiltrating CTL. Hence, TGF-β has been identified as a therapeutic target because of its tumor-promoting roles.[25] However, when applying TGF-β antagonistic agents, CD103 expression on CTL might be abrogated, as we show in **chapter 2**. As a consequence, CTLs might lose the ability to exert their cytolytic activity, for which near contact with E-cadherin on the tumor cells is needed.

Supporting evidence for this hypothesis comes from mouse studies on the immune system in the gut. Expression of CD103 has been described on a resident-memory population of intra-epithelial lymphocytes (IEL) in the gut of all vertebrate possessing a thymus. IEL play an important role regulating mucosal immune surveillance.[26] Mice with either a null mutation in the gene encoding TGF-βr1 or T cell–specific deletion of TGF-βr1 lacked IEL, whereas mice with transgenic overexpression of TGF-βr1 had a larger population of IEL.[27] In humans, TGF-βr1/2 mutations have also been described in the context of Loeys-Dietz syndrome (LDS). Like in the overexpressing mice, a mutation in either human TGF-βr1 or TGF-βr2 in LDS leads to an increase in the availability of TGF-β which appears to underlie the formation of abnormally weak connective tissue. Interestingly, the increased availability of TGF-β in LDS is associated with a higher prevalence of inflammatory bowel disease (IBD) when compared to the general population.[28] Since IBD has been linked to the expansion of IEL in Crohn's disease,[29] it would therefore be of great interest to investigate the presence, number and functionality of CD103-expressing cells in these patients.

Immunoscore

As discussed above, our results from **chapters 2 and 3**, demonstrate a superior prognostic value of CD103-positive T cells over CD8-positive T cells, suggesting that CD103 may be used as an immune marker to predict prognosis and/or response to standard therapy. In line with this notion, worldwide taskforces are currently making an effort to stratify patients based on their immune infiltrates for the prediction of prognosis and response to therapy. Galon et al. developed the Immunoscore as a method for standardized quantification of immune infiltrates within the tumor contexture.[30] This standardized scoring system is based on densities of two lymphocyte populations (CD3/CD45RO, CD3/CD8 or CD8/CD45RO) infiltrating the core and invasive margin of the tumor. The Immunoscore can provide a score ranging from Immunoscore 0, when low densities of both cell types are found in both regions, to Immunoscore 4, when high densities are found in both regions. To illustrate this, the Immunoscore approach was applied to

two large independent cohorts of colorectal cancer patients. Only 4.8% of patients with a high Immunoscore, relapsed after 5 years and 86.2% were alive. In comparison, 72% of patients with a low score experience tumor recurrence and only 27.5% were alive at five years.[31] These low Immunoscore patients potentially could have benefited from adjuvant (immuno)therapy that increases T cell infiltration to (re)populate the tumorenvironment. In line with this, Galon et al. advocate to incorporate the Immunoscore into the TNM-classification (tumor burden, lymph nodes, metastasis) for tumor staging as a tool for the prediction of prognosis and response to therapy.[32,33]

Based on our data, it could therefore be argued that the Immunoscore might even be improved by replacing CD3/CD8 or CD8/CD45RO with CD103 as marker for intratumoral T cells. This (modified) Immunoscore as described by Galon et al. in colorectal cancer, could also be of use for the prediction of prognosis and response to therapy in gynecological malignancies. Within the Netherlands, large randomized clinical trials have been performed in endometrial cancer patients, the Post-Operative Radiotherapy Endometrial Cancer 1-3 (PORTEC1-3) studies. The PORTEC studies investigate the effect of different postoperative radio(chemo)therapy strategies in endometrial cancer patients. These randomized PORTEC cohorts would therefore be ideal for validation of CD103 as prognostic biomarker for endometrial cancer patients in general, and in this case, response to adjuvant radio(chemo)therapy in particular.

Differentiation of TIL

Along with the number and localization of TIL, their differentiation status is also an important prognostic factor.[3] Following activation, (cancer) antigen-specific naïve T cells undergo a progressive differentiation towards distinct effector and memory-precursor phenotypes. During e.g. acute infections, the effector T cells progress towards a terminally differentiated state associated with high cytolytic activity towards target cells followed by programmed cell death during the so-called "resolution phase" of the immune response. Concurrently, pre-cursor memory T cells mature into long-lasting memory T cells capable of rapid response and protection upon re-exposure. In cancer, the chronic nature of the antigen-exposure is thought to significantly skew this normal differentiation leading to an "exhausted" state in the effector population and a defective formation of memory T cells. In **chapters 5-7**, we describe how T cells in the peripheral blood and in the tumors of ovarian cancer patients display highly heterogeneous differentiation patterns, associated with prognosis. Indeed, less-differentiated TIL in ovarian cancers, characterized by expression of CD27, were associated with a significantly improved prognosis, particularly when cytoreductive surgery was incomplete. Remarkably, we observed a similar heterogeneous expression of CD27 within the peripheral blood, although we were unable to directly link CD27 expression status in circulating and tumor-infiltrating

CD8+ T cells. Nevertheless, our data suggests prospective studies comparing differentiation of circulating T cells and TIL may help elucidate how chronic antigen-exposure in OC patients shapes the immune response and outcome for patients.

Patient selection for immunotherapy

Immunotherapy, and in particular ICB can induce long-lasting clinical responses and even curation of some advanced and metastatic cancers. ICB reinvigorates exhausted, tumor-specific T cells. Unfortunately, only a small subset of cancer patients responds to ICB. Other disadvantages of ICB are the high costs, and the occurrence of severe, but manageable, adverse events. Generally, patients with high levels of infiltrating T cells -immunological 'hot' tumors- are more likely to respond to ICB compared to patients with low levels of infiltrating T cells – immunological 'cold' tumors-. At the very least, patients with immunological hot tumors should therefore be selected for ICB. By contrast, checkpoint inhibition therapy is less likely to benefit patients with immunological cold tumors, as there are none or not enough T cells to reinvigorate. Immunological cold tumors should therefore first be (re)populated with tumor-specific T cells. This (re)population can be induced by stimulation of the immune system with a tumor-specific antigen ex vivo, by adoptive T cell transfer, or in vivo, by therapeutic vaccination.

As we show in **chapter 2**, one example of an immunologically more profoundly cold tumor type is ovarian cancer. Indeed, only 10% of HGSC tumors show high levels of tumor-infiltrating lymphocytes. This immunologically cold tumor type can roughly be explained by an intermediate mutational load. As a consequence of this intermediate mutational load, the abundance of neoantigens derived from point mutations is expected to be lower in this disease.[34–36] Identifying patients with these neo-antigen rich and exceptional immunologically hot tumors for treatment with ICB is therefore of interest.

One possible identifier might be breast cancer 1 (BRCA1)-mutation status as it has been described that TIL are particularly prominent in BRCA1-mutant tumors.[37,38] This can partially be explained by the finding that BRCA1/2-mutated ovarian cancers harbor a higher mutational load and a unique mutational signature with an elevated number of larger insertions or deletions (indels).[39,40] This mutational signature can lead to the formation of more tumor-specific neoantigens that stimulate the recruitment of TIL. However, this does not completely explain why this increased levels of TIL is specifically observed in BRCA1-mutant tumors and not in BRCA2-mutant tumors. In addition, approximately 50% of HGSCs are defective in Homologous Recombination (HR) DNA repair pathways (genetic and epigenetic, including BRCA1/2 mutations).[41] HR deficient HGSCs depend on alternative, low fidelity mechanisms for double-strand break (DSB) repair. This error-prone DSB repair mechanism leads to point mutations and indels. Theoretically, this should then also lead to similar formation of neoantigens. An explanation for the decreased immunogenicity of HGSC might be that factors other than point mutation load are therefore

likely to influence T cell infiltration. These other factors might involve other classes of tumor antigens, such as amplified or aberrant gene products arising from gene fusions, so-called copy number aberrations (CNA).[42] High level of chromosomal aberration has been described to correlate with poor clinical outcome in ovarian cancer.[43] Taken together, HGSC is characterized by chromosomal instability e.g. caused by HR-deficiency or CNA. However, for unknown reasons this chromosomal instability does not lead to subsequent formation of TIL-attracting tumor-specific neoantigens. Patients with immunological cold tumors could first be selected for therapeutic strategies that (re)populates the tumorenvironment with tumor-specific T cells by stimulation of the immune system with a tumor-specific antigen ex vivo, by adoptive T cell transfer, or in vivo, by therapeutic vaccination.

In contrast to ovarian cancer, endometrial cancer includes some tumors with the highest mutational loads across malignancies. In particular, ultramutated POLE exonuclease domain-mutant (POLe-mutant) and hypermutated microsatellite unstable (MSI) tumors are characterized by high levels of neoantigens. In follow up to our data on CD103 in endometrial cancer in **chapter 3**, Eggink et al. explored the immune profiles, including CD103 infiltration, of these subgroups within the TransPORTEC cohort, a high-risk endometrial cancer cohort.[44] High levels of CD103-positive TIL were seen in the POLe-mutant/MSI subtypes, whereas low levels of CD103-positive TIL were observed in the P53-mutant/no specific molecular profile (NSMP) subtypes. In line with this, significant therapeutic responses to ICB have recently been observed in patients presenting with mismatch repair-deficient (dMMR) and/or MSI tumors.[45–49] Based on these results, the FDA has recently approved the immune checkpoint inhibitor Pembrolizumab (anti-PD1 monoclonal antibody) for the treatment of dMMR/MSI solid tumors that have progressed following prior treatment and who have no satisfactory alternative treatment options.[50] This approval also includes MSI endometrial cancer patients. Importantly, this is the first tissue/site agnostic FDA treatment approval.

Finally, cervical cancer as an entity is arguably the most immunogenic of all gynecologic malignancies. Indeed, cervical cancer is characterized by the expression of the viral oncoproteins E6 and E7 of high-risk HPVs by both malignant and premalignant cells. As a result, E6 and E7 are recognized as non-self and therefore the perfect antigens to target with immunotherapy by therapeutic vaccination or autologous cellular transfer strategies.

In **chapter 4** we describe such a therapeutic vaccination in an animal model in which mice were inoculated with E6,E7 expressing tumor cells (TC-1). Tumor-bearing mice were treated with a Semliki Forest Virus (SFV)-based therapeutic vaccine encoding the E6,E7 oncoproteins of HPV16 (rSFVeE6,7). Previously, we demonstrated that therapeutic vaccination with rSFVeE6,7 resulted in complete eradication of TC-1 tumors and survival of vaccinated mice.[51–54] Secondly, therapeutic vaccination induced long-lasting systemic immune responses measured by E6,7-specific CTL.[51–

[54] These long-lasting immune responses even protected the mice 6 months after the initial immunization for the outgrowth of tumor upon a second tumor challenge, without additional vaccination.[51–54] Leveraging this model, we show in **chapter 4**, that therapeutic vaccination with rSFVeE6,7 induced infiltration of CD103-positive TIL into the tumor. Importantly, these CD103-positive TIL were largely E6,7-specific-CD8-positive-CTL. Within this experiment a suboptimal dosed vaccination scheme was used to be able to obtain tumor samples and analyze TIL. Furthermore, therapeutic vaccination was combined with radiation, which is used as standard-of-care in advanced-stage cervical cancer, showing a synergistic effect of this treatment combination resulting in an even higher increase in the infiltration of CD103-positive CTL into the tumor. Our results therefore indicate that CD103 should be explored further as a biomarker for response evaluation of immunotherapeutic (combination) strategies.

…to bedside.

The highly promising preclinical data on rSFVeE6,7, described in part above, resulted in the initiation of a first-in-human clinical trial with rSFVeE6,7 as Vvax001 (**chapter 8**). Perspectives on this Vvax001 therapeutic vaccination and other immunotherapeutic strategies in cervical cancer will be discussed in this "bedside section".

Therapeutic vaccination using Vvax001

Therapeutic vaccination for the treatment of cervical cancer can be deployed in two phases of development of the disease. Firstly, in precancerous lesions enhancing the immune response to HPV could inhibit progression of disease towards invasive cancer. Secondly, in cervical cancer, therapeutic vaccination may result in cancer cell death, which on itself, or when combined with e.g. radiochemotherapy and/or other immunotherapeutic strategies such as immune checkpoint blockade (ICB), might be curative.

As a result of population-based screening in western countries, cervical cancer is mostly diagnosed in a precancerous stage, so called cervical intraepithelial neoplasia (CIN). Currently, CIN lesions are surgically treated by a large-loop-excision of the transformation zone (LLETZ). This is mostly an effective procedure, however, direct and indirect complications can occur such as bleeding, infection, infertility and insufficiency of the cervix during pregnancy. Furthermore, this surgical LLETZ procedure does not necessarily eradicate the HPV infection. Therefore, new therapeutic strategies are warranted.

The promising preclinical results of rSFVeE6,7 therapeutic vaccination, published earlier and described in **chapter 4**, have led to the development of an investigational medicinal product, named Vvax001, for the treatment of (pre)malignant cervical lesions. Vvax001 therapeutic vaccine is currently under investigation in a phase I clinical trial in healthy women with a history of HPV-related (pre) malignant lesions of the cervix. **Chapter 8** describes the design of the first-

in-human phase 1 clinical trial. The primary aim of this phase I clinical study is to determine the immunogenicity of Vvax001 in humans. In addition, safety and tolerability is being investigated. When proof of immunogenicity has been established, we envision a phase 2 clinical study, in which the clinical efficacy of Vvax001 will be established in patients with active disease of the cervix. To evaluate the clinical efficacy, we intend to immunize patients with HPV16-positive high-grade CIN lesions (CIN2/3) with Vvax001, instead of the standard LLETZ treatment. After the Vvax001 immunization, patients will enter a watchful waiting phase. During this watchful waiting phase patients will be monitored by regular colposcopy. At a to be defined interval after vaccination (e.g. 6 months), a biopsy or if necessary LLETZ excision, will be performed. If progression of the disease is suspected during the watchful waiting phase, LLETZ excision will be performed. Within this phase 2 study, pre- and post-vaccination biopsies will be collected to investigate immunological effects by monitoring CD103-positive CTL infiltration levels. Furthermore, systemic E6,7-specific immune response will be monitored before and after vaccination, and up to 24 weeks to establish long-lasting immunological responses. This phase 2 study can give insight in the relation between clinical efficacy (clearance/regression of CIN lesion) and systemic and local immune responses. A possible advantage for patients who would participate in this proposed phase 2 trial, is that these patients –mostly women in fertile life phase- might avoid LLETZ excision if biopsy proves regression of the CIN lesion. In addition, therapeutic vaccination might induce immune memory, protecting for recurrences of disease.

When Vvax001 is proven to be well tolerated, immunogenic and therapeutically effective in these phase I and II clinical trials, SFV can be further expanded as an immunization platform e.g. for the treatment of other HPV types or for the treatment of other HPV-related malignancies such as head and neck squamous cell carcinoma. Indeed, while Vvax001 therapeutic vaccine is the first viral vector vaccine using the Semliki forest virus (SFV) as viral vector, it can be readily modified to encode a variety of cancer antigens, including e.g. neo-antigens.

Other immunotherapy in cervical neoplasia and cervical cancer

In addition to Vvax001, a number of agents aiming to stimulate the immune system against cervical lesions are currently under evaluation in the field of cervical lesions. A search on *ClinicalTrials.gov* revealed that interventional clinical studies have been registered in the past decade for the treatment of cervical intraepithelial neoplasia and/or cervical cancer involving immunotherapeutic agents as monotherapy or in combination with radio(chemo)therapy. Most agents target HPV-16 and/or 18, but also other HPV serotypes are targeted.

The majority of the registered clinical trials involve therapeutic vaccination strategies (27 studies). Most therapeutic vaccines target the E6 and E7 viral proteins of HPV-16 and/or HPV-18. In two studies, prophylactic HPV vaccines (Gardasil© and Gardasil©9) are being evaluated for their therapeutic efficacy in women with cervical intraepithelial neoplasia. Thus far, therapeutic

vaccines targeting HPV-16 or HPV-18 have shown clinical efficacy with clearance of HPV infection and clearance of precancerous lesions in phase 2 studies.[55–58] In advanced cervical cancer, therapeutic vaccination resulted in induction of immune responses but no clinical effect was observed.[59] In addition, also vaccination studies aiming for targets other than HPV were open for cervical cancer patients; e.g. studies investigating a peptide-vaccine targeting VEGFR2, 'preferentially expressed antigen in melanoma' (PRAME) and 'prostate-specific membrane antigen' (PSMA).[60]

The second most used immunotherapeutic strategy that is used in the field of cervical cancer is adoptive cellular transfer (ACT). Currently, 8 studies are registered on *clinicaltrials.gov* using ACT strategies. In advanced metastatic cervical cancer, E6,7-reactive autologous TIL were selected and transferred back into the patients. Initial results showed impressive clinical responses with the clearance of tumor masses.[61] Recently, the results of a clinical study administering genetically modified T cell receptor (TCR) t cells targeting melanoma-associated antigen-A3 (MAGE-A3) were published in which also 3 cervical cancer patients were included. A complete response, that is still ongoing at 29 months, was observed in one patient with metastatic cervical cancer. The other two cervical cancer patients showed no response to the therapy.[62] Ongoing studies use a variety of ACT strategies for the treatment of cervical cancer such as natural killer (NK) cellular transfer and chimeric antigen receptor (CAR) T cells targeting Mesothelin.

Lastly, immune checkpoint blockade is also under investigation for the treatment of cervical cancer. Preliminary results from the KEYNOTE-028 study, evaluating the safety and efficacy of Pembrolizumab (anti-PD1) in patients with advanced solid tumors were presented in 2016. This study included a cohort of 24 patients with advanced cervical cancer. Out of these 24 patients, 3 patients showed a partial response leading to stable disease with a medium duration of 19.6 weeks.[63] As these results are preliminary, the clinical benefit of Pembrolizumab will be further investigated. ICB monotherapy can be given to boost pre-existing immunity against E6,E7 antigens, in patients with a pre-existing immune response or maybe even CIN-patients for the prevention of transformation to invasive cancer. However, according to the preliminary results in advanced cervical cancer, ICB monotherapy does not induce complete responses. Therefore, ICB is now mostly being tested in combination with other immunotherapeutic strategies (ACT and therapeutic vaccination) that have shown to initiate an immune response or to augment the pre-existing immune response.

In current ongoing trials, 4 studies investigate multiple immunotherapeutic combination strategies. Examples of therapeutic vaccination combined with ICB are Atezolizumab or Durvalumab (both anti-PDL1) with autologous tumor cell vaccination or Nivolumab (anti-

PD1) combined with synthetic-Long-peptide (SLP) vaccination targeting HPV16. Furthermore one study involves combination therapy of ACT, in the form of E7 targeting TCR T cells, with or without ICB Pembrolizumab (anti-PD1).

Combining immunotherapy with standard-of-care treatment

Finally, the effects of standard treatment on systemic immunity and the tumor microenvironment are important to consider when proposing combination therapies. In cervical cancer it was shown by Welters et al. that chemotherapy resulted in a systemic decrease of myeloid derived suppressor cells (MDSC).[64] In **chapter 7** we show a similar trend in the depletion/decrease of MDSC in ovarian cancer patients during Carboplatin/Paclitaxel chemotherapy. These results indicate that Carboplatin/Paclitaxel chemotherapy can best be combined with immunotherapy e.g. therapeutic vaccination after 2-3 cycles, when the immune suppressive subset is at its nadir, and the proportion of circulating T cell subsets is not affected.

In line with this data on circulating T cells, we also did not observe T cell depletion after Carboplatin/Paclitaxel chemotherapy in the tumor microenvironment, (**chapters 2, 5 and 6**). However, there are some pitfalls worth mentioning; we compared tissue samples obtained from either primary surgery (PS) or interval debulking surgery (after three cycles of chemotherapy; NACT), but these cohorts are not matched per patient. Therefore no statements can be made on the direct effect of chemotherapy on T cell infiltration per patient. Furthermore, the cohorts must be approached as two independent cohorts as a selection bias is present due to the decision for treatment regimen by the physician; patients in the NACT cohort generally have a worse prognosis compared to patients in the PS cohort. Lastly, we determined the number of infiltrating T cells per mm^2. Assuming chemotherapy diminishes the amount of cancer cells, it could be possible that the effector to target ratio in the NACT cohort is overestimated. In contrast to our data, mouse studies evaluating the effect of different chemotherapeutics on immune infiltration, generally suggest that chemotherapy enhances T cell infiltration into the tumor.[65] In line with this, it could also be hypothesized that the NACT cohort has lower initial/pretreatment numbers of TIL, and that chemotherapy induces an increase of infiltrating T cells. Ideally, our recommendation would therefore be to evaluate the effects of chemotherapy on the tumor microenvironment in matched tumor samples. However, in ovarian cancer, but also in many other cancer types, it is not standard procedure to collect pre- and post-treatment samples and tumor heterogeneity may still affect outcome of such comparisons.

Our hypothesis that immunotherapy could be combined with MDSC-depleting Carboplatin/Paclitaxel is further supported by two lines of evidence. First, vaccination with an HPV E6/E6 SLP vaccine during Carboplatin/Paclitaxel-chemotherapy in cervical cancer patients significantly augmented the circulating anti-E6/E7 immune response.[64] Second, depletion of intratumoral MDSCs by Sunitinib, a clinically-applied broad receptor tyrosine kinase inhibitor, augmented

rSFVeE6,7 therapeutic vaccination in our HPV16+ tumor model described in **chapter 4**. Moreover, combining both low dose irradiation and Sunitinib with therapeutic vaccination even further enhanced the intratumoral ratio of antitumor effector T cells to MDSCs.[66,67] One note of caution is appropriate as clinically-applied radiotherapy has previously been linked to reduced immune function in cervical- and other cancer patients, although this immune-suppressive effect is likely exacerbated by the high dose of radiation used for eradicating tumor cells. Nevertheless, these results imply that off-label use of clinically used drugs such as Sunitinib should be evaluated to create an optimal immune environment supporting immunotherapeutic activation of tumor-killing T cells.

CONCLUSION

Taken together, the data published so far contribute to our understanding of the tumor immune biology of gynecological malignancies and may help guide therapeutic intervention in the near future.

REFERENCES

1. Barnes, T. A. & Amir, E. HYPE or HOPE: the prognostic value of infiltrating immune cells in cancer. *Br. J. Cancer* (2017). doi:10.1038/bjc.2017.220
2. Webb, J. R., Milne, K., Watson, P., Deleeuw, R. J. & Nelson, B. H. Tumor-infiltrating lymphocytes expressing the tissue resident memory marker CD103 are associated with increased survival in high-grade serous ovarian cancer. *Clin. Cancer Res.* 20, 434–44 (2014).
3. Mlecnik, B. *et al.* Comprehensive Intrametastatic Immune Quantification and Major Impact of Immunoscore on Survival. *J. Natl. Cancer Inst.* 110, (2018).
4. Salgado, R. *et al.* The evaluation of tumor-infiltrating lymphocytes (TILs) in breast cancer: recommendations by an International TILs Working Group 2014. *Ann. Oncol.* 26, 259–271 (2015).
5. Galon, J. *et al.* Type, density, and location of immune cells within human colorectal tumors predict clinical outcome. *Science* 313, 1960–4 (2006).
6. Mei, Z. *et al.* Tumour-infiltrating inflammation and prognosis in colorectal cancer: systematic review and meta-analysis. *Br. J. Cancer* 110, 1595–1605 (2014).
7. Jochems, C. & Schlom, J. Tumor-infiltrating immune cells and prognosis: the potential link between conventional cancer therapy and immunity. *Exp. Biol. Med. (Maywood).* 236, 567–79 (2011).
8. Leffers, N. *et al.* Prognostic significance of tumor-infiltrating T-lymphocytes in primary and metastatic lesions of advanced stage ovarian cancer. *Cancer Immunol. Immunother.* 58, 449–59 (2009).
9. Sato, E. *et al.* Intraepithelial CD8+ tumor-infiltrating lymphocytes and a high CD8+/regulatory T cell ratio are associated with favorable prognosis in ovarian cancer. *Proc. Natl. Acad. Sci. U. S. A.* 102, 18538–43 (2005).
10. Zhang, L. *et al.* Intratumoral T cells, recurrence, and survival in epithelial ovarian cancer. *N. Engl. J. Med.* 348, 203–13 (2003).
11. Hwang, W.-T., Adams, S. F., Tahirovic, E., Hagemann, I. S. & Coukos, G. Prognostic significance of tumor-infiltrating T cells in ovarian cancer: a meta-analysis. *Gynecol. Oncol.* 124, 192–8 (2012).
12. Geng, Y. *et al.* Prognostic Role of Tumor-Infiltrating Lymphocytes in Lung Cancer: a Meta-Analysis. *Cell. Physiol. Biochem.* 37, 1560–71 (2015).
13. Erdag, G. *et al.* Immunotype and Immunohistologic Characteristics of Tumor-Infiltrating Immune Cells Are Associated with Clinical Outcome in Metastatic Melanoma. *Cancer Res.* 72, 1070–1080 (2012).
14. Azimi, F. *et al.* Tumor-infiltrating lymphocyte grade is an independent predictor of sentinel lymph node status and survival in patients with cutaneous melanoma. *J. Clin. Oncol.* 30, 2678–83 (2012).
15. Geissler, K. *et al.* Immune signature of tumor infiltrating immune cells in renal cancer. *Oncoimmunology* 4, e985082 (2015).
16. Wallis, S. P., Stafford, N. D. & Greenman, J. Clinical relevance of immune parameters in the tumor microenvironment of head and neck cancers. *Head Neck* 37, 449–459 (2015).
17. Wang, B. *et al.* CD103+ Tumor Infiltrating Lymphocytes Predict a Favorable Prognosis in Urothelial Cell Carcinoma of the Bladder. *J. Urol.* 194, 556–62 (2015).
18. Djenidi, F. *et al.* CD8+CD103+ tumor-infiltrating lymphocytes are tumor-specific tissue-resident memory T cells and a prognostic factor for survival in lung cancer patients. *J. Immunol.* 194, 3475–86 (2015).
19. Webb, J. R., Milne, K. & Nelson, B. H. PD-1 and CD103 Are Widely Coexpressed on Prognostically Favorable Intraepithelial CD8 T Cells in Human Ovarian Cancer. *Cancer Immunol. Res.* 3, 926–935 (2015).
20. Webb, J. R., Milne, K. & Nelson, B. H. Location, location, location: CD103 demarcates intraepithelial, prognostically favorable CD8(+) tumor-infiltrating lymphocytes in ovarian cancer. *Oncoimmunology* 3, e27668 (2014).

21. Koh, J. *et al.* Prognostic implications of intratumoral CD103+ tumor-infiltrating lymphocytes in pulmonary squamous cell carcinoma. *Oncotarget* 8, 13762–13769 (2017).

22. Wang, Z.-Q. *et al.* CD103 and Intratumoral Immune Response in Breast Cancer. *Clin. Cancer Res.* 22, 6290–6297 (2016).

23. Floc'h, A. L. *et al.* Minimal Engagement of CD103 on Cytotoxic T Lymphocytes with an E-Cadherin-Fc Molecule Triggers Lytic Granule Polarization via a Phospholipase C -Dependent Pathway. *Cancer Res.* 71, 328–338 (2011).

24. Franciszkiewicz, K. *et al.* CD103 or LFA-1 engagement at the immune synapse between cytotoxic T cells and tumor cells promotes maturation and regulates T-cell effector functions. *Cancer Res.* 73, 617–28 (2013).

25. Yang, L., Pang, Y. & Moses, H. L. TGF-beta and immune cells: an important regulatory axis in the tumor microenvironment and progression. *Trends Immunol.* 31, 220–7 (2010).

26. van Wijk, F. & Cheroutre, H. Intestinal T cells: facing the mucosal immune dilemma with synergy and diversity. *Semin. Immunol.* 21, 130–8 (2009).

27. Konkel, J. E. *et al.* Control of the development of CD8αα+ intestinal intraepithelial lymphocytes by TGF-β. *Nat. Immunol.* 12, 312–319 (2011).

28. Guerrerio, A. L. *et al.* Increased Prevalence of Inflammatory Bowel Disease in Patients with Mutations in Genes Encoding the Receptor Subunits for TGFβ. *Inflamm. Bowel Dis.* 22, 2058–2062 (2016).

29. Ohri, N., Gerich, M. E., Fennimore, B. P. & Kuhn, K. Altered colonic intraepithelial lymphocyte composition and function in Crohn's Disease. *J. Immunol.* 196, 54.10 LP-54.10 (2016).

30. Galon, J. *et al.* Cancer classification using the Immunoscore: a worldwide task force. *J. Transl. Med.* 10, 205 (2012).

31. Pagès, F. *et al.* In situ cytotoxic and memory T cells predict outcome in patients with early-stage colorectal cancer. *J. Clin. Oncol.* 27, 5944–51 (2009).

32. Galon, J. *et al.* The immune score as a new possible approach for the classification of cancer. *J. Transl. Med.* 10, 1 (2012).

33. Galon, J. *et al.* Towards the introduction of the 'Immunoscore' in the classification of malignant tumours. *J. Pathol.* 232, 199–209 (2014).

34. Rooney, M. S., Shukla, S. A., Wu, C. J., Getz, G. & Hacohen, N. Molecular and genetic properties of tumors associated with local immune cytolytic activity. *Cell* 160, 48–61 (2015).

35. Wick, D. A. *et al.* Surveillance of the Tumor Mutanome by T Cells during Progression from Primary to Recurrent Ovarian Cancer. *Clin. Cancer Res.* 20, 1125–1134 (2014).

36. Bell, D. *et al.* Integrated genomic analyses of ovarian carcinoma. *Nature* 474, 609–615 (2011).

37. George, J. *et al.* Nonequivalent Gene Expression and Copy Number Alterations in High-Grade Serous Ovarian Cancers with BRCA1 and BRCA2 Mutations. *Clin. Cancer Res.* 19, 3474–3484 (2013).

38. Clarke, B. *et al.* Intraepithelial T cells and prognosis in ovarian carcinoma: novel associations with stage, tumor type, and BRCA1 loss. *Mod. Pathol.* 22, 393–402 (2009).

39. Birkbak, N. J. *et al.* Tumor Mutation Burden Forecasts Outcome in Ovarian Cancer with BRCA1 or BRCA2 Mutations. *PLoS One* 8, e80023 (2013).

40. Strickland, K. C. *et al.* Association and prognostic significance of BRCA1/2-mutation status with neoantigen load, number of tumor-infiltrating lymphocytes and expression of PD-1/PD-L1 in high grade serous ovarian cancer. *Oncotarget* 7, 13587–98 (2016).

41. Cancer Genome Atlas Research Network, T. C. G. A. R. Integrated genomic analyses of ovarian carcinoma. *Nature* 474, 609–15 (2011).

42. Vaughan, S. *et al.* Rethinking ovarian cancer: recommendations for improving outcomes. *Nat. Rev. Cancer* 11, 719–25 (2011).

43. Cope, L., Wu, R.-C., Shih, I.-M. & Wang, T.-L. High level of chromosomal aberration in ovarian cancer genome correlates with poor clinical outcome. *Gynecol. Oncol.* 128, 500–505 (2013).

44. Eggink, F. A. *et al.* Immunological profiling of molecularly classified high-risk endometrial cancers identifies *POLE* -mutant and microsatellite unstable carcinomas as candidates for checkpoint inhibition. *Oncoimmunology* 6, e1264565 (2017).

45. Nebot-Bral, L. *et al.* Hypermutated tumours in the era of immunotherapy: The paradigm of personalised medicine. *Eur. J. Cancer* 84, 290–303 (2017).

46. Seiwert, T. Y. *et al.* Safety and clinical activity of pembrolizumab for treatment of recurrent or metastatic squamous cell carcinoma of the head and neck (KEYNOTE-012): an open-label, multicentre, phase 1b trial. 17, (2016).

47. Le, D. T. *et al.* KEYNOTE-164: Phase II study of pembrolizumab (MK-3475) for patients with previously treated, microsatellite instability-high advanced colorectal carcinoma. *J. Clin. Oncol.* 34, TPS787-TPS787 (2016).

48. Le, D. T. *et al.* Mismatch repair deficiency predicts response of solid tumors to PD-1 blockade. *Science* 357, 409–413 (2017).

49. Ott, P. A. *et al.* Safety and Antitumor Activity of Pembrolizumab in Advanced Programmed Death Ligand 1-Positive Endometrial Cancer: Results From the KEYNOTE-028 Study. *J. Clin. Oncol.* 35, 2535–2541 (2017).

50. FDA. Approved Drugs - FDA grants accelerated approval to pembrolizumab for first tissue/site agnostic indication. Available at: https://www.fda.gov/Drugs/InformationOnDrugs/ApprovedDrugs/ucm560040.htm. (Accessed: 18th October 2017)

51. Daemen, T. *et al.* Genetic immunization against cervical carcinoma: induction of cytotoxic T lymphocyte activity with a recombinant alphavirus vector expressing human papillomavirus type 16 E6 and E7. *Gene Ther.* 7, 1859–66 (2000).

52. Daemen, T. *et al.* Eradication of established HPV16-transformed tumours after immunisation with recombinant Semliki Forest virus expressing a fusion protein of E6 and E7. *Vaccine* 21, 1082–8 (2003).

53. Riezebos-Brilman, A. *et al.* Induction of human papilloma virus E6/E7-specific cytotoxic T-lymphocyte activity in immune-tolerant, E6/E7-transgenic mice. *Gene Ther.* 12, 1410–1414 (2005).

54. Daemen, T., Regts, J., Holtrop, M. & Wilschut, J. Immunization strategy against cervical cancer involving an alphavirus vector expressing high levels of a stable fusion protein of human papillomavirus 16 E6 and E7. *Gene Ther.* 9, 85–94 (2002).

55. Muderspach, L. *et al.* A Phase I Trial of a Human Papillomavirus (HPV) Peptide Vaccine for Women with High-Grade Cervical and Vulvar Intraepithelial Neoplasia Who Are HPV 16 Positive 1.

56. Hallez, S. *et al.* Phase I/II trial of immunogenicity of a human papillomavirus (HPV) type 16 E7 protein–based vaccine in women with oncogenic HPV-positive cervical intraepithelial neoplasia. doi:10.1007/s00262-004-0501-4

57. Kenter, G. G. *et al.* Vaccination against HPV-16 oncoproteins for vulvar intraepithelial neoplasia. *N. Engl. J. Med.* 361, 1838–47 (2009).

58. Kim, T. J. *et al.* Clearance of persistent HPV infection and cervical lesion by therapeutic DNA vaccine in CIN3 patients. *Nat. Commun.* 5, 5317 (2014).

59. van Poelgeest, M. I. E. *et al.* HPV16 synthetic long peptide (HPV16-SLP) vaccination therapy of patients with advanced or recurrent HPV16-induced gynecological carcinoma, a phase II trial. *J. Transl. Med.* 11, 88 (2013).

60. Weber, J. S. *et al.* A phase 1 study of a vaccine targeting preferentially expressed antigen in melanoma and prostate-specific membrane antigen in patients with advanced solid tumors. *J. Immunother.* 34, 556–67 (2011).

61. Stevanović, S. *et al.* Complete Regression of Metastatic Cervical Cancer After Treatment With Human Papillomavirus–Targeted Tumor-Infiltrating T Cells. *J. Clin. Oncol.* 33, 1543–1550 (2015).

62. Lu, Y.-C. *et al.* Treatment of Patients With Metastatic Cancer Using a Major Histocompatibility Complex Class II–Restricted T-Cell Receptor Targeting the Cancer Germline Antigen MAGE-A3. *J. Clin. Oncol.* 35, 3322–3329 (2017).

63. Jean-Sebastien Frenel, Christophe Le Tourneau, Bert H. O'Neil, Patrick Alexander Ott, Sarina Anne Piha-Paul, Carlos Alberto Gomez-Roca, Emilie Van BruJean-Sebastien Frenel, Christophe Le Tourneau, Bert H. O'Neil, Patrick Alexander Ott, Sarina Anne Piha-Pa, and A. V. Pembrolizumab in patients with advanced cervical squamous

cell cancer: Preliminary results from the phase Ib KEYNOTE-028 study. *J. Clin. Oncol.* 34, 5515–5515 (2016).

64. Welters, M. J. *et al.* Vaccination during myeloid cell depletion by cancer chemotherapy fosters robust T cell responses. *Sci. Transl. Med.* 8, 334ra52 (2016).

65. Pfirschke, C. *et al.* Immunogenic Chemotherapy Sensitizes Tumors to Checkpoint Blockade Therapy. *Immunity* 44, 343–354 (2016).

66. Draghiciu, O., Nijman, H. W., Hoogeboom, B. N., Meijerhof, T. & Daemen, T. Sunitinib depletes myeloid-derived suppressor cells and synergizes with a cancer vaccine to enhance antigen-specific immune responses and tumor eradication. *Oncoimmunology* 4, e989764 (2015).

67. Draghiciu, O., Boerma, A., Hoogeboom, B. N., Nijman, H. W. & Daemen, T. A rationally designed combined treatment with an alphavirus-based cancer vaccine, sunitinib and low-dose tumor irradiation completely blocks tumor development. *Oncoimmunology* 4, e1029699 (2015).

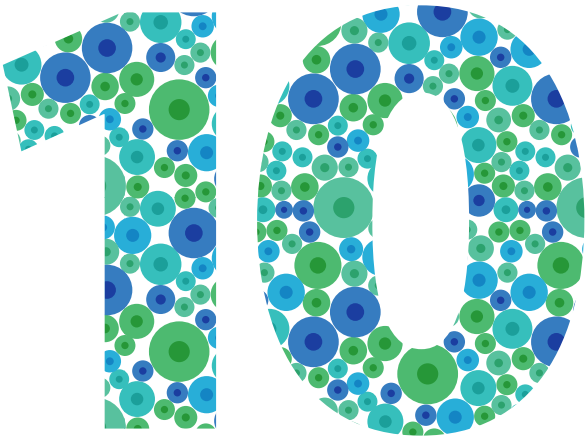

Nederlandse samenvatting

NEDERLANDSE SAMENVATTING

De studies beschreven in dit proefschrift hebben als doel bij te dragen aan de kennis over de interactie tussen het immuunsysteem en kanker. Deze kennis is nodig voor het optimaliseren van immuuntherapie voor de behandeling van patiënten met eierstokkanker, baarmoederkanker en baarmoederhalskanker.

HET IMMUUNSYSTEEM EN IMMUUNTHERAPIE

Het immuunsysteem speelt een belangrijke rol bij het elimineren van kankercellen. Immuun T-cellen in het bijzonder zijn zeer vaardig in het gericht herkennen en doden van kankercellen. T-cellen die zich in het tumorweefsel begeven worden ook wel tumor-infiltrerende lymfocyten (TIL) genoemd. Uit onderzoek bij verschillende vormen van kanker is gebleken dat de aanwezigheid van deze TIL gecorreleerd is met de prognose van patiënten; patiënten waarbij meer TIL aanwezig zijn hebben gemiddeld genomen een langere overlevingsduur, vergeleken met patiënten waarbij minder of geen TIL voorkomen. Uit onderzoek komt naar voren dat TIL kunnen worden geïnactiveerd door kankercellen en niet in staat om alle kankercellen te doden. Bij patiënten waarbij veel TIL aanwezig zijn, is het wenselijk om de aanwezige afweerreactie tegen de kankercellen te versterken, bijvoorbeeld door de TIL opnieuw te activeren. Bij patiënten waarbij weinig of geen TIL voorkomen moet allereerst een afweerreactie worden opgewekt tegen de kankercellen zodat het aantal TIL toeneemt.

Immuuntherapie bij kanker staat voor een therapie die erop gericht is om onderdelen van het immuunsysteem, zoals T-cellen, te activeren en te stimuleren kankercellen te doden. Sterk versimpeld kunnen we drie verschillende vormen van immuuntherapie onderscheiden die op dit moment sterk in de belangstelling staan; *checkpoint inhibitors*, therapeutische vaccinatie, en celtherapie. *Checkpoint inhibitors* hebben onder andere als doel om geïnactiveerde TIL te reactiveren. Dit gebeurt bijvoorbeeld door remmende factoren op de T-cellen op te heffen. Therapeutische vaccinatie heeft als doel om een nieuwe afweerreactie specifiek gericht tegen de kankercellen op te wekken. Bij celtherapie worden TIL die specifiek zijn voor de kankercellen geïsoleerd, buiten het lichaam opgekweekt en in grote hoeveelheden toegediend aan de patiënt.

Het is van belang om de juiste vorm van immuuntherapie toe te passen bij de juiste patiëntengroep. Patiënten waarbij al een afweerreactie is opgetreden en veel TIL aanwezig zijn kunnen baat hebben bij *checkpoint inhibitors*. Bij patiënten waarbij nog geen of onvoldoende afweerreactie is opgetreden (geen of weinig TIL in het tumorweefsel), kan deze afweerreactie eerst worden opgewekt door middel van therapeutische vaccinatie of celtherapie.

De aanwezigheid van TIL in tumorweefsel kan dus een belangrijke graadmeter zijn voor het bepalen van de behandelingsstrategie.

GYNAECOLOGISCHE MALIGNITEITEN

De studies in dit proefschrift richten zich op de drie meest voorkomende gynaecologische maligniteiten, namelijk eierstokkanker, baarmoederkanker en baarmoederhalskanker.

Eierstokkanker wordt over het algemeen in een laat stadium van de ziekte ontdekt, wat voor een deel te verklaren is omdat deze vorm van kanker pas laat klachten geeft. De behandeling bestaat uit een operatie waarbij gepoogd wordt al het tumorweefsel te verwijderen, voorafgegaan of gevolgd door chemotherapie. In ruim de helft van de patiënten wordt gestart met chemotherapie om de tumormassa te verkleinen en de kans op een succesvolle operatie te vergroten. De combinatie van chemotherapie en opereren is bij de meeste patiënten succesvol, helaas keert de ziekte bij veel patiënten terug.

Bij de meeste patiënten met eierstokkanker is er initieel geen of onvoldoende afweerreactie tegen de kankercellen tot stand gekomen. Bij de patiënten waarbij wel een initiële afweerreactie tot stand is gekomen zijn de afweercellen bij een overmaat aan tumormassa inactief geraakt. Immuuntherapie zou in de toekomst mogelijk kunnen worden toegepast om de behandeling en de prognose van patiënten met eierstokkanker te verbeteren.

Baarmoederkanker wordt over het algemeen juist in een vroeg stadium ontdekt doordat de kanker herkenbare klachten geeft (postmenopauzaal bloedverlies). De behandeling bestaat uit een operatie en wordt soms gevolgd door aanvullende behandeling (meestal bestraling). Bij een deel van de patiënten met baarmoederkanker zijn de kankercellen heel goed herkenbaar voor het immuunsysteem, we noemen deze kankercellen microsatelliet instabiel. Doordat deze kankercellen zo goed herkenbaar zijn voor het immuunsysteem ontstaat er bij deze patiëntengroep een zeer effectieve afweerreactie, te zien aan de hoeveelheid TIL in het tumorweefsel. Voor deze patiëntengroep is immuuntherapie -*checkpoint inhibitors*- recent goedgekeurd door de FDA voor de behandeling van teruggekeerde, uitgezaaide ziekte.

Baarmoederhalskanker wordt veroorzaakt door een infectie met een hoog-risico humaan papillomavirus (hr-HPV). In de meeste gevallen wordt het virus opgeruimd door het immuunsysteem. Als dit niet gebeurt dan is er een kans dat geïnfecteerde cellen veranderingen ondergaan die uiteindelijk kunnen leiden tot het ontstaan van kankercellen. Baarmoederhalskanker kan in een vroeg stadium worden opgespoord via het bevolkingsonderzoek waarbij getest wordt op infectie met hr-HPV en afwijkende cellen van de baarmoederhals. In een vroeg stadium wordt baarmoederhalskanker, of een voorstadium van baarmoederhalskanker, behandeld met

een chirurgische ingreep (lisexcisie). Deze ingreep kan zowel op korte als op lange termijn voor complicaties zorgen zoals bloeding, infectie, onvruchtbaarheid of vroeggeboorte. En de onderliggende oorzaak, het hr-HPV virus, wordt niet behandeld.

Cellen die door een infectie met hr-HPV in kankercellen veranderen, maken nog steeds sommige eiwitten van het HPV virus. Het immuunsysteem kan hierdoor baarmoederhalskankercellen herkennen als afwijkende cellen die aangevallen moeten worden. Dit maakt baarmoederhalskanker geschikt voor behandeling met therapeutische vaccinatie.

In **hoofdstuk 2** hebben wij onderzocht wat de kenmerken zijn van TIL die zich in het tumorweefsel van patiënten met eierstokkanker bevinden. Allereerst is het belangrijk om onderscheid te maken tussen afweercellen die zich in het kankerweefsel bevinden en afweercellen die zich in het omliggende bindweefsel, *het stroma*, bevinden. Bij het bestuderen van weefselcoupes is het onderscheid tussen afweercellen in kankerweefsel of in stroma niet altijd goed te maken. In de studie in hoofdstuk 2 laten wij zien dat de afweercellen die zich in het kankerweefsel bevinden gekenmerkt worden door expressie van de merker CD103 ($CD103^+$TIL). Deze studie laat zien dat de aanwezigheid van afweercellen in het kankerweefsel -en niet afweercellen in het stroma- een gunstig effect hebben op de prognose van patiënten met eierstokkanker. In de **hoofdstukken 3 en 4** bevestigen we deze bevindingen bij patiënten met baarmoederkanker en baarmoederhalskanker. Wij concluderen dat CD103 gebruikt kan worden als merker voor het bepalen van het aantal TIL dat zich in het kankerweefsel bevindt en dat de hoeveelheid $CD103^+$TIL een voorspellende waarde heeft voor de prognose van verschillende (gynaecologische) maligniteiten.

Het immuunsysteem blijkt niet altijd in staat om de groei van kankercellen te controleren en in bedwang te houden. Dit kan doordat het immuunsysteem de kankercellen niet goed kan herkennen of doordat het immuunsysteem geïnactiveerd is door de langdurige aanwezigheid van kankercellen. Bij eierstokkanker is er vaak sprake van een grote tumormassa, waarbij slechts bij een klein gedeelte van de patiënten (~10%) TIL aanwezig zijn. In de **hoofdstukken 5 en 6** laten we zien dat vooral de aanwezigheid van jonge, meer naïeve TIL een gunstig effect heeft op de prognose van patiënten met eierstokkanker. Deze jonge, meer naïeve TIL worden gekenmerkt door expressie van de merker CD27. Echter, wanneer de tumormassa te groot wordt, blijken ook de jonge, meer naïeve TIL onvoldoende in staat de prognose om te kunnen buigen. *Size matters!* Wij concludeerden dat zowel immuuntherapie om de initiële afweerreactie op te wekken (zoals therapeutische vaccinatie of celtherapie) als immuuntherapie om de geïnactiveerde afweercellen te reactiveren (zoals *checkpoint inhibitors*) zinvol zou kunnen zijn voor de behandeling van patiënten met eierstokkanker.

Chemotherapie is voor veel vormen van kanker onderdeel van de standaardbehandeling, zo ook voor de behandeling van eierstokkanker. In **hoofdstuk 7** beschrijven we een studie naar het effect van chemotherapie op de verschillende typen afweercellen in het bloed van patiënten met eierstokkanker. Hiervoor werd bij patiënten met eierstokkanker voor, tijdens en na chemotherapie, bloed afgenomen om naar de verhouding tussen de verschillende typen afweercellen te kijken. De uitkomst van deze studie was dat er een duidelijke daling was van myeloïde cellen tijdens de chemotherapie, wat zich herstelde na afronding van de chemotherapie. Myeloïde cellen zijn afweercellen die een afweer-onderdrukkende werking kunnen hebben. Wij concludeerden hieruit dat immuuntherapie goed toegepast kan worden tijdens chemotherapie, wanneer het aantal afweer-onderdrukkende myeloïde cellen gedaald is.

In het vervolg van **hoofdstuk 4** beschrijven we een nieuw therapeutisch vaccin voor de behandeling van baarmoederhalskanker. Zoals boven beschreven kan baarmoederhalskanker ontstaan na een infectie met een hr-HPV en kan het immuunsysteem deze cellen herkennen op basis van bepaalde eiwitten van het HPV virus. Dit zijn onder andere de eiwitten E6 en E7 van hr-HPV. Het nieuwe therapeutische vaccin wekt een afweerreactie op, welke specifiek gericht is tegen de E6 en E7 eiwitten van het HPV virus. In een muismodel voor door HPV-getransformeerde kankercellen hebben we onderzocht of dit therapeutische vaccin effectief is in het opwekken van een afweerreactie in de tumor. Wij toonden aan dat therapeutische vaccinatie ervoor zorgde dat er een afweerreactie werd opgewekt en dat er meer $CD103^+$ afweercellen de tumor infiltreerden.

Tot slot beschrijft **hoofdstuk 8** het onderzoeksprotocol van de Fase I klinische studie waarbij het nieuwe therapeutisch vaccin, genaamd Vvax001, voor het eerst zal worden toegepast in patiënten met (een voorstadium van) baarmoederhalskanker. Figuur 1 toont het beoogde werkingsmechanisme van het therapeutische vaccin. Het doel van deze eerste klinische studie is om, naast de veiligheid van het vaccin, te onderzoeken of het vaccin ook in de mens in staat is een afweerreactie op te wekken. Indien het therapeutische vaccin effectief blijkt in het opwekken van een afweerreactie zal in de toekomst mogelijk een chirurgische behandeling kunnen worden vervangen door therapeutische vaccinatie. Dit zal worden onderzocht in Fase II en Fase III studies.

CONCLUSIE

De studies beschreven in dit proefschrift dragen bij aan de kennis over de interactie tussen het immuunsysteem en gynaecologische kankers. We bestudeerden tumor-infiltrerende lymfocyten in de verschillende gynaecologische maligniteiten. De merker CD103 is voorspellend voor de

prognose van patiënten met een gynaecologische maligniteit en kan in de toekomst gebruikt worden om richting te geven bij de keus van de meest effectieve immuuntherapie voor de patiënt.

Tot slot beschrijven we een klinisch studieprotocol waarbij een nieuw therapeutisch vaccin voor het eerst zal worden toegepast voor de behandeling van patiënten met (een voorstadium van) baarmoederhalskanker.

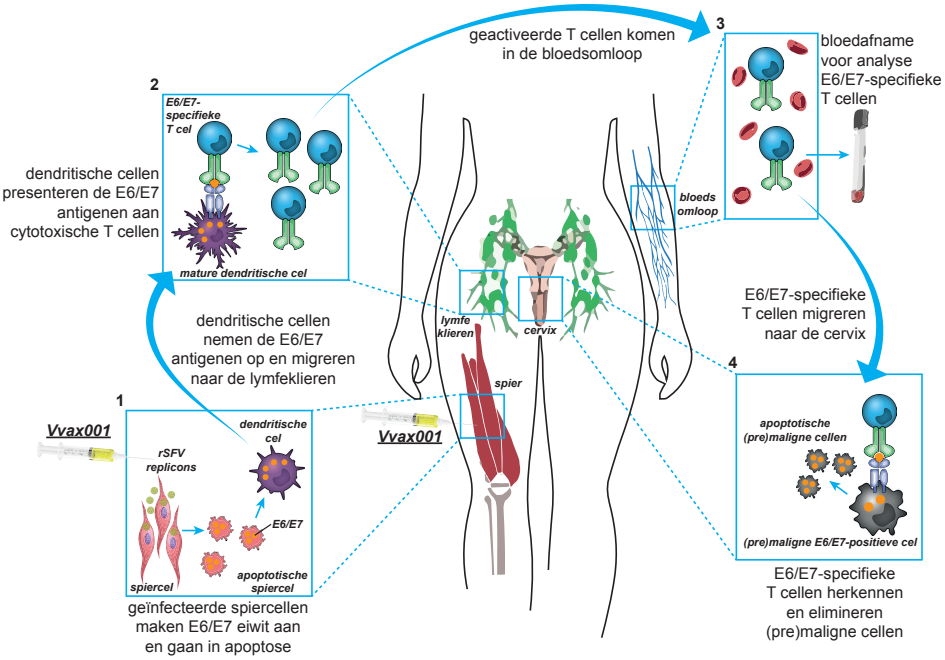

FIGUUR 1. Werkingsmechanisme Vvax001. Vvax001 bestaat uit repliconpartikels van een alfavirus, het Semliki Forest virus (SFV) die coderen voor HPV16-E6- en E7-eiwitten. rSFV is zodanig veranderd dat de repliconpartikels een cel kunnen infecteren en het RNA kunnen repliceren maar niet coderen voor de eiwitten die nodig zijn om nieuw virus te maken; immunisatie leidt dus niet tot de aanmaak van nieuw virus. De wetenschappelijke benaming van Vvax001 luidt rSFVeE6,7 **1.** rSFVeE6,7 maakt in een geïnfecteerde cel een grote hoeveelheid van een fusie-eiwit van E6 en E7 aan. Zo'n cel gaat 48 tot 72 uur na infectie dood. Deze celdood resulteert in celfragmenten die E6 en E7 bevatten die opgenomen kunnen worden door dendritische cellen. **2.** De dendritische cellen presenteren vervolgens stukjes van de E6- en E7 eiwitten aan T-cellen in de lymfeklieren. Hierdoor worden T-cellen opgewekt die gericht zijn tegen HPV16. **3.** De geactiveerde T-cellen komen in de bloedsomloop **4.** Deze T-cellen kunnen (pre) maligne cellen van de baarmoederhals (cervix) herkennen en doden.

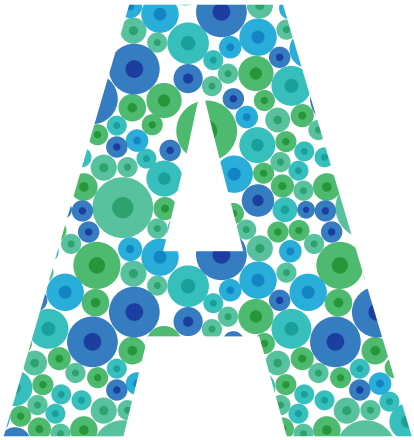

Appendix

DANKWOORD

Graag wil ik eenieder bedanken die heeft bijgedragen aan de totstandkoming van dit proefschrift.

Mijn eerste dank gaat uit naar de patiënten die hebben deelgenomen aan de klinische studies beschreven in dit proefschrift.

Geachte promotor Prof. Dr. H.W. Nijman, beste Hans, bedankt dat je me de kans hebt gegeven om na mijn wetenschappelijke stage door te gaan met dit promotietraject. Het was een ongelofelijke uitdaging om de fase I klinische studie op poten te zetten en ik vind het een eer dat je mij hiertoe in staat achtte. Jij wist tegenslagen te relativeren en wist me altijd weer te motiveren door jouw 'het is geen probleem, het is een uitdaging'-uitspraak. Ik heb met veel plezier deel uit gemaakt van jouw onderzoeksgroep.

Geachte promotor Prof. Dr. C.A.H.H. Daemen, beste Toos, bedankt voor je begeleiding. Ik heb veel van je geleerd over virale vector vaccins en de immunologische assays. Ook gaf je mij de kans mijn onderwijsvaardigheden te ontwikkelen, best spannend, zo'n collegezaal vol studenten. Ik vond het een eer om het stapje *from bench to bedside* met VVAX001 te mogen maken, het vaccin waar jij -met vele anderen- al zo lang aan hebt gewerkt.

Geachte copromotor Dr. M. de Bruyn, beste Marco, bedankt voor het delen van je enthousiasme voor de wetenschap! Gecombineerd met altijd fluitend door de gang te lopen, werkt dat erg aanstekelijk. Naast dat ik ontzettend veel van je heb geleerd, wil ik mijn bijzondere waardering uitspreken voor de wekelijkse brainstorm sessies over de toekomst van het onderzoek, carrière en de zin -en onzin- van het leven.

Graag bedank ik de leden van de leescommissie, Prof. dr. J.P. Medema, Prof. dr. R.K. Weersma en Prof. dr. S.A. Scherjon voor het beoordelen van mijn proefschrift.

Graag bedank ik alle co-auteurs voor onze productieve samenwerking.

Graag bedank ik het secretariaat van de afdeling Obstetrie & Gynaecologie voor de ondersteuning. In het bijzonder wil ik Diana en Janette bedanken. Ook wil ik Lida bedanken voor de ondersteuning bij de voorbereidingen van de klinische studie en de audits.

Graag bedank ik iedereen van onze Immuno-oncology onderzoeksgroep: Ninke, Maartje, Florine, Kim, Hagma, Joyce, Sterre, Arjan, Martha, Annechien en Nienke. Wat is het fijn om als groep samen te werken en van elkaar te kunnen leren. Keep up the good work! En drink een lekkere kop koffie als het even tegen zit!

Beste Student-onderzoekers, Thalina, Aline, Anouk, Bart en Jessica. Bedankt voor jullie hulp en samenwerking. Beste Jessica, speciale dank voor je inzet, enthousiasme en betrouwbaarheid. Je gaat vast een mooi promotietraject tegemoet.

Graag bedank ik eenieder die betrokken was bij de VVAX001 klinische studie. Naast Refika Yigit als principal investigator van de studie wil ik in het bijzonder Sterre en Jessica bedanken voor de klinische betrokkenheid. Het immunomonitoring team bestaande uit Stephanie, Boukje-Nynke, Annemarie, Amritha en Ruben, bedankt.

Graag bedank ik Janneke Meulenberg voor de prettige samenwerking vanuit Vicinivax bv. Jouw overzicht, precisie en vastberadenheid maakt dat we menig deadline hebben gehaald! Daarnaast wil ik eenieder bedanken die betrokken was bij de ontwikkeling van VVAX001. Ido, Annelies, en Jolande, ik heb veel van jullie geleerd over het drug-development proces tijdens de pre-klinische vergaderingen.

Graag wil ik al mijn kamergenoten van de afgelopen jaren bedanken voor de nodige afleiding, thee, koffie en motivatie! In semi-chronologische volgorde; Florine, Tom, Jan, Aniek, Meike, Anne, Petra, Violetta, Claudia, Thalita, Nienke, Lotte en Matty.

Lieve paranimfen, lieve Florine, 3.5 jaar samen onderzoek doen waarbij we lief en leed met elkaar konden delen. Wat was het fijn om jou als collega en vriendin te hebben. Lieve Ils, vanaf het eerste uur waren we huisgenoten in Groningen, na ongeveer 10 jaar splitsten onze wegen. Wat was het fijn om jou als huisgenoot en vriendin te hebben. Bedankt dat jullie mijn paranimfen willen zijn. Ik kan me niet anders voorstellen mijn proefschrift te verdedigen met jullie aan mijn zijde.

Lieve jo, jij mag natuurlijk niet ontbreken; bedankt voor je trouwe vriendschap. Nadat jij, Ils, en Flo me al voorgegaan zijn in het academiegebouw wordt het binnenkort weer tijd voor een mooi diner met zijn vieren!

Graag bedank ik mijn nieuwe collega's van de afdeling klinische genetica van het Amsterdam UMC. In het bijzonder mijn opleiders Mieke van Haelst en Mariet Elting voor het vertrouwen dat jullie in mij hadden in de 'mijn proefschrift is bijna af'-periode. Veel dank aan al mijn collega's, in het bijzonder Sanne, Mala en Bas, dankzij jullie voelde ik me al snel 'thuis' op mijn nieuwe werkplek.

Lieve huisgenootjes van Fort Noxx en clubgenootjes van JC LOS. Bedankt voor jullie vriendschap, gezelligheid, hapjes en drankjes, huisweekends, clubvakanties en klaverjasavonden. Moge er nog vele mooie momenten volgen!

Lieve pap, mam, bedankt voor jullie steun en het vertrouwen dat jullie hebben dat ik dit promotietraject tot een goed einde zal brengen. Lieve broers Bent en Jeppe, dankzij jullie ben ik er zelf in gaan geloven. De bijnaam *mini-professor* heeft hierbij erg geholpen!

Lieve Ruben, bedankt voor je steun, geduld en begrip tijdens het afronden van mijn promotietraject. Jij zorgt voor een fijn thuis waar ik heerlijk kan ontspannen, maar jij weet me ook aan het werk te zetten wanneer dat nodig is. Samen zijn we een topteam. Bedankt voor je liefde. Wie weet wat de toekomst ons zal brengen... Ik ook van jou!

Tot slot bedank ik Acda en de Munnik, Bob Marley en Ludovico Einaudi voor de muzikale ondersteuning tijdens het schijven van dit proefschrift.